The role of GPR65 and GALC in Multiple Sclerosis

Establishing the functional consequences of an MS associated variant on chromosome 14q31.3

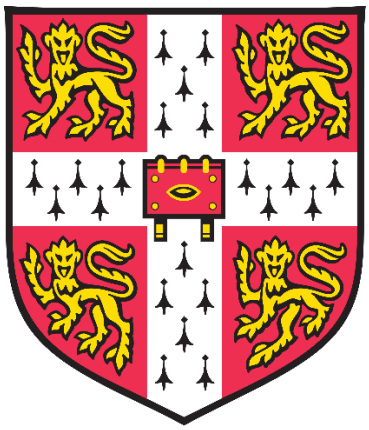

Wenjia Liao

Peterhouse

Department of Clinical Neuroscience

October 2018

This dissertation is submitted for the degree of Master of Science.

Declarations

This dissertation is the result of my own work and includes nothing which is the outcome of work done in collaboration except where specifically indicated in the text.

The word count is less than 60000.

Abstract – The role of GPR65 and GALC in Multiple Sclerosis

Wenjia Liao

Genome-wide association studies have identified an extensive catalogue of unequivocally associated genetic variants, each of which provides a clue to the aetiology of multiple sclerosis (MS). Unfortunately, for the vast majority of these quite how the genetic change contributes to the development of the disease is unknown. However, preliminary work undertaken by one of my predecessors suggested that the functionally relevant variant underlying the association identified on chromosome 14q31.3 might exert its effect by influencing T cell activation in a pH dependent manner. From a genetics perspective the ImmunoChip study showed that the lead most strongly associated single nucleotide polymorphism (SNP) tagging this association was rs74796499, which lies in a region of genome containing two protein coding genes; the lysosomal enzyme galactosylceramidase (*GALC*) and acid sensing surface receptor G-protein coupled receptor 65 (*GPR65*). In my thesis I attempted to validate and replicate this finding, and also to explore the possibility of other pH dependent effects of this SNP.

In order to undertake this work, I first developed a system capable of maintain cultured cells at a stable pH for prolonged periods. Using this system I was able to show that the activation of human lymphocytes to stimulation with anti-CD3/CD28 antibodies is maximal at neutral pH and reduced in both acidic and alkaline conditions. Unfortunately, I was unable to replicate the provisional finding that carrying the protective allele at rs74796499 resulted in greater inhibition of CD25 expression in acidic conditions. However, I did observe nominally significant evidence that the expression of the early activation marker CD69 was induced by culturing cells in unstimulated but acidic conditions, and that this expression was highest in individuals carrying the protective allele at rs74796499. In my first attempt to validate and replicate this new finding I not only found further evidence to support this effect on CD69 in unstimulated cells but also found nominally significant evidence that the expression of lactosylceramide (LacCer, CD17) was lower in ex-vivo cells from individuals carrying the protective allele at rs74796499. Unfortunately, in my final confirmatory experiments I was unable to replicate either of these effects. In summary despite carefully studying over 160 healthy subjects, I was unable to find any statistically significant evidence that rs74796499 genotype exerts any effects the expression of either CD25, CD69 or LacCer in ex-vivo cells or stimulated and unstimulated cells cultured under a range of pH conditions.

Table of Contents

Abbreviation

α-GalCer	alpha-galactocerebroside
ASIC	Acid-sensing Ion channels
B4GALT5	β-1,4-galatosyltransferase 5
BBB	Blood brain barrier
BCR	B cell receptor
BSA	Bovine serum albumin
cAMP	cyclic adenosine 5'-monophosphate
CCR7	C-C chemokine receptor type 7
CLL	Chronic Lymphocytic Leukaemia
CNS	Central nervous system
Co-IP	Co-immunoprecipitation
CREB	cAMP response element binding protein
CSF	Cerebrospinal fluid
Csk	C-terminal Src kinase
DC	Dendritic cell
DMEM	Dulbecco's Modified Eagle Medium
EAE	Experimental autoimmune encephalomyelitis
EBS	Epstein-Barr virus
eQTL	Expression quantitative trait loci
FACS	Fluorescence-activated cell sorting; Flow cytometry
FcR	Fc region
FDA	Food and Drug Administration
FMO	Fluorescence minus one
FSC/SSC	Forward-scatter/Side-scatter
GALC	Galactosylceramidase
GalC	Galactosylceramide
Gb3	Globotriaosylceramide
GBA	Glucosylceramidase beta
GC	Glucocorticoids
GM1	Monosialotetrahexosylganglioside
GPCR	G protein couple receptor
GPR65	G protein coupled receptor 65

GWAS	Genome-Wide Association Study
HEXB	Hexosaminidase B
HHV-6	Human Herpesvirus 6
HLA	Human Leukocyte Antigen
HRP	Horseradish peroxidase
IBD	Inflammatory bowel disease
ICAM-1	Intercellular Adhesion Molecule 1
IFN-γ	Interferon-gamma
IL-7	Interleukin 7
IMSGC	International Multiple Sclerosis Genetics Consortium
iNKT cell	invariant Natural killer cell
JAK2	Janus kinase 2
LacCer	Lactosylceramide
LD	Linkage disequilibrium
LLC	Lewis lung carcinoma
LPS	Lipopolysaccharide
MFI	Mean fluorescence intensity
MHC	Major histocompatibility complex
MMP	Matrix metalloproteinase
MS	Multiple Sclerosis
NK cell	Natural killer cell
PBMC	Peripheral blood mononuclear cell
PFA	Paraformaldehyde
PHGDH	phosphoglycerate dehydrogenase
PKA	Protein kinase A
RORC	RAR-related orphan receptor C
S1P	Sphingosine1-phosphate receptor
SLE	Systemic lupus erythematosus
SNP	Single nucleotide polymorphism
STAT3	Signal transducer and activator of transcription 3
TCR	T cell receptor
Th	T helper cell
TNF-α	Tumour necrosis factor-alpha

Treg	Regulatory T cell
TRPV1	Transient receptor potential channel vanilloid subfamily 1
TYK2	Tyrosine kinase 2
WTCCC	Wellcome Trust Case Control Consortium

Chapter 1: Introduction

1.1 Multiple sclerosis

1.1.1 Pathogenesis of multiple sclerosis

Multiple sclerosis (MS) is an autoimmune disease of the central nervous system (CNS) which in the developed world is a common cause of chronic neurological disability in young adults [1]. MS most frequently begins in the third of fourth decade of life and affects women more often than men [2]. Pathologically the disease is characterised by patchy inflammatory demyelination of the central nervous system accompanied by neurodegeneration [3]. Myelin is a lipid-rich membrane covering axons that is generated and maintained by oligodendrocytes. Damage or loss of myelin, and/or its supporting oligodendrocytes, impairs the ability of axons to transmit electrical impulses and thereby results in neurological dysfunction. As time passes the disease leads to axonal loss and neurodegeneration that results in the progressive accumulation of irreversible disability. Common symptoms include weakness, sensory upset, balance problems, sphincter disturbance and fatigue.

The clinical course of MS has been classified into four main types. In the majority of cases (80%) patients begin with what is referred to as relapsing-remitting MS (RRMS) where they have episodes of neurological upset, typically about one per year, from which recovery is generally complete [1, 4]. After a time these relapses tend to become less common but instead the patients have increasing accumulation of disability (secondary progressive MS). In 15-20% of patients, the disease progresses from onset with little to no recovery periods and accumulation of disability (primary progressive MS) [5]. Approximately 5% of patients have progressive-relapsing MS (PRMS) in which they have progressive disease from the onset but this is punctuated by occasional relapses [5]. Although the pathogenesis of MS remains unclear, available evidence suggests that the disease results from the effects of environmental factors acting in genetically susceptible individuals [6].

1.1.2 Environmental factors

The prevalence of MS varies across the world, being highest in temperate parts of the globe, such as North America and Europe (approximately 1:1000 in the UK) [7], and lowest in tropical areas, such as Asia and Africa [8]. Migration studies have shown that risk increases in people moving from low-risk to high-risk areas, and vice versa, particularly if they move before puberty (age 15 years) [9-11], with the result that changes in risk are greatest in second

generation migrants and minimal in adults from the first generation [12]. These data confirm the involvement of environmental factors in the development of MS but don't provide much information about what these factors might be. Both infective and non-infective factors have been considered [13, 14].

The role of viral infection in the pathogenesis of MS remains uncertain. Epstein-Barr virus (EBV) infection has been reported to be strongly associated with the susceptibility of MS [15] and increased levels of EBV antibodies are found in the serum and cerebrospinal fluid (CSF) in MS patients [16-18]. It has been suggested that EBV infection might generate T cells that cross-react with CNS antigens, or that MS might represent bystander damage caused by CD8+ T cells attacking EBV infected autoreactive B cells [19]. A role for human herpesvirus 6 (HHV-6) has also been suggested, particularly in disease relapses and progression [20], with HHV-6 DNA and antigens found in MS plaques and oligodendrocytes [21]. Non-infective factors such as sunlight/vitamin D [22, 23], smoking [23] and diet [24] have also been implicated, however no environmental risk factor has been firmly established as being unequivocally essential for the development of MS.

1.1.3 Genetic factors

Epidemiological studies have consistently identified clustering of the disease in families, with twin studies confirming that much of this clustering relates to shared genetic factors. In the Canadian twin study for example, researchers found that recurrence risk was 25.9% for identical (monozygotic) twins compared with just 2.3% for fraternal (dizygotic) twins [25]. Consistent results have been found in other populations, such as the Danish [26], UK [27] and Italian populations [28]. In a unique adoption study, only one case of MS was found among 1201 first-degree non-biological relatives of patients who had been adopted at an early age, which is equal to the general population prevalence rate (0.1%) for MS [29].

Association with variation in the Human Leukocyte Antigen (HLA) genes from the Major Histocompatibility Complex (MHC) was identified more than 40 years ago [30-32]. Subsequent studies of the MHC have shown that although many variants from this region show association with MS, most of these associations are secondary to linkage disequilibrium (LD) with *HLA-DRB1*15:01* the strongest genetic risk factor associated with MS identified to date [33-36]. The primary function of the HLA genes is to provide a means for the immune system to distinguish self, the body's own proteins and cells, from foreign material such as pathogens.

How and why this particular allele of DRB1 increases the risk of MS remains unknown, but most likely relates in some way to antigen presentation.

In the last 10 years genome-wide association studies (GWAS) have identified more than two hundred non-MHC common variants that increase the risk of developing MS, each of which exerts only a minor individual effect on risk [37]. Most of these associated variants lie close to immunologically relevant genes but how they affect the immune system is only known for a very few loci. For example, the risk allele of rs6897932 which maps within the spliced exon 6 of *IL-7Rα*, the gene for the α subunit of the interleukin 7 (IL-7) receptor, has been shown to increase the proportion of soluble as opposed to membrane bound receptor, and thereby inhibit IL-7 signalling [38, 39]. More recently evidence for interaction of this variant with rs2523506 from the *DDX39B* gene has emerged extending our understanding of the mechanism underlying this shift in alternate splicing [40]. Although many of the MS associated susceptibility variants also influence the risk of developing other autoimmune diseases [41], and thus presumably exert their effects by shifting the immune system towards autoreactivity, some of the risk variants appear to only influence the risk of developing MS. It seemed to me that these MS specific variants might be more revealing about why MS rather than some other autoimmune disease develops, and might therefore be interesting targets for functional analysis.

1.1.4 Current disease modifying therapies for MS

Currently, there is no cure for MS, but in the last 20 years a range of disease modifying therapies (DMTs) have emerged which modulate or suppress the immune system and thereby reduce the inflammatory activity of the disease (in particular the number of relapses). The first DMT licenced for patients with relapsing-remitting MS was β-interferon (IFN-β) which reduces proinflammatory type 1 T helper (Th1) cells and increases anti-inflammatory type 2 T helper (Th2) cells [42-44]. Another key effect of IFN-β is inhibition of matrix metalloproteinase (MMPs) expression which reduces the number of inflammatory macrophages that cross the blood brain barrier [45]. A clinical study showed that MS patients treated with IFN-β have increased levels of soluble CD73, a known neuroprotective molecule in serum [46]. Other medications including Alemtuzumab (Lemtrada) and Dacizumab (Zinbryta), both of which are monoclonal antibodies against CD52 or CD25 respectively, are also available to be used for the treatment of relapsing MS [47-49]. Therapies that reduce the trafficking of cells into the CNS are also used, in particular the oral therapy Fingolimod

(Gilenya) which reduces lymphocyte egress from lymph nodes by down-regulating sphingosine1-phosphate receptors (S1P) [50].

The most recent addition to the catalogue of MS DMTs is the anti-CD20 antibody ocrelizumab, which is the first and only drug approved by the US Food and Drug Administration (FDA) for the treatment of primary progressive MS. Ocrelizumab is a humanized monoclonal anti-CD20 antibody which reduces B cells by antibody-dependent cell mediated cytotoxicity [51, 52]. Clinical trials showed ocrelizumab slowed disability progression in primary progressive MS patients [53].

1.2 Immunology of multiple sclerosis

1.2.1 CD4+ helper T cells in MS

Studies in mouse models and MS patients suggest that inflammatory demyelination is primarily initiated by CD4+ T helper cells and maintained by pathogenic CD8+ effector T cells [1, 54]. In the mouse model of MS, experimental autoimmune encephalomyelitis (EAE), disease can be initiated by the passive transfer of myelin-specific CD4+ T cells alone, and effectively treated with anti-CD4 antibodies [55-57]. However, in a clinical trial long-term reduction of CD4+ T cell alone using anti-CD4 antibody showed no significant therapeutic effect [58]. The importance of CD4+ helper T cell is also suggested by the strong association with MHC class II, and many of the other genes implicated through genetic analysis, such as *TAGAP* and *IL-2RA*. Furthermore the actions of the drugs which have been found to be effective, such as Natalizumab which particularly blocks the passage of CD4+ T cells into the CNS [59-61] and the established efficacy of Alemtuzumab further support the importance of T cells (both of CD4+ and CD8+ T) [62, 63].

1.2.2 CD8+ T cells in MS

As the genetic analysis of the MHC region has been refined in recent years it has become clear that the disease is also associated with MHC class I genes as well as class II genes, implicating CD8+ alongside CD4+ T cells [33, 64]. CD8+ T cells are a vital part of the effector arm of the adaptive immune system, that recognise antigen presented in combination with MHC class I, release proinflammatory cytokines, including interferon-gamma (IFN-γ) and tumour necrosis factor-alpha (TNF-α), and also give rise to a memory population. CD8+ T cells reactive to

myelin basic protein (MBP) have a pathogenic role in the development of EAE [65]. In MS lesions CD8+ T cells can be 10 times more frequent than CD4+ T cells [66-68], which is a higher ratio than in the blood [69, 70].

1.2.3 Th17 cells and Treg in MS

In the last few years a new lineage of T helper cells distinct from the traditional Th1 (pro-inflammatory) and Th2 (anti-inflammatory) lineages, and characterized by the production of IL-17 has been identified, called Th17 cells [71]. Studies in MS patients have shown an increased proportion of Th17 cells in CSF and blood during a relapse and increased expression of the Th17 cell specific transcription factors RORγt and RORα (encoded by the receptor-related orphan receptor C gene; *RORC*) in peripheral blood mononuclear cells (PBMCs) from MS patients in comparison to healthy controls [72, 73]. In mouse models, the differentiation of naive T helper cells into Th17 cells has been shown to require IL-23 [74]. Deficiency in the expression of IL-23, or CCR7 (C-C chemokine receptor type 7), an essential ligand required for the production of IL-23 in dendritic cells (DC), causes a defect in the generation of Th17 cells, and protects against the development of EAE [75, 76]. Evidence suggests that the Th17 cell signature cytokine (IL-17A) also plays a pathogenic role as *IL-17* knockout mice are significantly protected from EAE, and adoptive transfer of IL-17 deficient (-/-) CD4+ T cells does not efficiently induce EAE [77].

Regulatory T cells (Treg) play a critical role in establishing peripheral tolerance and protecting against the development of autoimmune diseases and EAE [78-82]. FOXP3 is a key regulatory molecule in the maturation of Treg cells and genetic defects in the *FOXP3* gene are known to cause dysregulation of immune homeostasis [83]. Also, inactivation or depletion of Tregs with anti-CD25 monoclonal antibody led to exacerbated EAE in mice [82]. In humans, there is no difference in the frequency of Treg cells in peripheral blood between healthy controls and MS patients, however, several studies have shown that the maturation of Tregs from patients are functionally impaired [84-86].

1.2.4 NK and NKT cells in MS

Natural killer (NK) cells have become attractive target for MS research in recent years. It is widely accepted that NK cells can be divided into cytotoxic ‘mature’ NK cells and cytokine secreting ‘immature’ NK cells, which can be phenotypically distinguished by the surface expression of CD56 and CD16 in human [87]. *In vivo* studies have shown that cytotoxic NK

cells are able to directly kill myelin-specific encephalitogenic T cells, and that depletion of NK cells causes an increase in the production of Th1 cytokines, which in turn promote the development of EAE [88, 89]. In MS patients, many studies have reported the dysfunction of the cytotoxic NK cell in the blood [90-93], while expansion of NK cells (using IL-2 antibody complex) suppressed inflammation in EAE through the inhibition of the Th17 pathway [94]. Notably, clinical studies have also shown that the DMT IFN-β upregulates immunoregulatory immature NK cells in the periphery blood and reduces cytotoxic mature NK cells [95-98].

NKT cells are a subset of T cells which are characterized by the recognition of the MHC class I-related protein CD1d [99]. NKT cells can be divided into invariant NKT cells (iNKT) and variant NKT cells dependent on the expression of a semi-invariant T cell receptor (TCR), which consists of Vα24-Jα18 and Vβ11 chains in human [99-101]. Activation of iNKT cells with alpha-galactocerebroside (α-GalCer) protects against the development of EAE in a manner that is dependent upon IL-4 and IFN-γ [102]. Moreover, IFN-β treated patients show an expansion of iNKT cells which enhances their regulatory effects [103]. Further investigation suggests that IFN-β exerts its effects on iNKT cells by altering the antigen-presenting capacity of dendritic cells (DCs) [103].

1.2.5 Cytokines and chemokines in MS

The cytokine network is complex and several of the susceptibility loci identified in genetic studies map close to cytokine related genes [33]. Many studies have considered the effects of cytokines on the Th1 and Th17 pathways using transgenic knockout mice, recombinant proteins or antibodies; Table 1.1 below showed some key effects of cytokines in the mouse model EAE.

The blood brain barrier (BBB) is formed by cerebral vessel endothelial cells, and functions to separate the circulating blood from the CNS. Dysregulation of chemokines or chemokine receptors can lead to the migration of T cells across the BBB into the CNS in MS [104]. It has been reported that CCR6 plays a critical role in the regulation of inflammatory T cell migration, and that mice deficient in CCR6 are resistant to the induction of EAE [105, 106]. Furthermore, increased expression of CCR5 and CXCR3 on T cells have been found in blood and CSF in MS patients [107]. Other chemokines identified that are dysregulated in MS include CCR1, CCR2, CCR5, CXCR3 and CX3CR1 [108].

Table 1. 1: The phenotypic effects of cytokines, cytokine receptors and transcription factors in EAE mouse models. (continued on next page)

Cytokine	KO mice/treatment	Phenotype	Reference
IL-1	*IL-1*$^{-/-}$	Protected	[109]
	IL-1R$^{-/-}$	Protected	[110]
	IL-1α recombinant protein	exacerbated	[111]
IL-2	*IL-2*$^{-/-}$	protected	[112]
IL-3	*IL-3*$^{-/-}$	protected	[113]
	IL-3 recombinant protein	exacerbated	[113]
IL-4	*IL-4*$^{-/-}$	exacerbated	[114]
	IL-4$^{-/-}$	no phenotype	[115]
	IL-4Rα$^{-/-}$	protected	[116]
IL-6	*IL-6*$^{-/-}$	protected	[117]
	anti-IL-6 antibody	protected	[118]
	anti-IL-6R antibody	protected	[119]
IL-10	*IL-10*$^{-/-}$	exacerbated	[120]
	IL-10 transfection	protected	[121]
IL-12	*IL-12p35*$^{-/-}$	exacerbated	[122]
	IL-12p40$^{-/-}$	protected	[122]
	IL-12Rβ1$^{-/-}$	protected	[123]
	IL-12Rβ2$^{-/-}$	no phenotype	[123]
	IL-12Rβ2$^{-/-}$	protected from remitting stage	[124]
	anti-IL-12 antibody	protected	[125]
IL-17	*IL-17*$^{-/-}$	protected	[77]
	IL-17A$^{-/-}$	no phenotype	[126]
	Il-17F$^{-/-}$	no phenotype	[126]
IL-21	*IL-21*$^{-/-}$	protected	[127]
	IL-21$^{-/-}$	no phenotype	[128]
	IL-21R$^{-/-}$	protected	[127]
	IL-21R$^{-/-}$	no phenotype	[128]
IL-22	*IL-22*$^{-/-}$	no phenotype	[129]
IL-23	*IL-23p19*$^{-/-}$	protected	[130]
	IL-23R$^{-/-}$	protected	[127]

IFN-γ	anti-IFN-γ antibody	exacerbated	[131]
	anti-IFN-γ antibody	exacerbated	[132]
	IFN-γR$^{-/-}$	exacerbated	[133]
	IFN-γR$^{-/-}$	exacerbated	[134]
IFN-β	recombinant IFN-β	protected Th1-induced EAE	[135]
	recombinant IFN-β	exacerbated Th17 induced EAE	[135]
	IFN-β$^{-/-}$	exacerbated	[136]
	IFN-β$^{-/-}$	exacerbated	[137]
TNFα	*TNFα*$^{-/-}$	exacerbated	[138]
	TNFα$^{-/-}$	exacerbated	[139]
	anti-TNFα antibody	protected in early stage	[140]
GM CSF	*CSF2*$^{-/-}$	no phenotype	[141]
RORγt	*RORγt* transfection	exacerbated	[142]
T-bet	*T-bet* transfection	protected	[142]
	T-bet$^{-/-}$	protected	[143]

1.3 The genetic analysis of multiple sclerosis

1.3.1 Genome-wide studies

Linkage analysis is a highly effective way of mapping disease loci in families affected by highly penetrant Mendelian disorders. However, the approach has little power in the analysis of complex diseases where susceptibility is determined by multiple loci each exerting only modest effects on risk [144]. In MS genome-wide searches for linkage have failed to find any significant evidence for linkage anywhere except in the MHC region (related to the long established DRB1*15:01 risk allele) [145]. On the other hand, genome-wide association studies (GWAS) in adequate sample sizes have high power to identify common susceptibility variants (those with a minor allele frequency of >5%) [146]. The approach relies on the extensive correlation that exists between the alleles of tightly linked common variants, linkage disequilibrium (LD) [147], which means that only a small fraction of common variation needs to be actually typed; these typed variants effectively "tag" the much larger number of un-typed variants [148]. International collaborative efforts such as the HapMap project have identified most common variants in the human genome (as listed in publicly available resources such as dbSNP: https://www.ncbi.nlm.nih.gov/projects/SNP/) [149]. It is now well recognised that

genotyping a few hundred thousand carefully selected common variants effectively enables more than 80% of common variation to be tested [150].

The first GWAS for MS was completed by the International Multiple Sclerosis Genetics Consortium (IMSGC) in 2007 and considered 334,923 single nucleotide polymorphisms (SNPs) in 931 trio families (an affected individual and both their parents) in its screening phase [38]. In total three MS associated SNPs were identified two from the *IL-2RA* gene and one from the *IL-7RA* gene; these were the first non-MHC variants confirmed to be associated with the disease. Subsequently the IMSGC collaborated with the Wellcome Trust Case Control Consortium (WTCCC) and completed a significantly more powerful GWAS which was published in 2011 and included 9,772 cases and 17,736 controls tested at 465,434 SNPs in the screening phase [33]. This study brought the total number of non-MHC associated variants to 57. Following this the IMSGC fine mapped 184 genomic regions in 14,498 cases and 24,091 controls using the ImmunoChip, and extended the number of associated non-MHC variants to 110, each with genome-wide significant evidence for association ($p<5x10^{-8}$) [151]. Table 1.2 shows a summary of GWAS efforts in MS. Since completing the ImmunoChip analysis the IMSGC has performed a meta-analysis of MS GWAS and genotyped potentially associated variants on a custom "MSchip", a pre-print of this work has been published in Biorxiv and lists a total of 201 non-MHC associated variants [37], which together with the MHC account for about a 20% of the heritability of MS.

It is striking that nearly all the MS associated genetic variants are located in regulatory non-coding regions of the genome in or near to genes with known immunological functions [33, 151]. These data provide some of the strongest evidence supporting the importance of immunological processes in the aetiology of MS. However, because of the extensive LD between common variants, each of the associated SNPs implicates a genomic region rather than just the nearest gene. Thus, it is challenging to establish which specific genes and functional pathways are implicated by these associations.

1.3.2 The association of chromosome of 14q31.3 and MS

One of the most strongly associated SNPs identified in the 2011 GWAS was rs2119704 ($p=2.2x10^{-10}$) from chromosome 14q31.3 [33]. The region implicated by this SNP was also included in the ImmunoChip study, which enabled detailed fine mapping of the association that

identified rs74796499 ($p=8.47x10^{-11}$; $r^2 = 0.6$; D' = 0.993) as the lead most associated SNP in the region (Figure 1.1) [151]. Both the GWAS and ImmunoChip lead variants have a low minor allele frequency (MAF), 6% for rs2119704 and 3% for rs74796499 in the UK ImmunoChip data, with the minor allele being protective in each case. Within this associated region, there are two protein coding genes: galactosylceramidase (*GALC*) and G protein coupled receptor 65 (*GPR65*, also referred to as T cell death associated gene 8, *TDAG8*), and a long intergenic non-coding RNA gene *LINC01146*, the function of which is unknown [152]. Both *GALC* and *GPR65* have functions that make them logical and promising candidate genes in MS.

The associated variants in the region containing these two coding protein genes are in tight LD, making it difficult genetically to determine which gene is associated with the MS susceptibility SNP. The SNP rs2119704 lies downstream of *GPR65*, whilst rs74796499 lies within intron 8 of *GALC* (Figure 1.1).

Table 1. 2: Completed GWAS for MS listed on GWAS catalogue and the latest IMSGC papers. (continued on next page)

Year	Study	Tested SNPs	Sample size	Identified SNPs
2007	Risk alleles for multiple sclerosis identified by a genome-wide study [38].	335k	931 trio families	6
2009	Genome-wide association analysis of susceptibility and clinical phenotype in multiple sclerosis [153].	552k	883 controls 978 case	11
2009	Meta-analysis of genome scans and replication identify CD6, IRF8 and TNFRSF1A as new multiple sclerosis susceptibility loci [153].	2.56m	7220 controls 2624 cases	16
2009	Genome-wide association study identifies new multiple sclerosis susceptibility loci on chromosomes 12 and 20 [154].	302k	3413 controls 1618 cases	9
2010	Genome-wide association study in a high-risk isolate for multiple sclerosis reveals associated variants in STAT3 gene [155].	297k	136 controls 68 cases	2

2010	Variants within the immunoregulatory CBLB gene are associated with multiple Sclerosis [156].	6.6m	872 controls 882 cases	2
2011	Genome-wide meta-analysis identifies novel multiple sclerosis susceptibility loci [157].	2.5m	12153 controls 5545 cases	19
2011	Genetic risk and a primary role for cell-mediated immune mechanisms in multiple sclerosis [33].	660k	17376 controls 9772 cases	57
2013	Analysis of immune-related loci identifies 48 new susceptibility variants for multiple sclerosis [151].	161K	24091 controls 14,498 cases	110
2013	Fine-mapping the genetic association of the major histocompatibility complex in multiple sclerosis: HLA and non-HLA effects	3613	9595 controls 5091 cases	11
2016	Novel multiple sclerosis susceptibility loci implicated in epigenetic regulation [158].	883K	10395 controls 4888 cases	15

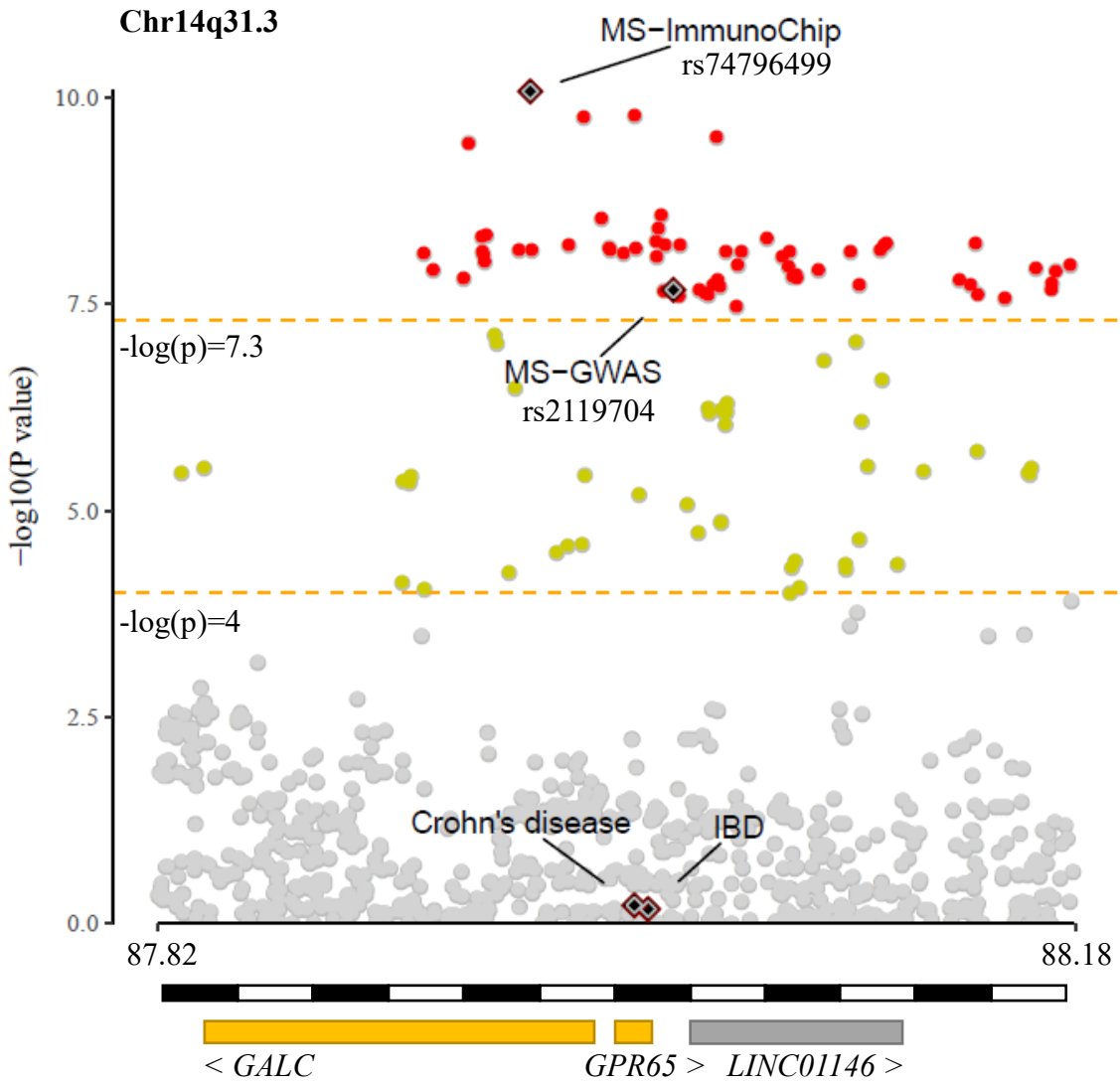

Figure 1. 1: Manhattan plot for the fine mapped region on chromosome 14q31.3 in the ImmunoChip study. The negative log p value of each SNP is plotted against the position on the chromosome. The horizontal dash lines indicate the GWAS significance threshold (-log (p) = 7.3) and the a priori discovery threshold in the ImmunoChip study (-log (p) = 4). Grey indicates –log (p) ≥ 4, yellow indicates –log (p) ≥ 4 and <7.3, while red indicates –log (p) ≤7.3. Full details can be found in ImmunoBase [151]. The figure was generated with help from my colleague Dr Wu.

1.4 GALC

1.4.1 The role of GALC in myelin metabolism

The *GALC* gene encodes the lysosomal enzyme β-galactosylceramidase, which plays an important role in the hydrolysis of specific galactolipids, including the otherwise non-degradable galactosylceramide (GalC) and galactosylsphingosine (psychosine) [159]. In the homozygous or compound heterozygous state, mutations in *GALC* that result in loss of function in β-galactosylceramidase lead to the development of Krabbe disease (also known as globoid-cell leukodystrophy, an autosomal recessive inherited neurodegenerative disorder) [160, 161]. More than 70 *GALC* gene mutations have been found in relation to the development of Krabbe disease. The crystal structure of GALC reveals that all parts of the protein contribute to the substrate binding site, which explains why the mutations causing Krabbe Disease are widely distributed across the gene [162].

GalC and its sulphate derivatives are essential components of the myelin produced by oligodendrocytes in the CNS [163] and lack of GalC in mice has been shown to alter oligodendrocyte maturation [164]. Psychosine, one of the potential breakdown products of myelin, is highly neurotoxic and has lethal effects [165]. Removal of psychosine is almost entirely dependent upon GALC such that this metabolite accumulates in patients with Krabbe disease and causes demyelination due to apoptosis of oligodendrocytes [166, 167]. This results from down-regulation of lipopolysaccharide (LPS) induced NF-kB and up-regulation of a pro-apoptotic AP-1 pathway by psychosine [168]. Many studies in the twitcher mouse model, a natural model of Krabbe disease, have shown psychosine induced apoptosis on glial cells and fibroblasts as well, however, only low level apoptotic cell death is seen in human lymphocytes [169-171]. On the other hand, a recent study found that the high psychosine concentration caused by GALC functional defects in the brainstem and spinal cord does not correlate with white matter loss or gliosis, suggesting that psychosine levels may not be the only factor responsible for demyelination [172].

1.4.2 The role of GALC in the immune system

Increased levels of proinflammatory cytokines and chemokines have been found in the CNS in Krabbe disease including increased levels of TNF-α, MIP-1β, MCP-1 and CD68 [173]. Furthermore, D-galactosyl-β1-1'-sphingosine (psychosine) and D-glucosyl-β1-1'-sphingosine, but not other lipids, are reported to induce chemotaxis and apoptosis of human NK cells in

vitro [174]. Also, both these glycosphingolipids have been shown to bind TDAG8 (GPR65) in mice. These results suggest a functional defect in GALC may alter GPR65 activity as a result of the accumulation of these particular glycosphingolipids, leading to an altered immune response.

A recent study investigating PBMCs from Krabbe patients found a low concentration (5 μM) of psychosine contributes to proinflammatory activation through increased TNF-α secretion, but that TNF-α was not affected at a higher concentration (20 μM) of psychosine [175]. These results suggest that in Krabbe disease, there is a proinflammatory activation of the immune system as well as psychosine induced glial cells apoptosis. In the twitcher mouse model elevated levels of IL-6 and TNF-α are seen in the CNS [176]. Interestingly, the IL-6 deficient mice also showed more severe Krabbe disease due to the damage or disruption of the blood-brain barrier, allowing T cells to cross over and attack myelin [177]. Disruption of the blood-brain barrier is one of the hallmarks of MS, and the role of GALC in this process needs to be explored further [178].

1.4.3 GALC and MS

Both Krabbe disease and MS are demyelinating diseases, however in MS the demyelination is a consequence of an autoimmune attack on myelin (see Chapter 1.1), while in Krabbe disease it is caused by the accumulation of toxic galactosylsphingolipid. There is no evidence to suggest that heterozygous carriers of Krabbe disease variants are at higher risk of developing MS.

Neither of the MS associated SNPs rs2119704 and rs74796499 are associated with Krabbe disease or any other complex trait. However, this region of the genome has also been linked to both Crohn's disease and ankylosing spondylosis (AS); the Crohn's disease associated variant rs8005161 ($p=1.3x10^{-8}$) [179] and the AS associated variant rs11624293 ($p=1.5x10^{-10}$) [180] being in complete LD ($r^2=1.0$) with each other, i.e. being perfect proxies for each other. This Crohn's disease/AS associated variant is not associated with MS, suggesting independent mechanisms for the two diseases.

1.5 GPR65

1.5.1 The function of GPR65

GPR65, a G protein couple receptor (GPCR), is a membrane protein containing 337 amino acids with a molecular mass of 39kD. It is predominantly found in lymph nodes, thymus and lymphoid tissues, including peripheral blood leukocytes [152, 181]. *GPR65* was first identified to be a gene through increased mRNA expression during T cell activation and thymocyte apoptosis with the treatment of anti-TCR (T cell receptor) antibody or glucocorticoid [181]. This study suggested that GPR65 may be involved in T cell apoptosis and thereby negative selection of immature thymocytes. However, another study showed that *GPR65* knockout mice had normal glucocorticoid induced thymocyte apoptosis [182].

Several studies have demonstrated that activation of GPR65 increases the intracellular second messenger cAMP (cyclic adenosine 5'-monophosphate) concentration and leads to triggering of the PKA (protein kinase A) signalling pathway [183-185]. In T cells, one the main effects of cAMP is to activate PKA, which disrupts lipid rafts in the plasma membrane and is thereby a negative regulator of T cell function [186-188]. A functional study showed cAMP induced PKA activity negatively regulates proximal TCR signalling by phosphorylation of tyrosine-protein kinase Csk (C-terminal Src kinase) and co-localizing with the TCR complex [189]. Elevation of cAMP also activates the transcription factor CREB (cAMP response element binding protein), leading to upregulation of cytokine expression including the anti-inflammatory cytokine IL-10 [190]. Recent studies also showed that activation of CREB by cAMP regulates FoxP3 expression to maintain the Treg phenotype [191, 192]. Furthermore, activation of GPR65 using a synthetic agonist BTB09089 has been shown to increase intracellular cAMP and thereby reduce production of IL-2, TNF-α and IL-6 [193]. Collectively, these studies suggest that activation of GPR65 regulates inflammatory cell activity, particular T cells and their cytokine production, through the cAMP/PKA pathway.

In addition in a cancer cell line investigators found a functional role for GPR65 in apoptosis in an acidic environment, with GPR65 upregulating anti-apoptotic bcl-2 in a manner dependent on mitogen-activated protein kinase/extracellular signal-regulated kinase (MEK/ERK) signalling pathway but independent of cAMP induced PKA [194]. In addition to cAMP/PKA and MEK/ERK pathways, GPR65 was also reported to be involved in actin reorganization through $G\alpha_{12/13}$ dependent activation of Rho [195].

1.5.2 Function of GPR65 in acidic microenvironment

GPR65, GPR4, OGR1 (GPR68) and G2A (GPR132) are all proton sensing receptors. At an acidic pH, proton transfer to the histidine residues in the first loop of GPR65 leads to a conformational change which alters function [196]. Mutations at amino acids 10, 14 or 243 (all histidine residues) have been shown to reduce the production of cAMP in acidic microenvironments and inhibits the proton-sensing response in an *in vitro* study. In mice the peak activation of GPR65 occurs when the extracellular environment is between pH 6.5 to pH 7.0 [181, 183]. Acidic microenvironments have been shown to increase the viability of eosinophils [185] and inhibit the production of proinflammatory cytokines including TNF-α in a cAMP and GPR65 dependent manner [197].

Given that inflammatory lesions are locally acidic the activation of GPR65 in acidic environments and its role in modulating immune function could have particular relevance in autoimmune diseases like MS [198]. Investigations in cancer, where the microenvironment within tumors is frequently acidic, have shown that GPR65 activity influences the development and growth of tumors. Overexpression of GPR65 in mouse lewis lung carcinoma cells promotes growth and resistance to acidification induced cell death by cAMP/PKA and ERK related pathways *in vitro* [199]. Similarly knockdown of *GPR65* in NCl-H460 human non-small cell lung cancer cells reduce the cells viability in an acidic environment [199]. On the other hand, GPR65 has also been reported to act as a tumor suppressor by reducing the expression of c-Myc oncogene in human lymphoma cells under acidosis [200], and expression of *GPR65* mRNA is decreased by 50% in human lymphoma samples in comparison to non-tumor lymphoid tissues [200].

1.5.3 GPR65 is a psychosine receptor

Interestingly it has been shown that psychosine and several related glycosphingolipids, including Lac-psychosine and lysosulfatide, are ligands for GPR65 [201]. However, the data regarding how these moieties affect GPR65 and consequently immune function is inconsistent. In a *GPR65* transgenic mouse activation of GPR65 with psychosine was shown to inhibit glucocorticoid induced cytokine production [201, 202]. However, other investigators saw no effect of psychosine on the immune system or glucocorticoid induced thymocyte apoptosis [182]. It has also been shown that the inhibitory effects of GPR65 induced by acidity can be antagonised by psychosine [183].

1.5.4 GPR65 and autoimmune diseases

Few studies have examined the function and expression of GPR65 in humans, but as described in Chapter 1.3, genetic variants in the region of *GPR65* are associated with MS [33], Crohn's disease [179, 203] and ankylosing spondylitis [180]. In mice the gene has been suggested to play a role in T cell mediated disease [152] and *GPR65* knockout mice show an enhanced tendency to develop anti-collagen type II antibody induced arthritis [193, 204, 205]. In addition, more severe induced adoptive transfer of delayed type hypersensitivity to methylated bovine serum albumin (BSA) has been observed in *GPR65* deficient transferred mice, but not in *GPR65* deficient recipient mice [206]. Finally, knocking down *GPR65* or carrying the *GPR65* Crohn's disease risk allele has been suggested to lead to increased lysosomal pH, resulting in impaired clearance of intracellular bacteria and accumulation of aberrant lysosomes [203]. *In vitro*, naive GPR65 deficient T cells differentiated 40% fewer IL-17A-producing cells, with a similar reduction observed in IL-23 treated memory cells. In the absence of GPR65 in T cells, mice are protected from EAE [207]. Furthermore, ChIP-Seq analysis indicated RORγt, the master transcription factor for Th17 cells, binds the promoter region of *GPR65* [208]. These data all suggest that GPR65 may influence the development of MS by altering Th17 cells.

1.6 Preliminary assessment of GALC and GPR65

In a pilot study my predecessor in the lab, Dr Tom Button, investigated the relationship between T cell activation and genotype at the MS associated SNP (rs2119704) at varying pH (7.0 - 7.4); the results of which are shown in Fig 1.2. His results suggested that rs2119704 genotype influenced T cell activation at pH levels below the normal physiological level. Given the known acid sensing function of GPR65 it seemed reasonable to hypothesize that genotype dependent variation in GPR65 function might underlie these observations.

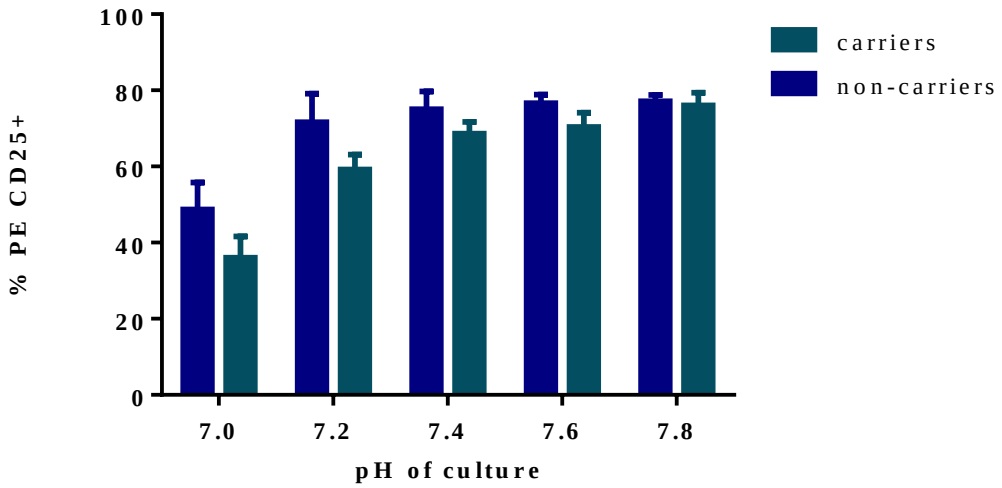

Figure 1. 2: Lymphocyte activation at varying pH in wild type homozygote and heterozygote individuals. Activation is measured after anti CD3/CD28 stimulation in terms of the % of CD25 positivity. Carriers of the protective allele (n = 5) and non-carriers (n = 9) are compared at the pH range 7.0-7.8. Figure generated by Dr Tom Button.

1.7 Summary

Although the genetic analysis of multiple sclerosis has identified over two hundred associated variants little is known about how these exert their effects on risk and result in the development of the disease. The association with rs74796499 on chromosome 14q31.3 implicates two interesting genes *GALC* and *GPR65,* both of which have the potential to be relevant in the pathogenesis of MS. The LD flanking the minor protective allele at rs74796499 implicates a range of variants over the region containing these genes, including a synonymous splice region variant in *GALC* (rs11552556). Other independent haplotypes in the region are associated with susceptibility to Crohn's disease and AS but the haplotype containing the minor allele at rs74796499 appears to exert an MS specific effect. Based on the preliminary results observed by my predecessor Dr Tom Button I decided to focus my efforts to understand this association on *GPR65*, as this acid sensing receptor seemed more likely to underlie an acid specific genotype dependent effect. It seemed to me that GALC was less likely to be relevant since there is no evidence that any of the loss of function mutations underlying Krabbe disease have any effect on the risk of MS.

Chapter 2: Materials and Methods

My research was approved by the South Central – Berkshire National Research Ethics Service (NRES) Committee (study reference number 15/SC/0087) and all study subjects gave fully informed written consent. The experimental procedures I used in my research are detailed below.

2.1 Human PBMC isolation and cell separation

Venous blood from healthy human individuals was collected in heparin tubes (Sarstedt, Germany) by research nurses and transferred to the lab where peripheral blood mononuclear cells (PBMCs) were isolated using Ficoll-Paque (GE Healthcare, UK) density gradient centrifugation. Collected cells were then washed twice in sterile phosphate-buffered saline (PBS) solution and counted using a Brightline haemocytometer (Hausser Scientific, US), with viability assessed using trypan blue dye exclusion (Sigma, UK).

Mononuclear cells were then suspended in magnetic activated cell sorting (MACS) buffer and positively separated using either CD56+ MACS MicroBeads and/or CD3+ MicroBeads (Miltenyi Biotec, UK) to isolated NK/NKT cells and T/NKT cells respectively. Cell separation was completed using the autoMACS Pro Separator (Miltenyi Biotec, UK) according to the manufacturer's protocol. For each subject, the remaining cells (CD56- and CD3- cells) and an aliquot of the separated T cells and NK cells (up to 1.5x 10^7 cells of each) were rapidly resuspended in 1 mL TRIzol reagent (Ambion, US) and stored at -80°C prior to DNA and RNA extraction.

2.2 Immunocytochemistry (ICC)

Freshly isolated human PBMCs were isolated by autoMACS Pro Separator into three groups: T cells (CD3+); NK cells (CD3- CD56+) and the remaining fraction a B cells and monocytes enriched population (CD3- CD56-) and fixed with 4% paraformaldehyde (PFA) for 15 min and then washed twice with PBS. Cells were then spread on a polysine-coated microscope slide and dried for 2 hours at room temperature followed by blocking with ICC blocking buffer for an hour at room temperature. Sections were then immune-labelled using rabbit anti-GPR65 antibody diluted 1 in 100 followed by the Alex Fluor 647 labelled polyclonal donkey anti-rabbit antibody (1 in 1000 dilution) provided by Prof Robin Franklin group. Cells were also stained with DAPI (4', 6-diamidino-2-phenylindole), a fluorescent stain, that selectively binds

nuclei with limited background of cytoplasm. Sections were coverslip mounted and imaged using an Axio Observer inverted microscope (Zeiss, Germany) at a magnification of x20.

2.3 Pierce bicinchoninic acid (BCA) protein assay

Protein concentration was determined using the Pierce BCA protein assay kit (Thermo Fisher, UK) completed according to the manufacturer's protocol. Unknown concentrations were determined using a plate specific standard curve created by serially diluting (1 in 2 dilution) a 2 µg/µL standard down to 15.625 ng/µL. Standards and samples were processed on a 96-well plate and gently shaken to mix reagents. The plate was incubated at 37°C for 30 min, then read on a micro plate reader (Bio-Rad). The average blank-corrected 562nm absorbance measurement of each serially diluted sample was used to create a standard curve. The concentration of unknown technically triplicated samples was calculated using the standard curve method.

2.4 Western blot

For each sample a total of $5x10^6$ cells were washed in PBS and centrifuged for 10 min at 300g. Cells were lysed on ice with cell lysis buffer followed by sonication. 20 or 30 µg protein from each sample and 10 µL prestained protein ladder (Bio-Rad, UK) were loaded onto a NuPAGE Novex Bis-Tris gel (Thermo Fisher, UK). Protein was transferred to a polyvinylidene difluoride (PVDF) membrane at 30V for 1 hour using the XCell Blot Module followed by blocking the membrane in 5% (w/v) non-fat dry milk in PBS-T for 1 hour at room temperature. The membrane was incubated with primary antibodies overnight at 4°C with gentle shaking. The membrane was then washed with PBS-T three times followed by incubation with or without Horseradish peroxidase (HRP) conjugated secondary antibodies (Dako, Glostrup Denmark) for 2 hours. The bound antibodies were detected by using HRP substrate ECL plus detection reagent (GE Healthcare, UK) and visualised using the ChemiDoc XRS+ Systems (Bio-Rad, UK). Protein expression was normalized to the loading control protein using Imagine J (version 1.49) analysis software.

Protein dephosphorylation

Dephosphorylation of tyrosine, threonine and serine residues in sample proteins was achieved by incubating protein lysate with Lambda protein phosphatase (New England Biolabs, UK) for

2 hours at 30°C. The enzyme was then inactivated by heating with Na_2EDTA for 1 hour at 65°C. Samples were then assessed by Western blot with anti-GPR65 antibody.

Protein deglycosylation

To remove cross-linked glycans, the protein deglycosylation mix kit (New England Biolabs, UK) was used under denaturing and non-denaturing conditions. For denaturing conditions 100 µg of sample protein was mixed to 10x glycoprotein denaturing buffer followed by heated to 100°C for 10 min and cooled down prior to the addition 10x glycoprotein denaturing buffer and deglycosylation enzyme cocktail. For non-denaturing condition, 100 µg of sample protein was directly mixed with deglycosylation enzyme cocktail gently. Both reactions were incubated at 37°C for 4 hours. The deglycosylated reactions were assessed by Western blot with the same GPR65 antibody used as described above.

2.5 Protein complex immunoprecipitation (Co-IP) and Mass Spectrometry analysis

Co-IP

In order to undertake Co-IP 10 µg of commercial GPR65 specific antibody were firstly combined with 1.5 mg of Pierce protein A/G magnetic beads (Thermo Fisher, UK). The mixture was washed with binding/wash buffer and Dynabeads labelled antibody collected with a magnetic stand. The Dynabeads labelled antibody was then added to protein lysates and the resulting precipitates collected. Elution buffer was added and incubated for 2 min with rotation to dissociate the Dynabeads from complexes. The Dynabeads were then removed from the antibody protein complexes using a magnetic stand.

Coomassie staining

Coomassie brilliant blue R-250 (Sigma, UK) was used to stain protein samples after electrophoretic separation in a Bis-Tris gel. The gel was incubated in 0.1% coomassie staining buffer for 1 hour in a sealable container with gentle shaking at room temperature. The gel was then washed and incubated in a de-staining buffer for 4 hours to remove excess staining buffer.

Mass spectrometer

The mass spectrometry analysis was performed by Cambridge Centre for Proteomics. The sample peptides were separated by high-resolution nanoscale chromatography. The mass

accuracy tandem mass spectra (MS/MS) were then acquired automatically. The results were then compared against all the entries in the latest NCBI database (Release number 211) to generate Mascot histograms.

2.6 siRNA transfection

GPR65 knockdown was attempted using the human T cell Nucleofector kit (Amaxa Lonza, USA). Specially, in each experiment 100 µL of transfection reagent was used to process $1x10^7$ freshly separated PBMCs.

To test the efficiency of the knockdown in human T cells, initial experiments were completed using a positive control pmax green fluorescent protein (pmaxGFP) vector to test the nucleofector programs. Cells were transfected using 2 nM pmaxGFP, and processed using electroporation programs U-014 or V-024 on a Nucleofector 2b device. Cells were then incubated in DMEM for 5 hours at 37°C in 5% CO_2, harvested and incubated again with anti-CD3 plus anti-CD28 antibodies for a further 18 hours. Flow cytometry was used to detect the expression of GFP. The efficiency of knockdown was expressed as the percentage of GFP expressing T cells.

2.7 DMEM pH measurement and adjustment

Dulbecco's Modified Eagle Medium (DMEM) was adjusted to the required pH (ranging from pH 6.2 to pH 7.6) with sodium bicarbonate (Sigma, UK) prior to cell culture in a 5% CO_2 humidified environment. The mass of bicarbonate needed to adjust the DMEM to the desired pH was calculated according to the Hendersion-Hasselach equation. Osmolality was balanced using sodium chloride (Sigma, UK). The pH pre-adjusted DMEM was then filtered with a 0.22 micron filter (Merck Millipore, Germany) and stored in a sterile environment at 4°C. To ensure the pH of the medium was maintained and consistent, the pH was pre-checked after incubation overnight with or without cells prior to use in the experiment. The pH value at 37°C were recorded using Orion Star A121 pH meter (Thermo Fisher, UK) with a precision of ± 0.05.

Hendersion-Hasselach equation:

$$\mathrm{pH} = 6.1 + \log\left(52 \times \frac{\mathrm{mg/mL\ NaHCO3}}{\%\mathrm{CO2}} - 1\right)$$

2.8 Cell culture

All cell cultures were undertaken in pre-made DMEM at 37°C in a humidified atmosphere containing 5% CO_2. In initial experiments designed to establish the conditions required to ensure stable extracellular pH throughout the period of culture, different cell numbers (0.5 or 1 x 10^6), culture plates (48-well or 96-well flat bottom plates, Nuclon, US), culture volumes (0.5 mL or 0.2 ml) and cell cultured medium (DEME or RPMI) were tested. Stimulation was performed using plate bound anti-CD3 and soluble anti-CD28 antibodies (Affymetrix eBioscience, US) at a final concentration of 1 µg/mL, or with Dynabeads™ Human T-Activator CD3/CD28 (Gibco by Life Technologies, US) at the same final concentration. To establish the length of culture needed to reach maximal T lymphocyte activation, the expression of CD25 and CD69 was measured at 6, 24, 32, 48, 56 and 72 hours following activation with plate bound anti-CD3/CD28 antibodies, at differing pH values.

T cell activation

Anti-CD3 antibody was incubated in 48-well flat bottom plates for 2 hours at the concentration of 1 µg/mL. Plates were then washed with PBS twice to remove unbound antibodies. The soluble anti-CD28 antibodies were added in and used to stimulate 1x10^6 PBMCs at final concentration of 1 µg/mL. Cells were then incubated for 18 hours for full T cell activation.

GPR65 functional assay

Previous studies have shown the synthetic molecule BTB09089 (Maybridge, UK) is a specific agonist of GPR65. Dimethyl sulfoxide (DMSO) was used to solubilise BTB09089. To investigate the impact of DMSO on T cell subtypes and T cell activation, a DMSO concentration titration experiment (ranging from 0 µM to 50 µM) was performed and proportion of T cell subtypes and T cell activation measured by flow cytometry. To determine the specific action of GPR65, 1x10^6 PBMCs were seeded onto an anti-CD3 coated plus soluble anti-CD28 48-well culture plate with DMEM at pH 6.2, pH 7.0 and pH 7.6 containing 20 µM BTB09089 and incubated for 18 hours. Activation of T cells, NKT cells and NK cells were measured by CD25 and/or CD69 expression using flow cytometry.

2.9 Flow cytometry

Cells were collected and washed twice in PBS. Fixable viability dye (eBioscience, US) were used for live/dead staining, diluted with PBS to a concentration of 1 µg/mL and incubated with

cells for 30 min. Cells were then washed twice with PBS and transferred to 96-well U-shape bottom plates (Corning, US). Cells were blocked with FACS buffer containing 2% mouse serum for 15 min, and labelled with fluorescent conjugated antibodies by incubating for 20 min at 4°C. The panel of fluorochrome antibodies used in each experiment is described in the respective chapters. Each antibody was titrated to determine the optimal concentration for flow cytometry. Annexin V Apoptosis Detection kit (eBioscience, UK) was used for labelling early apoptotic cell. Cells were washed with binding buffer and incubated with fluorochrome-conjugated Annexin V diluted with binding buffer at a concentration of 50 μg/mL for 15 min at room temperature. The binding buffer were then used to wash and remove the excess Annexin V. Cell fixation was performed with 100 μL 2% PFA incubated for 20 min at 4°C. Compensation matrices were created using single-stained cells or anti-mouse compensation particles (BD Bioscience, US) for each fluorochrome. Cells were then resuspended in 500 μL of FACS buffer for flow cytometry analysis. All flow cytometry was performed on the Fortessa II (BD Bioscience, US) and a total of 20,000 gated lymphocytes were recorded.

2.10 Flow cytometry gating strategy

The flow cytometry data were analysed using FlowJo software (version 10). Unstained controls were used to define negative gates (thresholds), except for the work described in Chapter 8 when fluorescence minus one (FMO) controls were used to define the LacCer and CD69 thresholds. In initial experiments I performed I found no significant difference using unstained controls, FMO controls or isotype controls. The gating strategy was outlined in Figure 2.1 and 2.2.

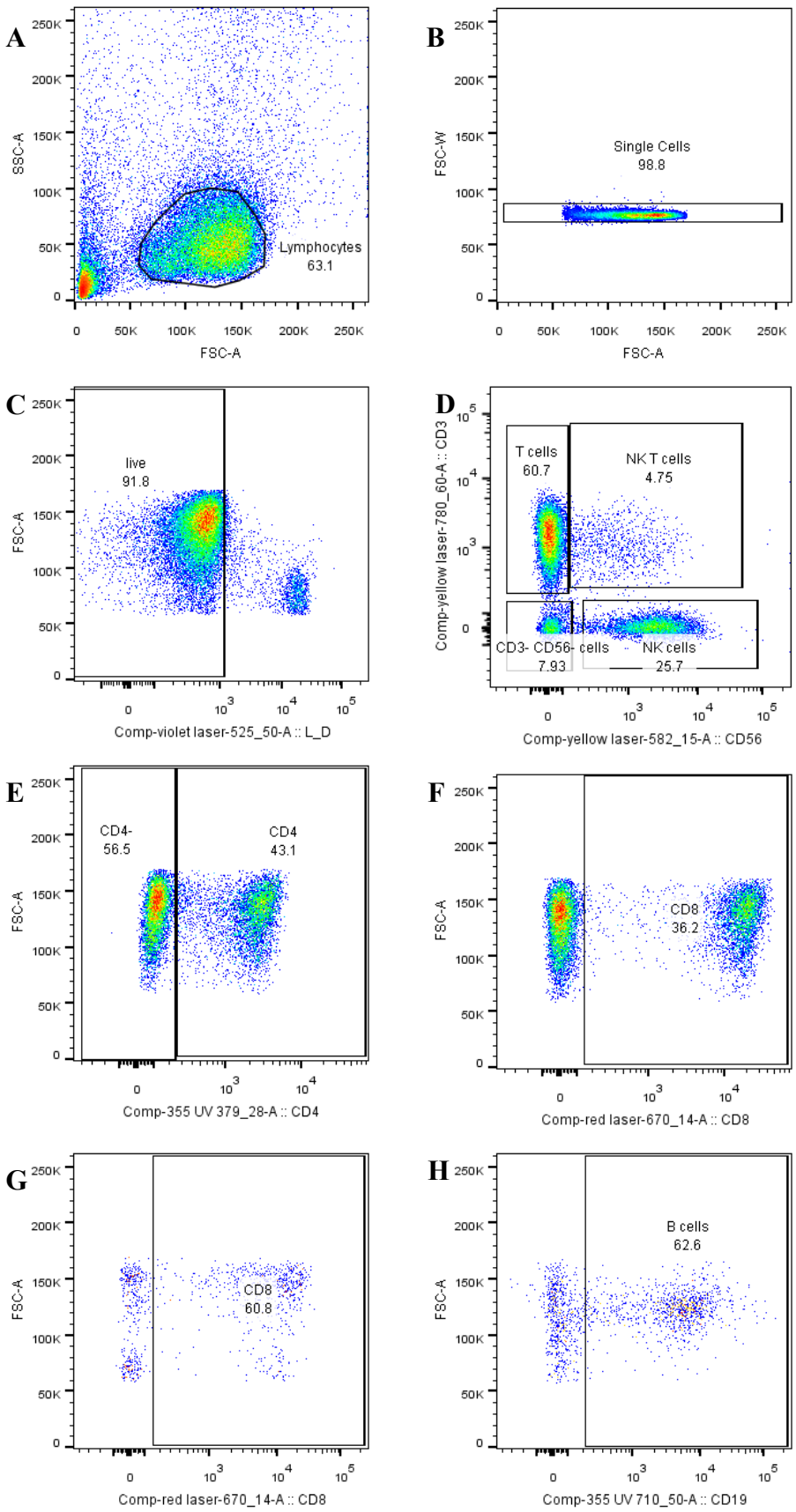

Figure 2. 1: Example analysis of human PBMC. **A**, FSC/SSC (lymphocyte gate). **B**, SCW/FSC (singlet gate). **C**, FSC/live/dead stain (live cell gate). **D**, CD3-PE-Cy7/CD56-PE (T cells, CD3-

CD56- cells, NKT cells, NK cells). **E**, FSC/CD4-BUV395 in T cells (CD4+ T cells). **F**, FSC/CD8-APC in T cells (CD8+ T cells). **G**, FSC/CD8-APC in NKT cells (CD8+ NKT cells). **H**, FSC/CD19-BUV737 in CD3- CD56- cells (B cells).

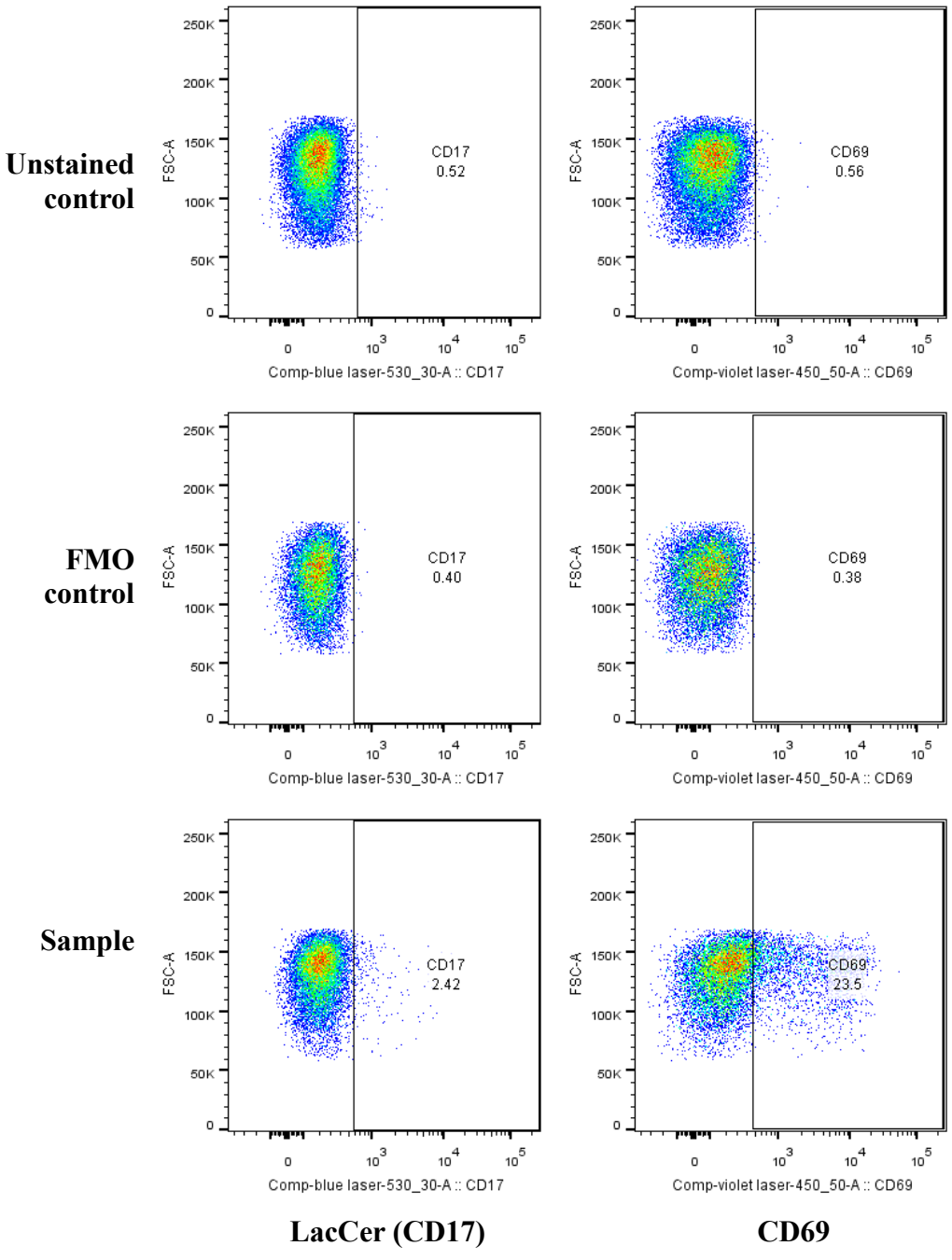

Figure 2. 2: Example of LacCer and CD69 negative gates in human cultured T cells. A total of 20,000 lymphocytes were collected and analysed as described above. LacCer and CD69 thresholds were presented on gated T cells in unstained controls, FMO controls and samples.

2.11 Lysosomal pH measurement

The LysoSensor Green DND-189 dye (Invitrogen, US) was used to measure intracellular pH. For this T cells (CD3+), monocytes (CD14+), B cells (CD19+ CD3- CD56-) NKT cells (CD3+ CD56+) and NK cells (CD3- CD56+) were labelled using appropriate antibodies then incubated with 1 µM LysoSensor Dye for exactly 5 min. After two washes with FACS buffer, the mean fluorescence intensity (MFI) was measured by flow cytometry and analysed by FlowJo software (version 10). Values were normalised against the antibodies bound to Compbeads (BD Bioscience, US) which were used as a positive control for each experiment. The incubation time and the dye concentration were optimized in initial experiment set up described in Chapter 7.2.

2.12 DNA/RNA extraction

Trizol was used for DNA/RNA extraction following the manufacture's protocol. Trizol stored samples were allowed to defrost to room temperature for 5 min to permit completely dissociation of the nucleoprotein complex. 200 µL chloroform was added in each homogenized sample followed by shaking and centrifugation to separate the mixture into a lower red phenol-chloroform phase, a DNA contained interphase and a colourless RNA contained upper aqueous phase.

RNA isolation

The RNA contained aqueous phase was transferred to a new eppendorf and mixed with 500 µL isopropanol and then incubated on ice for 30 min. Samples were then centrifuged at 12,000 g for 15 min at 4°C to precipitate RNA as a pellet. After washing with 1 mL 75% ethanol and air-drying for 5 min, RNA was then resuspended in RNase-free water at 55°C – 60°C. The concentration of RNA was measured using spectrophotometry.

DNA isolation

The phenol-chloroform phase and the DNA contained interphase were mixed with 100% ethanol by gentle shaking. Normally the DNA pellets became visible. Samples were then centrifuged and organic phenol-chloroform phase stored at -80°C for protein analysis. The DNA pellets were then washed twice with 0.1 M sodium citrate buffer then stored in 75% ethanol for a week. Finally, the DNA was dissolved in DNase-free water at 4°C.

Spectrophotometry

DNA and RNA concentration were measured and calculated from the absorbance at 260 nm using a Nanodrop ND-1000 spectrophotometer (Thermo Scientific, US).

2.13 DNase treatment and clean-up

DNase I (Invitrogen, UK) was used to remove any contaminating genomic DNA (gDNA) from the RNA samples. One unit of DNase I enzyme was used for each 1 µg RNA with the proprietary reaction buffer, the mixture being incubated for 30 min at 37°C. The same amount of 50 mM EDTA (Ethylenediaminetetraacetic acid) was added as an exonuclease inhibitor and incubated for 15 min at 65°C to terminate the reaction. DNase I treated sample was purified and concentrated using RNeasy MinElute Cleanup kit (Qiagen, Germany) according to the manufacturer's instructions. RNA was eluted in RNase/DNase free water.

2.14 Bioanalyzer for RNA integrity number

RNA quality was examined by capillary electrophoresis using the Agilent 2100 Bioanalyzer system (Agilent Technologies, US) according to the manufacturer's protocol. The RNA integrity number (RIN), an algorithm for assigning the RNA integrity, was automatically calculated and generated within Agilent 2100 Expert software (Agilent Technologies, US) [209]. RIN values range from 1 to 10, with 10 being the highest quality of RNA. In general, the electropherogram for a typical sample shows a small 5S peak, a larger 18S peak and a 28S peak (Figure 2.3). As 28S ribosomal RNA (rRNA) tends to be degraded more quickly than 18S rRNA, the ratio of the area under the 18S and 28S rRNA peak provides a measure of the

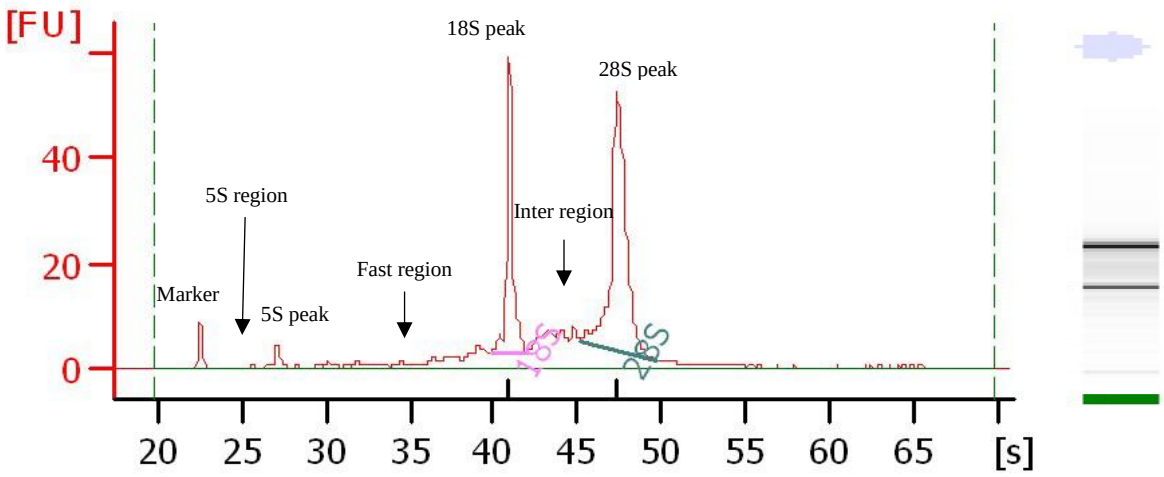

Figure 2. 3: An example of the Bioanalyzer electropherogram and computer modelled gel plots.

degradation of rRNA. An aliquot of 2 µL RNA were taken for concentration measurement and Quality control. All samples analysed had a RIN > 8.0.

2.15 cDNA synthesis

I used the SuperScript™ III First-Strand Synthesis System (ThermoFisher, US) which contains SuperScript III reverse transcriptase, Oligo-dT and random hexamers to synthesise cDNA in accordance with the manufacturer's instructions. In this 1 µg of cleaned-up RNA was mixed with the cDNA synthesis kit regents (Table 2.1) and processed according to the manufacturer's instruction (see Table 2.2 for more details). Samples were finally collected and chilled in an ice block then stored at -20°C.

Table 2. 1: cDNA synthesis reagent mixture

	Components	Volume for each reaction
Mixture A		
	10 mM dNTP mix	1 µL
	50 µM oligo (dT)	0.5 µL
	Random Hexamer	0.5 µL
	RNase free water	Top up to 13 µL
Mixture B		
	5x First Strand Buffer	4 µL
	0.1 M DTT	1 µL
	RNaseOUT (40 U/ µL)	1 µL
	SuperScript III RT (200 U/ µL)	1 µL

Table 2. 2: cDNA Reverse Transcription Kit Reagents and thermal cycle program.

Step	Temperature	Time	Reagents for each reaction
1	65°C	5 min	Mixture A and RNA sample
2	25°C	60 min	Added Mixture B
3	50°C	10 min	
4	70°C	15 min	
storage	-20°C	∞	

2.16 quantitative PCR

Gene expression was assessed by quantitative PCR (qPCR) of cDNA from either ex-vivo NK (CD56+) /non-NK cells or T (CD3+) /non-T cells. These reactions were performed in 384 well-plates, with each reaction containing 2 µL cDNA, 20x pre-designed primers (Table 2.3), 2x Universal Master Mix (Life Technologies, US) made up to 10 µl with DNase/RNase free water. The relative abundance of cDNA was determined in triplicate by qPCR analysis using the QuantStudio 7 Flex system (Applied Biosystems, US) and standard Taqman program (Table 2.4). Each gene was normalized to the housekeeping gene *β-ACTIN* prior to calculation of the relative expression in order to correct for variation in cDNA concentrations.

Quantification of the expression of target genes

The relative standard method was used to calculate and compare the target gene expression. The standard curve is generated by qPCR of a 5 folds serial dilution of a stock cDNA with the Ct (cycle threshold) determined for each dilution. The quantity of target genes and housekeeping gene *β-ACTIN* (endogenous control) were calculated by interpolating from the standard curve followed by normalization to their housekeeping gene (see equation below). The normalized target genes were compared by genotypes.

The relative gene expression:

$$\textbf{Normalized target gene expression} := \frac{\text{Target}}{\text{Housekeeping gene}}$$

Table 2. 3: qPCR primers

Primer	Amplicon (bp)	Hs assay code	Vender
β-ACTIN	171	Hs99999903	Life Technologies
CD69	94	Hs00156399	Life Technologies
GALC	82	Hs01012300	Life Technologies
GPR65	86	Hs01087326	Life Technologies
GPR65	124	Hs00269247	Life Technologies
RORC	62	Hs01076112	Life Technologies
LINC01146			Provided by Dr Ban

Table 2. 4: qPCR program

Step	Temperature	Time	Cycles
Initial denaturation	95°C	10 min	
Denaturation	95°C	15 sec	Repeat these 2 steps for 40 cycles
Annealing	60°C	1 min	
Hold	4°C	∞	

2.17 Genotyping

Genotyping was performed in 384 well-plates with 25 ng of dried down genomic DNA in each well. A total of 5 µL of genotyping PCR reaction mix was then added to each well; consisting of 1x Taqman genotyping Master Mix, 0.5x primer/probe mix made up to 5ul with DNase-free water. The target SNPs were genotyped in duplicate using the pre-designed primers (Life Technologies, US) listed in Table 2.5. The genotyping PCR program (Table 2.6) was run and read on the QuantStudio 7 Flex system (ThermoFisher, US). Quantstudio software was used to determine genotypes. Observed allele frequencies were comparable to those seen in the 1000 Genomes Project Phase 3.

Table 2. 5: Genotyping primers.

SNP	Genotype	Sequence
rs11052877 C_32169538	CD69	TAGTACCAACATCTAACTCCTTCCA[A/G]TAGTGC AAATGCATGAAGGGCTCTC
rs17785991 C_33663616	SLC9A8	TCCATATTCAGATCTCTGATGTTCT[A/T]GTCACC AAACCATTTACTTTTTCCT
rs28533072 C_63304041	GALC	TCTGTTTTTGTCCCAGGAACTTTAT[C/T]ACCCTG AATCTACCTACAATATCCT
rs3742704 C_1928640	GPR65	GAGAATCATAAAACTACTTGTCAGC[A/C]TCACA GTTACTTTTGTCTTATGCTT
rs3943657 C_27507588	GPR65	GTTTGTGTTTCTTATGTTTCTTAAT[G/T]ATAATCT TTTTCTTTTGAAAAGCAA
rs6020055 C_2701156	B4GALT5	GTGCTTGTGACCTGCAACACTCAGT[A/G]ACTGC CAGTCATCTTTCATAAACTA

rs666930 C_970234	PHGDH	GTGAAGAGACTACAGCATAAATCTT[C/T]ACAAG GGAGATCCATCCAGAGAGTC
rs74796499 C_104289723	GPR65	CAAATAAAGGCTTTGTGCATACCTA[A/C]TTTCCT TTCAACAGTCAGCCTTCTT

Table 2. 6: PCR program for genotyping

Step	Temperature	Time	Cycles
Initial denaturation	95°C	10 min	
Denaturation	95°C	15 sec	Repeat these 2 steps for 40 cycles.
Anneal	60°C	1 min	
Final extension	60°C	30 sec	
End Plate read			

2.18 Buffers and mediums

All buffers and media used in the experiments are outlined in Table 2.7.

Table 2. 7: List buffers and mediums

Buffer/Media	Components	Manufacturer
Cell lysis buffer	RIPA buffer	Sigma
	Mini proteinase inhibitor cocktail	Roche
Coomassie de-stain buffer	200 mL methanol	Sigma
	100 mL glacial acetic acid	Fisher Chemical
	700 mL Millii-Q-H_2O	
Coomassie staining buffer	1g coomassie R250	Sigma
	400 mL methanol	Sigma
	100 mL glacial acetic acid	Fisher Chemical
	500 mL Millii-Q-H_2O	
DMEM	13.7g DMEM	Sigma
	1 L Milli-Q-H_2O	
	1 M HCL/ 1 M NaOH for pH adjustment	Sigma
	NaCl for osmolarity adjustment	Sigma

FACS Buffer	1x PBS 0.1% BSA 0.01% sodium azide	Fisher Scientific Millipore Sigma
Fixing buffer	2% paraformaldehyde in PBS/FACS buffer	Sigma
Immunocytochemistry dilution buffer	1x PBS 1% BSA 1% normal donkey serum 0.3% Trition X-100 0.01% sodium azide	Fisher Scientific Millipore Sigma Sigma Sigma
Immunocytochemistry blocking buffer	10% normal donkey serum 0.3% Triton X-100	Sigma Sigma
Loading buffer	NuPAGE 4x LDS sample buffer	Invitrogen
MACS Buffer	1x PBS 2 mM EDTA 2% BSA	Fisher Scientific Fisher Scientific Millipore
PBS-T	1x PBS 0.1% Tween-20	Fisher Scientific Sigma
RPMI	RPMI medium 1640	Life Technologies
Running buffer	NuPAGE 20x MES SDS running buffer	Invitrogen
0.1M Sodium citrate buffer	14.7 g 1 M Sodium citrate 50 mL ethanol 450 mL Millii-Q-H_2O	Sigma Sigma
Transfer buffer	20% Methanol NuPAGE 20x transfer buffer	Sigma Invitrogen
TBS buffer (10x)	24.23g Tris-HCl 5.6g Tris-Base 87.66g NaCl 1 L Millii-Q-H_2O 1 M HCL for pH adjustment	Sigma Sigma Sigma Sigma

2.19 Antibodies and dyes

All antibodies used in Western blot, Immunocytochemistry and immunoprecipitation (Co-IP) are in Table 2.8. All antibodies and dyes used in flow cytometry are listed in Table 2.9.

Table 2. 8: List of antibodies for immunocytochemistry, Western blot and Co-IP.

Application	Target	Immunogen	Host	Vender
Immunocytochemistry	GPR65	36-51	Rabbit	Abcam
Western blot; Co-IP	GPR65	245-275	Rabbit	Abcam
Western blot	GPR65	72-89	Rabbit	Bioss Antibodies
Western blot	GPR65	238-267	Rabbit	LifeSpan BioSciences
Western blot; Co-IP	β-actin	1-100	Mouse	Abcam
Western blot	Cofilin	150-C-terminus	Mouse	Abcam
Western blot	Tubulin	Full length	Mouse	Abcam

Table 2. 9: List of antibodies and dyes for flow cytometry.

Marker	Fluorochrome	Clone	Manufacturer
Annexin V staining	FITC		eBioscience
CD3	PE-Cy7	SK7	BD Bioscience
CD4	v500 BUV395	RPA-T4	BD Bioscience BD Bioscience
CD8	APC	RPA-T8	BD Bioscience
CD14	APC	M5E2	BD Bioscience
CD17 (Lactosyleramide)	FITC	Huly-m13	LifeSpan BioSciences
CD19	BUV737	SJ25C1	BD Bioscience
CD25	FITC	M-A251	BD Bioscience
CD56	PE	B156	BD Bioscience
CD69	v450	FN50	BD Bioscience
Fixable far red dead stain	APC-Cy7		Life Technologies
Fixable Viability Dye	eFluor 506		eBioscience
TCR Vα24-Jα18 (iNKT cell)	PerCP/Cy5.5	6B11	Biolegend

Chapter 3: Alternate attempts to characterise GPR65

3.1 Introduction

In this chapter I will describe a number of antibody based approaches which I attempted to employ but did not have sufficient time to adequately optimise and was therefore unable to utilise. Each of these methods had the potential to quantify important characteristics of GPR65 protein expression which I had hoped to correlate with genotype. However, in each case my pilot efforts revealed that considerable time and resources would be required to establish a reliable assay, I therefore decided to focus my effort primarily on pH dependent functions and did not employ these methods further in my search for genotype dependent biology.

Since 1975 when Kohler and Milstein described their hybridoma based technique for producing monoclonal antibodies, the exquisitely specific binding properties of these agents has been extensively used in the study of protein expression [210, 211]. Numerous biopharmaceutical companies now provide a wide range of protein specific monoclonal antibodies which in principle enable the localisation and quantification of protein expression to be studied in great detail. It seemed logical to begin my analysis of GPR65 using an antibody based approach to examine protein expression and quantification. Unfortunately, despite the fact that GPR65 has been recognised since the 1990s, only polyclonal GPR65 antibodies are currently available; furthermore, there are no published papers validating or describing the use of any of these antibodies. I had hoped to find a monoclonal antibody recognizing a unique GPR65 epitope in order to minimise non-specific binding and maximise specificity. The mouse anti-GPR65 monoclonal antibody previously produced by TransGenic (CABT-19961MH, Creative BioMart; KX443) has been discontinued. The currently available polyclonal antibodies are listed in Table 2.9 in Chapter 2. Each was generated in rabbit by immunization with a KLH (keyhole limpet hemocyanin; the most common peptide carrier for immunization) conjugated synthetic peptide sequence from the C-terminal end of human GPR65, and purified by protein A antibody-binding ligands.

There are no published data describing the expression of GPR65 at the protein level. However, at the level of transcription *GPR65* has been shown to be expressed in lung, spleen, liver, bone marrow and immune cells; with transcription being particularly high in thymocytes and NK cells (Data available in the human protein ATLAS website: https://www.proteinatlas.org/). In mice, the transcription of *GPR65* is rapidly induced by glucocorticoids (GC) [182]. In this

context, it seemed logical to attempt to use the available polyclonal antibodies to establish the expression profile of GPR65 at the protein level, with a view to subsequently exploring the influence of genotype and extracellular pH on this expression.

3.2 Results

3.2.1 Immunocytochemistry

In an attempt to determine the expression of GPR65 at the protein level in human leukocyte subtypes, I performed immunocytochemical staining of freshly isolated T cells (CD3+), NK cells (CD3- CD56+), CD3- CD56- cells, and total PBMCs from two healthy individuals using the Abcam polyclonal anti-GPR65 antibody (Figure 3.1). These studies showed heterogeneous staining in each cell type, with the highest frequency of intensely expressing cells seeming to occur in the CD3- CD56- population. The low-resolution microscope used to image the staining did not allow accurate localisation of the antibody staining relative to the DAPI nuclear staining but suggested surface or cytoplasmic staining rather than nuclear staining.

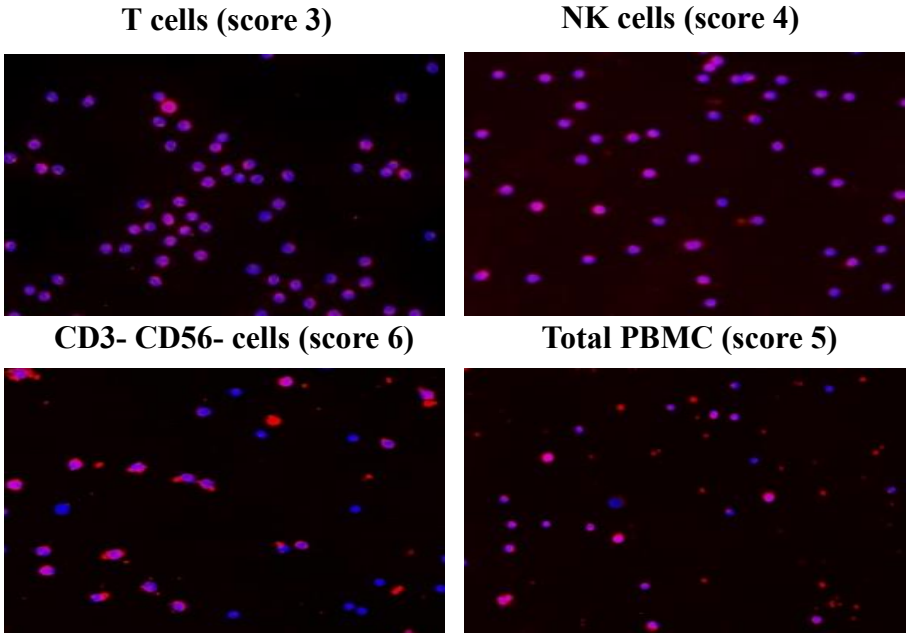

Figure 3. 1: Immunocytochemistry using Abcam anti-GPR65 antibodies. Staining is shown for CD3+ lymphocytes (T cells), CD3- CD56+ lymphocytes (NK cells), CD3- CD56- cells and total PBMCs, at a magnification of x20. The manual weight parameter score is based on the red fluorescence to investigate the GPR65 expression in cell subtypes.

3.2.2 Western blot

Loading control selection

Having detected apparent GPR65 expression in the immunocytochemistry experiment I next attempted to quantify this using Western blotting. To do this I first tested the suitability of β-actin (42kD), Cofilin (20kD) and α-tubulin (57kD) as potential loading controls, by undertaking cell subtype specific Western blotting of these proteins in HeLa cells and lymphocytes from healthy controls. These efforts revealed that α-tubulin is only weakly expressed in human PBMCs (Figure 3.2A). While β-actin gave a band size similar to that expected for GPR65, and my result using cultured lymphocytes also showed that the expression of β-actin is significantly altered following cell proliferation and simulation (Figure 3.2B), further limiting its utility as a suitable control for cultured cells. I therefore concluded that for most of my experiments Cofilin would be the most logical protein to use as a loading control.

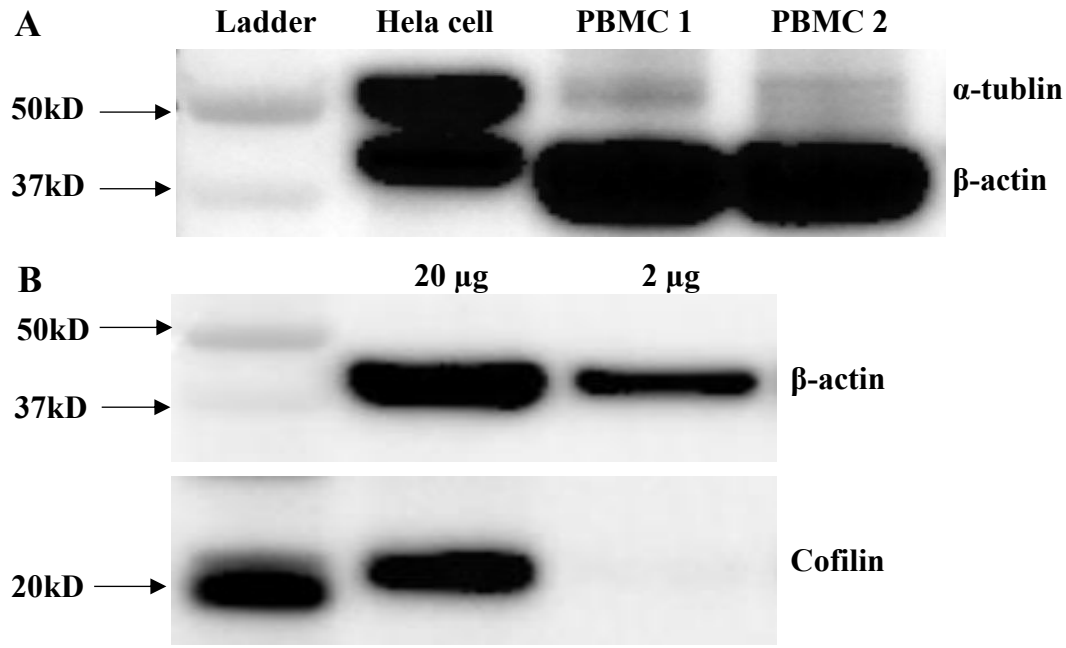

Figure 3. 2: Western blotting of housekeeping proteins α–tubulin, β–actin and Cofilin. Comparison of α-tubulin and β-actin was made in 20 µg of lysate from Hela cells and 20 µg of lysate from cultured PBMCs (mainly lymphocytes) **(A)**. Comparison of β-actin and cofilin was made in 20 µg and 2 µg of lysate from anti-CD3/CD28 antibodies activated lymphocytes **(B)**.

GPR65

The full length GPR65 protein includes 337 amino acids and has an expected molecular weight of 39kD. However, in Western blot using the Abcam polyclonal anti-GPR65 antibody I found a strong band at 52kD, a weak band at 20kD and only faint evidence of a band at the expected size of 39kD when loading high amount (30 µg) of ex-vivo PBMC protein lysate (see lane 1 in Figure 3.3). In cultured lymphocytes without stimulation I saw no 39kD band and an increased ratio of the 20kD band compared to the 52kD band (see lane 2 and independent sample in lane 3 in Figure 3.3). Equivalent results were seen with each of the two alternate anti-GPR65 antibodies binding to different epitopes (Bioss, US; LifeSpan BioSciences, US).

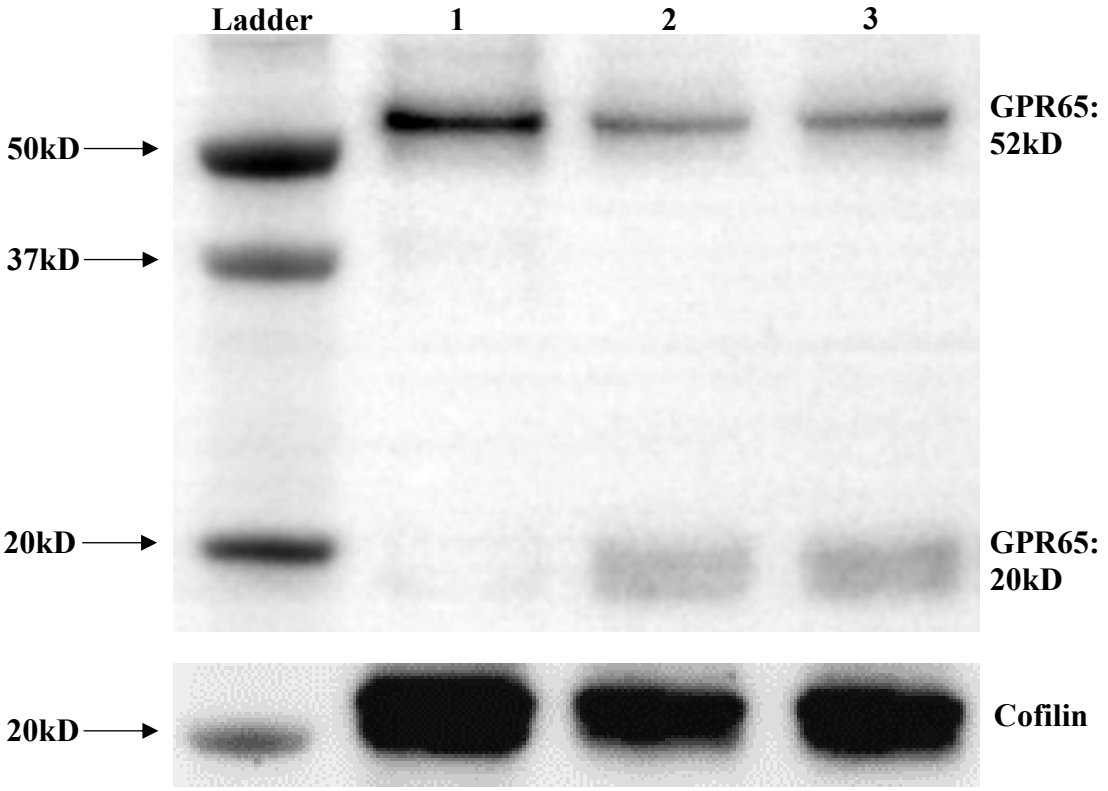

Figure 3. 3: GPR65 expression in Western Blot. Lane 1 contains 30 µg of ex-vivo PBMC lysate while lanes 2 and 3 (biological replicate) contain 20 µg of lysate from lymphocytes cultured without stimulation for 18 hours. The lysates were loaded onto a NuPAGE Novex Bix-Tris Gel and expression was determined using polyclonal anti-GPR65 specific antibody (Abcam). Cofilin was used as a loading control. Faint evidence of a band at 39kD was only apparent in lane 1 when large volume of lysate was included.

I next repeated the Western blot in PBMCs and specific lymphocyte subtypes from two MS patients and one healthy individual. Both MS samples were collected from patients attending the disease modifying clinic at Addenbrooke's hospital; the first patient was on treatment with Fingolimod, while the second was on treatment with Copaxone. In the first MS patient, I observed the anticipated 39kD band as well as the 20kD and 52kD bands seen previously (Figure 3.4 Left). The sample from the second MS patient was separated into NK cells and T cells prior to loading on the Western blot (Figure 3.4 Middle). I found that the 20kD band was primarily expressed in the NK cells, the 52kD band primarily in the T cells and the 39kD band only in the remaining lymphocytes (CD3- CD56-). The cell type specific difference seen in the context of MS patients was less evident in a further healthy control I tested (Figure 3.4 Right). Given the manufactures claims of extremely high specificity for these antibodies I reasoned that the unexpected band sizes might be the result of post-translational modification such as cross-linking with phosphate groups and glycans, or cleavage of GPR65 into a smaller molecule.

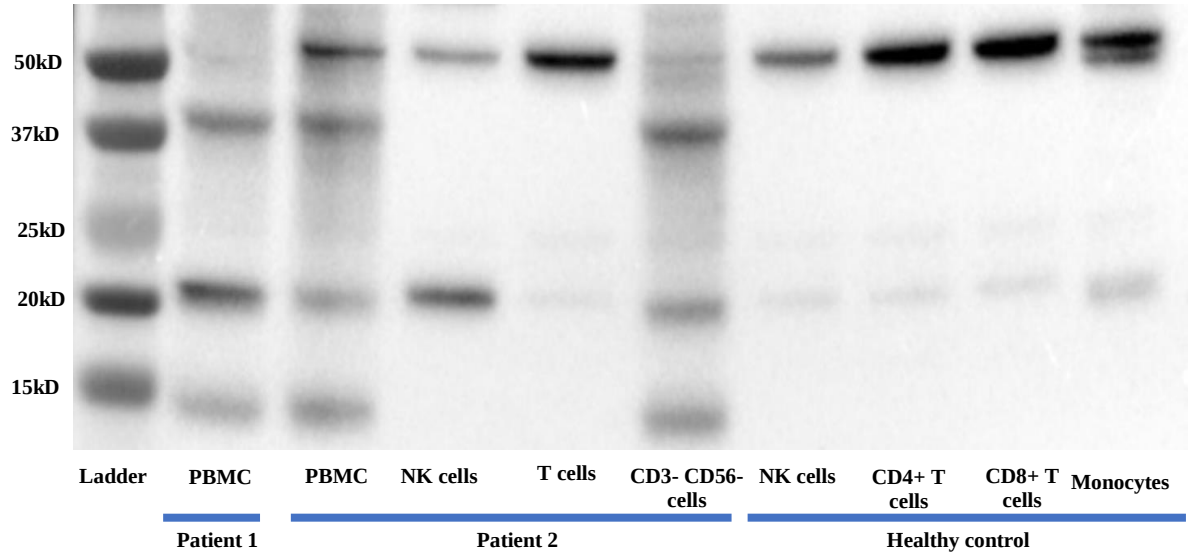

Figure 3. 4: Western blot using the Abcam anti-GPR65 antibodies in two MS patients and in a healthy control. NK cells and T cells were separated from PBMCs prior to the Western blot analysis using autoMACS Pro Separator. 20 μg protein lysates was loaded into each well. No loading control was included in this experiment

Dephosphorylation and deglycosylation

It is known that the activity of GPR65 is regulated by phosphorylation, and that the protein includes three sites where N-linked glycosylation might occur (the 2nd, 79th and 166th are histidine residues) [183]. Either of the phosphate groups or cross-linking glycan may contribute to the increased size. I therefore performed dephosphorylation and deglycosylation on PBMCs collected from a healthy individual prior to Western blot but found that there was no significant effect on the 52kD band (Figure 3.5), suggesting that the observed size difference was not related to phosphorylation or glycosylation.

3.2.3 Analysis of antibodies bound proteins

I then reasoned that perhaps the GPR65 protein was bound with other proteins in a complex having a combined mass of 52kD, or that the commercially available antibodies I had been using might not be as specific as the manufactures claimed; i.e. were in fact binding to proteins other than GPR65. Since 52kD is substantially less than 2x39kD (78kD), it seems unlikely that this band represents a dimer of GPR65. To explore these possibilities, I attempted to use mass spectrometry to analyse what the proteins bound by these antibodies are.

Using a PBMC and T cell lysate from a healthy individual I firstly performed SDS-PAGE followed by coomassie staining to separate all proteins based on their molecular weights (Figure 3.6). According to my previous Western blot results, the proteins at molecular weight 52kD, 39kD and 20kD in PBMC lysate and 52kD in T cell lysate (red rectangles) were processed by my collaborator Dr Deery from Cambridge Centre for Proteomics at Department of Biochemistry and run through the mass spectrometer. Unfortunately, no human GPR65 protein was detected. This may be due to the complex and abundant protein background in cell lysates, and the relatively low expression of GPR65 which may be masked by other similar size proteins, such as Talin-1 and pyruvate kinase enzymes, both of which were expressed extremely highly in all analysed proteins (Figure 3.6). A similar finding of human PBMCs analysed by mass spectrometry showing high expression of Talin-1 and other cytoskeletal proteins has recently been reported [212]. Therefore, I decided to perform protein complex immunoprecipitation (Co-IP) using the same GPR65 antibody to reduce the background noise, followed by mass spectrometry analysis of the proteins bound by the GPR65 antibody.

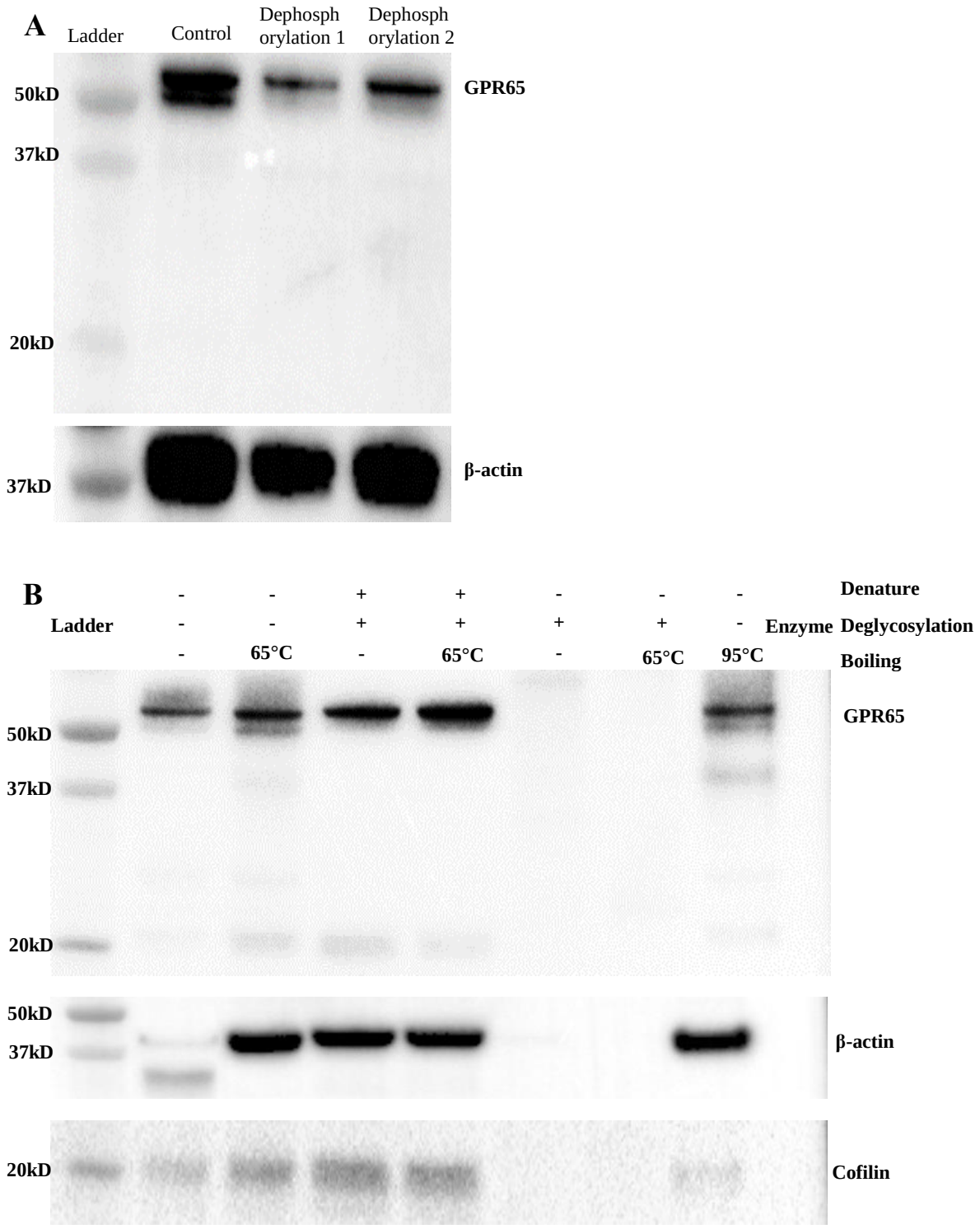

Figure 3. 5: Western blot using Abcam anti-GPR65 antibodies after dephosphorylation **(A)** and deglycosylation **(B)**. PBMC lysates were collected from healthy control subjects and processed by dephosphorylation or deglycosylation respectively before Western blot.

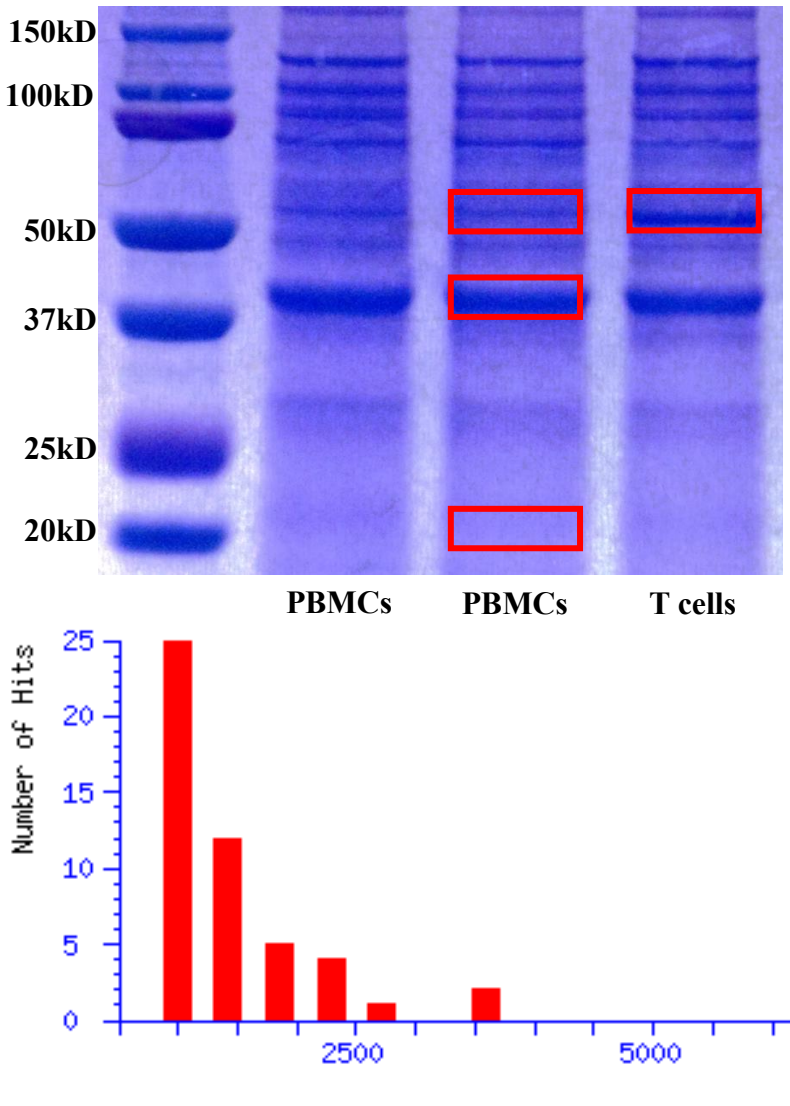

Top 5 matching proteins:

1. Talin-1 [Homo sapiens]
2. Serum albumin [Homo sapiens]
3. Albumin (Fragment) [Homo sapiens]
4. Epididymis luminal protein 113 [Homo sapiens]
5. Pyruvate kinase [Homo sapiens]

Figure 3. 6: List of PBMC lysate proteins of 52kD and their Mascot Scores identified by mass spectrometer. The protein bands stained by coomasive blue in red squares were cut for mass spectrometry analysis. The Mascot Score of the lysated PBMC protein is 52kD. Protein scores are derived from ions scores as a non-probabilistic basis for ranking protein hits ($p<0.05$). This graph automatically generated by mass spectrometry represents a similar finding for other proteins analysed including 39kD and 20kD in PBMCs and 52kD in T cells.

Following the Co-IP, the coomassie staining confirmed that the PBMC lysate from the healthy control individual I studied included only a band of 125kD (Figure 3.7A). This increased size is the result of bound antibodies. I then repeated the experiments using both PBMC and T cell lysates from other two independent healthy controls, the same band of 125kD was observed in both PBMC and isolated T cell lysates. Also, two faint bands at approximately 39kD and 52kD were also identified in T cell lysates (Figure 3.7B). I sent these samples (red rectangles) for analysis by mass spectrometer. The analysis showed that the protein in the 52kD band were most likely human keratins and Rabbit (Oryctolagus cuniculus) IgG heavy chains; in particular human type II cytoskeletal epidermal Keratin and Keratin 1 (Figure 3.8). Although human keratins have a molecular weight in the range of 44kD to 66kD, these proteins are not normally expressed in circulating leukocytes [213]. Similar results were observed for the 39kD protein in T cells and 125kD in PBMCs. Previous studies have reported that keratin from user or trypsin from reagents are the most common contaminating peptides [214]. Thus, given that the Abcam antibodies I used are rabbit IgG antibodies, it seems most likely that the faint 52kD band seen after Co-IP is in fact just free IgG heavy chains (which have a molecular weight of approximately 50kD) and sample contaminated with human keratin. Similar results were found for the band of 39kD suggesting that this is likely also to be a rabbit antibody fragment. In short, my attempt at Co-IP failed and I was unable to determine the protein bound by the commercial antibodies.

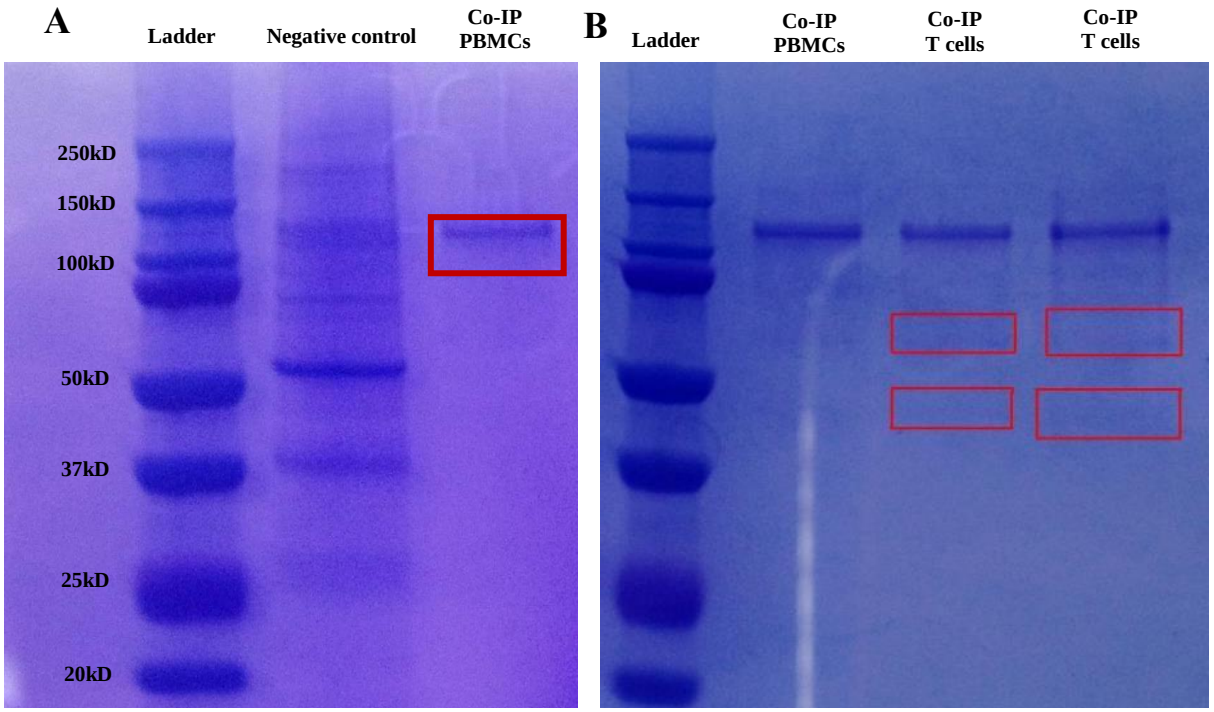

Figure 3. 7: Coomassie staining of precipitated proteins after Co-IP with Abcam anti-GPR65 antibodies. Dynabead labelled Abcam anti-GPR65 antibody were used to precipitate out proteins and protein complexes bound by these antibodies in PBMC **(A)** and T cell **(B)** lysates. Antibodies were then dissociated from these bound proteins and the resulting product Western blotted and stained with coomassie blue. The Co-IP bands in the gel at the relevant sizes (red rectangles) were then cut out for mass spectrometry analysis.

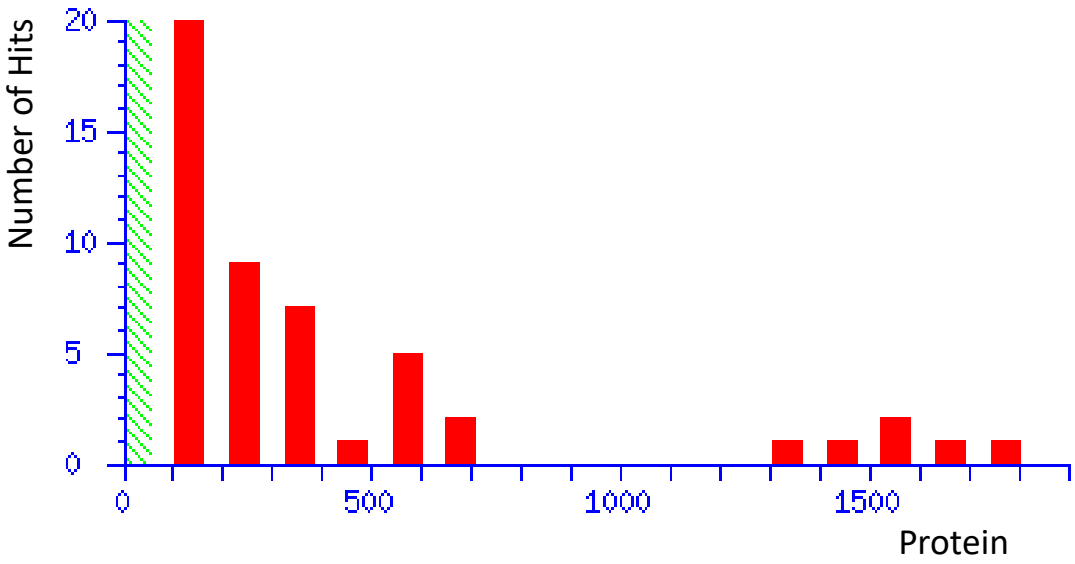

Top 5 matching proteins:

1. epidermal cytokeratin 2 [Homo sapiens]
2. keratin 1 [Homo sapiens]
3. unnamed protein product [Homo sapiens] (matched keratin family)
4. immunoglobulin gamma1 constant region [Oryctolagus cuniculus]
5. Ig gamma H-chain [Oryctolagus cuniculus]

Figure 3. 8: Mascot Score of precipitated proteins after Co-IP. Co-IP eluted proteins were analysed by MS/MS. The list above are top five matching proteins.

3.2.4 siRNA transfection

To determine the most efficiency means to measure siRNA transfection in T cells, I transfected freshly collected PBMCs with 2 nM pmaxGFP. In transfecting T cells I found that the electroporation programme V-024 was significantly ($p<0.0001$) more efficient (88.3%) than the U-014 programme (62.6%) (Figure 3.9), although the number of dead cells was calculated to be higher in NKT cells (U-014: 18.35%; V-024: 37.65%) and NK cells (U-014: 41.75%; V-024: 69.9%). Further optimisation would be needed to properly optimise the balance between transfection efficiency and cell death. However, as I could not validate the anti-GPR65 specific antibody used to confirm the protein knockdown, it was no meaningful to further investigate GPR65 siRNA transfection.

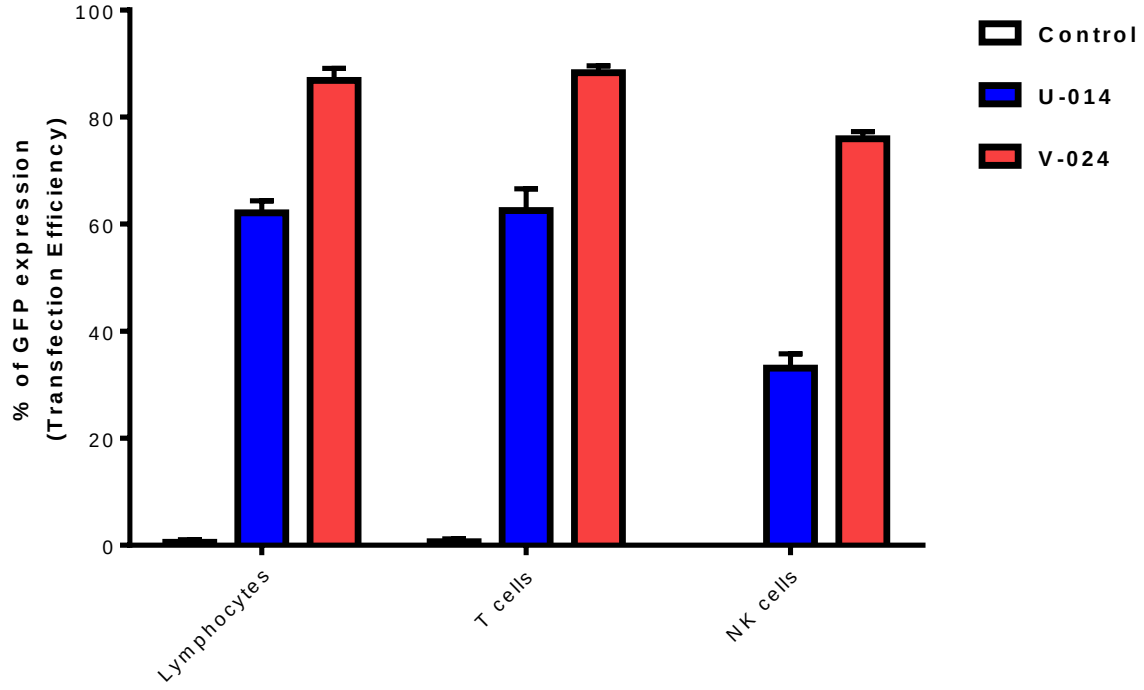

Figure 3. 9: siRNA transfection in different subtypes of lymphocytes comparing electroporation programmes U-014 and V-024. Cells were transfected using 2 µg pmaxGFP followed by culture and T cell activation. The GFP expression in harvested cells were analysed using flow cytometry.

3.3 Discussion

I had hoped that I would be able to establish an antibody based assay for GPR65 that would allow me to quantify GPR65 expression at the protein level, and perhaps establish its

expression pattern and cellular localisation. Unfortunately, each of the assays required extensive optimisation and I was unable to establish an adequately reliable assay in these pilot efforts. Although GPR65 was identified more than two decades ago [181] and has been characterised to some extent in mice [215], its role in humans has been studied very little. Recent studies in human chronic lymphocytic leukaemia (CLL) cells showed correlation between the mRNA expression of *GPR65* and the expression of anti-apoptotic genes, suggesting that GPR65 might enable lymphocytes to tolerate extracellular acidosis [216]. Unfortunately, my pilot efforts to quantify and localise the expression of GPR65 at the protein level were unsuccessful. Under standard conditions I found that the available polyclonal antibodies did not bind to GPR65 protein, and the mass spectrometry revealed only contaminating by keratin and GPR65 antibody itself. As a previous study had suggested GPR65 conformational changes by pH [196], if I had had the time I would have attempted to optimise the Western blot, it would have been particularly interesting to see if perhaps the anti-GPR65 antibody binding was itself pH dependent, perhaps confirming a pH dependent conformational change in GPR65. In addition, the failure of the Co-IP efforts was inevitable given the lack of specificity in the Western blot itself. Given the lack of specificity in the Western blot it seems unwise to read much, if anything, into the Immunocytochemical staining of cell types; these results could easily be confounded by non-specific or off target binding. Given that the commercially available anti-GPR65 antibodies are polyclonal an alternative approach would have been to develop a monoclonal antibody of my own. Such an antibody would be invaluable for GPR65 protein expression studies in the future but would undoubtedly have taken considerable time and resources.

Chapter 4: pH effects on lymphocyte activation

4.1 Introduction

In health, the extracellular hydrogen ion concentration (pH) is tightly regulated and lies slightly on the alkaline side of neutral; with normal values in arterial blood ranging from 7.35 to 7.45 [217]. However, at sites of inflammation, and within tumours, the extracellular space frequently becomes acidic [218-222]. In mice such changes in extracellular pH have been shown to affect immune cell proliferation [223], NK cell cytotoxicity [224] and macrophage phagocytosis [225]. While in humans extracellular pH has been shown to affect immune cell metabolism [226], survival [227], differentiation [228], apoptosis [229] and cytotoxicity [230]. To further refine the effects of extracellular pH on human immune cell activation I cultured PBMCs with and without stimulation and assessed the expression of CD25 and CD69 in CD4+ T cells, CD8+ T cells, NKT cells and NK cells. To avoid any confounding related to the tendency for pH to fall during cell culture I employed a culture system capable of maintaining a stable pH throughout the duration of the experiments.

In a standard culture system, a former Ph.D. student in the lab (Dr Tom Button), found preliminary evidence that human lymphocyte activation was reduced when the extracellular pH was on the alkaline side of physiological pH (pH 7.2 and pH 7.4). This reduction in activation seemed to be greatest in those carrying the protective minor allele at the MS associated SNP rs2119704. In mice, acidic pH (below pH 7.0) rather than alkaline pH has been shown to reduce the expression of activation markers and inhibit proinflammatory cytokine production [197]. Given that GPR65 is known to be sensitive to extracellular pH [183], it seemed reasonable to hypothesise that this gene might influence lymphocyte activation and function in an acidic environment, and that these effects might be important in the aetiology of MS. I therefore decided to explore how extracellular pH affects human lymphocyte activation.

4.2 Determining the effects of extracellular pH on immune cells

In order to follow up Dr Button's findings I first wanted to establish robust methods for testing the effects of extracellular pH and to confirm that pH does indeed effect immune cell activation. To do this I undertook the following experiments; using the flow cytometry antibody panel is shown in Table 4.1 to assess expression of activation markers in different lymphocyte subsets.

Table 4. 1: Flow cytometry staining dyes and antibody panel.

Marker	Fluorochrome	Clone	Manufacturer
Annexin V staining	FITC		eBioscience
CD3	PE-Cy7	SK7	BD Bioscience
CD4	v500	RPA-T4	BD Bioscience
CD8	APC	RPA-T8	BD Bioscience
CD25	FITC	M-A251	BD Bioscience
CD56	PE	B156	BD Bioscience
CD69	v450	FN50	BD Bioscience
Fixable far red dead stain	APC-Cy7		Life Technologies

4.2.1 Establishing a pH stable culture system

In standard cultures pH tends to fall over time as cells metabolise nutrients and buffering capacity becomes exhausted. To avoid confounding related to such changes and to reliably establish the effects of extracellular pH, I first tested the stability of the culture medium pH after 24 and 36 hours of culture using 5 x 10^5 or 1 x 10^6 PBMCs in a final volume of 0.2 mL or 0.5 mL per well. These efforts showed that culturing 5 x 10^5 cells in 0.5 mL resulted in very little change in the medium pH after either 24 hours or 36 hours. However, there was a dramatic drop in pH when 1 x 10^6 cells were incubated for 36 hours or in a final volume of 0.2 mL. In the larger volume system, with or without cultured cells, I observed that the fall in pH was less than 0.05 pH units during cultures of 24 or 36 hours. I also tested a HEPES buffering system and found similar results but decided that the sodium bicarbonate based system was optimal as this allowed me to ensure equivalence of pH, osmolality and sodium concentration in all cultures.

Having established a cell culture procedure in which extracellular pH remained constant for a prolonged period, I next compared the most effective method for T cell activation by activating cells using either plate bound anti-CD3 and soluble anti-CD28 antibodies or Dynabeads™ Human T-Activator anti-CD3/CD28. The extent of stimulation was assessed by measuring the expression of late (CD25) and early (CD69) T cell activation markers; unstimulated T cells were used as a negative control. As expected both protocols resulted in a highly significant increased expression of these two markers compared with unstimulated T cells. However, the

plate bound anti-CD3/CD28 antibodies were more effective at stimulating T cells than the anti-CD3/CD28 Dynabeads and I therefore elected to use these in my exploration of pH effects on stimulation (Figure 4.1).

I next undertook a time course analysis of T cell activation in order to establish the optimal length of culture time to employ. In this I established cultures at differing pH and assessed the expression of CD25 and CD69 from total T cells, CD4+ T cells, CD8+ T cells, NKT cells and NK cells at multiple time points (6, 24, 30, 48, 54, 72 hours following activation with anti-CD3/CD28 antibodies) and at different pH values (pH 6.2, pH 7.0 and pH 7.6). Results for T cells are shown in Figure 4.2, and indicate that maximum expression of CD25 and CD69 occurs within the first 24 hours. Similar results were also seen for other cell types at different pHs.

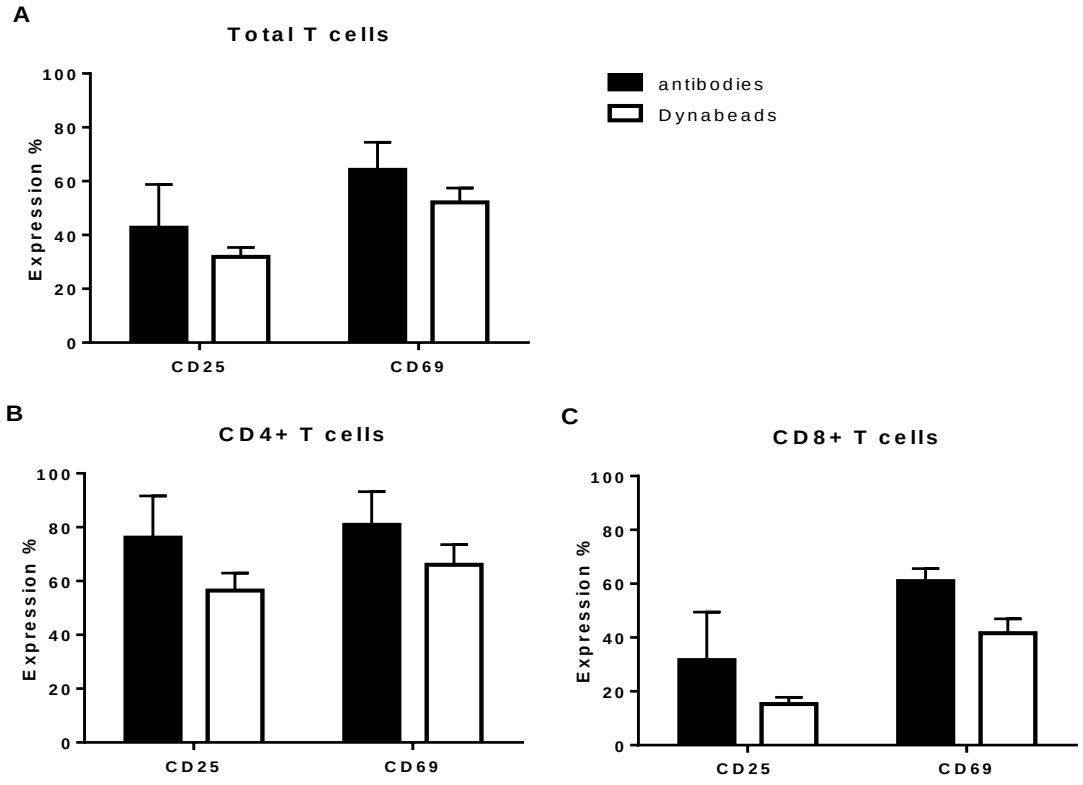

Figure 4. 1: Comparison of stimulation reagents. Activation of lymphocyte subtypes with plate bound anti-CD3/CD28 antibodies and with anti-CD3/CD28 Dynabeads. Cells were stimulated with 1 µg/mL plate bound anti-CD3/CD28 antibodies or 1 µg/mL anti-CD3 Dynabeads for 18 hours. Activation was assessed as % of CD25 and % of CD69 on total T cells (A) and CD4+ T cells (B) and CD8+ T cells (C). Results show the mean ± standard deviation (SD) of triplicate measures.

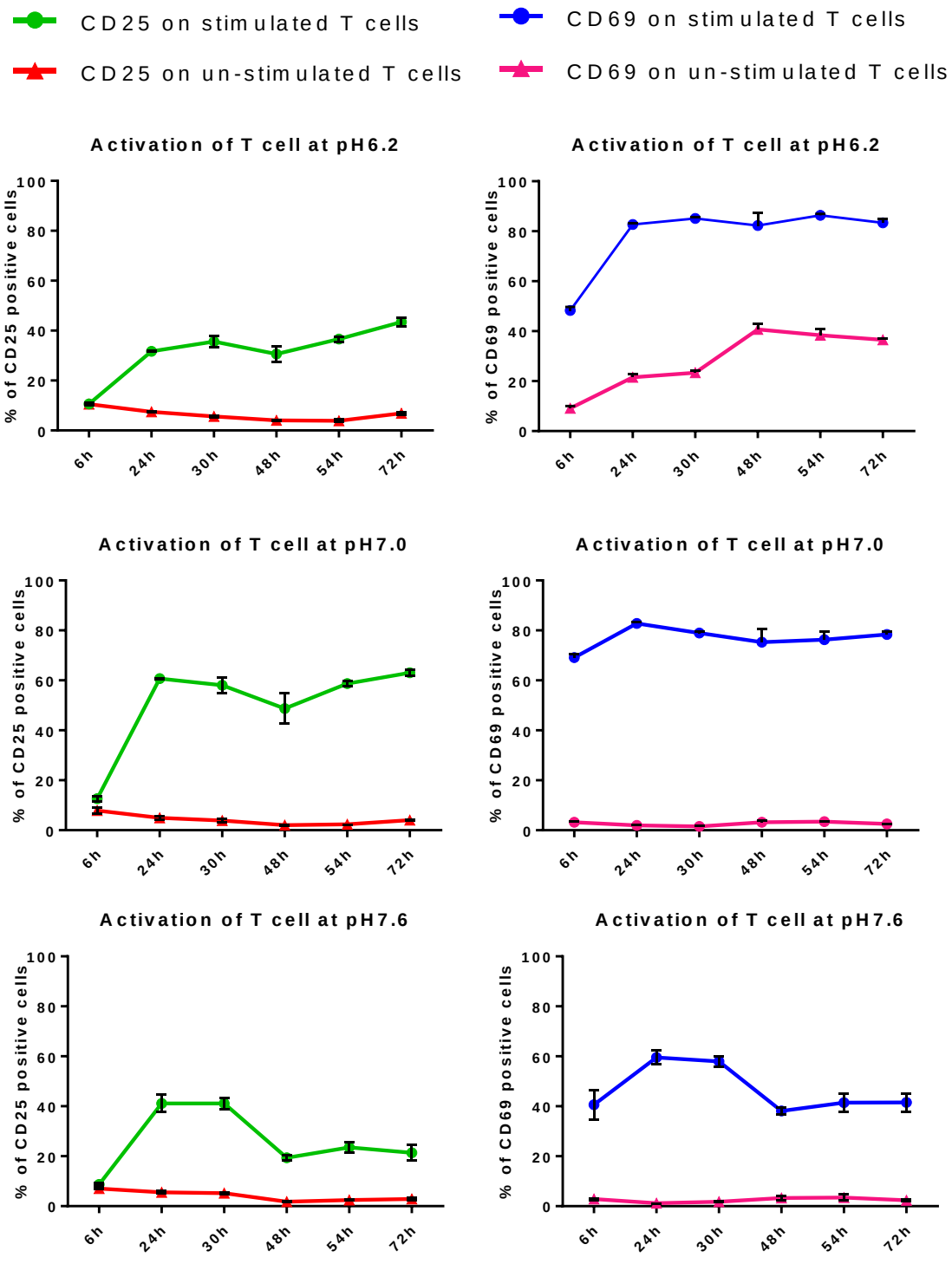

Figure 4. 2: The time course analysis of lymphocyte activation at different pHs. PBMCs were incubated with or without anti-CD3/CD28 antibodies stimulation for up to 72 hours at pH 6.2 pH 7.0 and pH 7.6. The maximal activation of T cells was achieved at 24 hours. Measures shown are the mean of technical triplicates.

One further concern was that my efforts might be confounded if stimulation substantially affected cell viability. To explore this question, I measured the viability of lymphocytes using Annexin V (an early stage apoptotic cell marker) and Live/Dead fixable far red stain (a dead cell marker) to identify the number of dead and viable cells present after culture. These experiments showed that the activation of lymphocytes resulted in a degree of apoptosis but that this was modest in cultures of less than 48 hours duration (Figure 4.3). Only 11% of cells were dead after 48 hours of culture, although a further one third of lymphocytes were in the early stage of apoptosis. This analysis also showed that lymphocyte apoptosis induced by anti-CD3/CD28 co-stimulation was approximately three times greater than in unstimulated cells. Based on these data, I decided to assess the effects of pH after 18 hours of culture, a time point before the expression was maximal to avoid ceiling effects masking pH dependent differences, and before significant cell death induced by stimulation which again might confound my ability to detect pH dependent differences.

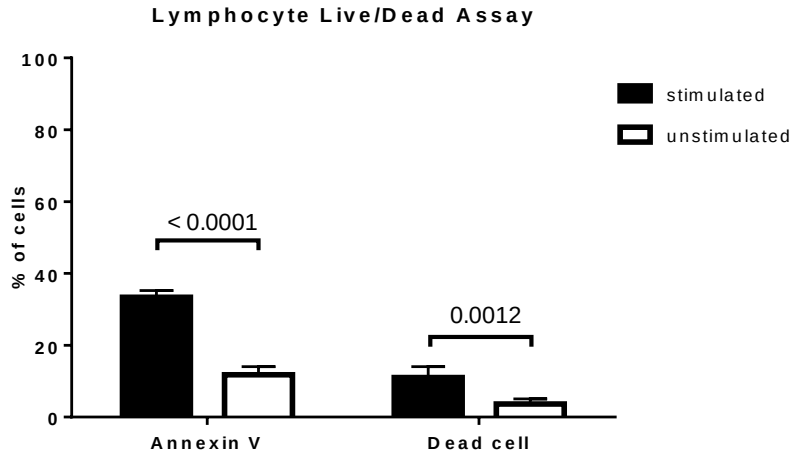

Figure 4. 3: Live/dead staining in lymphocytes after 48 hours stimulation. Cells were labelled with Annexin V (early apoptotic marker) and Live/Dead fixable far red stain (dead cell marker) after 48 hours stimulation. Flow cytometry measures are based on the mean of 5 technical replicates.

4.2.2 Exploring the effects of extracellular pH on lymphocyte activation

To examine the effect of extracellular pH on lymphocyte activation, I cultured cells for 18 hours at a range of pHs (pH 6.2, 6.5, 6.8, 7.0, 7.2, 7.4 and 7.6) with and without T cell stimulation and determined the expression of CD25 and CD69 in specific lymphocyte subtypes

(total T cells, CD4+ T cells, CD8+ T cells, NKT cells and NK cells), see Figure 4.4 and 4.5. In the absence of stimulation extracellular pH had no effect on basal expression of CD25 but tended to slightly increase the expression of CD69 at acidic pH (< pH 6.8). For stimulated T cells an inverted U shape response curve was observed with the highest activation occurring at pH 7.0, although statistical analysis showed no statistically definitive differences between pH 6.8 and pH 7.0 ($p=0.0505$). Either side of neutral pH the expression of CD25 declined more sharply at acidic pH than at alkaline pH. Considering T cell subtypes, CD4+ T cells and CD8+ T cells showed similar patterns of activation as assessed by CD25 expression but some differences were observed for CD69 proportion in stimulated cells at acidic pH. Since NKT cells are mainly CD8+, the pattern of CD69 expression was in fact more similar between CD8+ T cells and NK cell subsets (Figure 4.5). These results confirm that lymphocyte activation is indeed dependent upon extracellular pH, with the peak activation occurring at approximately pH 7.0 and both acidic and alkaline pH generally reducing activation.

While NK cells are not directly stimulated by anti-CD3/CD28 antibodies, they might be activated in a by stander manner as a result of cytokines released by activated T cells [231, 232]. However, I did not observe such indirect activation but instead I saw activation of both stimulated and unstimulated NK cells at acidic pH (Figure 4.5). This suggests that NK cells may become activated when the extracellular space becomes acidic. As might be expected NKT cells, which share properties of both T cells and NK cells [233], showed a pattern of pH dependency reflecting a combination of the patterns seen for T cells and NK cells.

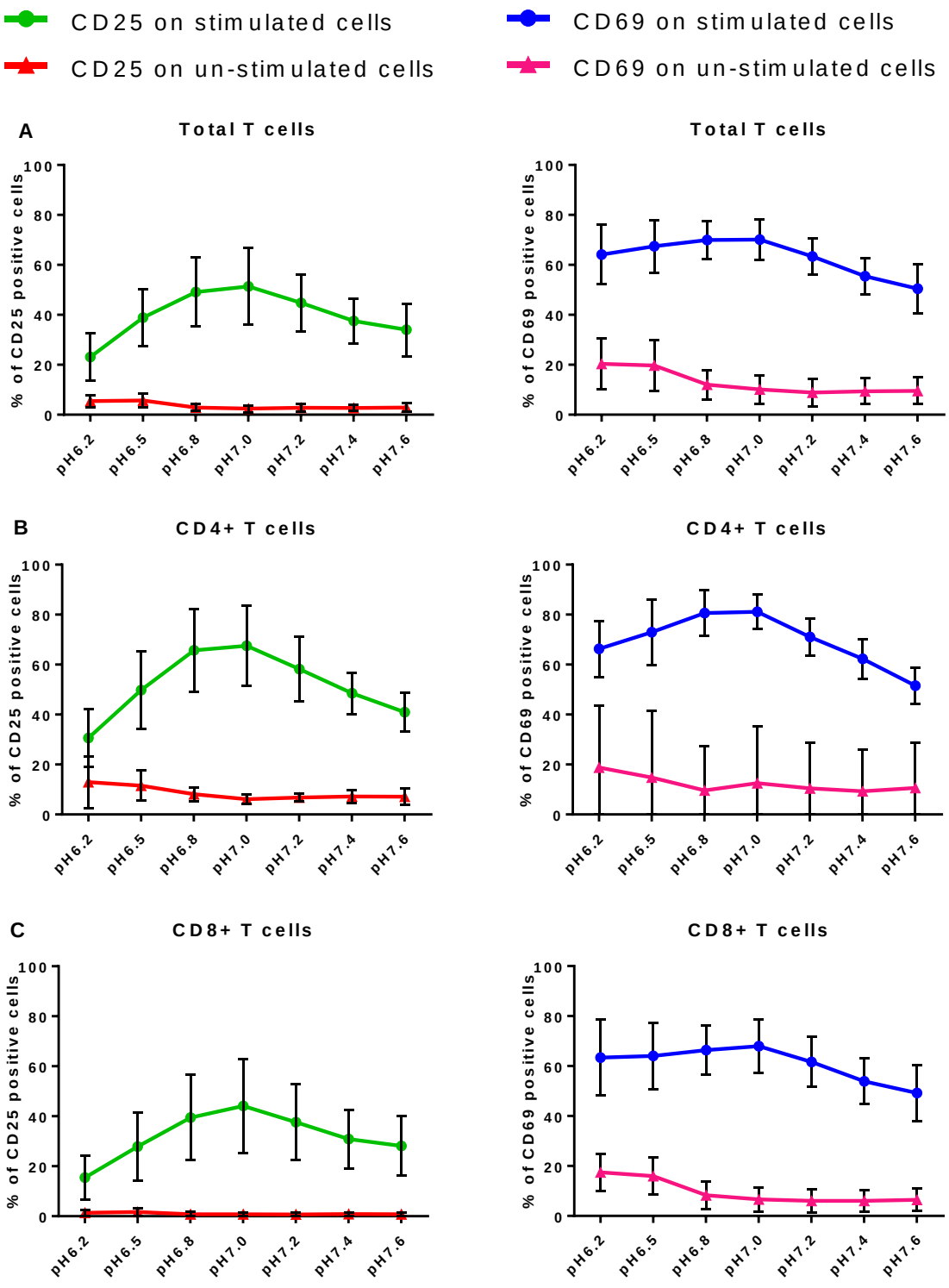

Figure 4. 4: Expression of CD25 and CD69 in activated human lymphocytes after 18 hours of culture at differing extracellular pH. Results are shown for total T cells **(A)**, CD4+ T cells **(B)**, CD8+ T cells **(C)**. Each mean ± SD is based on duplicate measures from 10 individuals.

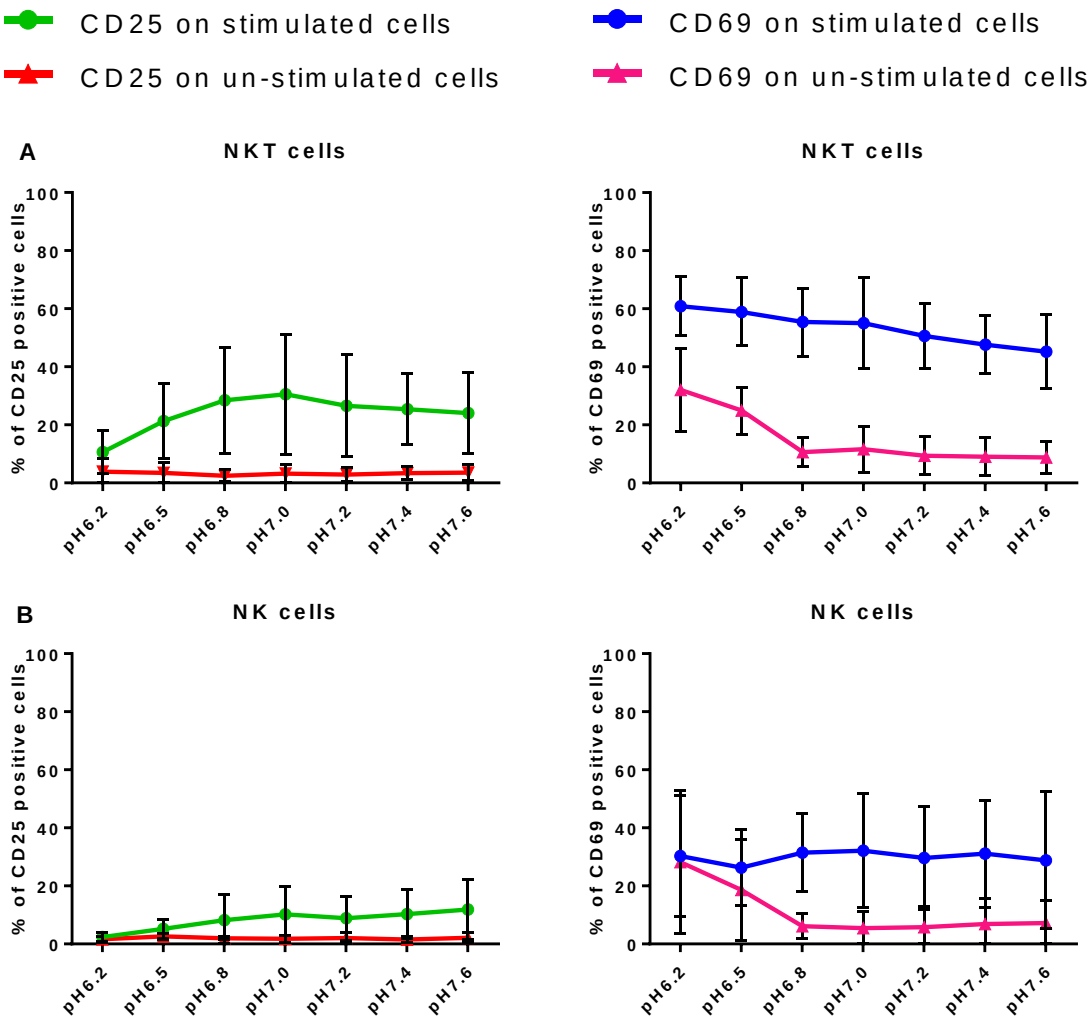

Figure 4. 5: Expression of CD25 and CD69 in activated human lymphocytes after 18 hours of culture at differing extracellular pH. Results are shown for NKT cells **(A)** and NK cells **(B)**. Each mean ± SD is based on duplicate measures from 10 individuals.

To examine whether pH or stimulation might alter the relative proportions of the different lymphocyte subtypes, I compared the proportion of T cells, CD4+ T cells, CD8+ T cells, NKT cells and NK cells. I observed that stimulation upregulated the proportion of CD4+ T cells at all tested pH (Figure 4.6). However, there is no significant differences in the proportion of other cell subtypes or in the ratio of CD4 to CD8 cells.

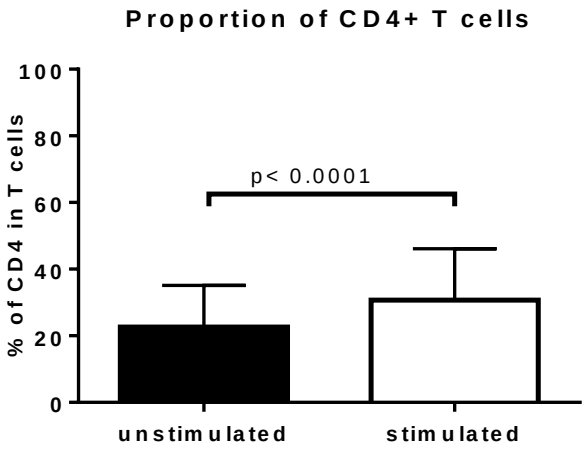

Figure 4. 6: The proportion of cultured CD4+ T cells in stimulated and unstimulated cultures. The proportion of human CD4+ T cells is increased by stimulation. Data were analysed by paired sample t-test and based on 10 individuals.

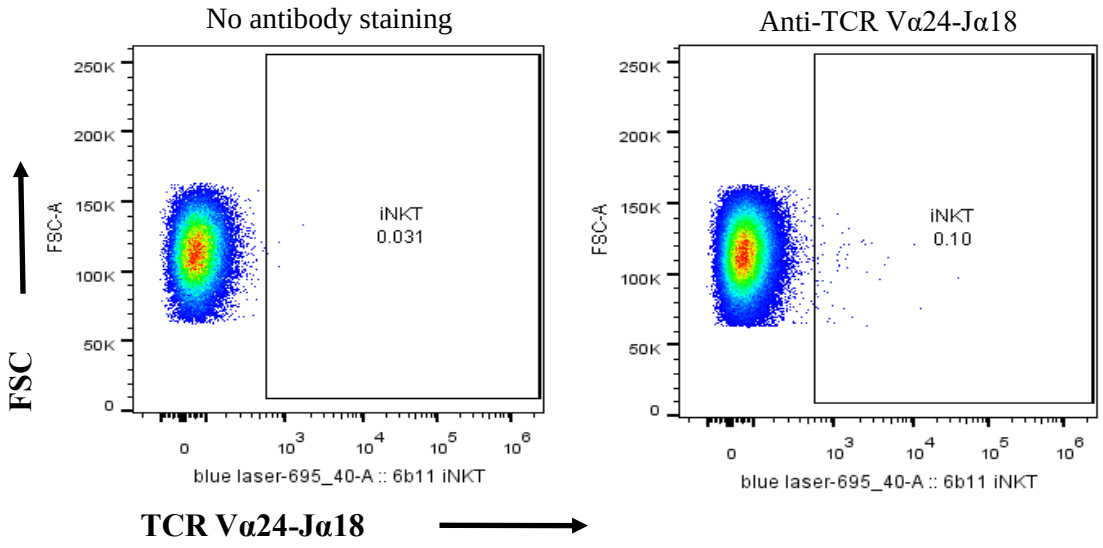

Figure 4. 7: Human peripheral blood lymphocytes stained with FITC conjugated anti-iNKT cell antibodies (right) or without any antibody (left).

I had hoped to be able to look specifically at iNKT cells using an antibody for the relevant T cell receptor Vα24-Jα18. Unfortunately, for each 100,000 lymphocytes captured there was only around 100 cells that were positive for Vα24-Jα18. Thus, given that iNKT cells only make up approximately 0.1% of the human ex-vivo lymphocyte population, it proved impossible to do this.

4.3 Discussion

The large volume bicarbonate based culture system I developed provides a simple method to maintain pH during prolonged cell culture and enabled me to reliably investigate the effect of extracellular pH on human lymphocytes in the context of T cell activation. This protocol maintains a stable medium pH for at least 24 hours without any non-CO_2 dependent buffer. During this time, the T cell viability is maintained at around 90%. Using this system, I have been able to show that lymphocyte activation as assessed by CD25 expression on the cell surface in response to anti-CD3/CD28 stimulation is pH dependent and maximal when extracellular pH is neutral, i.e. slightly on the acidic side of physiological pH. While I also found a similar observation for CD69 expression in stimulated cells the observation of an increased expression of CD69 at acidic pH in unstimulated cells was unexpected. Interestingly a similar finding was recently reported in human lymphocytes, whereby higher expression of CD69 was observed in human PBMCs at acidic pH (pH 6.0) compared to pH 7.3 [234]. I identified that the increased expression of CD69 in unstimulated cells at acidic pH is not only found in both CD4+ and CD8+ T cells but was particularly prominent in NK cells.

In recent work, several studies have suggested that CD69, a C-type transmembrane lectin, plays an essential role in regulating inflammatory responses in CD4+ T cells [235, 236], and have also indicated that activation of CD69 modulates Th17 lymphocyte differentiation [237, 238]. In NK cells the expression of CD69 is rapidly induced after activation by IL-2, IFN-α or the cross-linking stimulation of FcγRIII [239-242]. Furthermore, extracellular acidosis has been shown to inhibit the cytotoxic activity of NK cells and their production of cytokines such as TNF-α, INF-γ, IL-10, IL-12 and transforming growth factor-β1 [243]. In contrast, another study suggests acidic microenvironment enhances the microbicidal activity and perforin degranulation of NK cells [244]. Further work is required to establish the function of CD69 on both T cells and NK cells, particular in an acidic environment but my results suggests that some of these effects may result directly from pH sensing properties of these cells.

A number of mechanisms by which cells can sense and respond to changes in the extracellular pH have been identified, including acid-sensing Ion channels (ASICs), transient receptor potential channel vanilloid subfamily 1 (TRPV1) and proton sensing G-protein coupled receptors (GPCRs). ASICs are sodium channels playing important roles in mechanosensation and synaptic plasticity that are mainly expressed on neurons in the nervous system [245, 246].

TRPV1 has recently been shown to induce Ca^{2+} influx which contributes to CD4+ T cell activation and increase the pro-inflammatory cytokine production [247]. Inhibition of TRPV1 has also been shown to suppress Th2/Th17 cytokine production in CD4+ T cells through the inhibition of MAP kinase [248]. The proton sensing GPCRs including GPR4, GPR65, GPR68 (ovarian cancer G-protein couple receptor 1, ORG1), and GPR132 (G2A) have all been reported to be involved in inflammatory responses. Activation of GPR4 by extracellular acidosis induces the NF-κB pathway which in turns increase the expression of inflammatory genes in endothelial cells [249]. The function of GPR4 is similar to GPR65, which responds to extracellular pH changes through cAMP formation. GPR68 has been shown to mediate IL-8 production in human pancreatic B cells [250], and a hyperresponse to T-cell receptor stimulation was reported in GPR132 deficient T cells in mice [251]. These studies highlight the importance of proton sensing receptors and channels on immune system regulation in response to extracellular pH.

In summary, in this chapter I have established a simple method of undertaking cultures with a stable pH and using this have demonstrated that human lymphocyte activation is pH dependent confirming and refining the observations made by my predecessor, Dr Button. Interestingly I also found that an acidic extracellular pH alone is sufficient to activate an increased expression of CD69 particularly in NK cells.

Chapter 5: Investigates the effect of rs74796499 genotype on lymphocyte activation

5.1 Introduction

In his pilot experiment Dr Button found preliminary evidence suggesting that the genotype at the MS associated SNP rs2119704 influences the extent of T cell activation between pH 7.2 - pH 7.4 but had no effect on the extent of activation at alkaline pH (pH > 7.4); individuals carrying the protective allele (A) showing lower activation than individuals homozygous for the risk allele (C) (Figure 1.2). Given the limited sample size in Dr Button's pilot study (5 protective carriers in a total of 14 healthy individuals) and his use of standard cultures, in which the pH will have drifted during his experiment, I wanted to see if this observation could be replicated using my pH stable culture system in a larger cohort of individuals. As described in Chapter 1 the association of MS with rs2119704, which lies in the downstream of the *GPR65* gene (Figure 5.1), was first reported in the 2011 GWAS [33], and was subsequently partially fine mapped in the ImmunoChip study from 2013 [151]. In the ImmunoChip study the SNP rs74796499 was found to be the lead (most associated) SNP in this region.

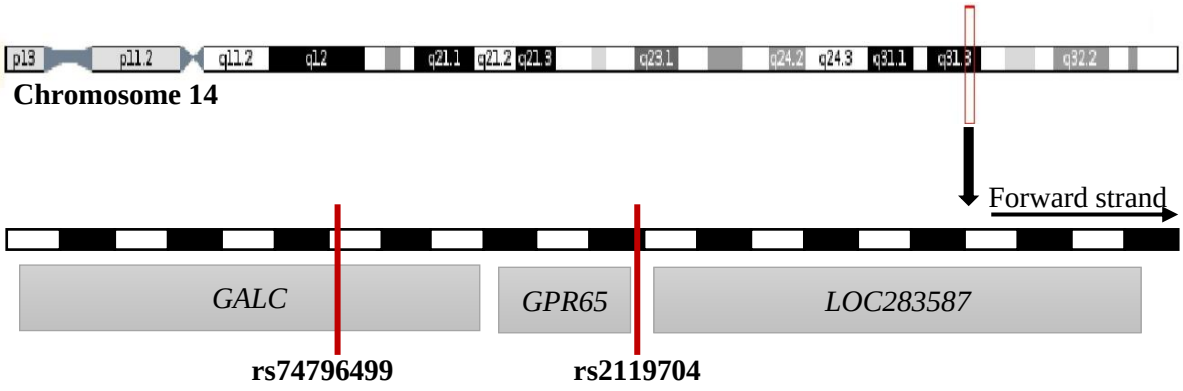

Figure 5. 1: Map indicating the relative position of the MS associated SNPs and potential candidate genes on Chromosome 14q31.3.

The primary aim of the work described in this chapter was thus to establish whether the MS associated SNP rs74796499 exerts any influence on T cell activation (as measured by the surface expression of CD25) at pH 7.0; this pH corresponding to the level resulting in maximal stimulation induced expression of CD25. Given my own additional observation that CD69 expression was upregulated at acidic pH in both T cells and NK cells in the unstimulated state, I also wanted to investigate whether the MS associated SNP influenced this effect. Given that

GPR65 has been shown to inhibit inflammation when the extracellular pH is on the acidic side of physiological pH (especially below pH 7.2) [185, 193], it seems reasonable to hypothesise that GPR65 might be involved in acidic pH induced upregulation of CD69 on T cells and NK cells and that the MS associated SNP rs74796499 might influence this process.

5.2 My approach to determine the effects of rs74796499 on lymphocyte activation

To achieve my primary experimental aim, I measured the surface expression of CD25 on total T cells, CD4+ T cells and CD8+ T cells from PBMCs stimulated with anti-CD3/CD28 antibodies for 18 hours at pH 7.0. For my secondary aim, I measured the surface expression of CD69 on total T cells, NKT cells and NK cells from PBMCs cultured for 18 hours at pH 6.2 without stimulation. I then tested each of these observed measures for evidence of association with rs74796499. Given the low frequency of the protective allele (A) of rs74796499 in the British population (2% in 1000 genomes project), random collection of study subjects would have been highly inefficient, as practically everyone recruited in such a way would have been homozygous for the common (risk) allele (C). I therefore recruited healthy volunteers from the Cambridge BioResource so that these could be selected on the basis of their genotype and I was able to process samples in pairs consisting of one risk allele homozygote (C/C) and one heterozygote (A/C). Individuals homozygous for the protective minor allele (A/A) are rare (even in the BioResource) and at the time of this experiment genotyping of the BioResource was incomplete and only a very few individuals with this third genotype were available. I therefore decided not to include these at this stage. In total, I processed 23 pairs of subjects (a total of 46 individuals) through this pipeline. All my sample processing and expression measurements were conducted blind to the genotypes, which were only revealed to me after all samples had been fully processed and the collected data had been finalised. Ten technical replicates were performed to calculate a robust mean value for each expression level measured. The flow cytometry antibody panel I used is shown in Table 5.1. Statistical significance of observed differences was determined using a paired student t-test.

Table 5. 1: Flow cytometry antibody panel.

Marker	Fluorochrome	Clone	Manufacturer
CD3	PE-Cy7	SK7	BD Bioscience
CD4	v500	RPA-T4	BD Bioscience

CD8	APC	RPA-T8	BD Bioscience
CD25	FITC	M-A251	BD Bioscience
CD56	PE	B156	BD Bioscience
CD69	v450	FN50	BD Bioscience

5.2.1 CD25 expression on T cells stimulated at pH 7.0

In my analysis of CD25+ T cells stimulated with anti-CD3/CD28 antibodies for 18 hours at pH 7.0 I found no evidence for association with carriage of the protective allele (A) and CD25 expression, in total T cells (p=0.7271), CD4+ T cells (p=0.7435) or CD8+ T cells (p=0.4043) (Figure 5.2). I was thus unable to replicate the effect suggested by Dr Button.

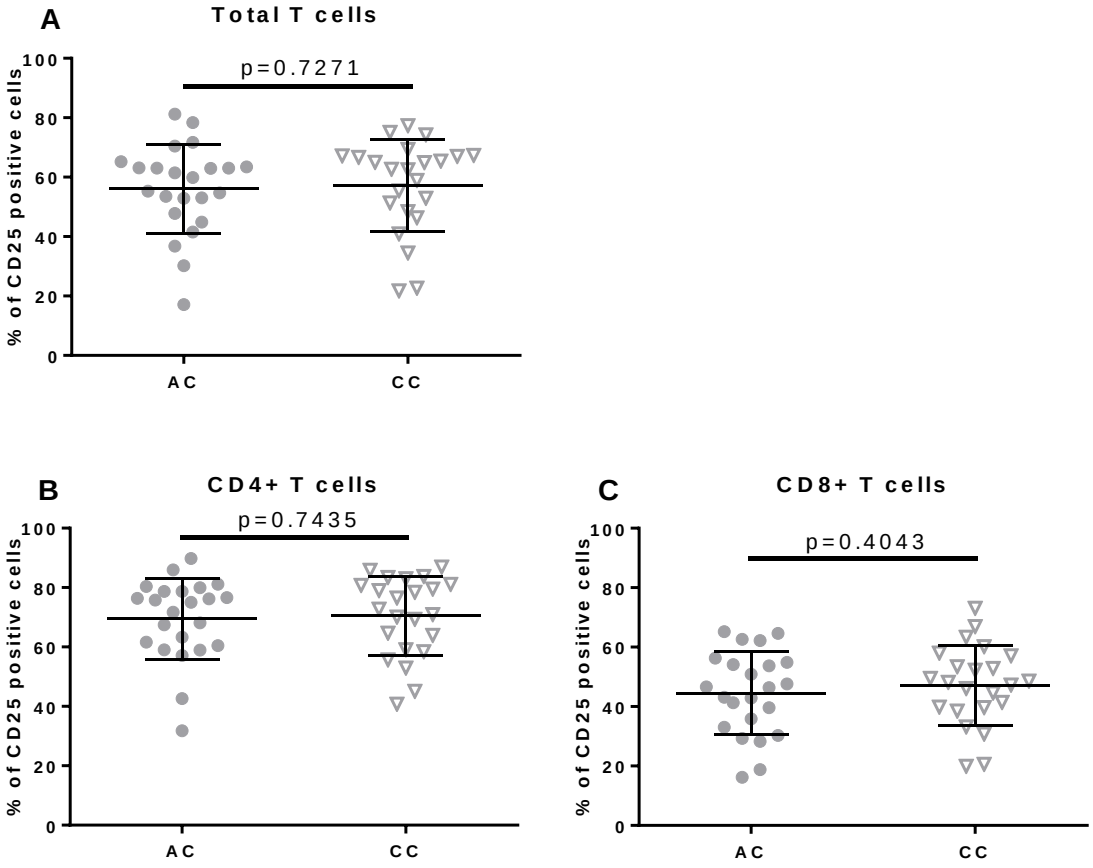

Figure 5. 2: CD25 expression on T cells after 18 hours stimulated with anti-CD3/CD28 antibodies at pH 7.0, comparing protective allele carriers (A/C, n=23) and non-carrier (C/C, n=23); total T cells (A), CD4+ T cells (B) and CD8+ T cells (C).

5.2.2 CD69 expression on T cells, NKT cells and NK cells unstimulated at pH 6.2

In my analysis of CD69 on total T cells, NKT and NK cells from 18 hours unstimulated cultures at pH 6.2, I found the CD69 expression on T cells is increased in individuals carrying the protective allele (p=0.0291) (Figure 5.3). While not significant a similar trend was observed in NKT cells (p=0.0689).

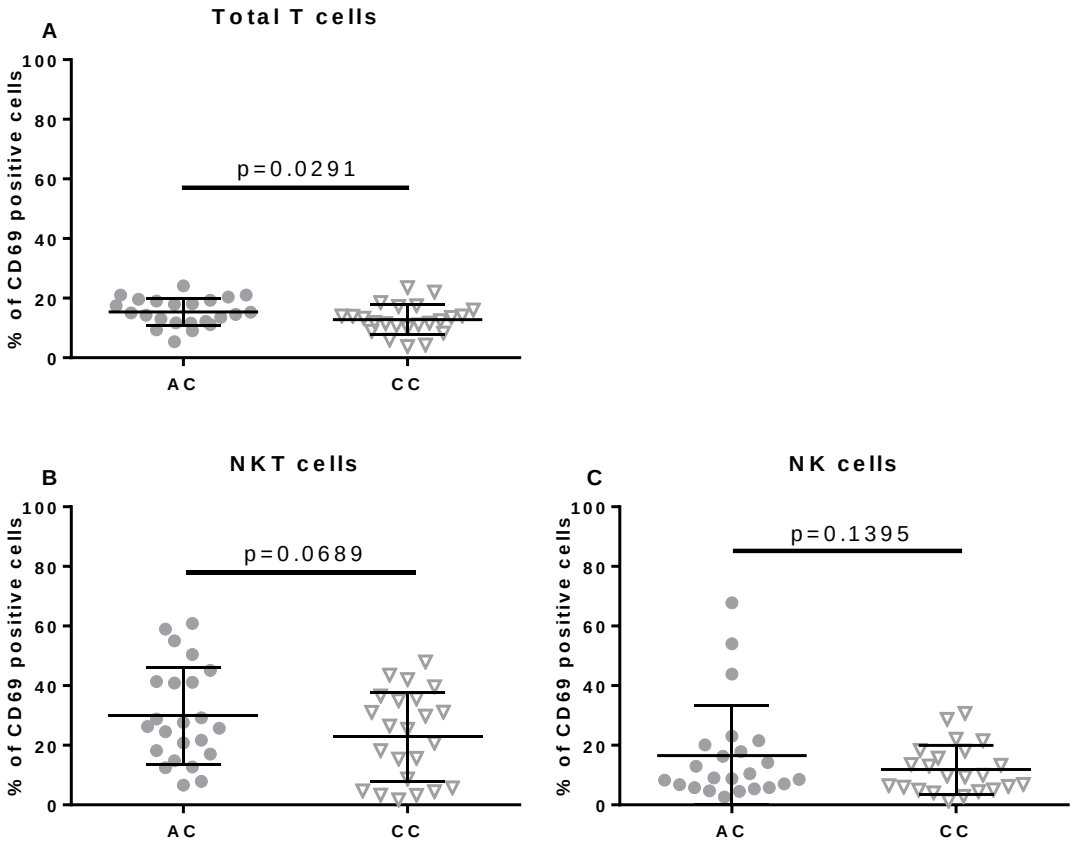

Figure 5. 3: CD69 expression on total T cells, NKT cells and NK cells from unstimulated cultures at pH 6.2 comparing protective allele carriers (A/C, n=23) and non-carrier (C/C, n=23); total T cells (A) NKT cells (B) and NK cells (C).

5.3 Discussion

In these carefully conducted experiments I was unable to replicate the preliminary observations made by Dr Button. In my analysis I found no evidence that the MS associated SNP rs74796499 influences T cell activation at pH 7.0, the optimal pH for T cell stimulation. However, given that studies in mice showed that there is little activation of GPR65 at pH 7.0, it occurred to me that perhaps the genotype only affects activation at more acidic pH [199]. Given that Dr Button

used standard culture methods the actual pH in his cultures may have drifted to lower values during the period of his experiments, this would not have happened during my experiments. I therefore decided to explore the genotype correlation experiment at a lower pH.

Currently, there are four known pH sensing G protein coupled receptors, each of which is thought to respond to extracellular protons via the effects of these on histidine residues present in their extracellular domains [196, 252]. In contrast to GPR65, the receptor GPR68 (also known as OGR-1) exerts pro-inflammatory effects in acidic environments [253, 254], through increased production of IL-6 [253]. Unsurprisingly OGR-1 has also been suggested to play a key role in the regulation of T cell responses during autoimmunity [255]. Research on GPR4, which is ubiquitously expresses in all cells including lymphocytes (the human protein ATLAS website: https://www.proteinatlas.org/), suggests that this receptor exerts its greatest effects on intracellular cAMP signalling at pH 6.8 [196]. It therefore, seems reasonable to suspect that the effects of GPR65 might only be relevant at lower pH levels than 7.0 and that the anti-inflammatory effects of GPR65 might be offset by other acid sensing receptors at particular pH values.

Another possible reason for the lack of replication of Dr Button's original finding that I have presented in this chapter is of course that rs74796499 may not directly affect the function of GPR65 at all but rather might be influencing GALC or the regulation of some other genes. In support of this view it is noteworthy that rs74796499 is located in an intron of *GALC* and is in complete linkage disequilibrium with 4 SNPs that are all located in *GALC* (shown in Appendix); including one synonymous coding variant (rs11552556, which is predicted to be a splice region variant). However, there is considerable LD associated with the minor allele of rs74796499 such that it is also correlated with variants in *GPR65* and the nearby non-coding RNA (*LINC01146*). If *GALC* is the relevant gene it might be that carriers of the protective allele have altered GALC function perhaps leading to increased level of psychosine or some other glycolipid. Psychosine has a direct apoptotic effect on oligodendrocytes and indirectly acts as an antagonist of GPR65, which inhibits the negative inflammatory function of GPR65. The fact that common variants known to alter the function of GALC are not associated with MS argues against any change in GALC function being simple.

Finally, studies in knockout mice have shown that GPR65 plays an important role in the development of anti-collagen type II antibody-induced arthritis and delayed-type

hypersensitivity, both of which are believed to be T and B cell independent effects that are mediated by macrophages and neutrophils [193]. It is likely that the influence of rs74796499 on risk of MS is cell type dependent, so it is possible that I have focused the efforts presented here in the wrong cell types. On the other hand, *GPR65* is highly expressed in NK cells [174]. As my results to date indicate that acidic pH induces the activation of NKT and NK cells and that the expression of CD69 on T cells is higher in protective allele carriers it therefore seemed reasonable to further extend the analysis of the associated variant in T cells, NKT and NK cells at low extracellular pH.

Chapter 6: Attempts to refine the relationship between genotype and pH dependent expression

6.1 Introduction

In the previous chapters I found that the expression of CD69 was upregulated on T cells when the extracellular pH is acidic, and also found evidence suggesting that the extent of this upregulation is dependent upon the genotype at the MS associated SNP rs74796499. In this chapter I therefore wanted to see if I could replicate and confirm these observations, and also try to establish if GPR65 might be involved in mediating these effects. To do this I repeated the experiments performed previously but this time included additional cultures that included BTB09089; a synthetic GPR65 ligand (see below) [193].

I also wanted to take the opportunity provided by repeating these experiments to simultaneously consider the possibility that the rs74796499 variant might exert effects on the other protein coding gene from this region galactosylceramidase (GALC), an essential lysosomal enzyme responsible for the catabolism of many myelin related sphingolipids, including galactosylceramide, galactosylsphingosine and lactosylceramide (LacCer) through the hydrolysis of their galactose ester bonds. These sphingolipids are important components of the membrane microdomains known as lipid rafts, where they act to increase the rigidity of the plasma membrane so that it can link to the cellular cytoskeleton and hold together the clusters of molecular components required in cell surface functional units [256, 257]. The role of lipid rafts in signal transduction has been shown to be important in the pathogenesis of various diseases including Alzheimer's disease, Parkinson's disease and systemic lupus erythematosus (SLE) [258]. Recent studies indicate lipid rafts also play a key role in immune cell activation [259, 260], via T cell receptor (TCR) and the Fc regions (FcR) of the B cell receptor (BCR) [261]. It therefore, seemed reasonable to hypothesise that altered lipid metabolism might alter lipid raft formation and thereby affect lymphocyte functioning. In support of this it is known that LacCer, an important intermediate in the catabolism of many of the complex glycosphingolipid found in myelin, is involved in cell-cell interaction and signalling transduction [262, 263]. A recent study found that the expression of LacCer and of its synthase enzyme (B4GALT6) is upregulated in astrocytes in MS lesion; both of which are involved in the recruitment and activation of CNS infiltrating monocytes and microglia in EAE [264]. This research group also observed inhibition of local CNS innate immunity when LacCer synthesis was inhibited, with resulting protection from EAE [264]. Increased expression of lipid raft-

associated glycosphingolipids, including LacCer, globotriaosylceramide (Gb3) and monosialotetrahexosylganglioside (GM1) has also been observed in CD4+ T cells from patients with SLE [265, 266]. So in the repeat experiments described in this chapter I decided to measure LacCer in ex-vivo cells.

As described in Chapter 1 the neurodegeneration seen in Krabbe's Disease (the autosomal recessive demyelinating disease resulting from loss of function mutations in *GALC*) is thought primarily to results from the toxic effects of the galactosyl-sphingolipid psychosine [167]. This moiety is a naturally occurring ligand for GPR65, and thus, although at face value the two genes from this region don't seem to have any immediately obvious relationship to each other, in fact one of the most important substrates for the one gene (*GALC*) is a ligand for the second (*GPR65*). Furthermore, given that galacto-sphingolipids are almost exclusively found in nervous tissue it seems likely that this interaction will be particularly relevant in areas of CNS inflammation where myelin breakdown will result in large amounts of galactosphingolipids needing to be catabolised and inflammation will result in reduction of local pH.

6.2 The synthetic GPR65 ligand - BTB09089

Given that activation of GPR65 has been shown to reduce the production of pro-inflammatory cytokines, and that knocking this gene out in mice results in exacerbation of various immune mediated inflammatory diseases [193, 206] Onozawa et al screened a library of compounds looking for an agonist for this receptor and found the molecule (3-[(2,4-dichlorobenzyl)thio]-1,6-dimethyl-5,6-dihydro-1H-pyridazino[4,5-e][1,3,4] thiadiazin -5-one) which they designated BTB09089. Despite the extensive homology between GPR65 and other acid-sensing G-protein coupled receptors, such as OGR1 and GPR4, BTB09089 has been shown to only activate GPR65 [193, 267] and has also been shown to reduce the production of IL-2 from splenocytes stimulated with anti-CD3/CD28 antibodies [193]. This molecule thus seems to act as a highly selective agonist of GPR65 and thus provides a means to test whether GPR65 is involved in the pH dependent effects I saw previously. However, because BTB09089 is hydrophobic I first needed to solubilise it, and to do this I used DMSO (as recommended by the manufacturer). In order to ensure that the use of DMSO in this way would not influence my results, I tested the effects of DMSO itself on my cultures and found that at concentrations up to 1% (v/v) DMSO did not significantly alter the expression of CD25 or CD69 on any of

the lymphocyte subtypes I wanted to test, or their relative proportions (Figure 6.1). It is well established that DMSO does not have any significant short term cytotoxic effect on lymphocytes at concentrations less than 1% (v/v) [268-270]. Having established that the use of DMSO would not confound my experiments I next performed a BTB09089 titration experiment with and without anti-CD3/CD28 stimulation at pH 7.0 (Figure 6.2). This confirmed that at the tested concentrations BTB09089 had no effect on the relative proportions of the different cell subtypes but substantially reduced the expression of both CD25 and CD69 in the stimulated cultures in a concentration dependent manner. My results were consistent with those from previous investigators [193] with a substantial effect at a concentration of 20 μM; which required the use of only 0.2% (v/v) DMSO. I then tested this concentration of BTB09089 in stimulated cultures at a range of pH values (Figure 6.3) and confirmed that it suppressed expression of CD25 and CD69 in all cases, although the effects in NK cells were limited.

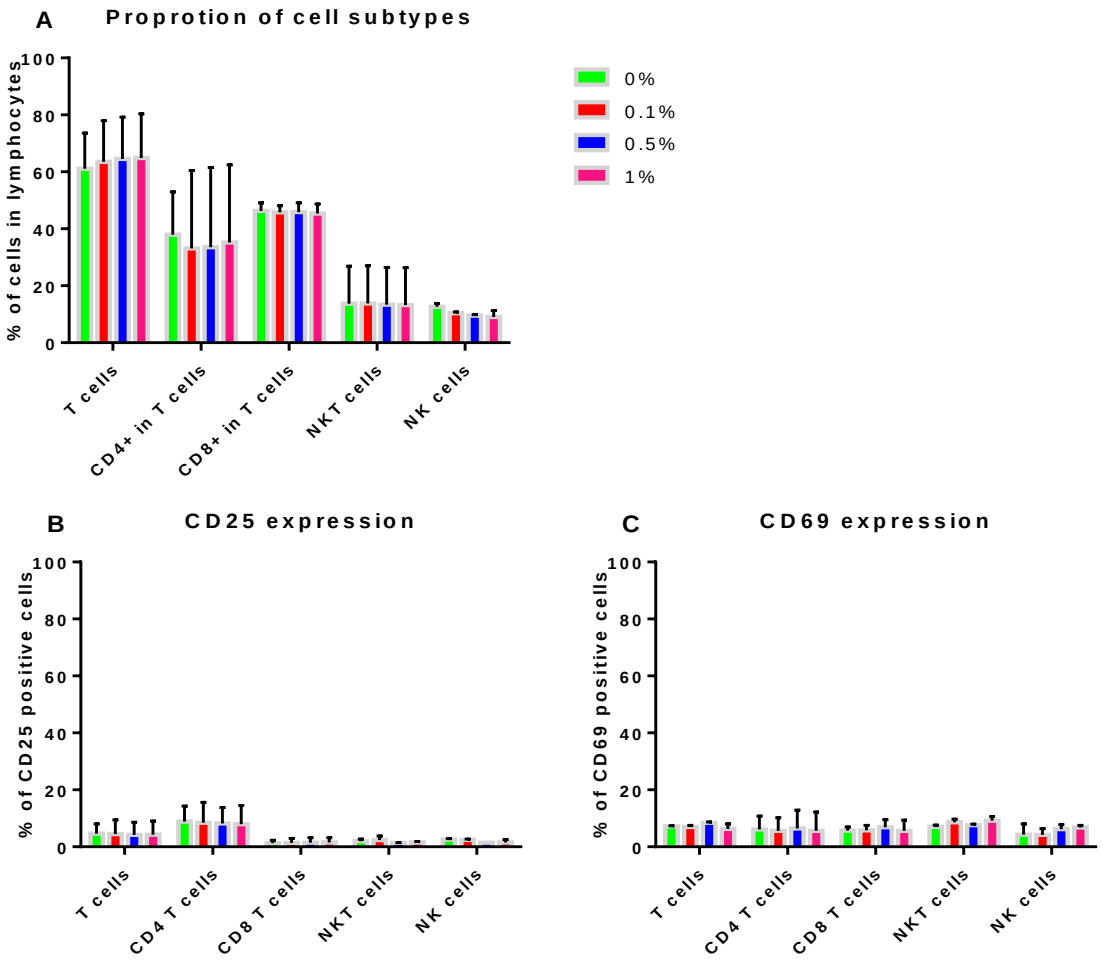

Figure 6. 1: Influence of DMSO on PBMCs cultured for 18 hours at pH 7.0. The proportion of lymphocyte subtypes (A), expression of CD25 (B) and CD69 (C) were assessed. Data is based on measures from 2 subjects each tested in duplicate.

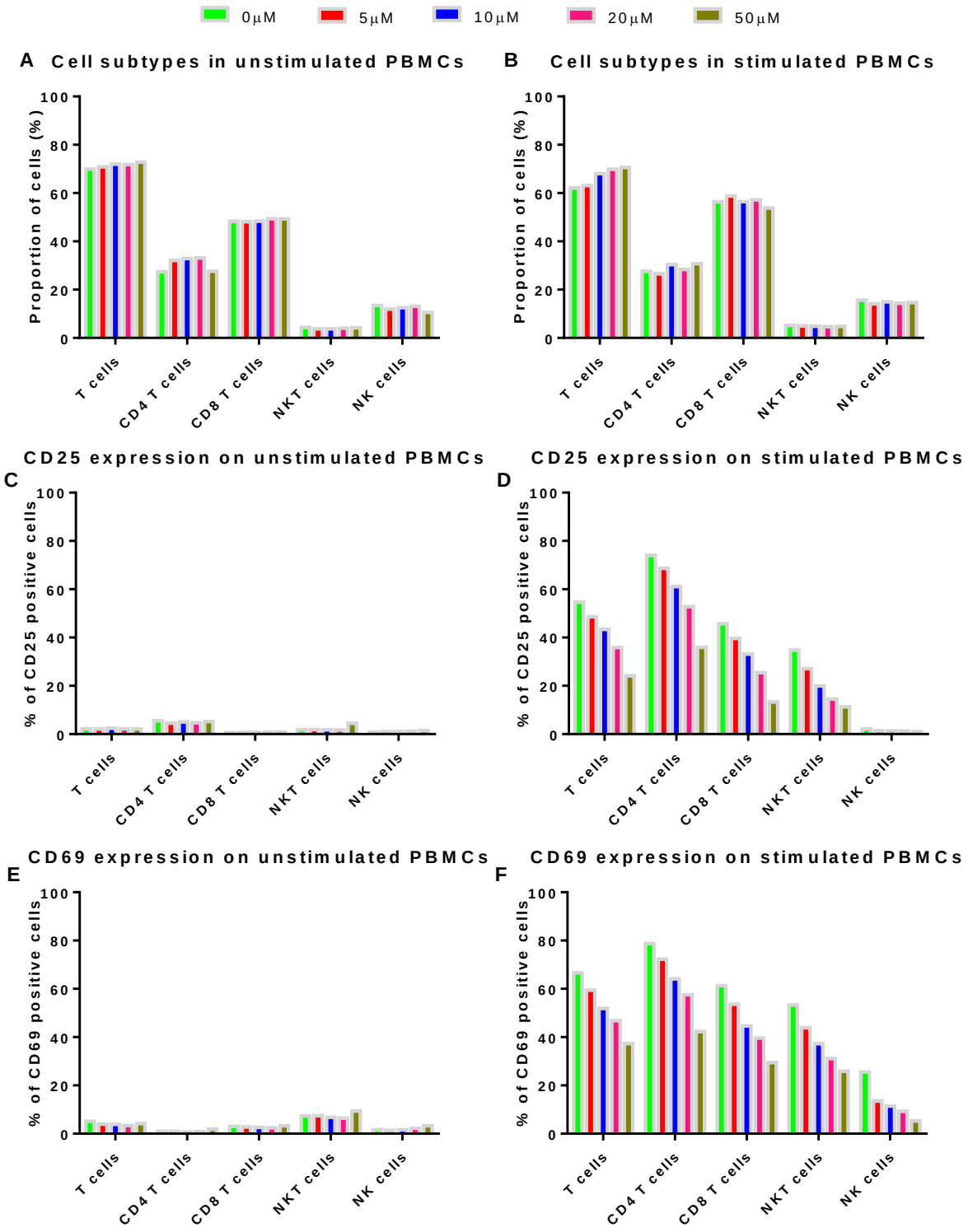

Figure 6. 2: BTB09089 titration assay. PBMCs were cultured at pH 7.0 for 18 hours unstimulated and stimulated in the presence of a range of BTB09089 concentrations. The proportion of lymphocyte subtypes in unstimulated (A) and stimulated (B) condition are shown together with the expression of CD25 and CD69 in unstimulated (C and E) and stimulated (D and F) cultures in each of the cell types to be considered. These data are based on testing one subject in duplicate.

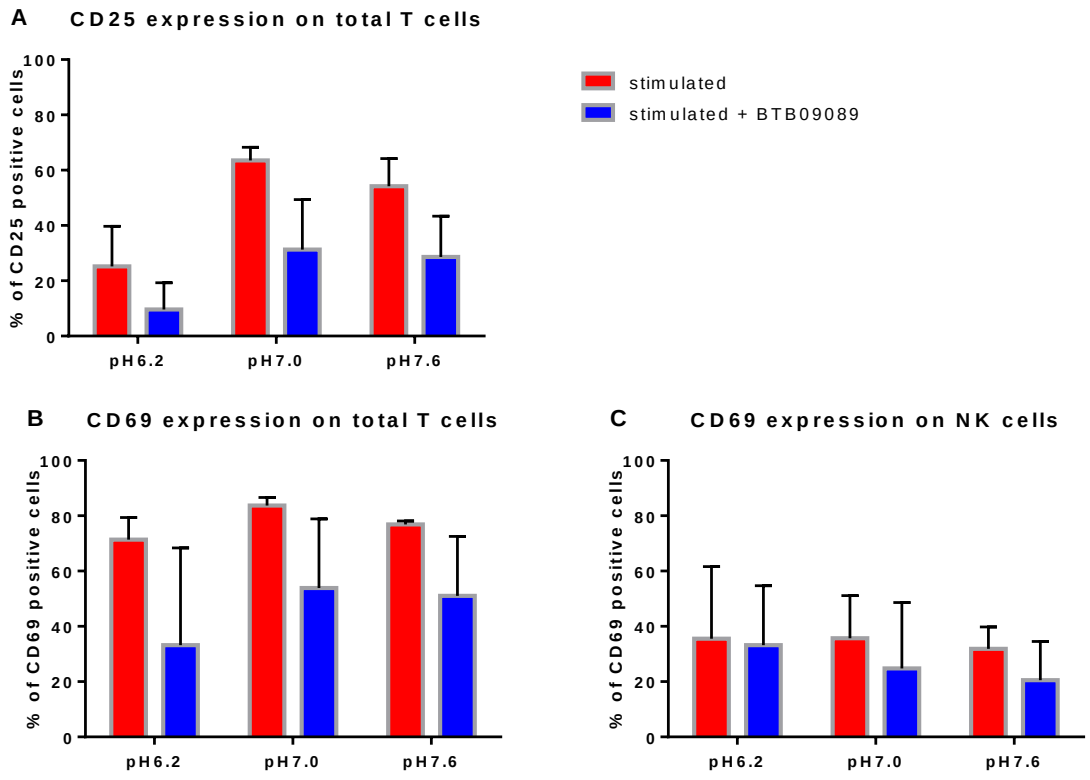

Figure 6. 3: BTB09089 induced suppression of CD25 and CD69 expression in stimulated cultures across a range of pHs. PBMCs were stimulated with anti-CD3/CD28 antibodies supplemented with 20 μM BTB09089 for 18 hours at pH 6.2, pH 7.0 and pH 7.6. Expression of CD25 (A) and CD69 (B) on total T cells, and CD69 on NK cells (C) were assessed. Data are based on one subject tested in duplicate.

6.3 Replication experiment outline

In this phase of my work, I processed samples from 50 healthy individuals (25 heterozygotes and 25 major risk allele homozygotes) that were all recruited from Cambridge BioResource on the basis of their genotype. Samples were collected and processed in genotype matched pairs with one homozygote (C/C) and one heterozygote (A/C) in each pair. I was blind to the genotypes until all sample processing and measurements had been completed and finalised. For each individual, I measured the surface expression of LacCer (CD17) on freshly collected ex-vivo T cells, CD4+ T cells, CD8+ T cells, NKT cells and NK cells. I also separated CD56+ cells (NKT and NK cells) and CD56- cells using the autoMACS Pro Separator and extracted RNA from these cells as described in Chapter 2. In parallel to processing the ex-vivo cells I

also set up three PBMC cultures at pH 6.2 and three at pH 7.0. At each pH one culture was established with anti-CD3/CD28 stimulation alone, a second was established with anti-CD3/CD28 stimulation in the presence of BTB09089, and a third was unstimulated (with no anti-CD3/CD28 antibodies and no BTB09089). Following 18 hours incubation of each of the 6 cultures I measured the surface expression of CD25 and CD69 on total T cells, CD4+ T cells, CD8+ T cells, NKT cells and NK cells. The flow cytometry antibody panels used for the ex-vivo cell analysis and the cultured PBMC analysis are shown in Table 6.1 and Table 6.2 respectively. For each measure I performed four technical replicates. Because the samples were supplied from the Cambridge BioResource in pairs I was able to analyse the resulting protein expression data using a paired student t-test which controls for any batch effect differences related to processing the samples on different days. For each of the five cell types (total T cells, CD4+ T cells, CD8+ T cells, NKT cells and NK cells) I measured CD17 in ex-vivo cells and CD25 and CD69 in each of the 6 culture settings. In each of the 6 culture settings I also measured CD25 and CD69 expression in the residual lymphocytes (i.e. the cells that were CD3- and CD56- and are therefore B cell enriched) and in the NKT cells that were also CD8+. There was no meaningful expression of CD25 in NK cells or in the B cell enriched residual cells (those that were both CD3- and CD56-) so no analysis was made for these groups. This gives a total of 77 expression phenotypes that were tested for association with genotype. Since many of these expression phenotypes are necessarily correlated the effective number of independent phenotypes was established using an R script provided by Prof Frank Dudbridge (using 10,000 permutations). This script, which determines the effective number of independent phenotypes empirically, showed that my 77 phenotypes were equivalent to 37.6 independent phenotypes and I therefore set a threshold of $p<0.0013$ for declaring statistical significance in order to correct for multiple testing.

In addition, I also measured cell proportions. In the ex-vivo cells I measured the % of lymphocytes that were T cells, NKT cells and NK cells, and also measured the proportion of NKT cells that were CD8+, the proportion of CD4+ T cells and CD8+ T cells, and the ratio of CD4+/CD8+ T cells. In each of the 6 culture settings I measured the % of lymphocytes that were of each subtype (total T cells, CD4+ T cells, CD8+ T cells, NKT cells, NK cells and CD8+ NKT cells). In each of the 6 culture settings I also measured the proportion of T cells that were CD4+, CD69+ and CD25- (this set of cells has been suggested to act as a new subset of regulatory T cells, that inhibits T cell proliferation) [236], the % of lymphocytes that were both CD4+ and CD69+ and the % of lymphocytes that were CD4+, CD69+ and CD25+. In

total, I thus measure 61 proportions which again are extensively correlated. Using the script from Prof Dudbridge these were found to be equivalent to 29.6 independent phenotypes and I therefore set a significance threshold of 0.0017 to correct for multiple testing in this group of tests.

Table 6. 1: Flow cytometry antibody panel for LacCer experiment on ex-vivo cells.

Marker	Fluorochrome	Clone	Manufacturer
CD3	PE-Cy7	SK7	BD Bioscience
CD4	BUV737	SK3	BD Bioscience
CD8	APC	RPA-T8	BD Bioscience
CD56	PE	B156	BD Bioscience
LacCer	FITC	Huly-m13	LifeSpan Biosciences

Table 6. 2: Flow cytometry antibody panel for GPR65 functional assay on cultured cells.

Marker	Fluorochrome	Clone	Manufacturer
CD3	PE-Cy7	SK7	BD Bioscience
CD4	BUV737	SK3	BD Bioscience
CD8	APC	RPA-T8	BD Bioscience
CD25	FITC	M-A251	BD Bioscience
CD56	PE	B156	BD Bioscience
CD69	v450	FN50	BD Bioscience

6.3.1 LacCer (CD17) expression in ex-vivo cells

In my analysis of ex-vivo cells I found evidence that was just significant after correcting for multiple testing that carrying the protective allele at rs74796499 (A) reduces the LacCer expression on the surface of T cells, with similar effects in both CD4+ and CD8+ subtypes (Figure 6.4). The same trend is seen in NK cells but this does not remain significant after correction for multiple testing and no evidence of an effect is seen in the NKT cells (Figure 6.4).

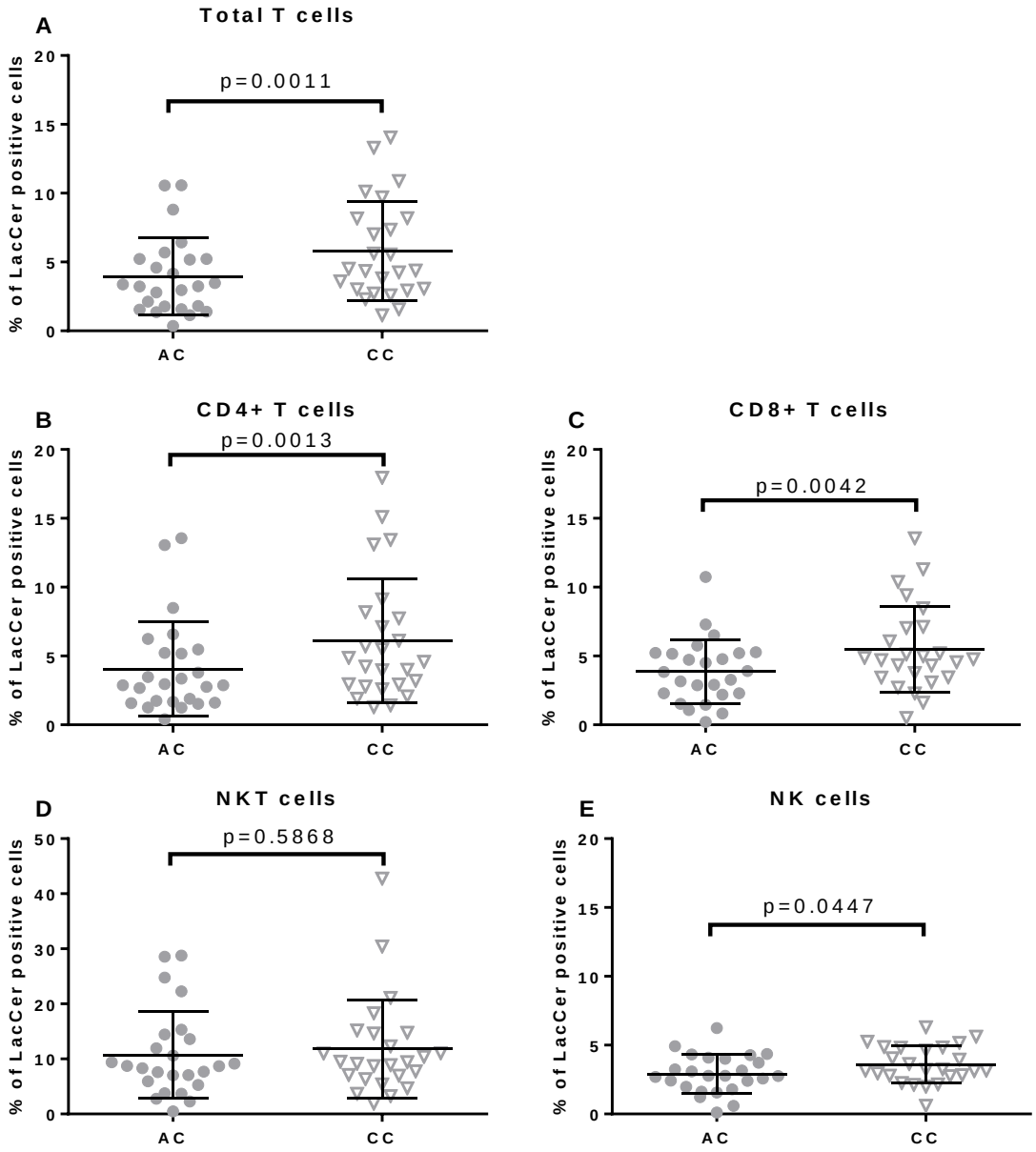

Figure 6. 4: LacCer expression on ex-vivo lymphocytes. Carriers of the protective allele (A/C) and non-carriers (C/C) are compared for total T cells (A), CD4+ T cells (B), CD8+ T cells (C), NKT cells (D) and NK cells (E).

6.3.2 CD25 and CD69 expression after pH specific cultures

As anticipated BTB09089 suppressed both CD25 and CD69 expression in stimulated cultures with a much larger effect in the acidic extracellular environment (pH=6.2) than at neutral pH (pH=7.0) (Figure 6.5 and 6.6). These differences at both pH are all statistically significantly different with $p<0.0001$ (unstimulated vs stimulated; stimulated vs stimulated with BTB09089) except for the suppression in NK cells at acid pH $p=0.1327$ (Figure 6.6B).

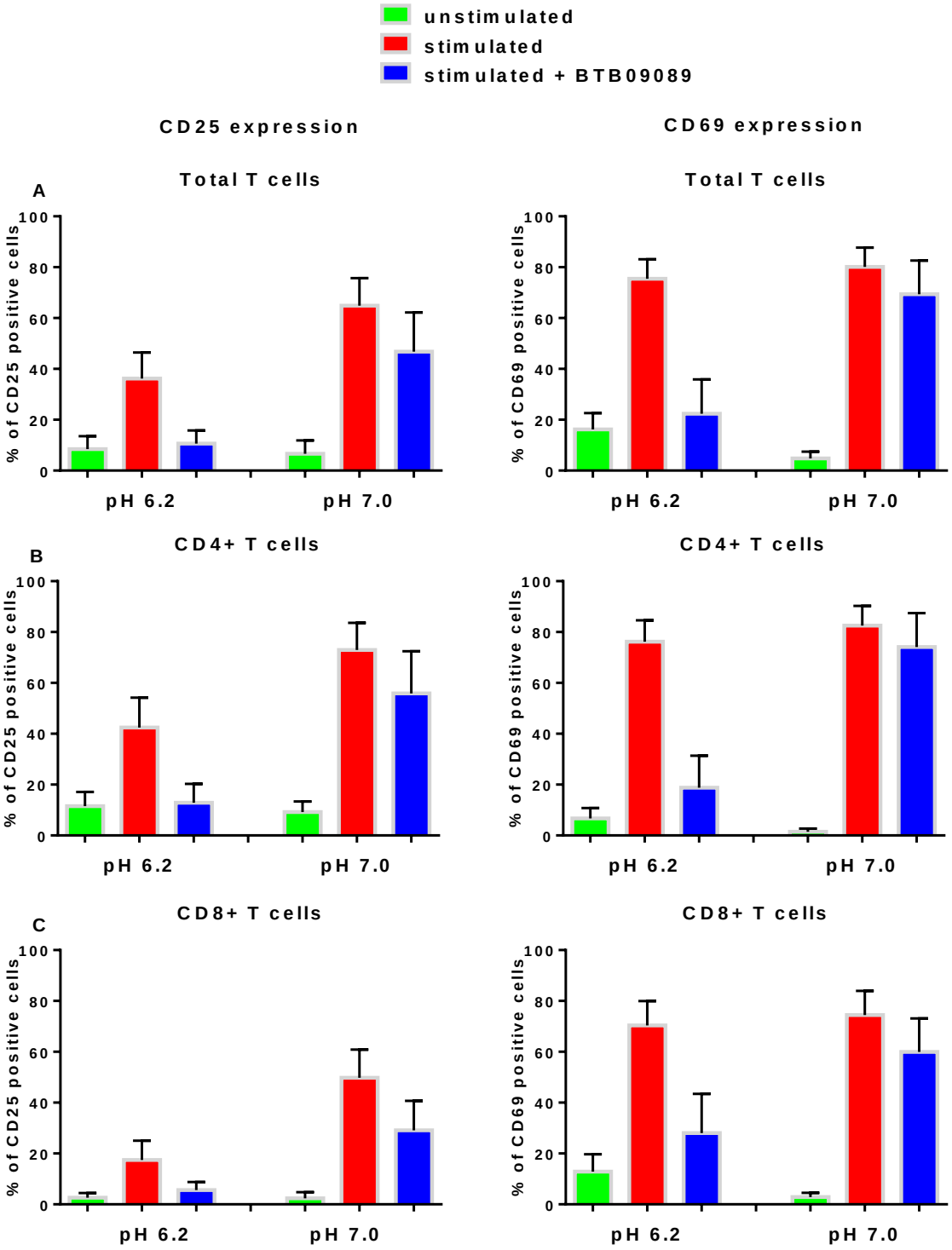

Figure 6. 5: CD25 and CD69 expression in total T cells (A), CD4+ T cells (B) and CD8+ T cells (C) unstimulated (green), stimulated without BTB09089 (red) and stimulated with BTB09089 (blue) in 18 hours cultures at pH 6.2 and pH 7.0. Histograms are based on the mean expression across all 50 samples with 4 technical replicates for each individual.

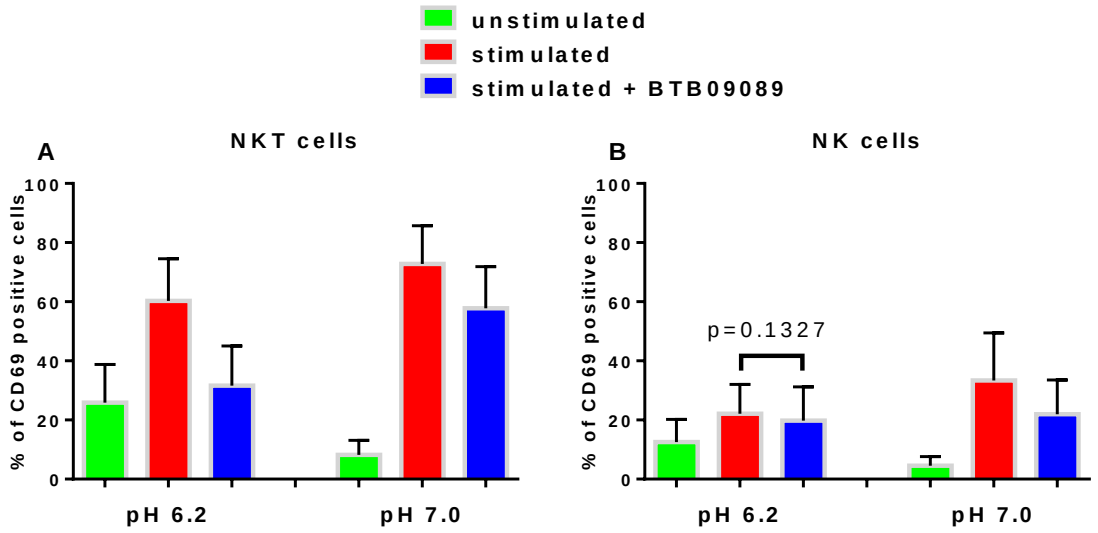

Figure 6. 6: CD25 and CD69 expression in NKT cells (A) and NK cells (B) unstimulated (green), stimulated without BTB09089 (red) and stimulated with BTB09089 (blue) in 18 hours cultures at pH 6.2 and pH 7.0. Histograms are based on the mean expression across all 50 samples with 4 technical replicates for each individual.

6.3.3 Surface expression of CD69

Figures 6.7, 6.8, 6.9, 6.10, 6.11, 6.12 and 6.13 show the effects of rs74796499 genotype on CD69 expression in each culture setting and at each pH for total T cells, CD4+ T cells, CD8+ T cells, NKT cells, CD8+ NKT cells, NK cells and B cell enriched lymphocytes (CD3-, CD56-) respectively. In keeping with my earlier results in unstimulated cultures at acidic pH (pH=6.2) I saw greater expression of CD69 in T cells from individuals carrying a protective allele at rs74796499 (Figure 6.7) although this difference did not survive correction for multiple testing. In Chapter 5, I measured CD69 in total T cells, NKT cells and NK cells after 18 hours of cultures at pH 6.2 (without anti-CD3/CD28 stimulation or BTB09089) in 23 genotyped matched pairs (46 individuals). Eleven of these subjects were also included in the analysis described in this chapter; including one complete genotyped matched pair and nine single individuals from other pairs. Removing the 11 overlapping subjects from the Chapter 5 data together with their 9 counterpart subjects left a total of 13 genotype matched pairs (26 individuals) that were non-overlapping with the data described in this chapter. Combining the non-overlapping data enabled an analysis of 38 genotyped matched pairs (76 individuals) for CD69 expression in total T cells, NKT cells and NK cells after 18 hours of unstimulated culture at pH 6.2 (without BTB09089), but there was no meaningful change in the results, with no

significant evidence of any genotype dependent difference in NKT cells or NK cells, but a higher proportion of CD69 positive T cells in the protective allele carriers (Figure 6.14).

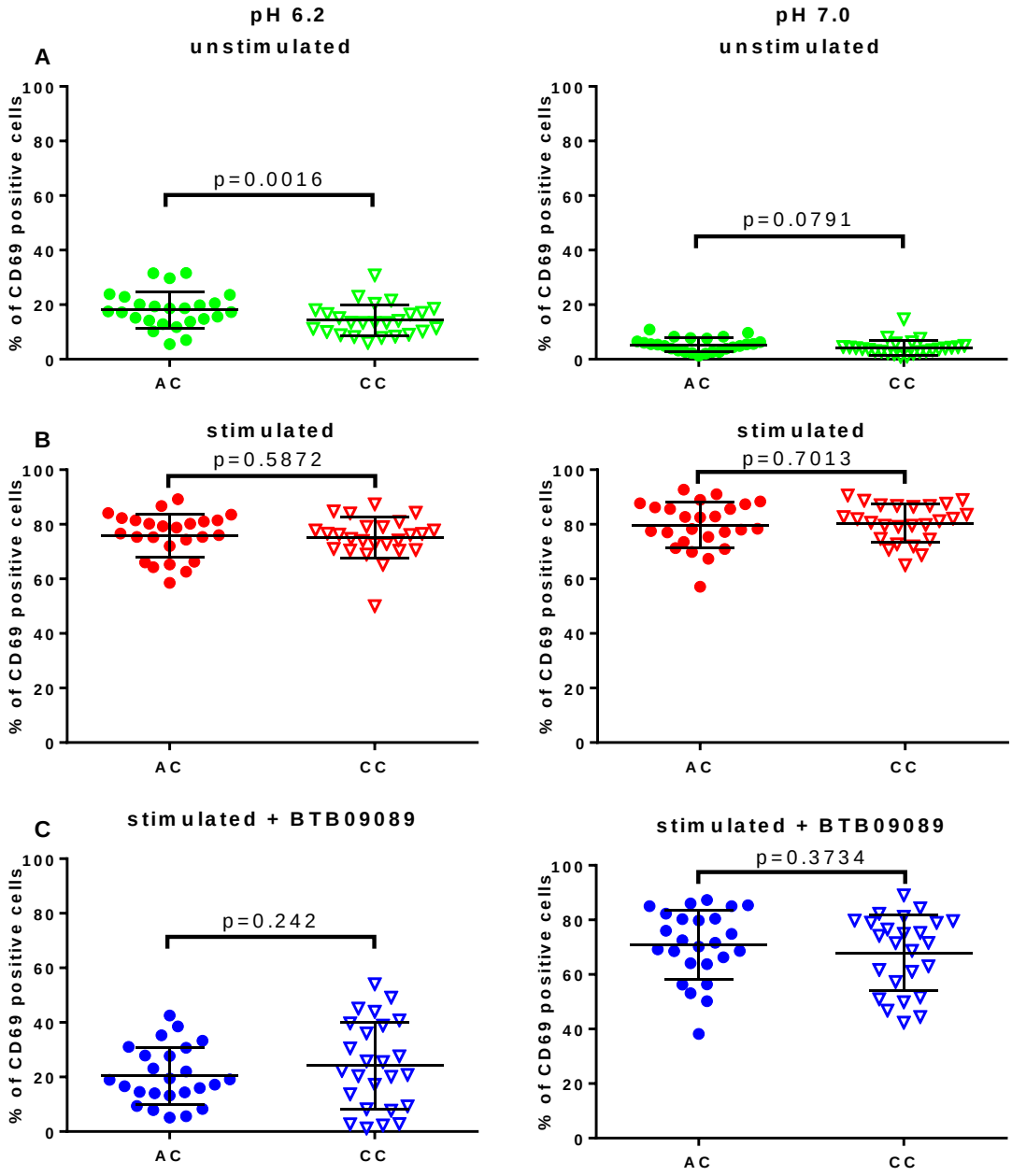

Figure 6. 7: Expression of CD69 on total T cells in protective allele carriers (circles) and risk allele homozygotes (inverted triangles) after 18 hours culture at pH 6.2 and pH 7.0 for each of the three culture settings; unstimulated (green), stimulated in the absence of BTB09089 (red) and stimulated in the presence of BTB09089 (blue).

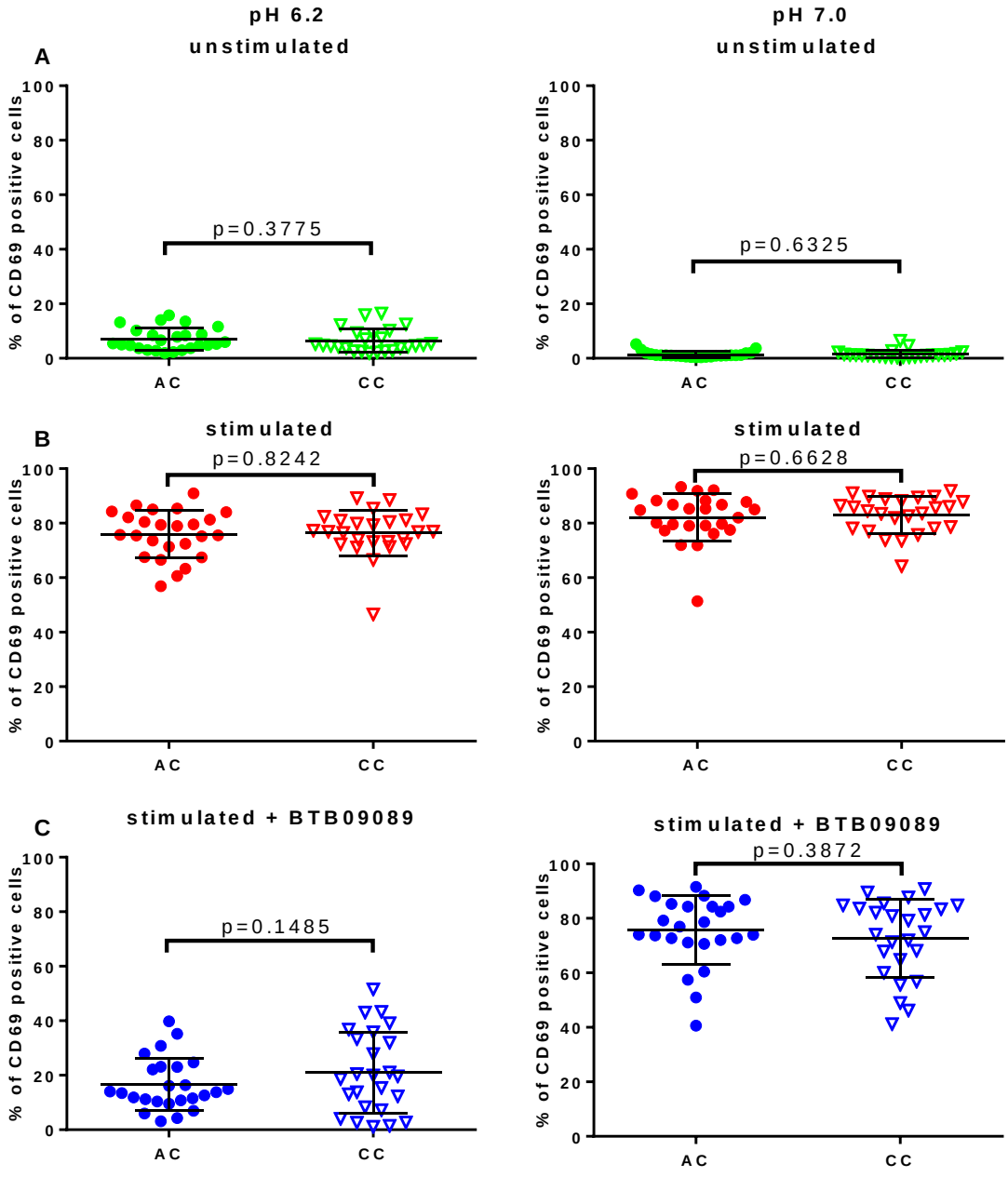

Figure 6. 8: Expression of CD69 on CD4+ T cells in protective allele carriers (circles) and risk allele homozygotes (inverted triangles) after 18 hours culture at pH 6.2 and pH 7.0 for each of the three culture settings; unstimulated (green), stimulated in the absence of BTB09089 (red) and stimulated in the presence of BTB09089 (blue).

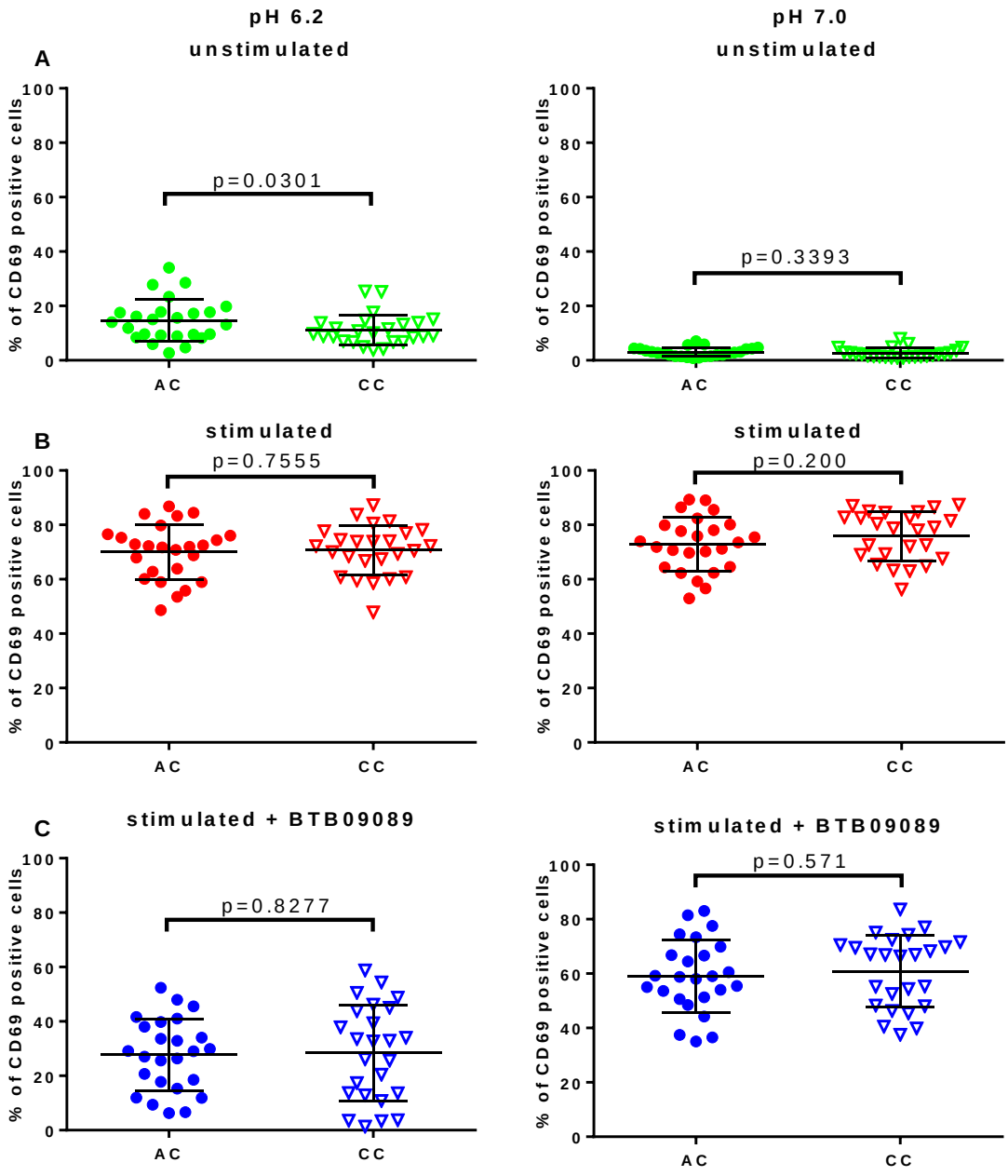

Figure 6. 9: Expression of CD69 on CD8+ T cells in protective allele carriers (circles) and risk allele homozygotes (inverted triangles) after 18 hours culture at pH 6.2 and pH 7.0 for each of the three culture settings; unstimulated (green), stimulated in the absence of BTB09089 (red) and stimulated in the presence of BTB09089 (blue).

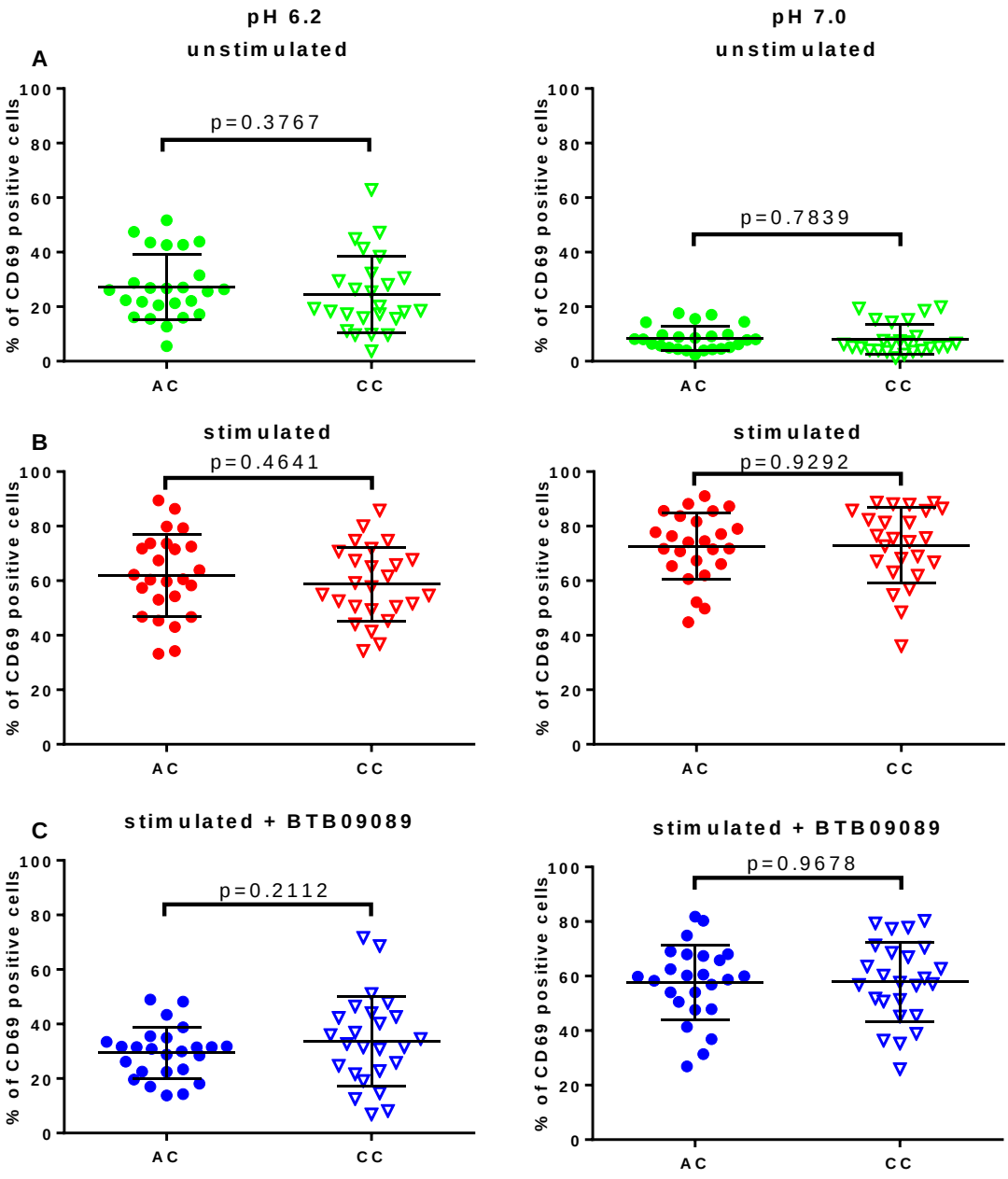

Figure 6. 10: Expression of CD69 on NKT cells in protective allele carriers (circles) and risk allele homozygotes (inverted triangles) after 18 hours culture at pH 6.2 and pH 7.0 for each of the three culture settings; unstimulated (green), stimulated in the absence of BTB09089 (red) and stimulated in the presence of BTB09089 (blue).

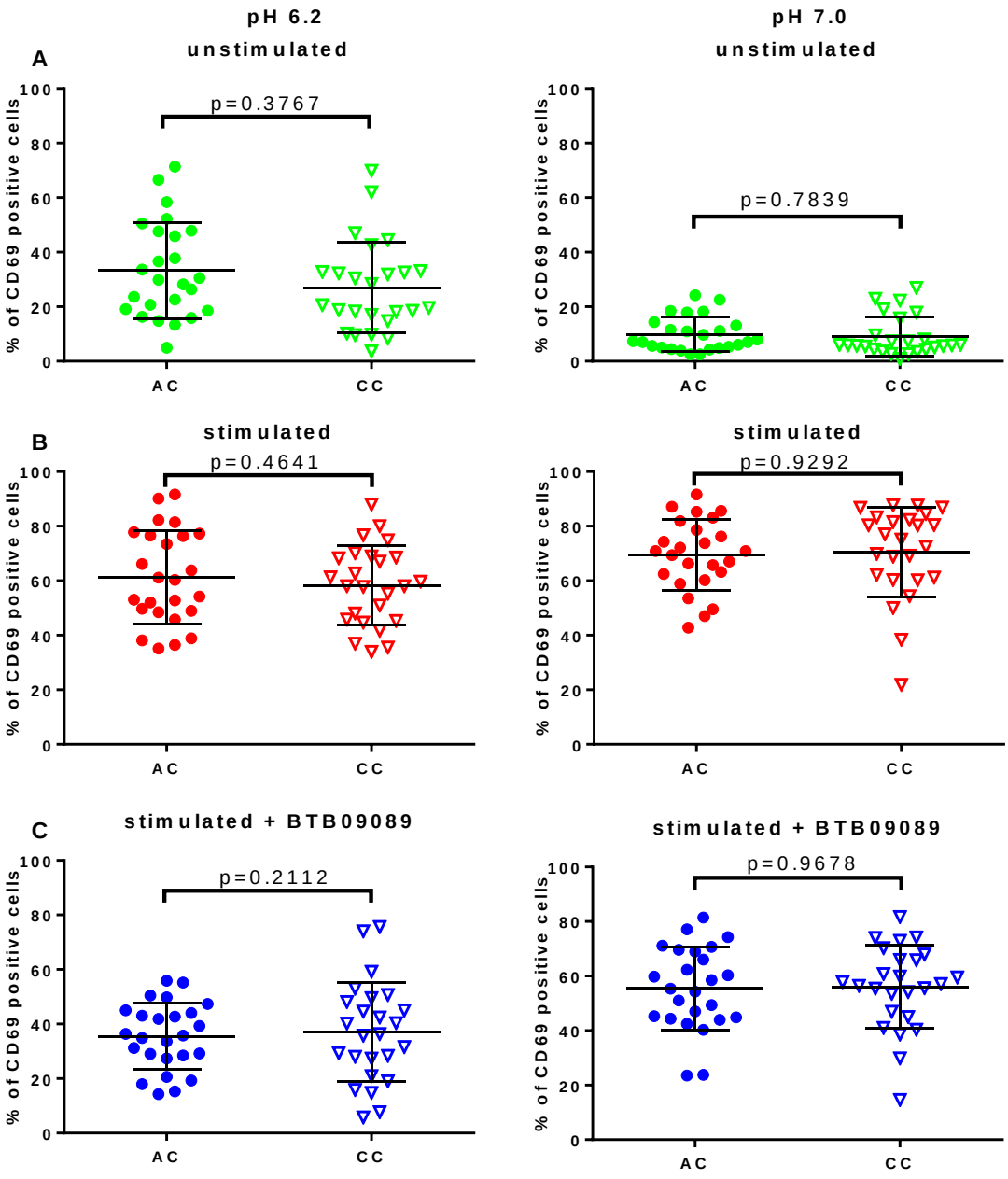

Figure 6. 11: Expression of CD69 on CD8+ NKT cells in protective allele carriers (circles) and risk allele homozygotes (inverted triangles) after 18 hours culture at pH 6.2 and pH 7.0 for each of the three culture settings; unstimulated (green), stimulated in the absence of BTB09089 (red) and stimulated in the presence of BTB09089 (blue).

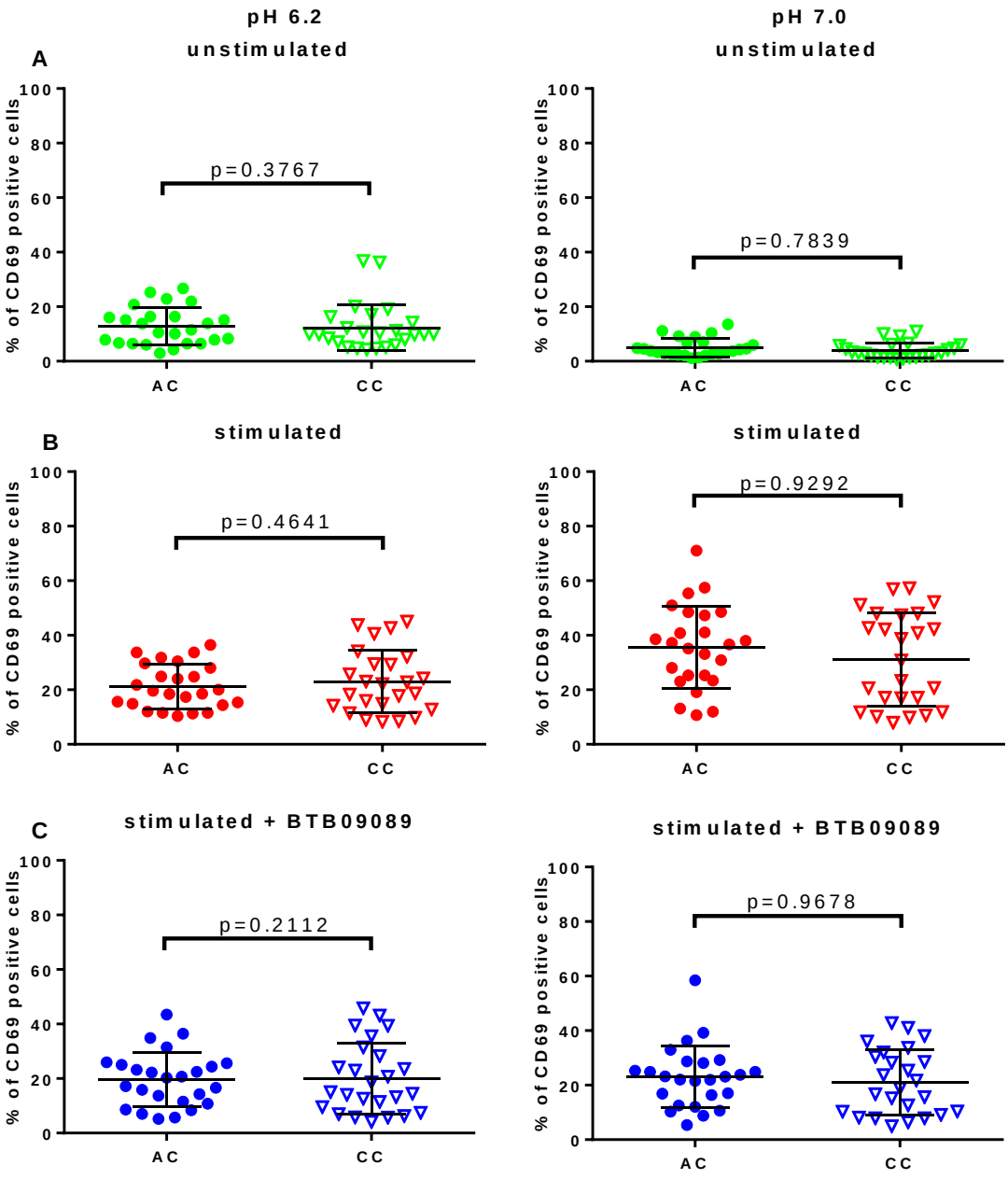

Figure 6. 12: Expression of CD69 on NK cells in protective allele carriers (circles) and risk allele homozygotes (inverted triangles) after 18 hours culture at pH 6.2 and pH 7.0 for each of the three culture settings; unstimulated (green), stimulated in the absence of BTB09089 (red) and stimulated in the presence of BTB09089 (blue).

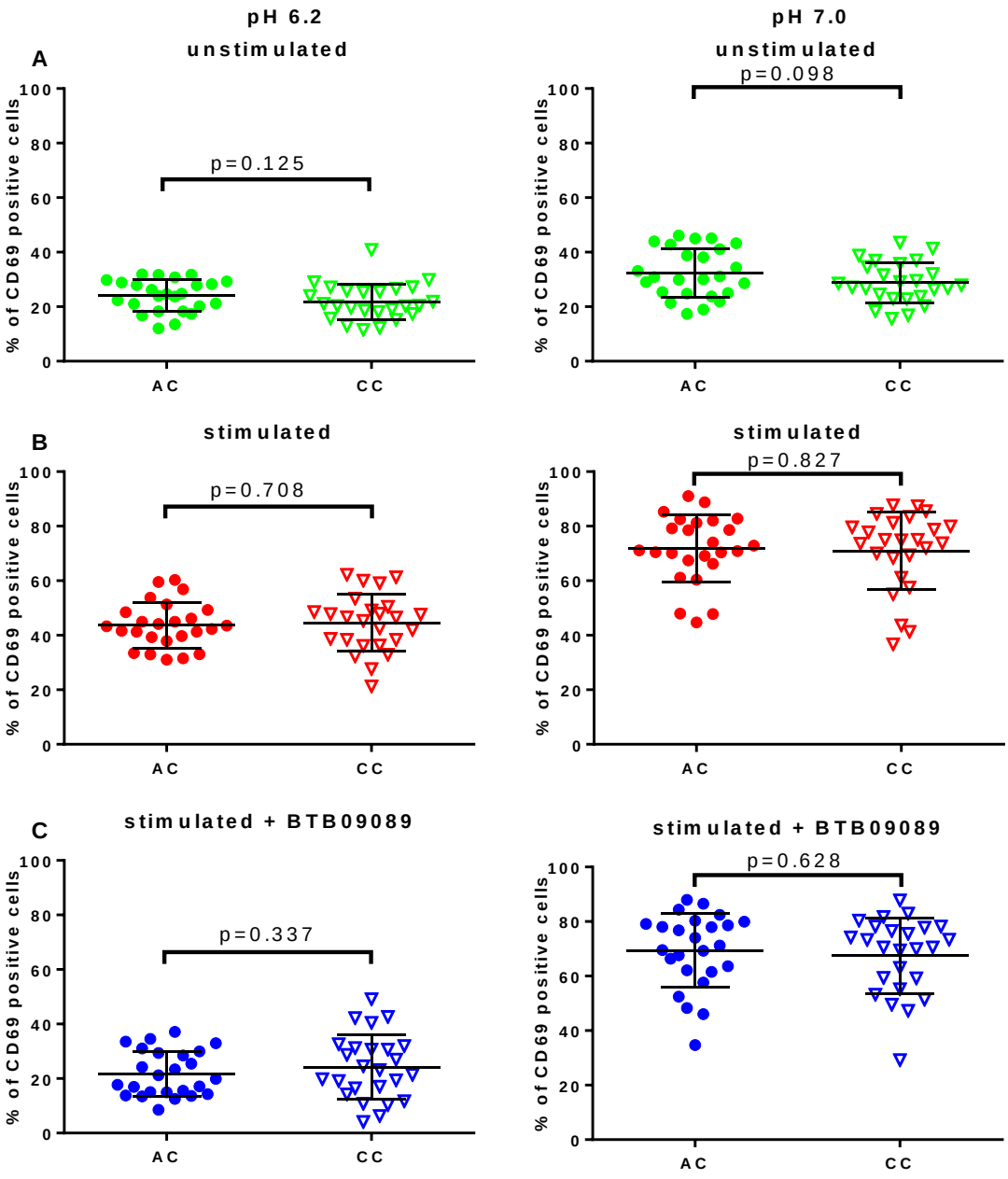

Figure 6. 13: Expression of CD69 on CD3- CD56- lymphocytes in protective allele carriers (circles) and risk allele homozygotes (inverted triangles) after 18 hours culture at pH 6.2 and pH 7.0 for each of the three culture settings; unstimulated (green), stimulated in the absence of BTB09089 (red) and stimulated in the presence of BTB09089 (blue).

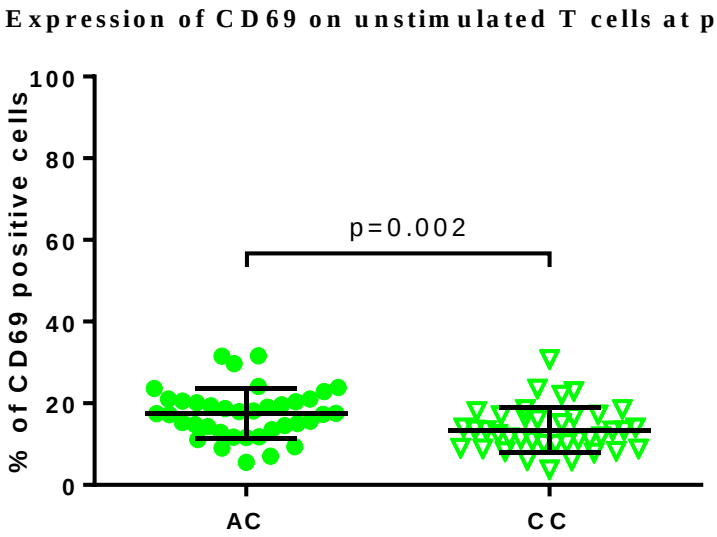

Figure 6. 14: Expression of CD69 on total T cells in protective allele carriers (circles) and risk allele homozygotes (inverted triangles) after 18 hours culture at pH 6.2 without any stimulation with anti-CD3/CD28 antibodies and without any BTB09089.

6.3.4 Surface expression of CD25

Figures 6.15, 6.16, 6.17, 6.18 and 6.19 show the effects of rs74796499 genotype on CD25 expression in each culture setting and at each pH for total T cells, CD4+ T cells, CD8+ T cells, NKT cells and CD8+ NKT cells (the number of CD25 positive NK cells or enriched B cells is very low, these cell types were therefore not analysed). Extending the analysis for T cells, CD4+ T cells and CD8+ T cells for the stimulated without BTB09089 at pH 7.0 using the data from the 13 non-overlapping pairs from Chapter 5 (as described above) did not reveal any significant associations.

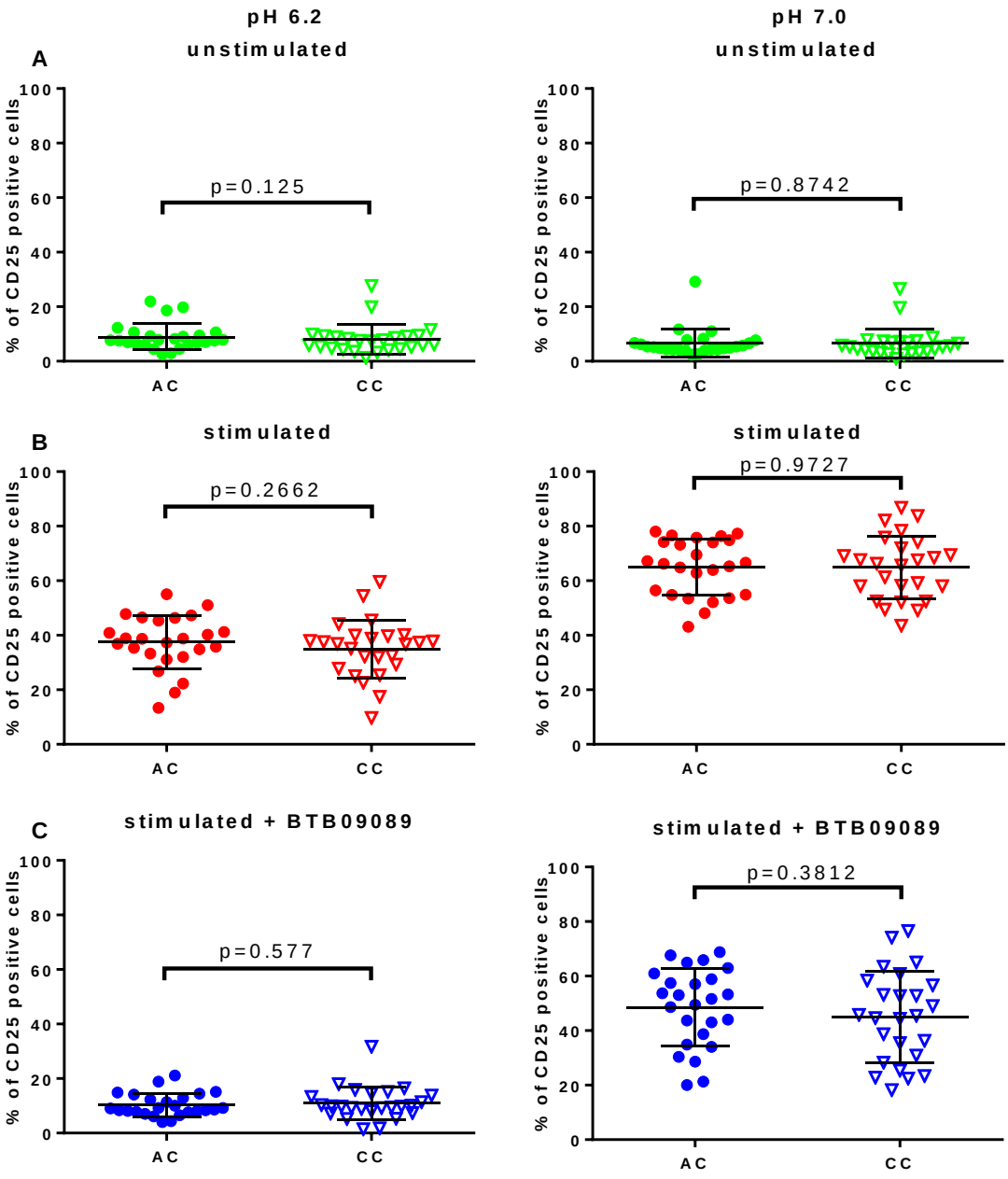

Figure 6. 15: Expression of CD25 on total T cells in protective allele carriers (circles) and risk allele homozygotes (inverted triangles) after 18 hours culture at pH 6.2 and pH 7.0 for each of the three culture settings; unstimulated (green), stimulated in the absence of BTB09089 (red) and stimulated in the presence of BTB09089 (blue).

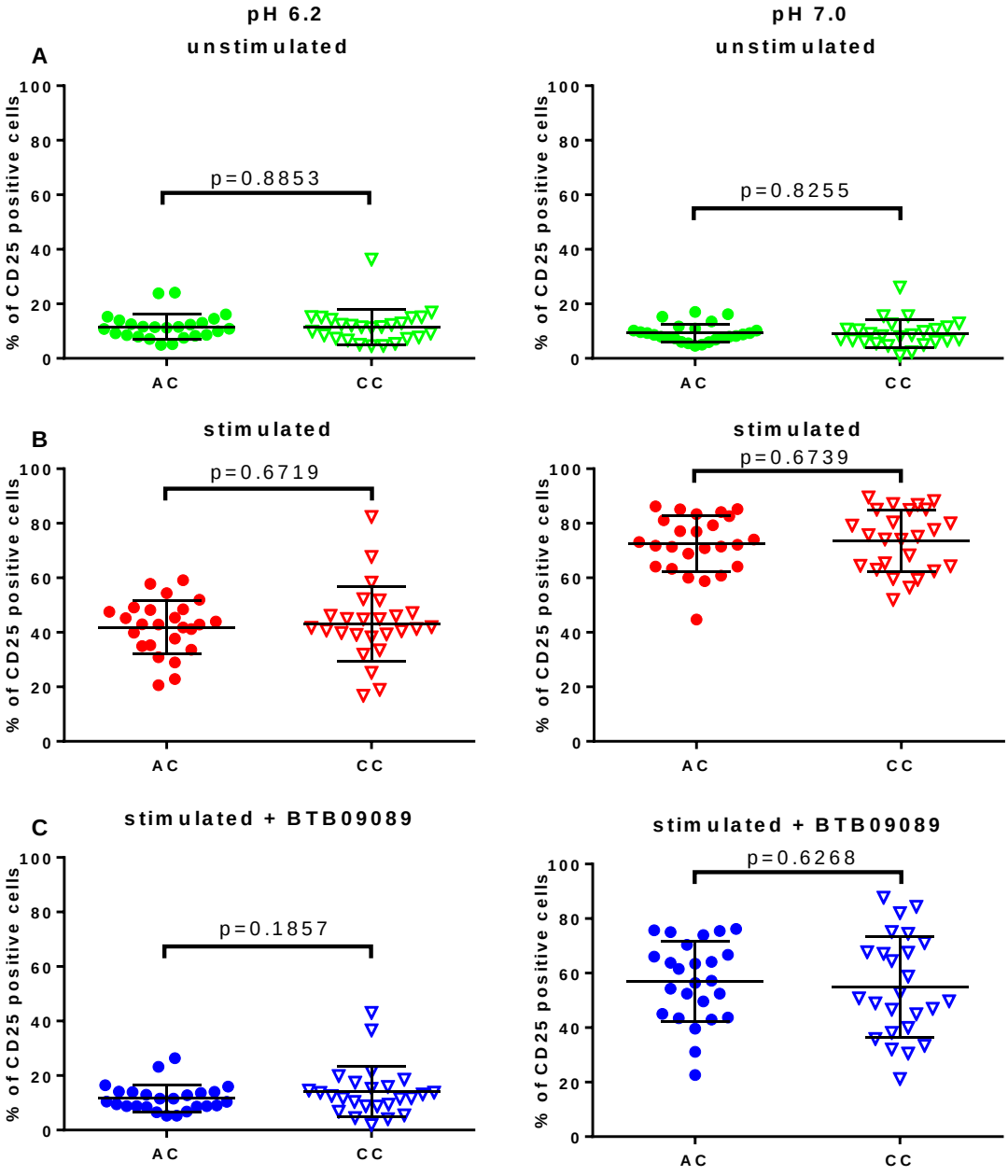

Figure 6. 16: Expression of CD25 on CD4+ T cells in protective allele carriers (circles) and risk allele homozygotes (inverted triangles) after 18 hours culture at pH 6.2 and pH 7.0 for each of the three culture settings; unstimulated (green), stimulated in the absence of BTB09089 (red) and stimulated in the presence of BTB09089 (blue).

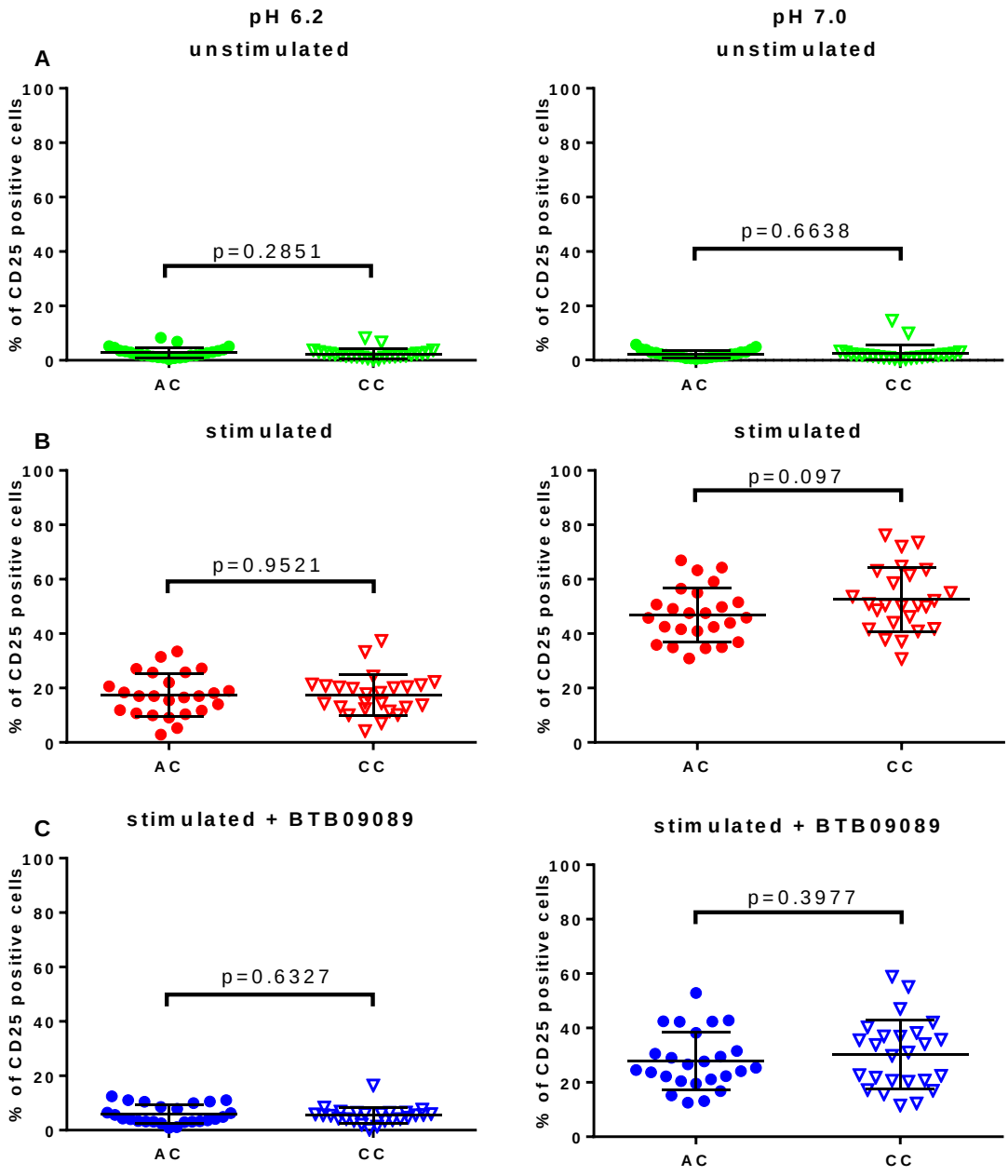

Figure 6. 17: Expression of CD25 on CD8+ T cells in protective allele carriers (circles) and risk allele homozygotes (inverted triangles) after 18 hours culture at pH 6.2 and pH 7.0 for each of the three culture settings; unstimulated (green), stimulated in the absence of BTB09089 (red) and stimulated in the presence of BTB09089 (blue).

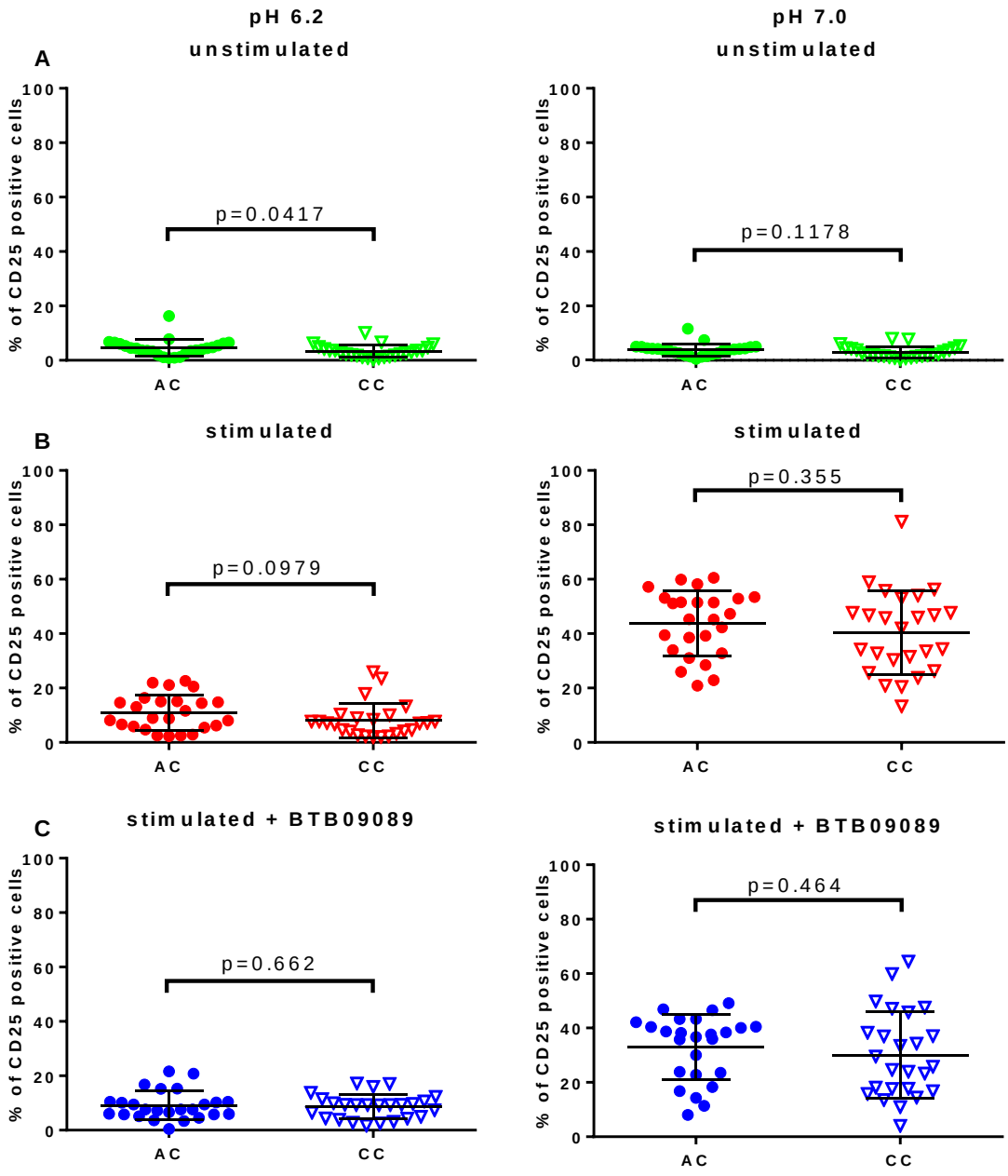

Figure 6. 18: Expression of CD25 on NKT cells in protective allele carriers (circles) and risk allele homozygotes (inverted triangles) after 18 hours culture at pH 6.2 and pH 7.0 for each of the three culture settings; unstimulated (green), stimulated in the absence of BTB09089 (red) and stimulated in the presence of BTB09089 (blue).

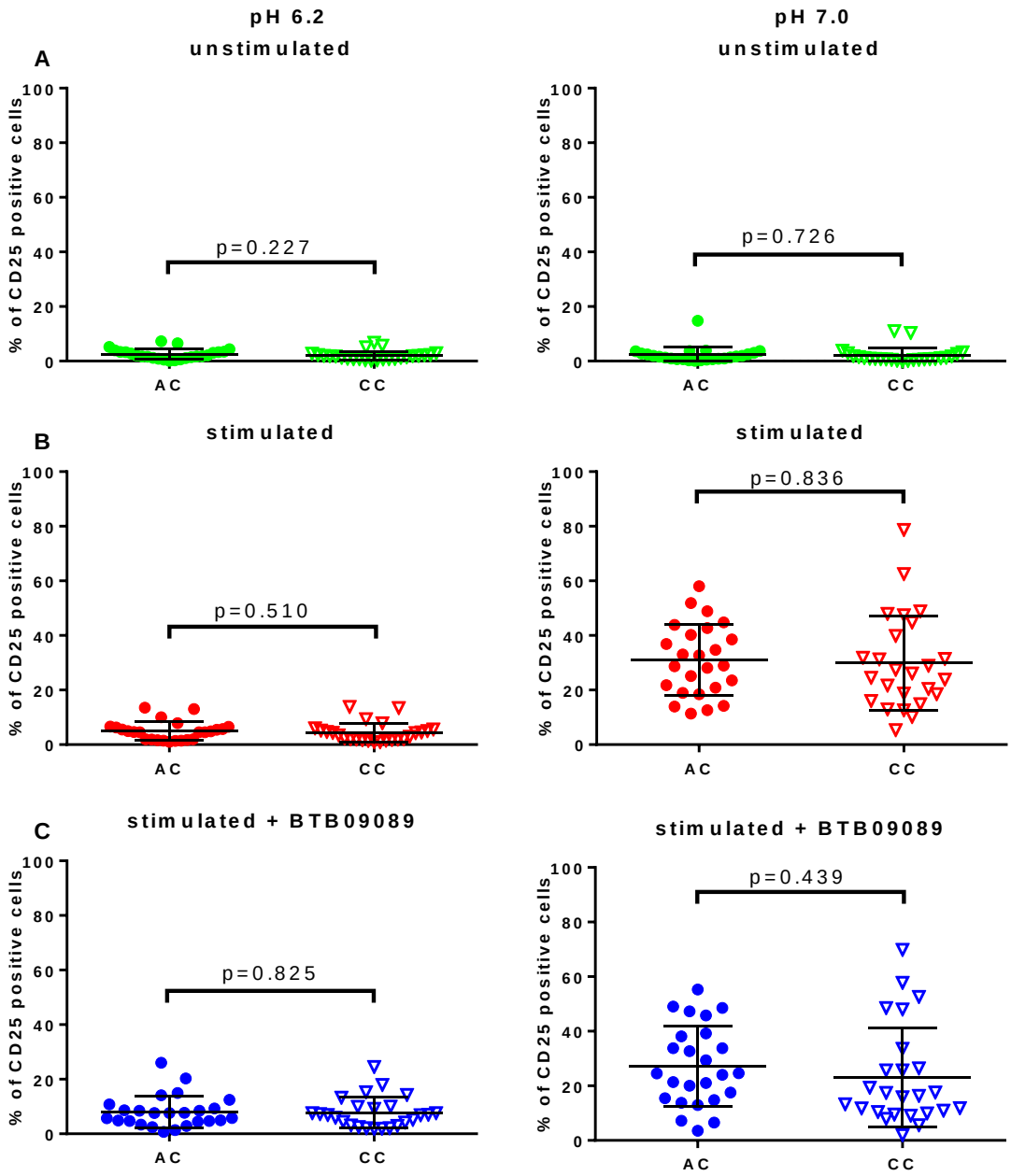

Figure 6. 19: Expression of CD25 on CD8+ NKT cells in protective allele carriers (circles) and risk allele homozygotes (inverted triangles) after 18 hours culture at pH 6.2 and pH 7.0 for each of the three culture settings; unstimulated (green), stimulated in the absence of BTB09089 (red) and stimulated in the presence of BTB09089 (blue).

6.4 Cell subtype proportion results

6.4.1 Cell subtype proportions in ex-vivo cells

Figures 6.20 shows the influence of the rs74796499 genotype on the proportion of ex-vivo T cells, CD4+ T cells, CD8+ T, NKT cells and CD8+ NKT cells and NK cells, as well as the

CD4/CD8 ratio. Although the p value did not survive correction for multiple testing, this analysis revealed a trend towards rs74796499 genotype influencing the CD4/CD8 ratio.

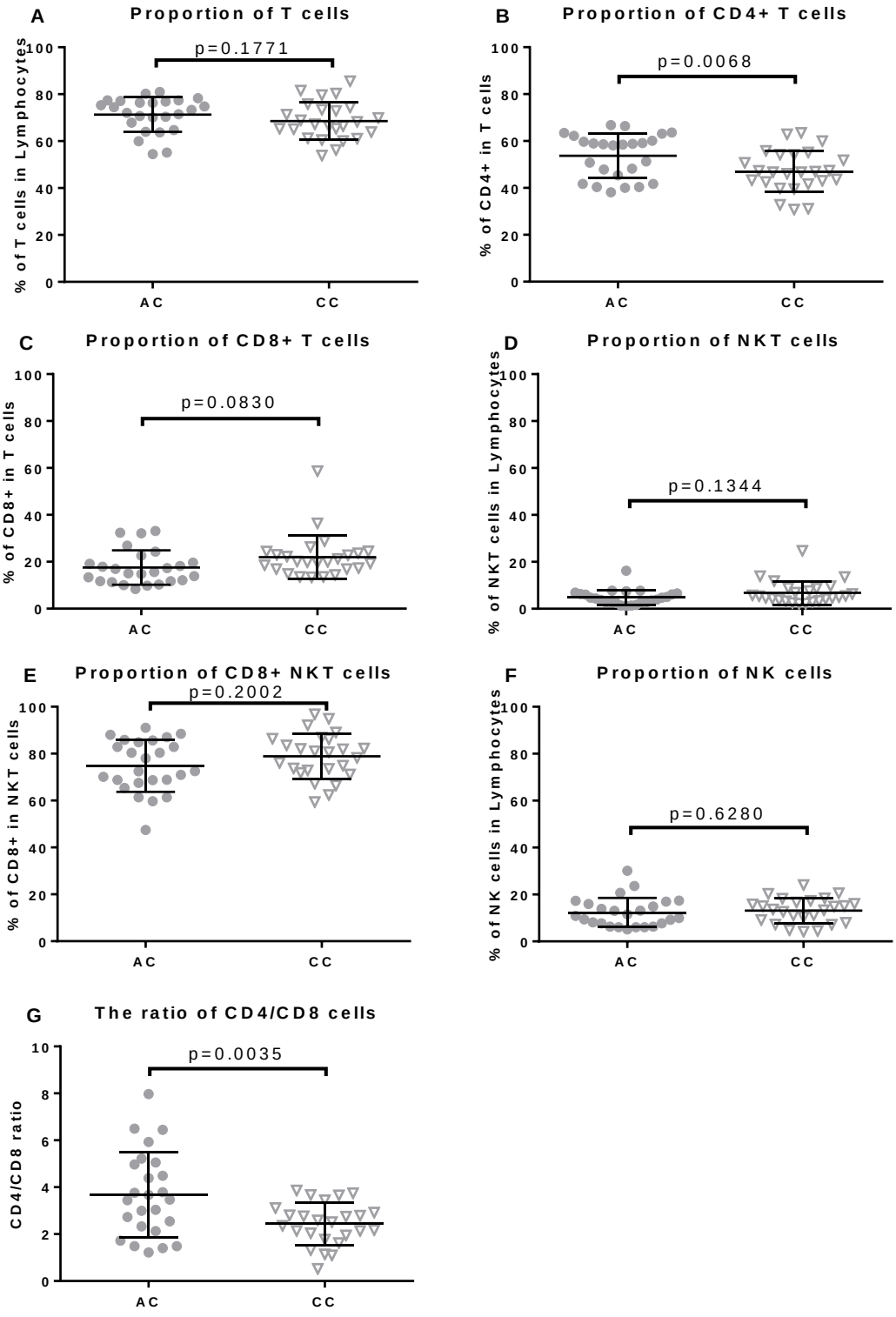

Figure 6. 20: The influence of genotype on the proportion of T cells that were CD4+ and CD8+, NKT cells and NK cells in ex-vivo cells, also the percentage of NKT cells that were CD8+. Figure (G) shows the ratio of CD4+/CD8+ T cells in ex-vivo cells.

6.4.2 Proportions of T cell subtypes after culture

Figures 6.21, 6.22 and 6.23 show the effects of rs74796499 genotype on cell subtype proportions in each culture setting and at each pH for the proportion of T cells that are CD4+, CD8+, and the ratio of CD4/CD8.

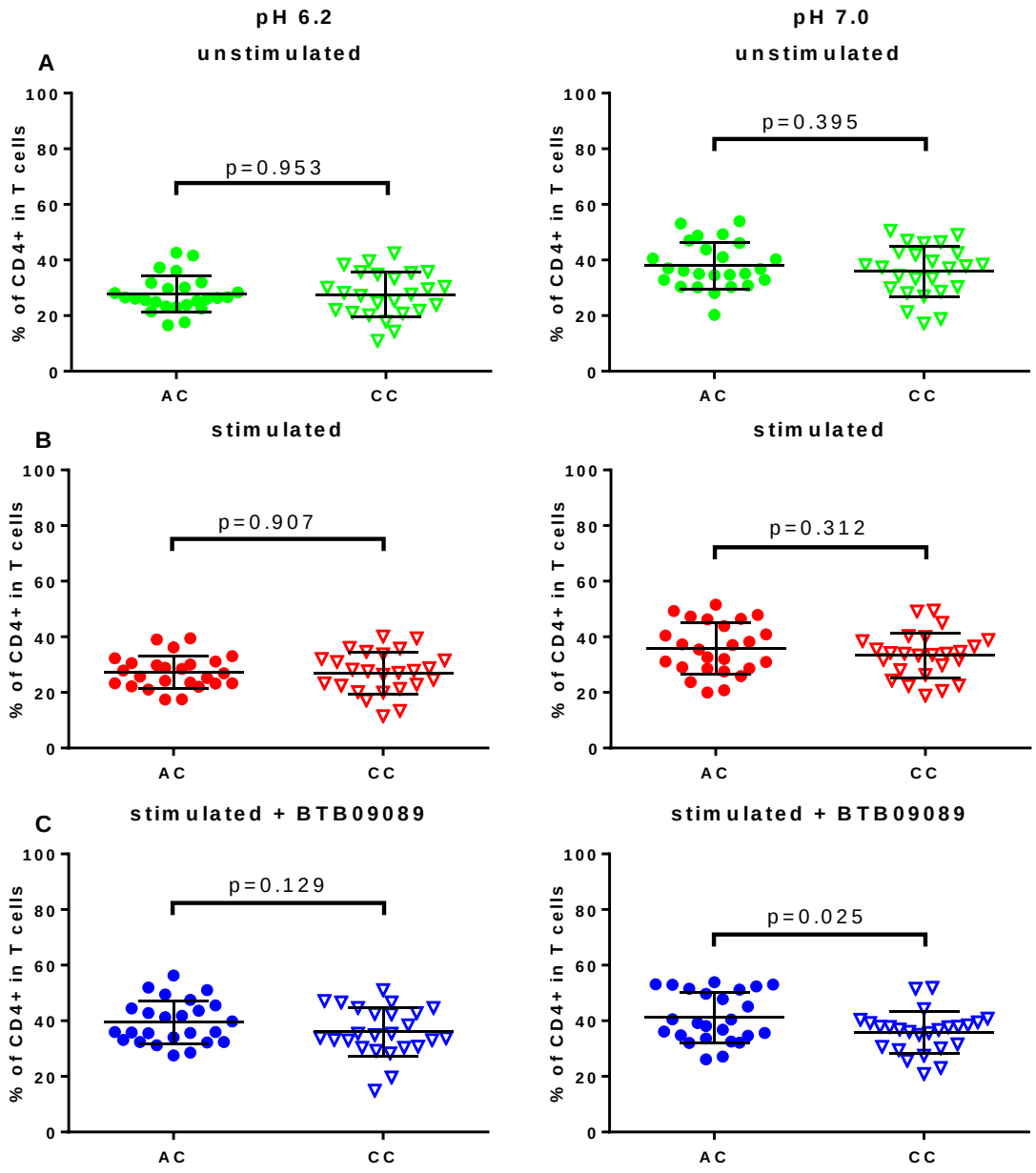

Figure 6. 21: Proportion of T cells that are CD4+ in protective allele carriers (circles) and risk allele homozygotes (inverted triangles) after 18 hours culture at pH 6.2 and pH 7.0 for each of the three culture settings; unstimulated (green), stimulated in the absence of BTB09089 (red) and stimulated in the presence of BTB09089 (blue).

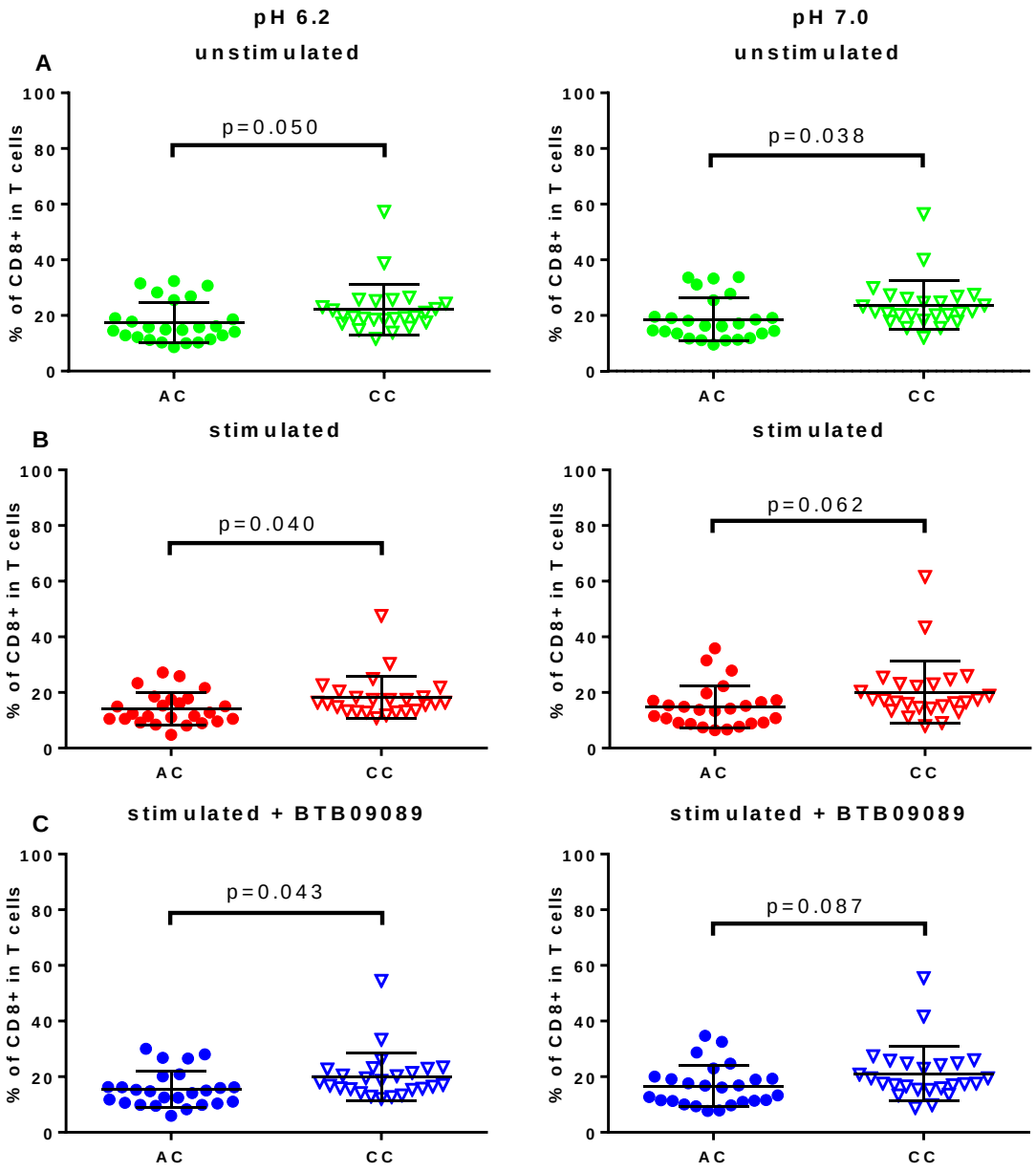

Figure 6. 22: Proportion of T cells that are CD8+ in protective allele carriers (circles) and risk allele homozygotes (inverted triangles) after 18 hours culture at pH 6.2 and pH 7.0 for each of the three culture settings; unstimulated (green), stimulated in the absence of BTB09089 (red) and stimulated in the presence of BTB09089 (blue).

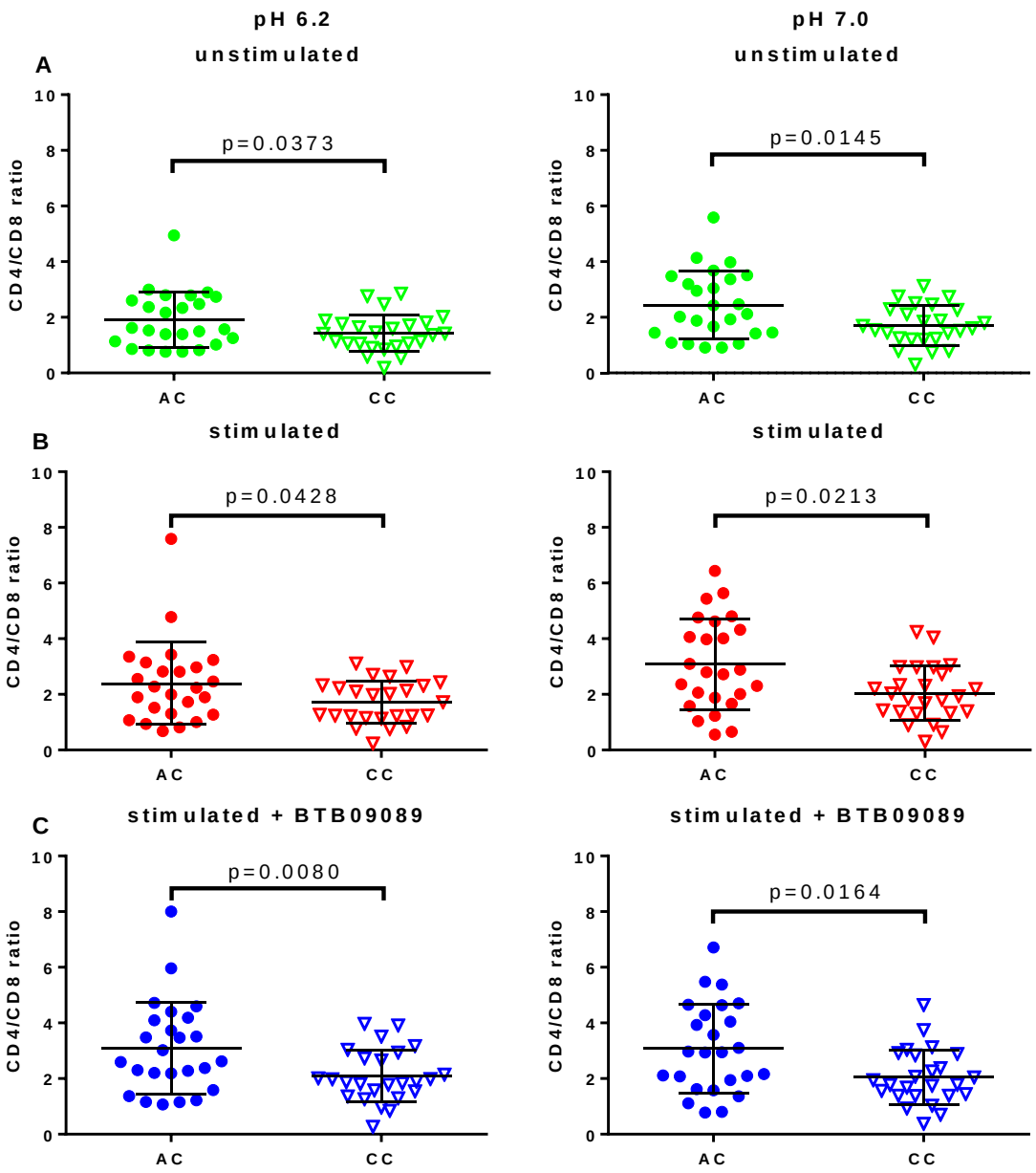

Figure 6. 23: The CD4/CD8 ratio in protective allele carriers (circles) and risk allele homozygotes (inverted triangles) after 18 hours culture at pH 6.2 and pH 7.0 for each of the three culture settings; unstimulated (green), stimulated in the absence of BTB09089 (red) and stimulated in the presence of BTB09089 (blue).

6.4.3 Proportion of NKT cells that are CD8+

In each of the culture settings I found that on average the proportion of NKT cells that are CD8+ (also known as CD8+ T cell that are CD56+) was lower in individuals carrying the protective allele than in risk allele homozygotes (Figure 6.10), with all but one of these differences being nominally significant but again none survived correction for multiple testing.

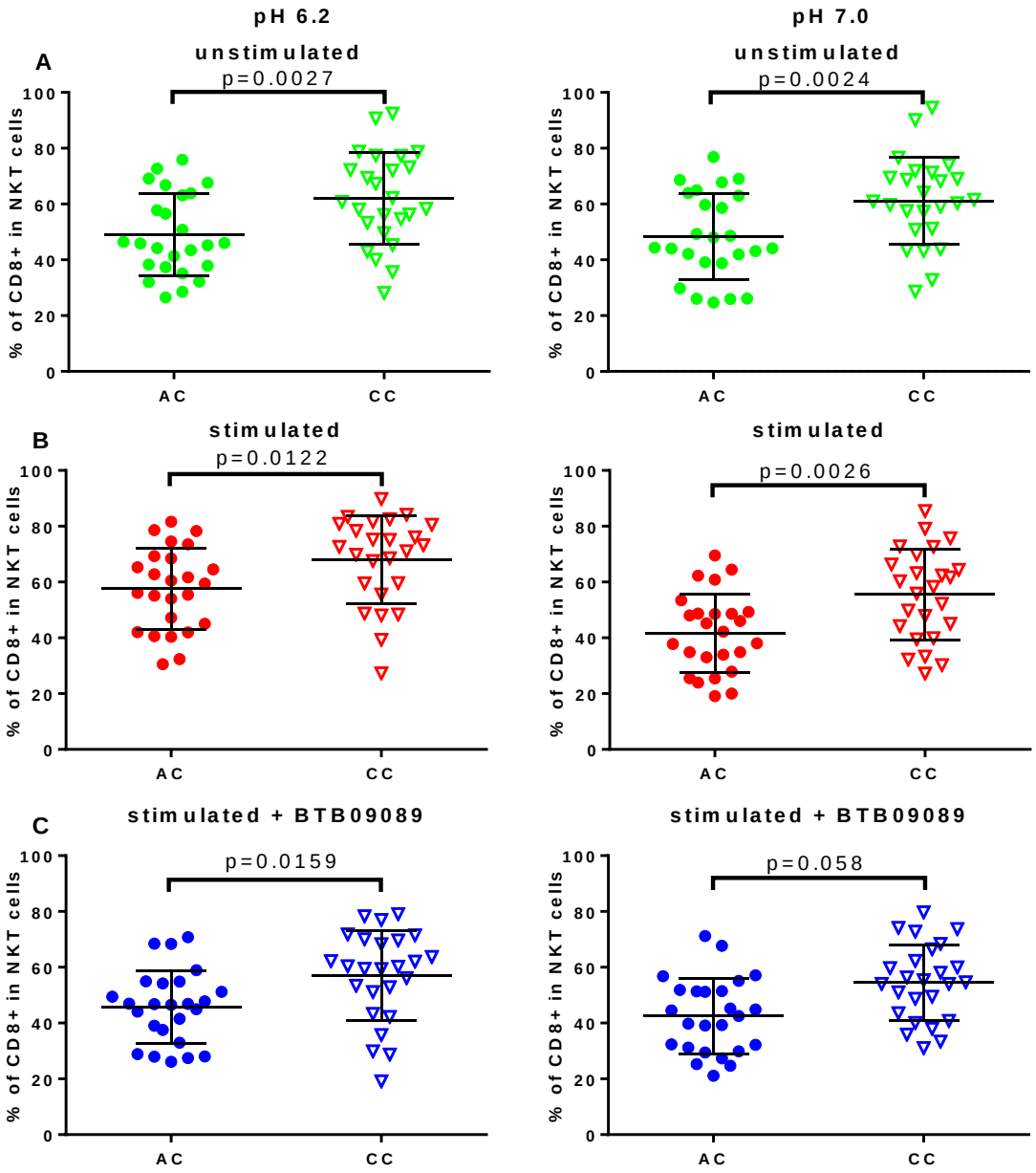

Figure 6. 24: Proportion of NKT cells that are CD8+ in protective allele carriers (circles) and risk allele homozygotes (inverted triangles) after 18 hours culture at pH 6.2 and pH 7.0 for each of the three culture settings; unstimulated (green), stimulated in the absence of BTB09089 (red) and stimulated in the presence of BTB09089 (blue).

6.5 MS associated variant - rs11052877

Given of the suggestion that the expression of CD69 might be influenced by the genotype at rs74796499 it seemed logical to also consider the effects of rs11052877, an independent SNP which was identified as a susceptibility variant in the MS Immunochip study and maps to the 3' UTR of the CD69 gene on chromosome 12p13 [151]. I therefore genotyped the rs11052877 variant in my 50 samples and found 18 protective allele homozygotes (A/A), 26 heterozygotes (A/G) and 5 risk allele homozygotes (G/G). I then tested the CD69 expression data from each of the cell types in each of the culture settings for association with this SNP. Since all three genotypes were included in this data set I completed the analysis using the logistic regression option in PLINK. Because the paired processing of samples was based on the genotype at rs74796499 many of these pairs had the same genotype at rs11052877, I was therefore not able to include the pair ID as categorical covariates. The results for each cell type are shown in Figures 6.25, 6.26, 6.27, 6.28, 6.29 and 6.30. As with rs74796499 a trend towards higher expression in carriers of the rs11052877 protective allele was seen in many cells subtypes; this trend being most statistically significant in NK cells.

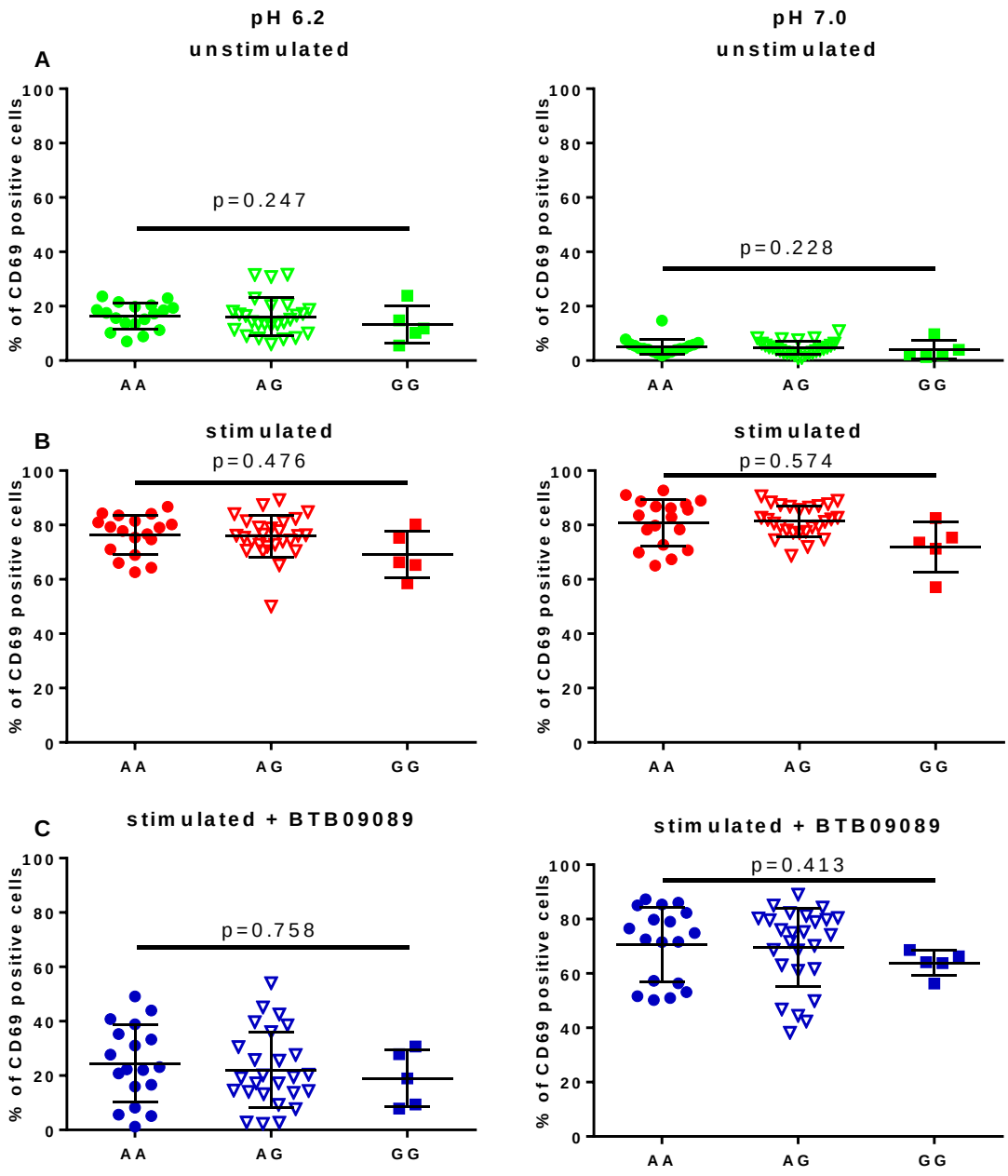

Figure 6. 25: Expression of CD69 on total T cells in protective allele homozygotes (circles), heterozygotes (inverted triangles) and risk allele homozygotes (squares) after 18 hours culture at pH 6.2 and pH 7.0 for each of the three culture settings; unstimulated (green), stimulated in the absence of BTB09089 (red) and stimulated in the presence of BTB09089 (blue).

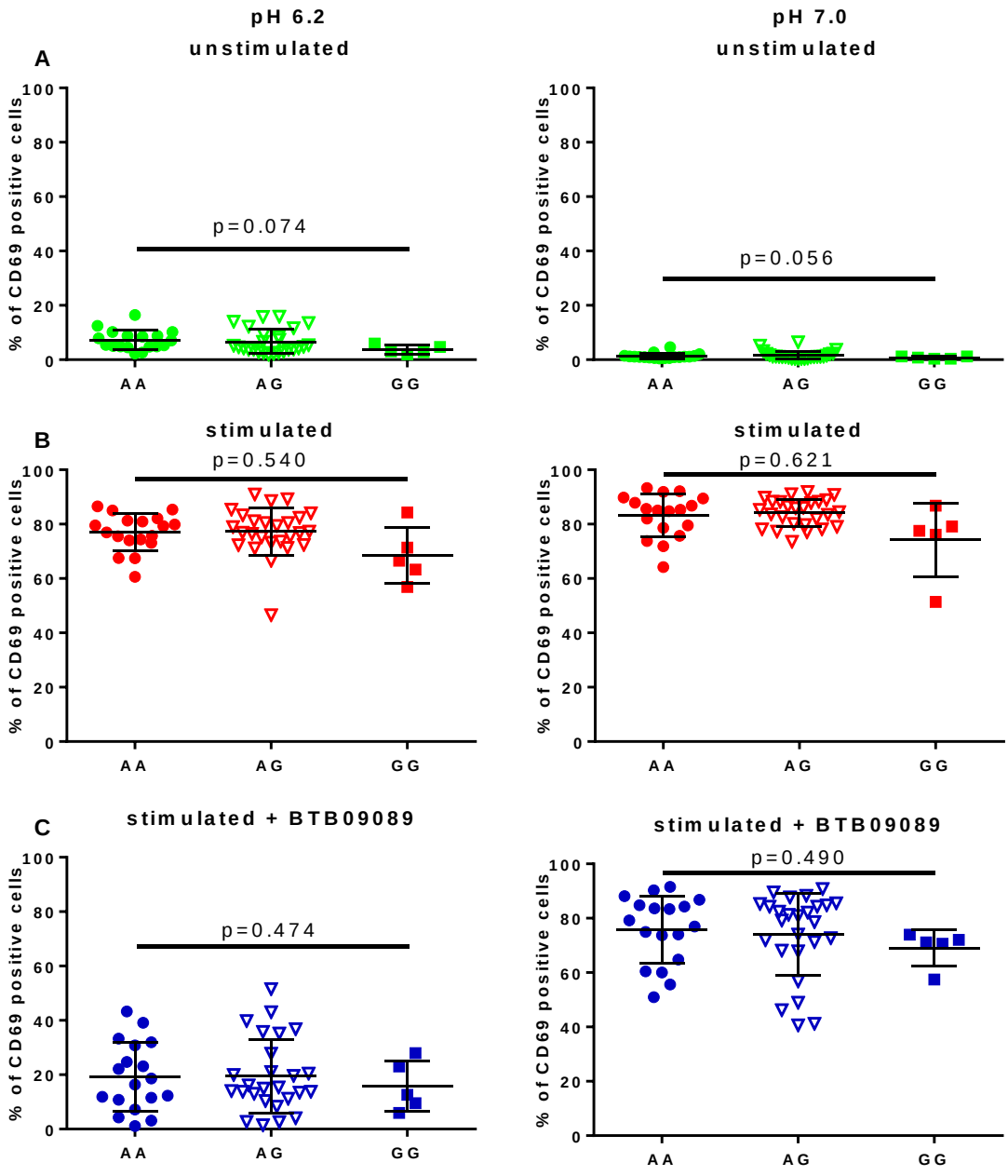

Figure 6. 26: Expression of CD69 on CD4+ T cells in protective allele homozygotes (circles), heterozygotes (inverted triangles) and risk allele homozygotes (squares) after 18 hours culture at pH 6.2 and pH 7.0 for each of the three culture settings; unstimulated (green), stimulated in the absence of BTB09089 (red) and stimulated in the presence of BTB09089 (blue).

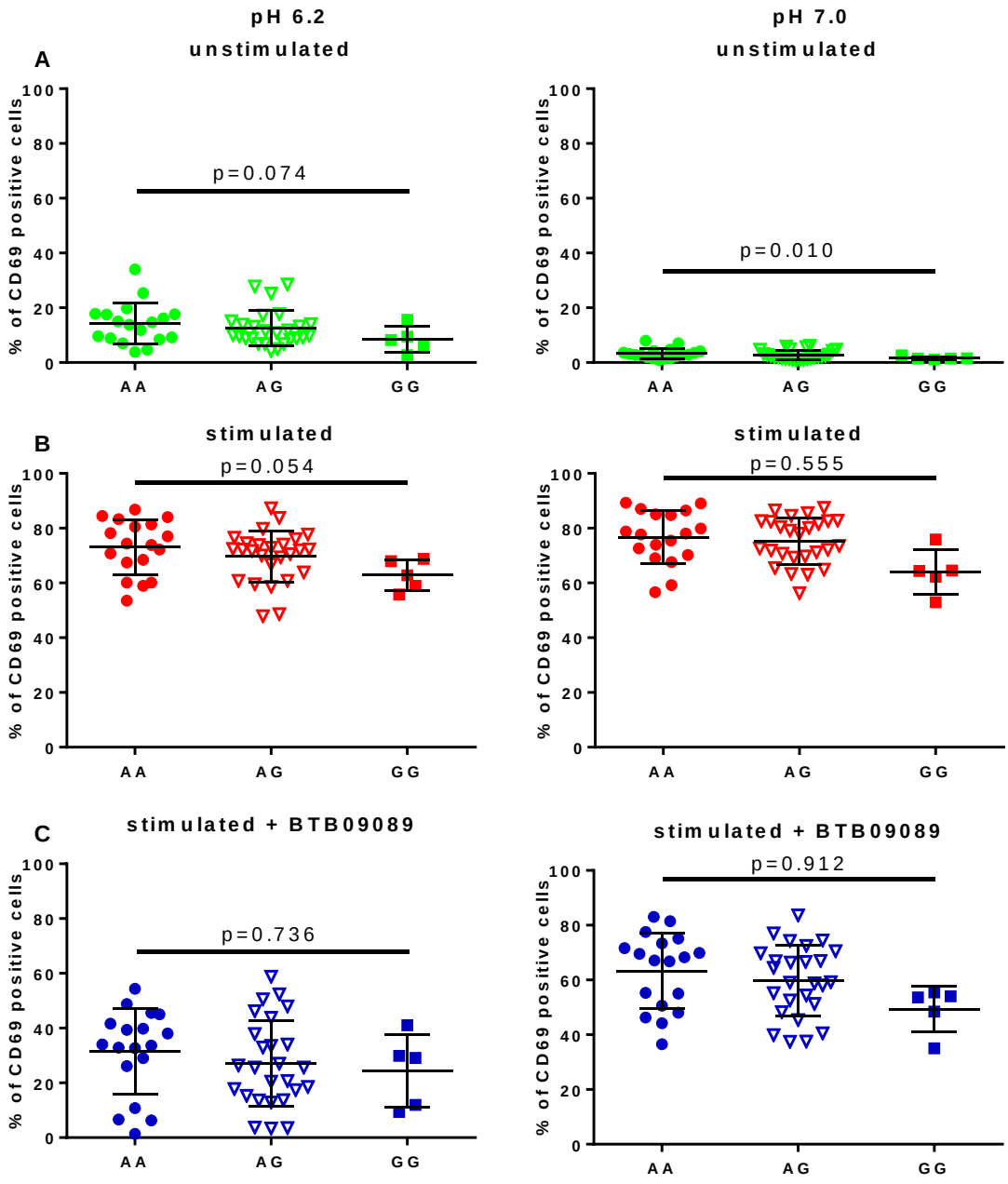

Figure 6. 27: Expression of CD69 on CD8+ T cells in protective allele homozygotes (circles), heterozygotes (inverted triangles) and risk allele homozygotes (squares) after 18 hours culture at pH 6.2 and pH 7.0 for each of the three culture settings; unstimulated (green), stimulated in the absence of BTB09089 (red) and stimulated in the presence of BTB09089 (blue).

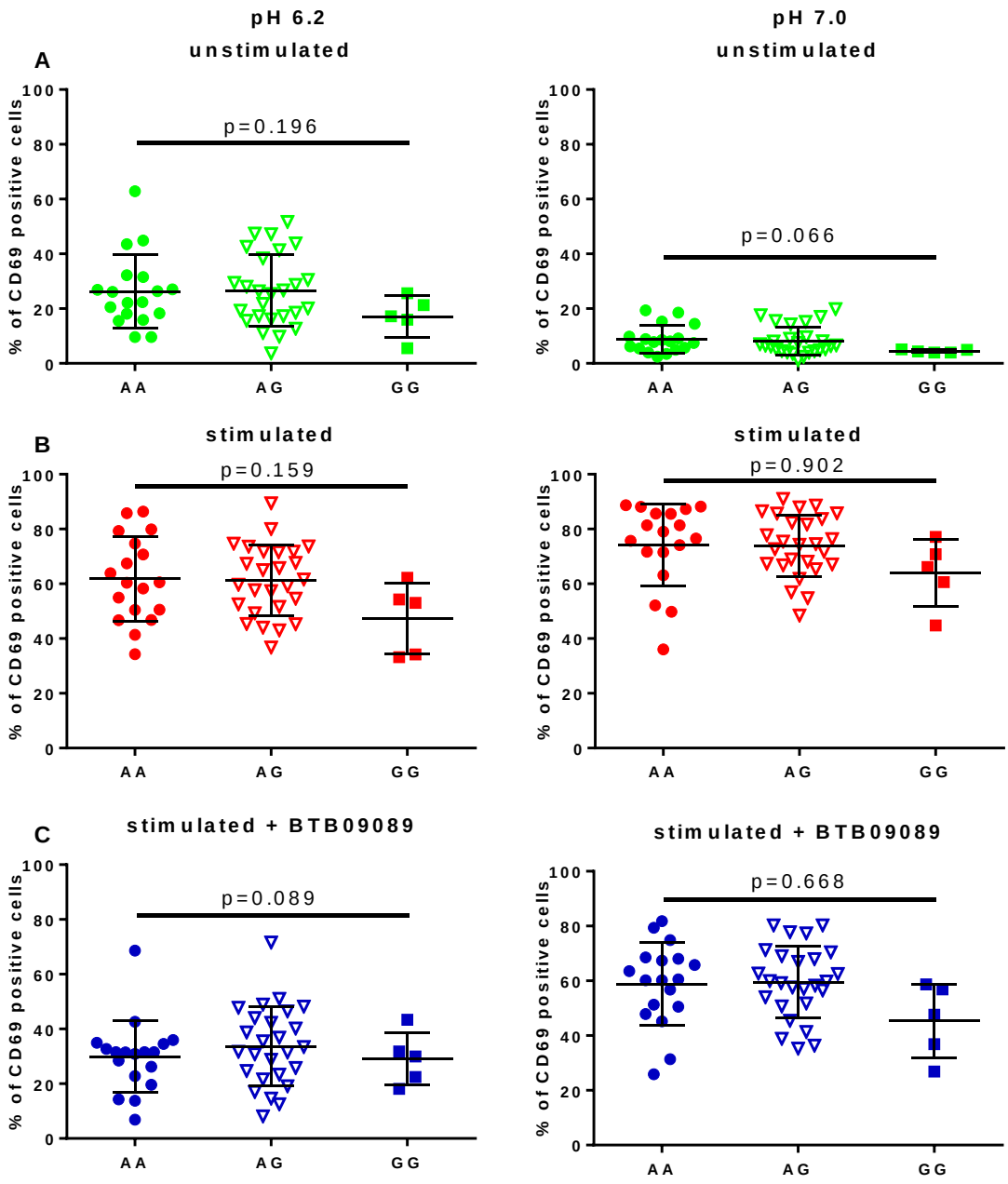

Figure 6. 28: Expression of CD69 on NKT cells in protective allele homozygotes (circles), heterozygotes (inverted triangles) and risk allele homozygotes (squares) after 18 hours culture at pH 6.2 and pH 7.0 for each of the three culture settings; unstimulated (green), stimulated in the absence of BTB09089 (red) and stimulated in the presence of BTB09089 (blue).

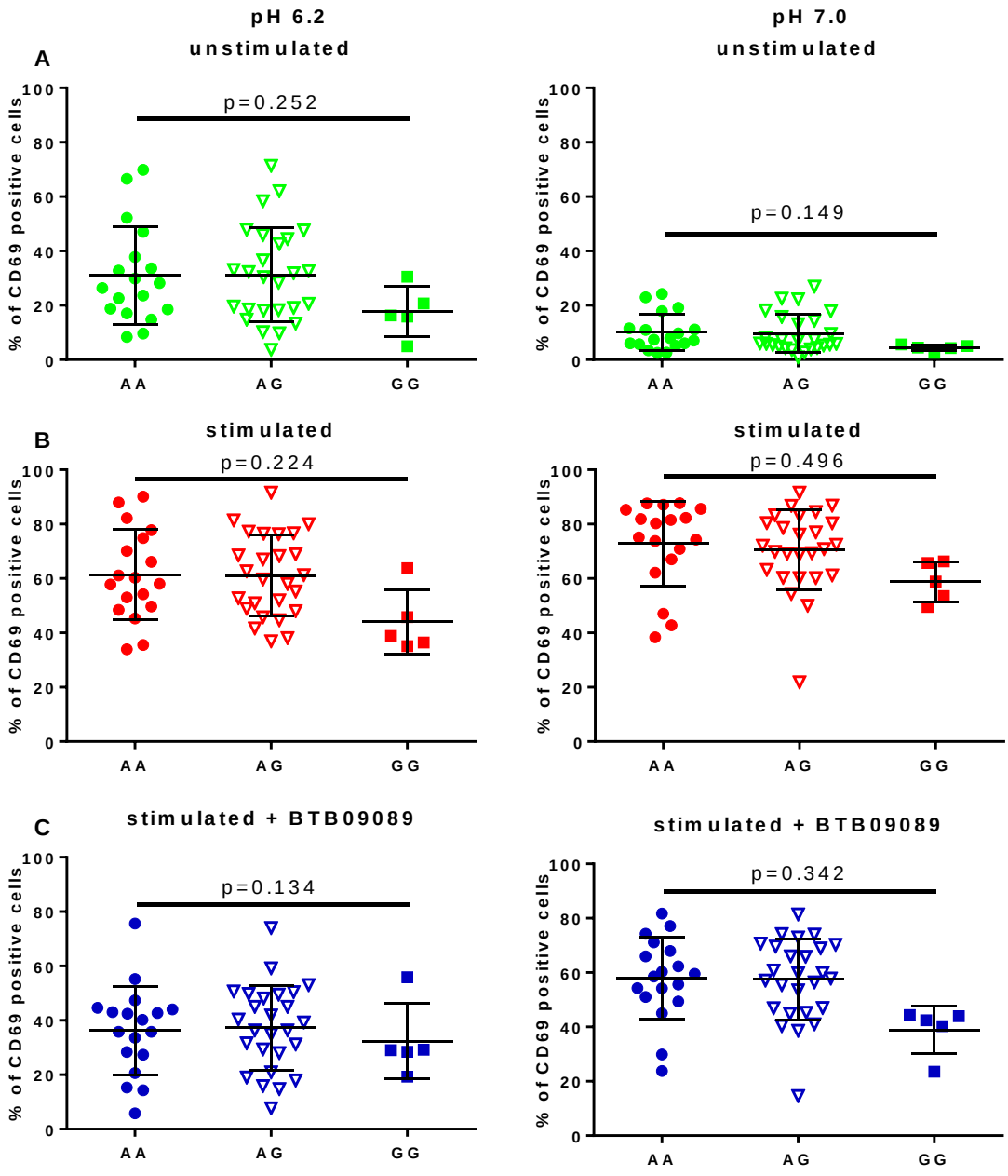

Figure 6. 29: Expression of CD69 on CD8+ NKT cells in protective allele homozygotes (circles), heterozygotes (inverted triangles) and risk allele homozygotes (squares) after 18 hours culture at pH 6.2 and pH 7.0 for each of the three culture settings; unstimulated (green), stimulated in the absence of BTB09089 (red) and stimulated in the presence of BTB09089 (blue).

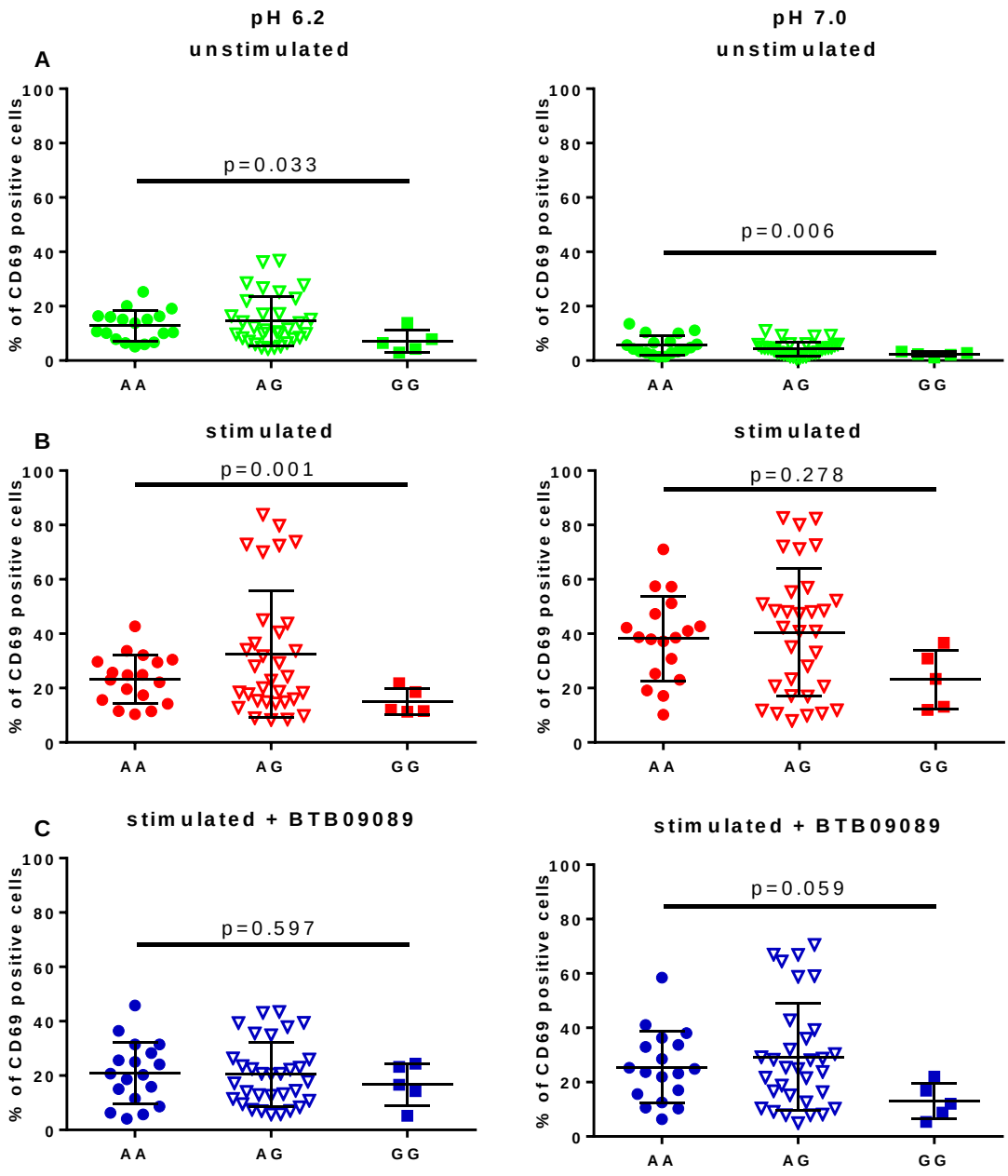

Figure 6. 30: Expression of CD69 on NK cells in protective allele homozygotes (circles), heterozygotes (inverted triangles) and risk allele homozygotes (squares) after 18 hours culture at pH 6.2 and pH 7.0 for each of the three culture settings; unstimulated (green), stimulated in the absence of BTB09089 (red) and stimulated in the presence of BTB09089 (blue).

6.6 Investigating mRNA expression in ex-vivo cells

In the RNA I collected from CD56+ and CD56- ex-vivo cells, I measured the mRNA expression of *GPR65*, *GALC* and *CD69* using quantitative PCR. As described in Chapter 2 this expression was quantified relative to the housekeeping gene *β-ACTIN* using the standard curve method. I found no evidence that either of the MS associated SNPs (rs74796499 and rs11052877) influenced the mRNA expression of these genes (Figures 6.31 and 6.32). In short, I found no evidence to suggest that either of these SNPs are expression Quantitative Trait Loci (eQTLs) for these genes.

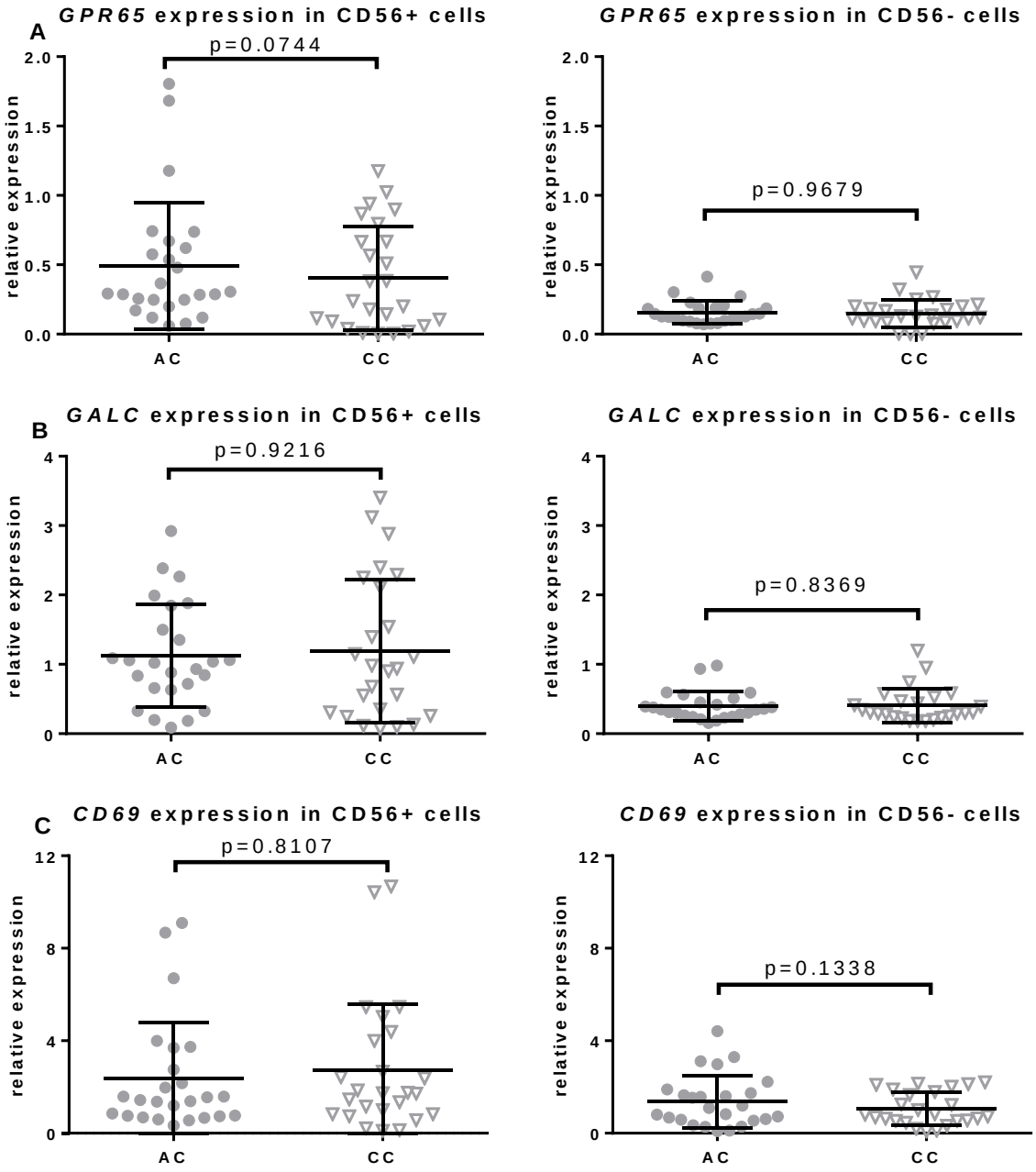

Figure 6. 31: *GPR65* (A), *GALC* (B) and *CD69* (C) mRNA expression in CD56+ cells (left hand panels) and CD56- cells (right hand panels) comparing rs74796499 heterozygotes (A/C) with risk allele homozygotes (C/C).

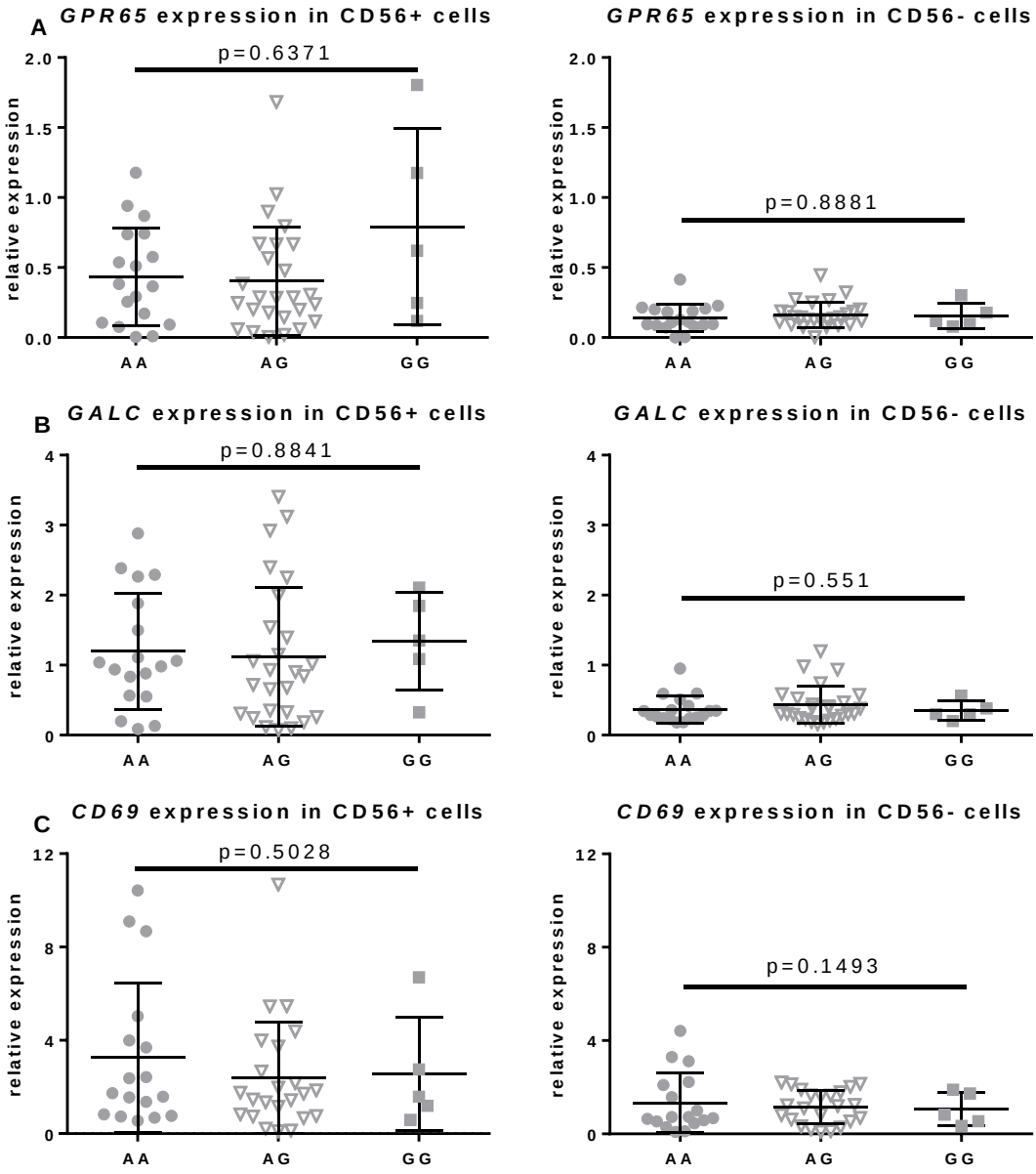

Figure 6. 32: *GPR65* (A), *GALC* (B) and *CD69* (C) mRNA expression in CD56+ cells (left hand panels) and CD56- cells (right hand panels) comparing rs11052877, protective allele homozygotes (A/A), heterozygotes (A/G) with risk allele homozygotes (G/G).

In 2016 the results from a Sardinian eQTL study became available online and on searching these I identified an eQTL for *GPR65* in PBMCs, rs3943657 (p=1.49e-21) [271]. At that time, I could not find any other publicly available databases listing eQTLs for *GPR65* or *GALC* in immune related tissues. I successfully genotyped 45 of my 50 subjects for rs3943657 (5 samples failed to genotype) and tested these data for evidence of association with the expression of *GPR65* as a positive control. I replicated the Sardinian observation that this SNP is indeed an eQTL for *GPR65* (Figure 6.33).

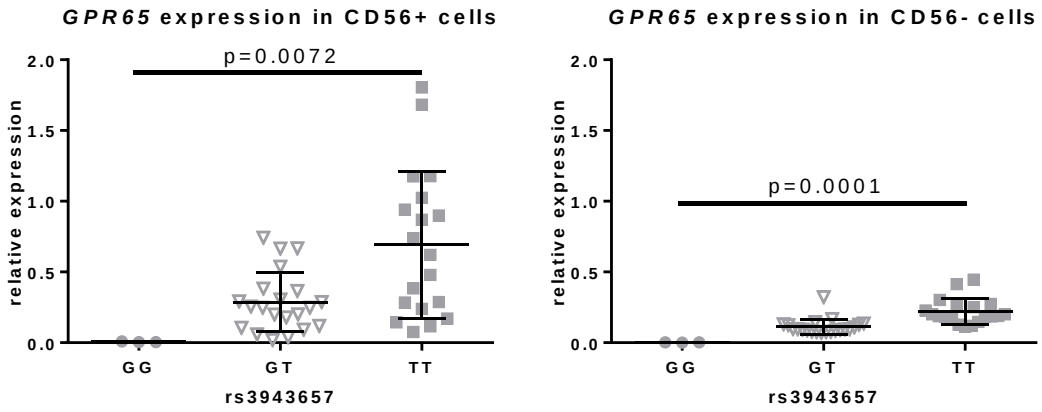

Figure 6. 33: *GPR65* mRNA expression in CD56+ cells (left hand panel) and CD56- cells (right hand panel) comparing rs3943657 minor allele homozygotes (G/G, n=3), heterozygotes (G/T, n=22) and major allele homozygotes (T/T, n=20). NB 5 samples failed to genotype in this assay.

6.7 Analysis of additional potentially related SNPs

Although rs74796499 appears to only be relevant in MS, genome-wide analysis of other autoimmune diseases has identified independent genetic variants from the chromosome 14q31.3 region that influence the risk of Crohn's disease (rs8005161) [179] and ankylosing spondylitis (rs11624293) [180]; as described in Chapter 1 these variants are perfect proxies for each other indicating that it is likely that a variant in this region influences the risk of both these diseases. In the inflammatory bowel disease (IBD) ImmunoChip study rs28533072 emerged as the lead SNP driving the Crohn's association [272]. In my data I found no evidence that this SNP influences the expression of *GPR65* or *GALC* in lymphocytes (Figure 6.34). However, in my cell subtype proportions data I observed a nominally significant trend suggesting that the minor allele at this SNP (T/T) might increase the proportion of NKT cells that are CD8+ (Figure 6.35).

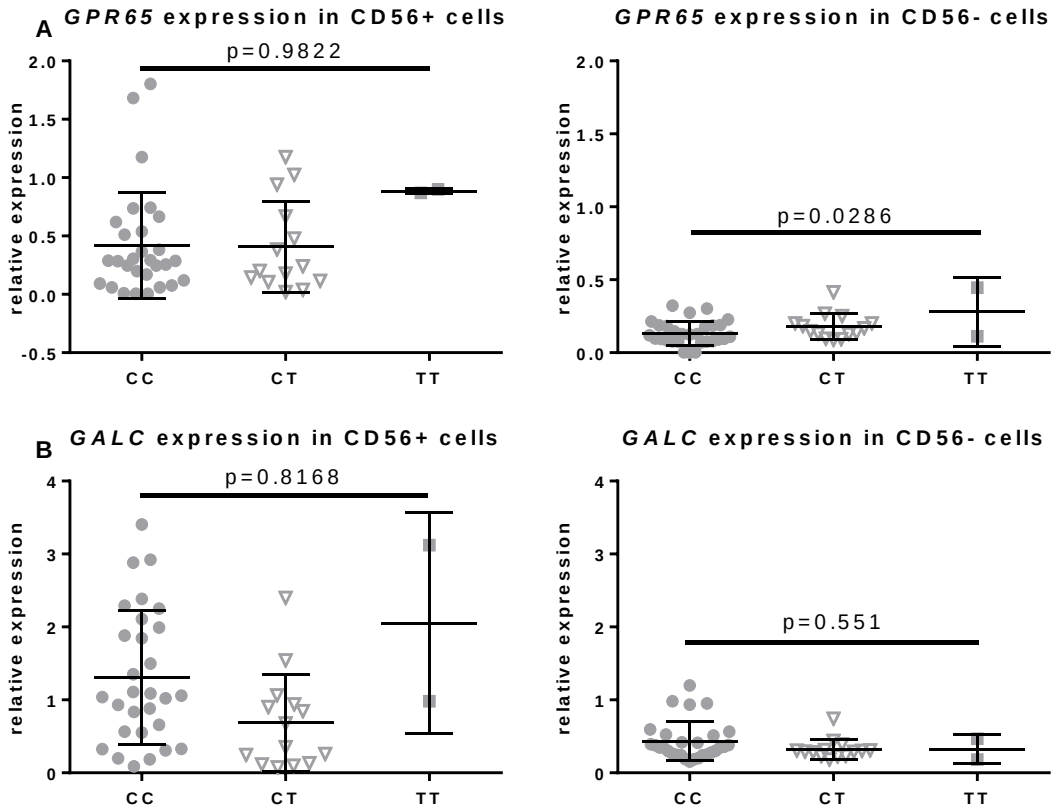

Figure 6. 34: *GPR65* and *GALC* mRNA expression in CD56+ cells (left hand panel) and CD56- cells (right hand panel) comparing rs28533072 major allele homozygotes (C/C, n=29), heterozygotes (C/T, n=14) and minor allele homozygotes (T/T, n=2). NB 5 samples failed to genotype in this assay.

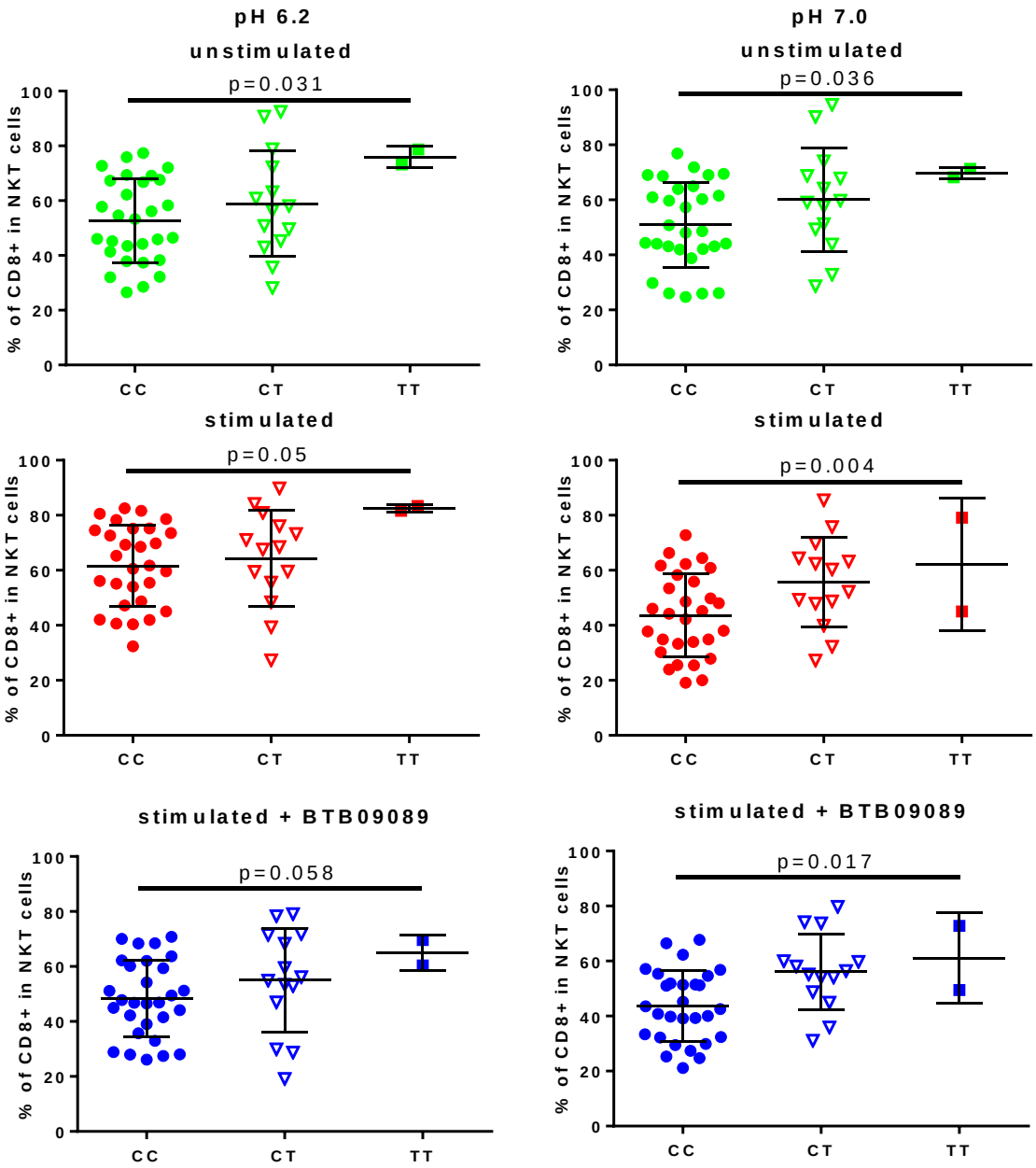

Figure 6. 35: Proportion of NKT cells that are CD8+ in rs28533072 major allele homozygotes (circles), heterozygotes (inverted triangles) and minor allele homozygotes (squares) after 18 hours culture at pH 6.2 and pH 7.0 for each of the three culture settings; unstimulated (green), stimulated in the absence of BTB09089 (red) and stimulated in the presence of BTB09089 (blue).

In the MS ImmunoChip study phosphoglycerate dehydrogenase (PHGDH) was highlighted as a potential candidate susceptibility gene [151], with rs666930 listed as the lead (most associated) SNP. Since this enzyme catalyses the rate limiting step in the synthesis of the amino

acid L-serine, which is an essential precursor required for the formation of myelin glycolipids, it seemed logical to also look for any association of this SNP with my results. Especially since in their metabolomics GWAS Shin et al. had clearly demonstrated that cis genetic variation in the region of PHGDH significantly influenced the circulating level of L-serine [273]. Unfortunately, the lead SNP from the metabolomics GWAS (rs1163251) was not genotyped in the ImmunoChip study [274], which included very few markers in this region of the genome. There is only very modest LD (r^2=0.1) between rs1163251 and rs666930 but no better tag SNPs were included on ImmunoChip. Looking further at the list of established MS susceptibility loci I noticed that one of the other associated SNPs, rs17785991 from chromosome 20q13, maps close to another myelin glycolipid relevant gene, B4GALT5, a key beta-galatosyltransferase enzymes [151]. In the latest results from the IMSGC meta-analysis, I found a further MS associated SNP (a low frequency variant) that also maps to the region containing the B4GALT5 gene, rs6020055 [37]. Given the relevance of these genes in sphingolipid metabolism I genotyped these three SNPs (rs666930, rs6020055 and rs17785991) in my 50 samples; unfortunately, none of these showed any evidence of association with the expression of LacCer (CD17).

Analysis of rs7476499 was performed using a paired t-test (as this cohort was recruited to contain just 2 genotypes), while other SNPs were analysed using the logistic regression option in PLINK. The pair IDs were not included as covariates, but covariates were included based on the batching of samples for RNA extraction, RNA clean-up and cDNA conversion.

6.8 Discussion

Many studies have shown that glycosphingolipids are important in the development of Th17 cells. For example, intracellular lipidome biosynthesis has been suggested to influence the quality and/or quantity of available RORγt ligand, and thereby affect the differentiation of helper cells into a Th17 phenotype [275]. Similarly, altering the glycosphingolipid composition of lipid rafts by reducing glycosphingolipid level in CD4+ T cells has been found to inhibit the Th17 cell differentiation [276]. LacCer is involved in multiple signal transduction pathways that lead to critical phenotypic changes in cells, and has been shown to be important in diverse processes including cell proliferation, adhesion, autophagy, inflammation and apoptosis [277-280]. LacCer is also involved in signalling and has been shown to regulate the activation of

astrocytes and influence the development of EAE [281]. The activity of adhesion molecules such as intercellular adhesion molecule 1 (ICAM-1) in monocytes and neutrophils has also been shown to be regulated by the expression of LacCer on the cell membrane [278]. In this context it seems reasonable to speculate that the genotype dependent changes I have seen in LacCer expression could result in important differences in the function of lymphocytes from rs74796499 protective allele carriers.

It's not immediately clear how rs74796499 might alter the expression of LacCer. Given that GALC is involved in the metabolism of glycolipids, it's possible that the change in LacCer might perhaps result from a change in the enzyme activity of GALC. However, since none of the common coding variants in *GALC* that are known to influence the catalytic activity of the enzyme (rs398607 (p.Ile562Thr), rs1805078 (p.Arg184Cys) and rs34362748 (p.Asp248Asn)) are associated with MS [282], it seems unlikely that any effects of rs74796499 on GALC is a simple as changing its catalytic activity. I found no evidence that rs74796499 alters the expression of *GALC* itself. However, the lead MS associated variant rs74796499 is in tight LD with a coding variant in *GALC* (rs11552556), which is predicted to be a splice region variant. The effect of this variant on *GALC* alternate transcription is at present unknown. In IBD the coding variant in *GPR65*, rs3742704 (I231L) has been suggested to alter the lysosomal pH and could thus affect the activity of GALC. However, the Crohn's disease associated variation from this region (which is in LD with this functionally relevant GPR65 coding variant) is not associated with MS and does not affect any of the phenotypes I measured. There is little LD between the MS associated variant rs74796499 and the Crohn's associated variant rs28533072 (R^2=0.02) but it remains possible that the MS variant might also influence lysosomal pH but in a different setting.

Despite suggestions to the contrary [193, 200] I found that BTB09089 is highly efficient at suppressing the activation of lymphocytes induced by anti-CD3/CD28 antibodies. Further studies are required to determine if BTB09089 can influence the expression of CD69 (or whether this agent might have blocked the influence of genotype on this acid induced expression).

In this chapter I successfully replicated my previous observation that CD69 expression is induced by culturing cells in an acid microenvironment and that the extent of this expression is dependent upon the genotype at the MS associated SNP rs74796499, but because of sample

overlap did not greatly increase the statistical significance of the evidence supporting this association in a combined analysis. In addition, I found that the independent associated SNP rs11052877 showed a trend towards a similar influence on the expression of CD69. For each of these two SNPs the protective allele increased the expression of CD69 suggesting that increased expression of CD69 on T cells in areas of inflammation (where pH will be acidic) is protective in MS. CD69 is a type II transmembrane glycoprotein with a C-type lectin domain in the extracellular side of the plasma membrane [283]. CD69 is considered an early activation marker in various lymphocyte subsets, and recent studies have indicated that CD69 has immune regulatory functions [284-286]. CD69 knockout mice have an increased propensity towards chronic inflammation, including collagen-induced arthritis [287], allergic asthma [238] and autoimmune cardiomyopathy [288], with recent studies suggesting that the increased susceptibility of these mice to different inflammatory diseases is primarily mediated via effects on Th17 cells [289]. Quite how CD69 influences the balance between Treg and Th17 cells is unclear. It has been shown that CD69 inhibits sphingosine 1-phosphate receptor (S1P1) signalling via the mTOR/HIF1a and JAK2/STAT3 pathways both of which are important in the development of the Th17 phenotype [290-292]. Sphingosine-1-phosphate (S1P) is involved in extracellular signalling [293-295] and influences astrocytosis in mice [296]. Clinical trials have shown that Fingolimod, an S1P receptor modulator, is an effective disease modifying treatment for MS [297, 298]. Lipid rafts, and therefore LacCer and other glycosphingolipids, are important at cell surface sites where CD3/CD28 stimulation occurs and where CD69 is expressed [299, 300].

In addition, there are data suggesting that CD69 is important in maintaining the balance between the master transcription factors in Treg (Foxp3) and Th17 cells (RORγt) through the JAK/STAT5 intracellular pathway [238, 301, 302]. Furthermore, *GPR65* knockout mice have been shown to produce less IL-17A and to be resistant to the development of EAE [275]; and ChiP-seq analysis has shown that RORγt (the Th17 cell master transcription factor) binds to the *GPR65* promoter region [275]. Given my analysis showing that the MS associated SNP rs74796499 influenced CD69 expression it is possible that the MS associated variant rs74796499 influence the Th17 and Treg balance through the regulation of CD69 expression.

It is also worth remembering that GPR65 was first identified through its involvement in thymocytes apoptosis mediated by T cell receptor engagement, suggesting the gene might have a role in the negative selection of thymocytes [181] and thus that the MS associated variant

might exert its effect by altering the balance of lymphocyte subtypes or numbers. Studies where GPR65 was over expressed lewis lung carcinoma (LLC) cells showed enhanced cell proliferation and glycolysis [199] while *GPR65* knockout mice showed normal immune development and glucocorticoid-induced thymocyte apoptosis [182]. In my analysis I found that the proportions of T lymphocyte subtypes were not significantly influenced by the MS associated SNP rs74796499, suggesting that any involvement of GPR65 in apoptotic functions may not be of critical importance.

In conclusion I validated and partially replicated my earlier observation that carrying the protective allele at rs74796499 increases the expression of CD69 on T cells cultured in acidic microenvironments, and extended this by showing that this allele might also reduce the expression of LacCer (CD17) on human T cells. Given the known roles of CD69 and LacCer in T cell development it is possible that the genotype dependent changes induced by the protective alleles at these SNPs favour the development of Tregs over Th17 cells and thereby protect against the development of MS.

Chapter 7: Lysosomal pH

7.1 Introduction

Lysosomes are membrane-bound organelles that contain hydrolytic enzymes required for the breakdown of both extracellular and intracellular biomolecules, including proteins, nucleic acids, carbohydrates and lipids [303]. Loss of function mutations in the genes that encode these enzymes result in the accumulation of substrates that cannot be metabolised by alternate means and produce so called "lysosomal storage diseases". For example, in Gaucher's disease homozygous (or compound heterozygous) mutations in the *GBA* (Glucosylceramidase beta) gene on chromosome 1, result in the intracellular accumulation of glucosylceramide [304, 305], while in the much rarer Sandhoff disease (SD) mutations in the *HEXB* (hexosaminidase B) gene from chromosome 5 results in the accumulation of the brain lipid GM2 ganglioside [306]. These lysosomal enzymes require an acidic environment for their optimal activity, and therefore the pH in lysosomes is typically maintained between 4.6 and 5.0 [307]. Active proton transports (proton pumping V-type ATPase) and ion channels in the lysosomal membrane maintain this pH which is substantially below the cytoplasmic pH of 7.2 [307, 308]. The extracellular material degraded in lysosomes through processes such as endocytosis, phagocytosis and autophagy include lipid molecules many of which are recycled back into metabolism via lysosomes [309-311]. A bidirectional relationship exists between lipids and lysosomes, with lysosome activity regulating lipid metabolism, and lipids in turn regulating lysosomal function [312].

Given the observation in IBD that activation of GPR65 influences the metabolism of glycosphingolipids by altering lysosomal pH it seemed logical to explore whether the MS associated variant rs74796499 might also exert effects on lysosomal pH. To investigate this, I measured the lysosomal pH in immune cell subtypes from ex-vivo PBMCs and correlated this with genotype.

7.2 LysoSensor dye

Thermo Scientific manufacture a range of fluorescent LysoSensor dyes. Ideally, I would have liked to use their LysoSensor Yellow/Blue DND-160 system which employs a yellow dye with a peak florescence in acidic environments together with a blue dye with a peak florescence in alkaline conditions. The ratio of these two emissions thus enabling a determination of the actual

pH. Unfortunately, this kit, which is primarily designed for fluorescence microscopy work, is currently incompatible with flow cytometry (BD Fortessa). I therefore used a single dye system (LysoSensor Yellow DND-189) and chose a dye with an emission spectra that was as different as possible from the other fluorophores I needed to use in the antibody panel. This dye reaches all intracellular compartments but only fluoresces in those with an acidic pH, and therefore effectively only reflects the pH of the acidic intracellular organelles, which are primarily the lysosomes. Because only one colour dye was used all measures were relative rather than absolute, with higher emission corresponding to lower (more acidic) pH. To measure lysosomal pH in specific immune cell subtypes from ex-vivo PBMCs I used the flow cytometry antibody panel shown in Table 7.1

Table 7. 1: Flow cytometry antibody panel used to assess lysosomal pH.

Marker	Fluorochrome	Clone	Manufacturer
CD3	PE-Cy7	SK7	BD Bioscience
CD14	APC	M5E2	BD Bioscience
CD19	BUV737	SJ25C1	BD Bioscience
CD56	PE	B156	BD Bioscience
LysoSensor DND-189	FITC		Thermo Fisher

7.2.1 Optimising pH measurement using the LysoSensor dye method

The manufacturer's handbook points out that prolonged incubation with the LysoSensor dye can increase the pH of lysosomes. To ensure that I avoided any potential confounding from this 'alkalizing effect' I performed an incubation time course experiment which confirmed that there was no change in the mean fluorescence intensity (MFI) from the dye for incubation times of 1 and 5 minutes (Figure 7.1). I then also investigated the effect of varying the interval between incubating cells with the dye and undertaking flow cytometric analysis, and found that there was no significant changes of MFI as long as the flow cytometry was completed within 6 hours of the incubation (Figure 7.2). Finally, I also examined the effects of flow cytometry voltage setting and confirmed that inevitably the MFI from the LysoSensor dye was critically dependent upon the blue laser (FITC) voltage but was little affected by voltage for the FSC/SSC (forward-scatter/side-scatter) detectors (Figure 7.3). To avoid any confounding from variation in the blue laser voltage during the assessment of samples I included a Compbead standard and

measured the LysoSensor signal (lysosomal pH) relative to this. I found no significant change in the signal from the Compbeads when the amount of antibody or beads were varied (see Appendix).

On the basis of these results I incubated antibody labelled PBMCs with LysoSensor dye for 5 min and performed flow cytometry within 2 hours of this incubation. LysoSensor MFI measures were normalised with Compbeads (1 drop of Compbeads and 5 µL of standard antibody).

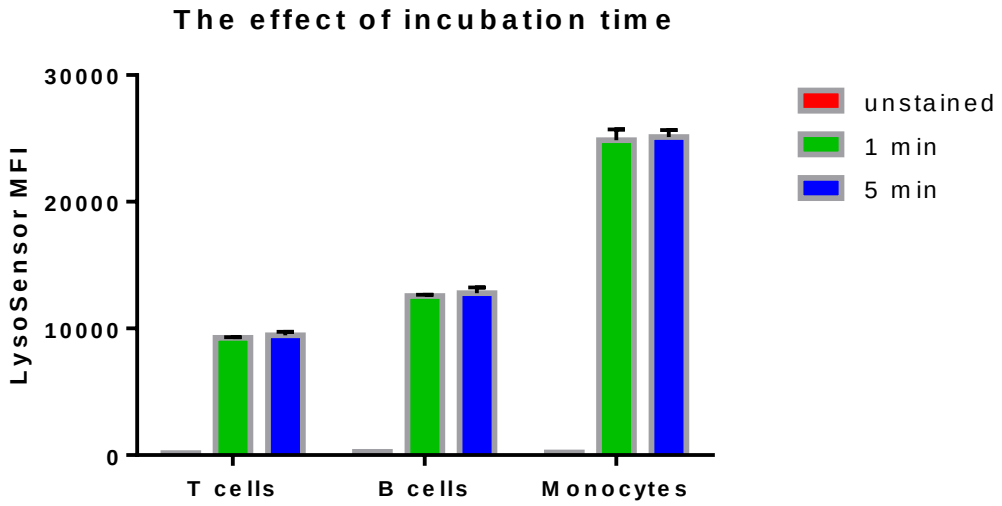

Figure 7. 1: Variation in LysoSensor MFI with incubation time.

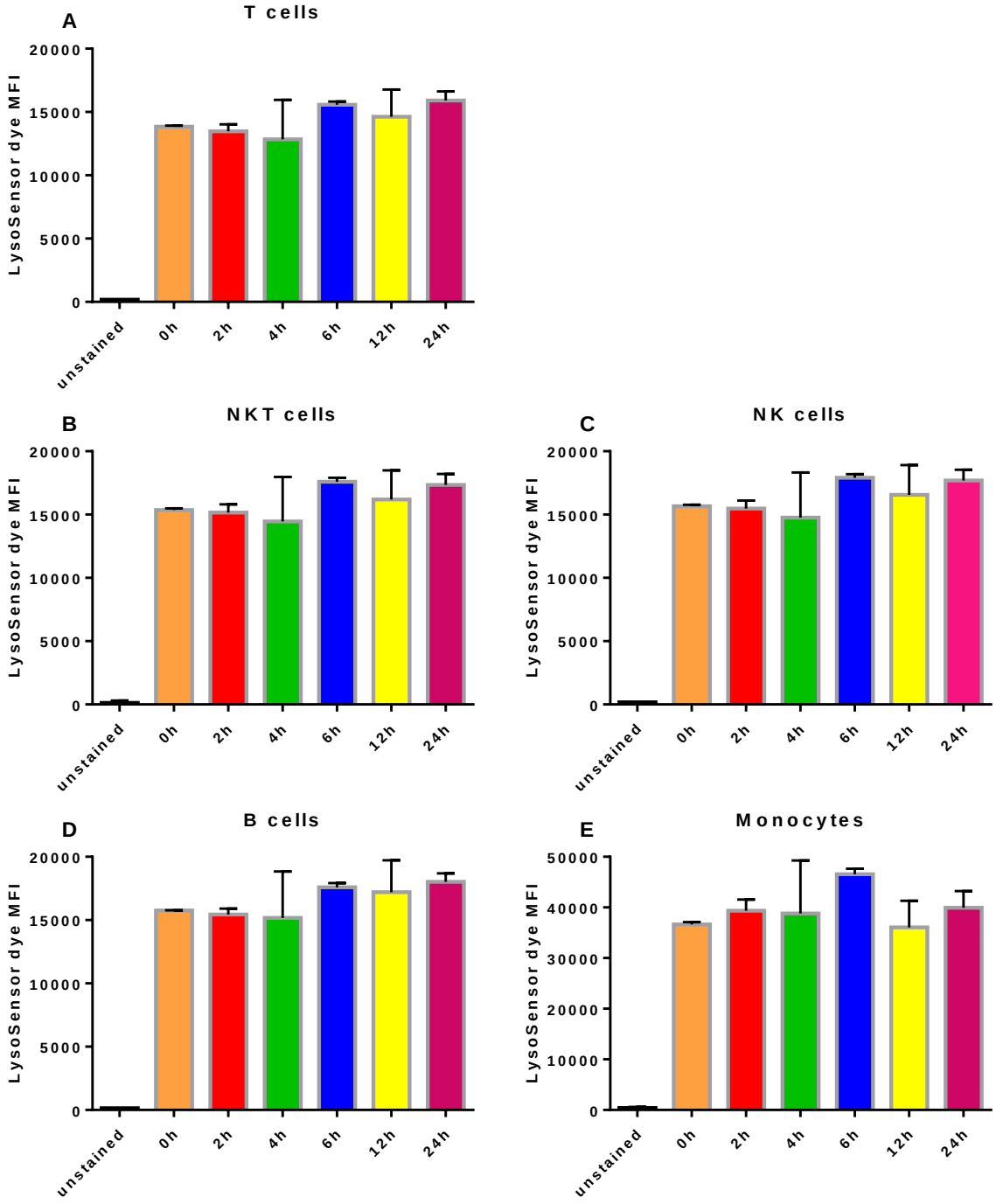

Figure 7. 2: LysoSensor MFI incubation to FACS analysis time course in T cells (A), NKT cells (B), NK cells (C), B cells (D) and monocytes (E).

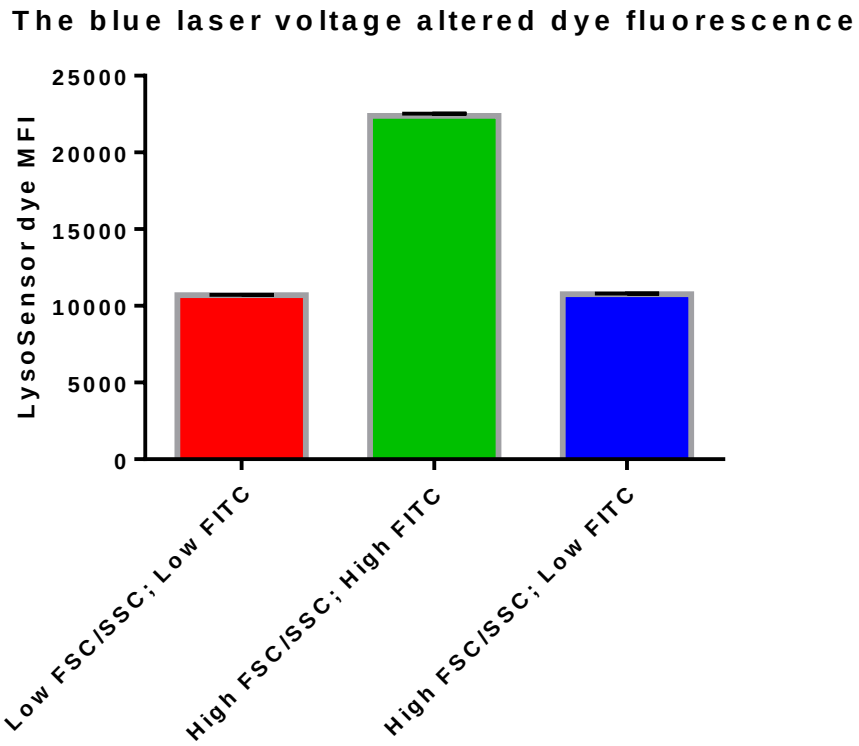

Figure 7. 3: The effect of the FSC/SSC and blue laser (FITC) voltage on LysoSensor MFI.

7.3 Results

7.3.1 Lysosomal pH in different cell subtypes

To explore the influence of genotype on lysosomal pH I collected ex-vivo PBMCs from 60 healthy donors recruited from Cambridge BioResource on the basis of genotype at rs74796499; 30 protective allele carriers (7 protective allele homozygotes and 23 heterozygotes) and 30 major allele (risk allele) homozygotes. For each subject, I measured Compbead normalised LysoSensor MFI in total T cells, NKT cells, NK cells, B cells and monocytes (all measures were made in triplicate). The average measure across all samples showed that lysosomal pH is most acidic in monocytes, followed by NK cells, and least acidity in T cells (Figure 7.4).

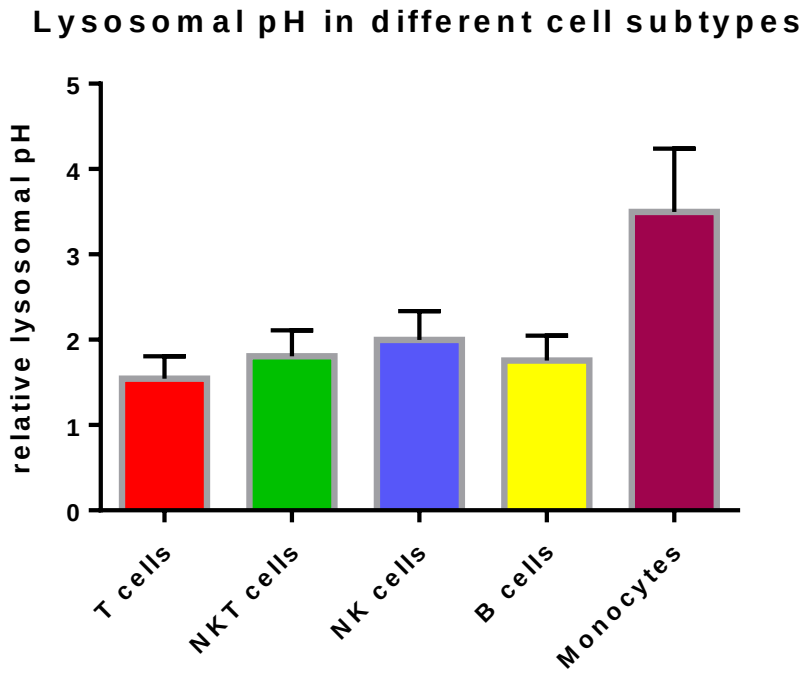

Figure 7. 4: Mean Compbead normalised LysoSensor MFI in ex-vivo T cells, NKT cells, NK cells, B cells and monocytes (the more acidic the lysosomal pH the higher relative MFI). Histograms are based on the mean expression across all 60 samples with technical triplicates for each individual.

7.3.2 Cell subtype specific effects of the MS associated SNP rs74796499 on lysosomal pH

The Cambridge BioResource supplied the genotype of rs74796499 for the 60 subjects considered, which I confirmed by independent genotyping. Genotype specific lysosomal pH measures are shown for each cell subtype in Figure 7.5. There was no evidence that this genetic variant is associated to the lysosomal pH in any of the ex-vivo cell subtypes considered.

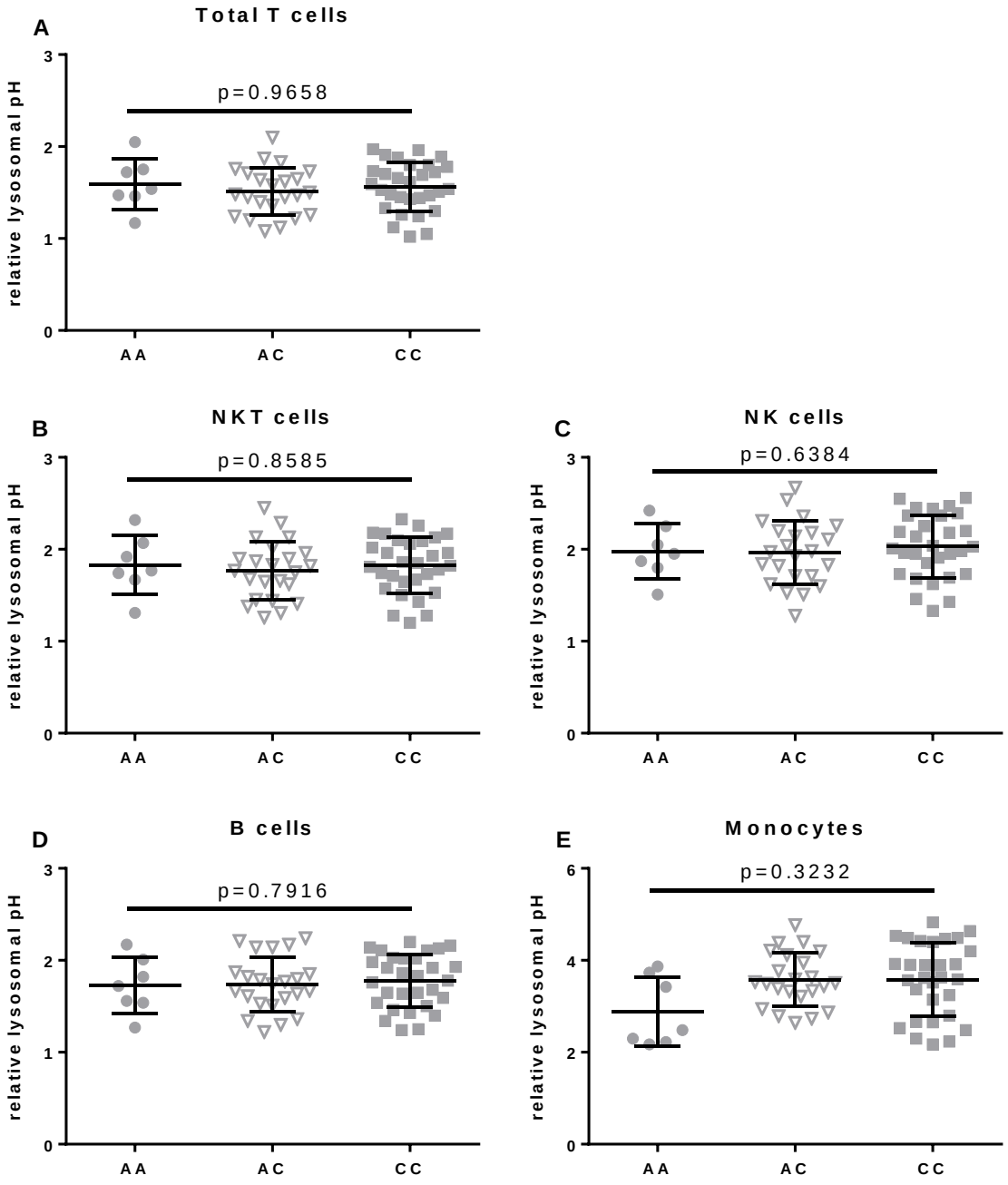

Figure 7. 5: rs74796499 genotype specific relative lysosomal pH in ex-vivo T cells (A), NKT cells (B), NK cells (C), B cells (D) and monocytes (E). Each measure is the average of three technical replicates.

7.3.3 Cell subtype specific effects of the IBD associated SNP rs3742704 on lysosomal pH

Figure 7.6 shows the same data from Figure 7.5 stratified by the IBD associated SNP rs3742704. I found no evidence to support the suggestion that this SNP influences lysosomal pH.

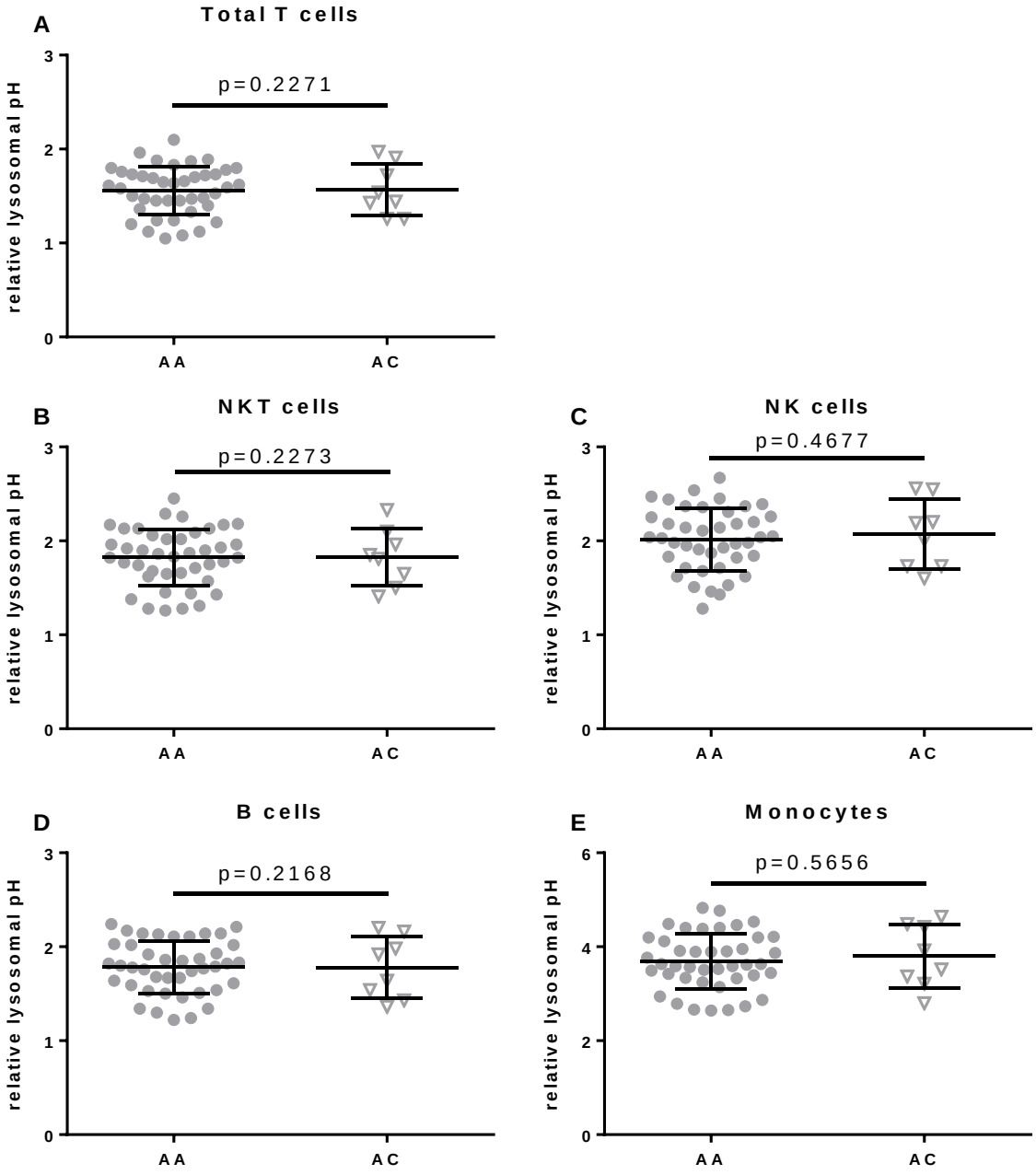

Figure 7. 6: rs3742704 genotype specific relative lysosomal pH in ex-vivo T cells (A), NKT cells (B), NK cells (C), B cells (D) and monocytes (E). NB: In these 60 subjects there were no risk allele homozygotes (C/C), so only protective allele homozygotes and heterozygotes could be tested.

7.3.4 Cell subtype specific effects of the Sardinian GPR65 eQTL SNP rs3943657 on lysosomal pH

Rather than directly measuring *GPR65* expression in the ex-vivo cells, I instead genotyped the Sardinian GPR65 eQTL SNP rs3943657 which I had previously confirmed influences *GPR65* expression. Again, I saw no evidence that this SNP is associated with lysosomal pH (Figure 7.7).

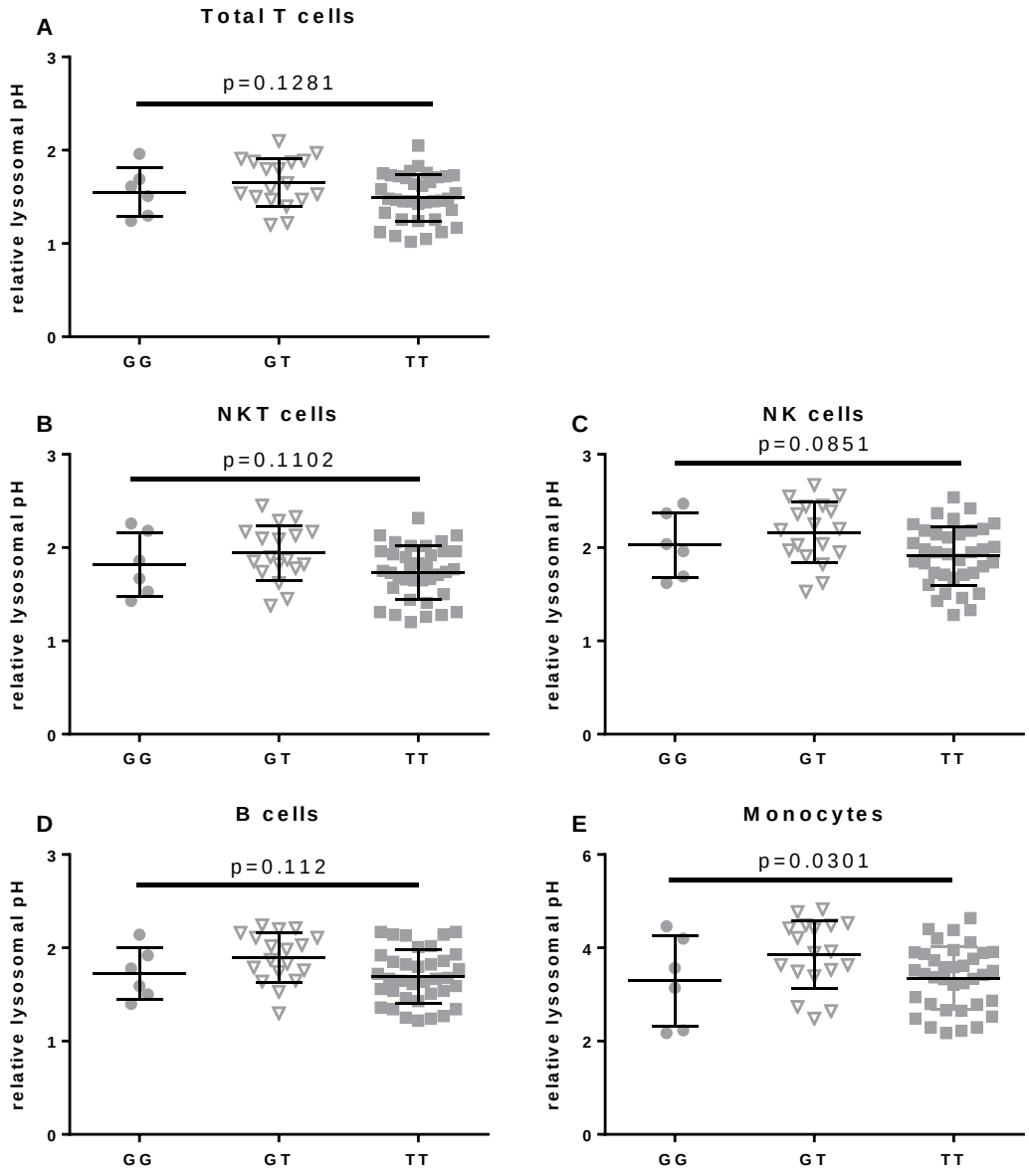

Figure 7. 7: rs3943657 genotype specific relative lysosomal pH in ex-vivo total T cells (A), NKT cells (B), NK cells (C), B cells (D) and monocytes (E).

7.3.5 The effect of activating GPR65 on lysosomal pH

I next undertook a pilot study to explore the effects of extracellular acidosis and GPR65 activation on lysosomal pH. In this experiment, I cultured PBMCs from three healthy volunteers for 18 hours in three settings.

1) Normal physiological pH (pH=7.4) without any BTB09089
2) Acidic pH (pH=6.2) without any BTB09089
3) Acidic pH (pH=6.2) with 20 μM BTB09089

The LysoSensor MFI was generally lower at acidic pH than at physiological pH (except in the monocytes), indicating that extracellular acidity results in a higher (i.e. less acidic) lysosomal pH (Figure 7.8). Stimulation of GPR65 with 20 μM BTB09089, results in further lowering of the LysoSensor MFI, i.e. a less acidic lysosomal pH in all cell types.

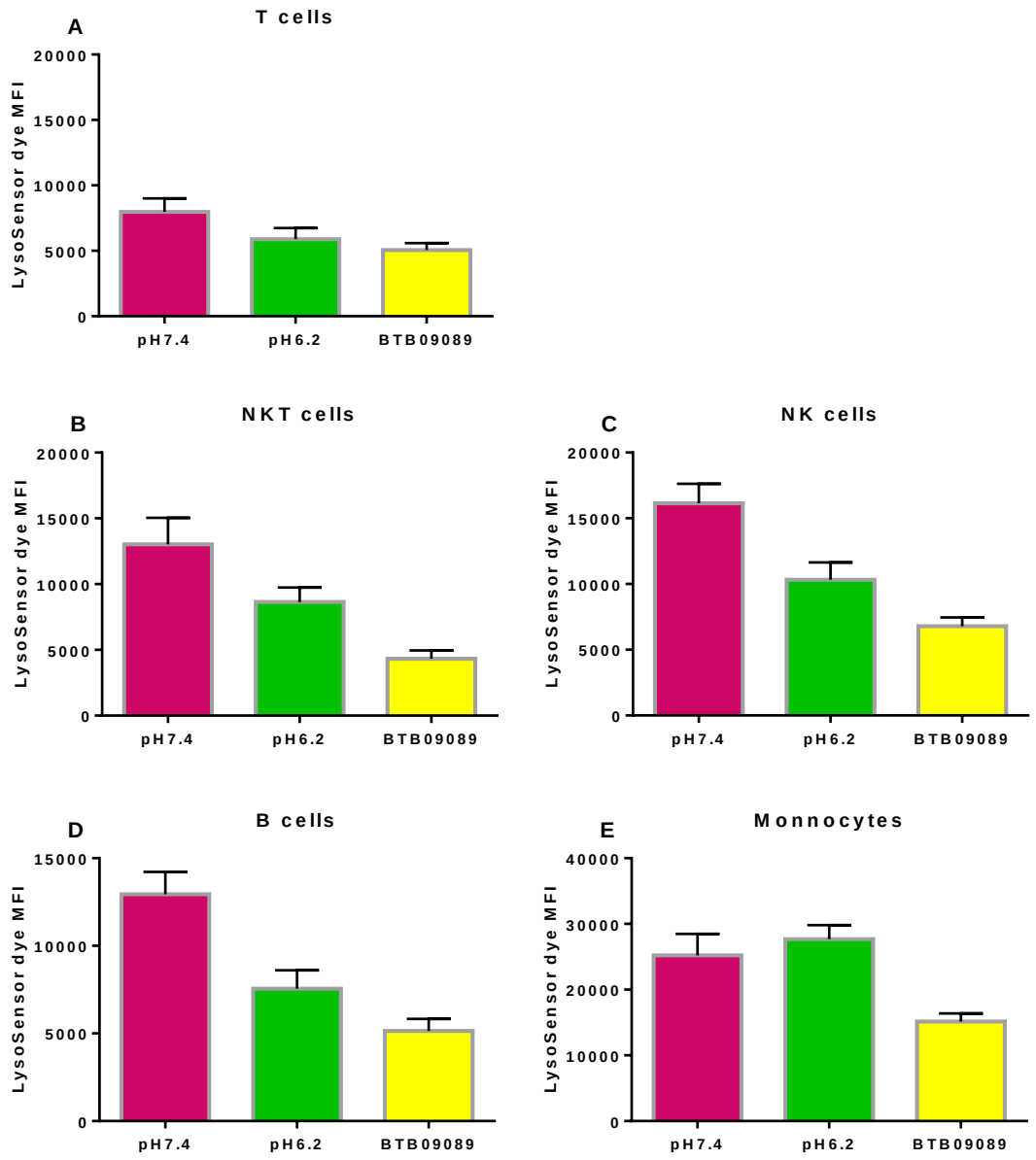

Figure 7. 8: Influence of extracellular pH and BTB09089 stimulation on LysoSensor MFI in T cells (A), NKT cells (B), NK cells (C), B cells (D) and monocytes (E). Each mean ± SD is based on technical triplicate measures from three samples.

7.4 Discussion

In their study Lassen et al. [203] showed that lysosomal pH is significantly raised (less acidic) in *GPR65* knockout mice and suggested that the GPR65 coding variant (rs3742704) that is also associated with increased risk of IBD, but more modestly, raises lysosomal pH and thereby disrupts lipid metabolism [203]. This SNP lies within a transmembrane domain of GPR65 and thus most likely alters GPR65 functioning by impairing intracellular signalling transduction

[152]. In my study I was unable to confirm the suggested effects of this SNP on lysosomal pH. It is possible that the effect of this IBD associated SNP may only be apparent in a cell subtype that I did not test, or perhaps is fully recessive and only occurs in risk allele (C/C) homozygotes, which were not included amongst the subjects I studied. It is also possible that perhaps this effect is too weak to detect with 60 subjects and that more individuals would need to be studied to provide enough power to confirm its presence.

I also found no evidence that the MS associated SNP rs74796499 influences lysosomal pH in any of the cell subtypes from ex-vivo PBMCs. These data suggest that it is unlikely that rs74796499 exerts its effects on MS risk by altering lysosomal pH but leave in question whether perhaps the variant is only relevant when GPR65 is activated, by extracellular pH and/or its ligand. In a pilot study, I found evidence that both acidic extracellular pH and the synthetic GPR65 ligand (BTB09089) result in less acidic lysosomal pH. However, I was not able test whether these effects are influenced by the MS associated variant rs74796499.

Altered lysosomal function has been described in MS, with fragile lysosomes observed in cerebral white matter from MS patients [313], and also excess lipid accumulation and increase autophagic activity seen in cortical neurons from MS patients [314, 315]. Furthermore, activation of lysosomal enzymes, including acid phosphatase and β-glucuronidase, has been confirmed in both lymphocytes and granulocytes during MS relapse [316]. In a recent study it was shown that exposure to psychosine disrupts lipid homeostasis and alters lysosomal pH [317]. Given the weight of evidence demonstrating the importance of GPR65 activity in determining lysosomal pH, and the profound effect of this pH on lysosomal function, it seemed logical to explore the effects of the MS associated variant on lysosomal pH. Unfortunately, I found no evidence to suggest any such effect in the experiments I conducted.

Chapter 8: LacCer and CD69 in a final cohort

8.1 Introduction

In Chapter 6, I extended the evidence indicating that carrying the protective allele at rs74796499 increases the surface expression of CD69 on T cells cultured in an acid environment. However, this effect was only apparent in unstimulated cultures, despite the substantial increase in the expression of CD25 and CD69 induced by stimulation with anti-CD3/CD28 antibodies. Furthermore, although the GPR65 agonist BTB09089 significantly reduced the expression induced by anti-CD3/CD28 stimulation I found no evidence that genotype influenced the final level of expression regardless of extracellular pH. In these earlier experiments, I did not consider the effects of BTB09089 in unstimulated cultures as I had wrongly anticipated that the effect of the genotype would be stronger in stimulated cultures and therefore it would be easier to establish the involvement of GPR65 in the context of stimulation. In this chapter I therefore wanted to explore the effect of BTB09089 in the unstimulated cultures where there was an apparent effect of genotype on CD69 expression. In this chapter I also wanted to extend the analysis to include individuals that are homozygous for the protective allele at rs74796499; I had not tested these in my previous work, raising the possibility that I could have missed recessive protective effects, as have been observed with variation in the *TYK2* gene [318]. The main reason for not considering these before was the practical difficulty of finding such individuals. The low frequency of the rs74796499 protective allele in the UK population (1.6%; 1000 Genomes Project Phase 3) means that only approximately 3 in 10,000 subjects are homozygous for this allele; which means that even in a large cohort like the Cambridge BioResource there are only a modest number of such subjects who might be willing to be involved in research. Given that CD69 expression has been shown to alter the balance between pro-inflammatory Th17 cell and anti-inflammatory Treg cells [301, 319], I also wanted to extend my experiments to explore whether the genotype dependent changes in CD69 expression that I had observed previously were accompanied by any changes in the ratio of these T cell subtypes. Unfortunately, the costs associated with undertaking such an analysis using the necessary surface markers were prohibitive, however, I was able to explore the mRNA expression of the key Th17 transcription factor, *RORC*. Furthermore, in Chapter 6 I found evidence suggesting that protective allele of rs74796499 was associated with lower expression of the glycosphingolipid LacCer (CD17) in ex-vivo cells. However, despite the evidence from IBD that genetic variation in *GPR65* can alter glycosphingolipid metabolism by changing lysosomal pH [320] I found no evidence that rs74796499 exerts any such effect

on the pH in these organelles (see Chapter 7, the work in Chapter 7 was performed in parallel to the work described in this chapter and employed the same samples – including the protective allele homozygotes). Finally, in this chapter I wanted to assess the expression of LacCer in cultured cells (with and without BTB09089 stimulation) as well as ex-vivo cells.

To undertake this next phase of my work I established two flow cytometry antibody panels, the first to assess the expression of CD69 and LacCer in ex-vivo cells (Table 8.1) and the second to assess the expression of CD69 and LacCer in unstimulated cultured cells at normal (pH=7.4) and acidic (pH=6.2) conditions both with and without exposure to BTB09089 (Table 8.2).

Table 8. 1: Flow cytometry panel for assessing ex-vivo cells.

Marker	**Fluorochrome**	**Clone**	**Manufacturer**
CD3	PE-Cy7	SK7	BD Bioscience
CD4	BUV395	RPA-T4	BD Bioscience
CD8	APC	RPA-T8	BD Bioscience
CD17	FITC	Huly-m13	LifeSpan Biosciences
CD19	BUV737	SJ25C1	BD Bioscience
CD56	PE	B156	BD Bioscience
CD69	v450	FN50	BD Bioscience

Table 8. 2: Flow cytometry for assessing cultured cells.

Marker	**Fluorochrome**	**Clone**	**Manufacturer**
CD3	PE-Cy7	SK7	BD Bioscience
CD4	BUV395	RPA-T4	BD Bioscience
CD8	APC	RPA-T8	BD Bioscience
CD17	FITC	Huly-m13	LifeSpan Biosciences
CD19	BUV737	SJ25C1	BD Bioscience
CD56	PE	B156	BD Bioscience
CD69	v450	FN50	BD Bioscience
Fixable viability dye	eFluor 450		eBioscience

8.2 Extending the analysis of LacCer expression

8.2.1 LacCer in ex-vivo PBMC subtypes

As lipid rafts are essential in all cells I first measured LacCer expression in a range of ex-vivo PBMC subtypes, including T cells, CD4+ T cells. CD8+ T cells, NKT cells, NK cells, B cells, classic monocytes (CD14+ CD16-) and non-classic monocytes (CD14+ CD16+) (Figure 8.1), in order to establish to what extent each of these express this molecule. Interestingly, LacCer was most highly expressed in monocytes (nearly 100%) and I therefore decide to not include this cell type in my assessment of the effects of MS associated genetic variant on LacCer expression.

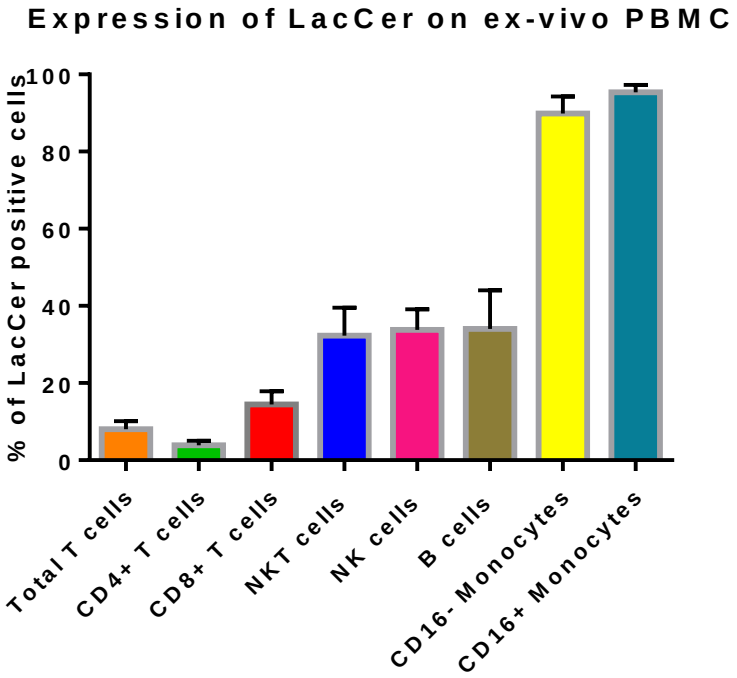

Figure 8. 1: Expression of LacCer on the surface of ex-vivo PBMC subtypes. Samples (n=2) with 3 technical replicates.

8.3 Refining the use of GPR65 ligands

Before embarking on the main work described in this chapter I wanted to establish if it would be possible to use the naturally occurring GPR65 ligand psychosine rather than its synthetic agonist BTB09089. Unlike BTB09089, which is an agonist of GPR65 [193], psychosine is an antagonist [183], and would therefore be expected to reduce the effects of acidic pH rather than mimic these effects. Furthermore, as psychosine is highly toxic to cells its utility might be

limited by its toxic effects; it is believed that most of the neurodegeneration seen in Krabbe's disease results from the toxic effects of psychosine [295]. Like BTB09089, psychosine is hydrophobic but can be solubilised using DMSO.

8.3.1 Considering psychosine as a GPR65 antagonist

In order to establish what concentrations of psychosine might have toxic effects in my culture systems I first stimulated PBMCs with anti-CD3/CD28 antibodies in acidic conditions (pH=6.2) for 18 hours in the presence of differing concentrations of psychosine between 0 µM to 20 µM. At concentrations below 1 µM there was very little change in the proportion of cells falling within a lymphocyte gate, however at concentrations above 10 µM the proportion fell significantly presumably as a result of cell death (Figure: 8.2).

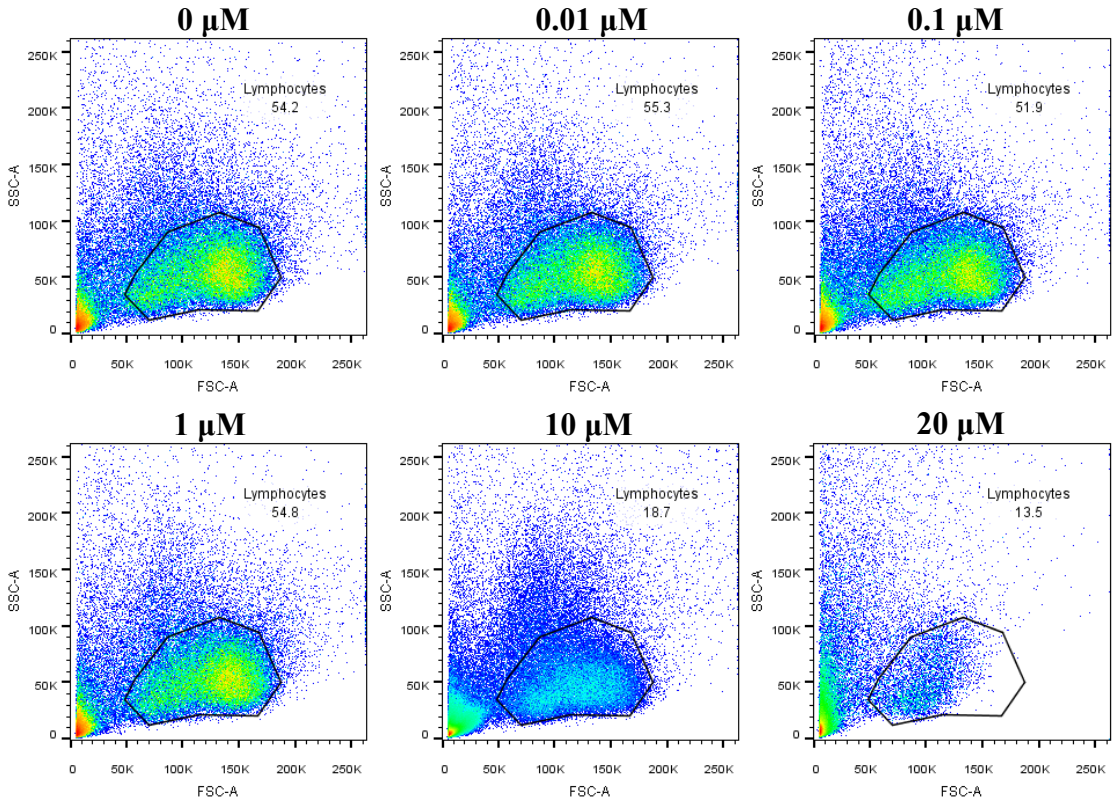

Figure 8. 2: Proportion of cells within a lymphocyte gate after 18 hours of stimulated culture in the presence of differing psychosine concentrations.

Having established that psychosine seemed to have little toxicity at concentrations below 1 µM but was clearly toxic at concentrations above 10 µM, I set up further PBMC cultures in the

presence of psychosine concentrations up to a maximum of 5 μM. In these experiments I set up unstimulated and anti-CD3/CD28 stimulated PBMC cultures in acidic conditions (pH=6.2) and measured the proportion of LacCer and CD69 positive cells in a range of cell subtypes after 18 hours of culture. There was little effect of anti-CD3/CD28 stimulation on LacCer expression (Figure 8.3) and the expected increase in expression of CD69 was seen (Figure 8.4). At concentrations of 1 μM and below psychosine seemed to have little effect on the expression of LacCer or CD69. Whereas at a concentration of 5 μM the expression of LacCer was notably increased in all tested cell subtypes, while the expression of CD69 was generally little changed. These effects are in contrast to the inhibitory effects of BTB09089 and thus in keeping with an antagonistic effect of psychosine. However, at this concentration the toxic effects of psychosine are likely to overwhelm its specific effects via GPR65 activation.

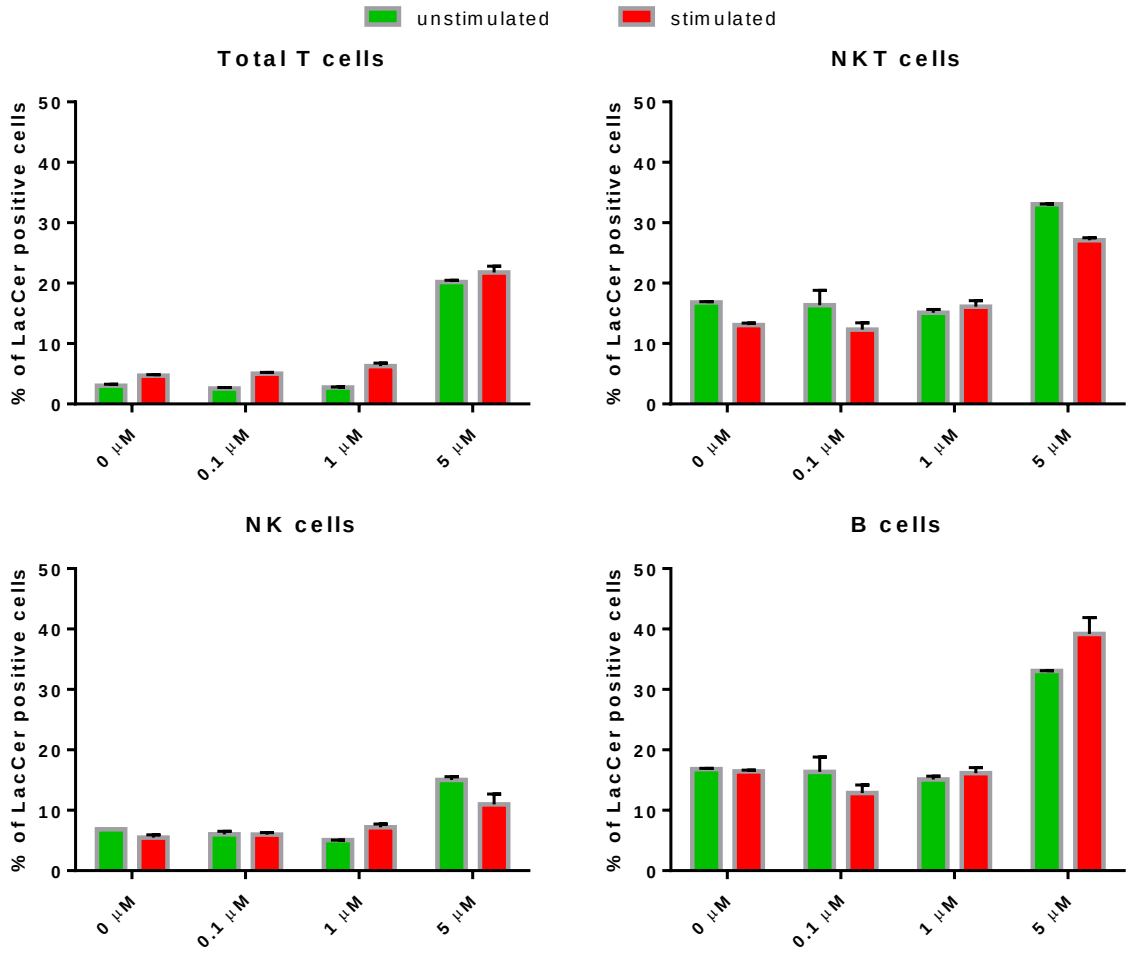

Figure 8. 3: LacCer expression in cell subtypes from PBMC cultures with and without anti-CD3/CD28 stimulation at a range of psychosine concentrations between 0 μM to 5 μM. Measures were made from two samples in technical triplicate.

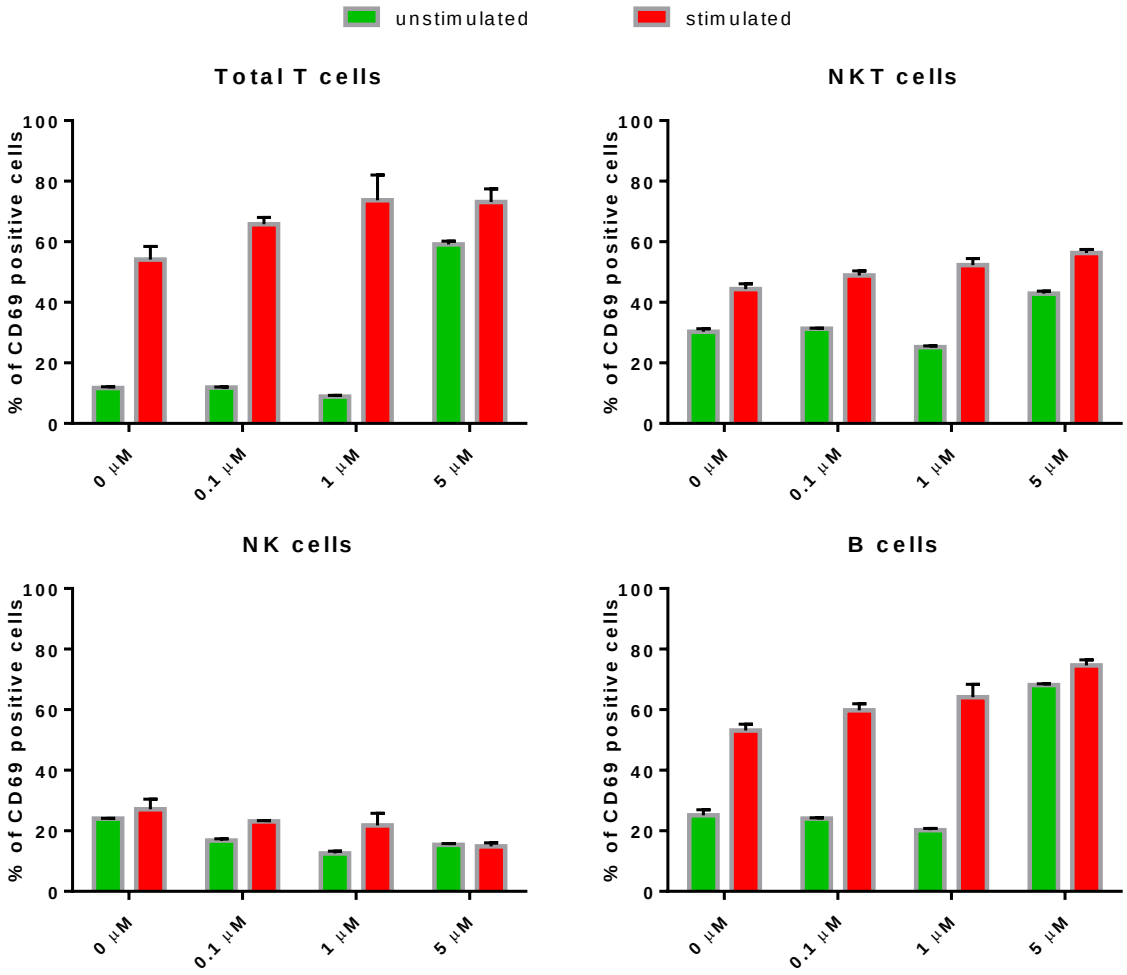

Figure 8. 4: CD69 expression in cell subtypes from PBMC cultures with and without anti-CD3/CD28 stimulation at a range of psychosine concentrations between 0 µM to 5 µM. Measures were made from each sample (n=2) in triplicate.

These experiments thus show that unfortunately non-toxic levels of psychosine had no major effect on expression. At higher (toxic) levels of psychosine increased expression but could not be reliably distinguished from toxic effects of psychosine. Based on these data and the report that psychosine might also influence GPR4 and OGR1 [183], I decided to continue using the synthetic ligand BT09089 which has no toxic effects at concentrations sufficient to activate GPR65.

8.3.2 LacCer and CD69 expression on dead cells

The observation that toxic concentrations of psychosine results in increased levels of LacCer suggested that perhaps dead or dying cells have increased expression of this marker. To

investigate this possibility, I cultured PBMCs for 18 hours (without stimulation) under acidic (pH=6.2) and physiological (pH=7.4) conditions both with and without BTB09089, and then compared LacCer (and CD69) expression in live and dead cells; dead cells were identified using fixable viability dye as described previously. As anticipated from the work described in Chapter 4 only very low levels of dead cells were seen (4-6% of FACS captured events), however a very much proportion of dead cells expressed LacCer although the proportion that express CD69 is little different (Figure 8.5). Given the prominent expression of LacCer on dead cells I excluded such cells from used all my subsequent experiments using a live-dead stain.

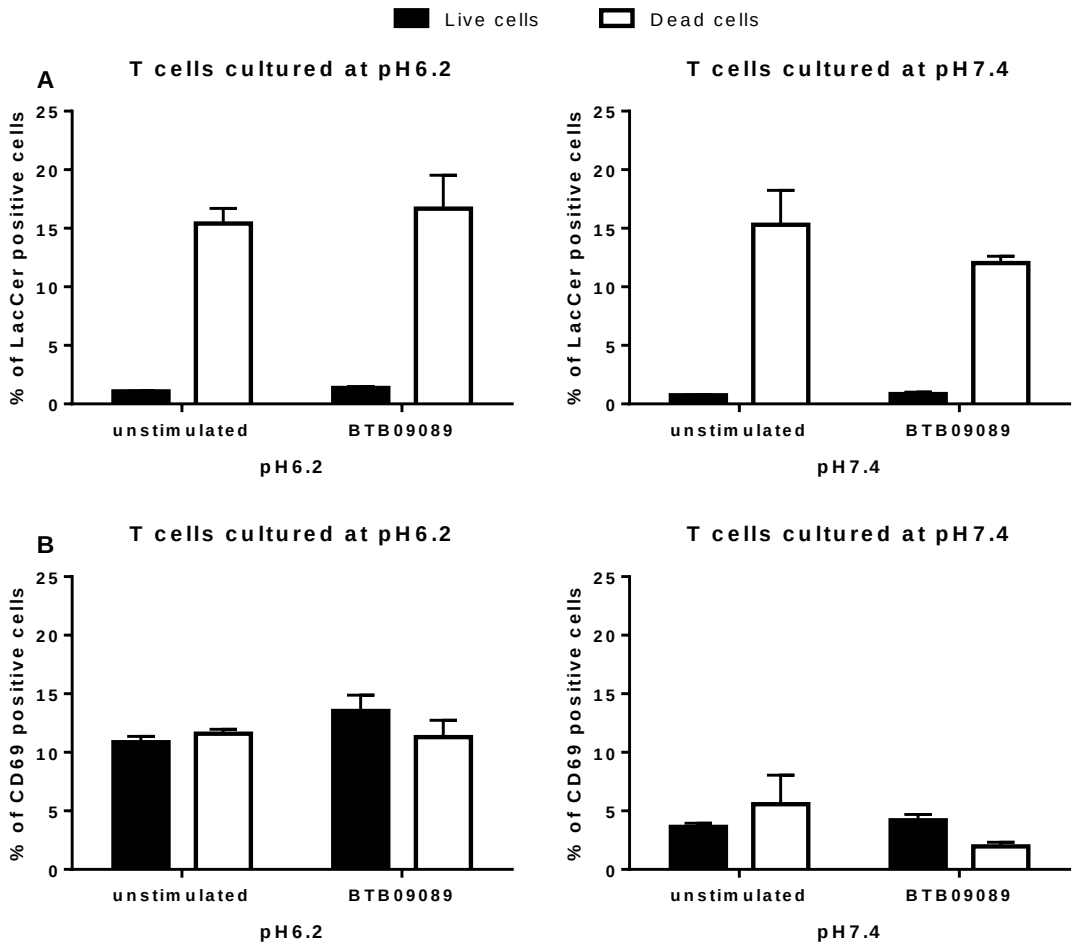

Figure 8. 5: Comparison of LacCer (A) and CD69 (B) expression in live and dead T cells after 18 hours of culture (unstimulated) at pH 6.2 (Left) and pH 7.4 (Right). Measures were made from one sample in triplicate.

8.4 Reassessing the effects of rs74796499 genotype on the expression of LacCer and CD69

In order to search for genotype dependent effects on the expression of LacCer and CD69, a total of 60 healthy donors were recruited from the Cambridge BioResource on the basis of their rs74796499 genotype; including 7 protective allele homozygotes (A/A), 23 heterozygotes (A/C) and 30 risk allele homozygotes (C/C) (these are the same subjects considered in Chapter 7). These individuals were recruited and sampled in pairs with the protective allele carrier (A/A or A/C) always paired with a risk allele homozygote (C/C). As before I was blind to sample genotypes until all experiments were completed and measures finalised. In total 139 phenotypes were tested for association with genotype. However, since many of these are necessarily correlated the effective number of independent phenotypes was again established using the R script provided by Prof Frank Dudbridge (using 10,000 permutations). This script, established that the effective number of independent phenotypes was 60 and I therefore set a threshold of $p<0.00083$ for declaring statistical significance in order to correct for multiple testing.

Figure 8.6 shows the mean expression of LacCer and CD69 across these 60 samples in each ex-vivo lymphocyte subtype; T cells, CD4+ T cells, CD8+ T cells, NKT cells, NK cells and B cells. This figure show that the highest expression of LacCer is seen on B cells and NKT cells, whereas, NKT cells and NK cells show the highest expression of CD69.

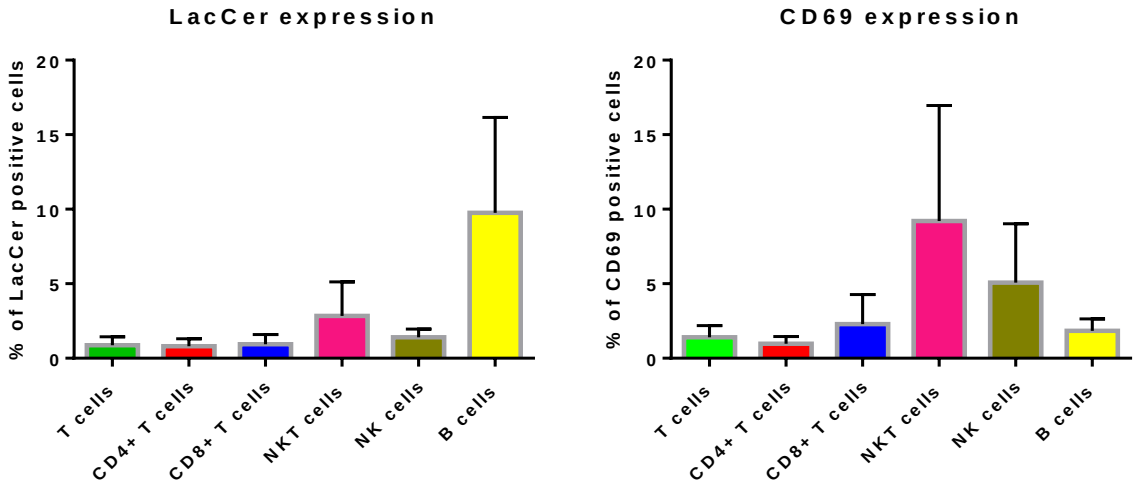

Figure 8. 6: Mean proportion of ex-vivo lymphocyte subtypes expressing LacCer and CD69. Sample specific expression was measured in duplicate.

Figures 8.7 and 8.8 show the mean proportion of lymphocyte subtypes expressing LacCer and CD69 after unstimulated culture, with and without BTB09089, in acidic (pH=6.2) and physiological (pH=7.4) environments. In contrast to the preliminary observations shown in Figure 8.2 this much larger data set shows that in fact BTB09089 tends to increase the expression of LacCer in all lymphocyte subtypes although this effect is only notable in NKT cells from acidic culture conditions (Figure 8.7). For CD69 the preliminary observations were largely reproduced apart from in NK cells where BTB09089 may slightly increase CD69 expression (Figure 8.8). Interestingly BTB09089 seems to have relatively little effect on the expression of either moiety at physiological pH, which is of course slightly alkaline of neutral (Figures 8.7 and 8.8). As anticipated BTB09089 had no meaningful effect on the proportion of dead cells after culture.

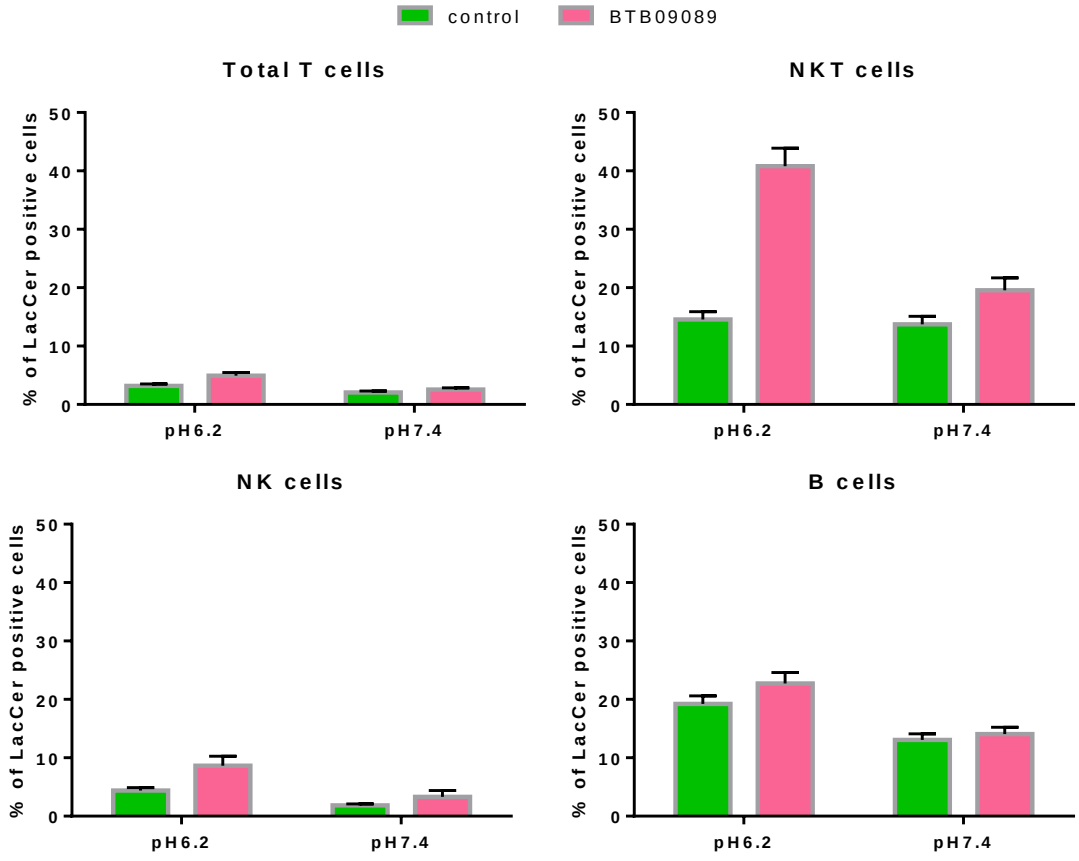

Figure 8. 7: Mean LacCer expression across all 60 individuals in lymphocyte subtypes after culture. Sample specific expression was measured in triplicate.

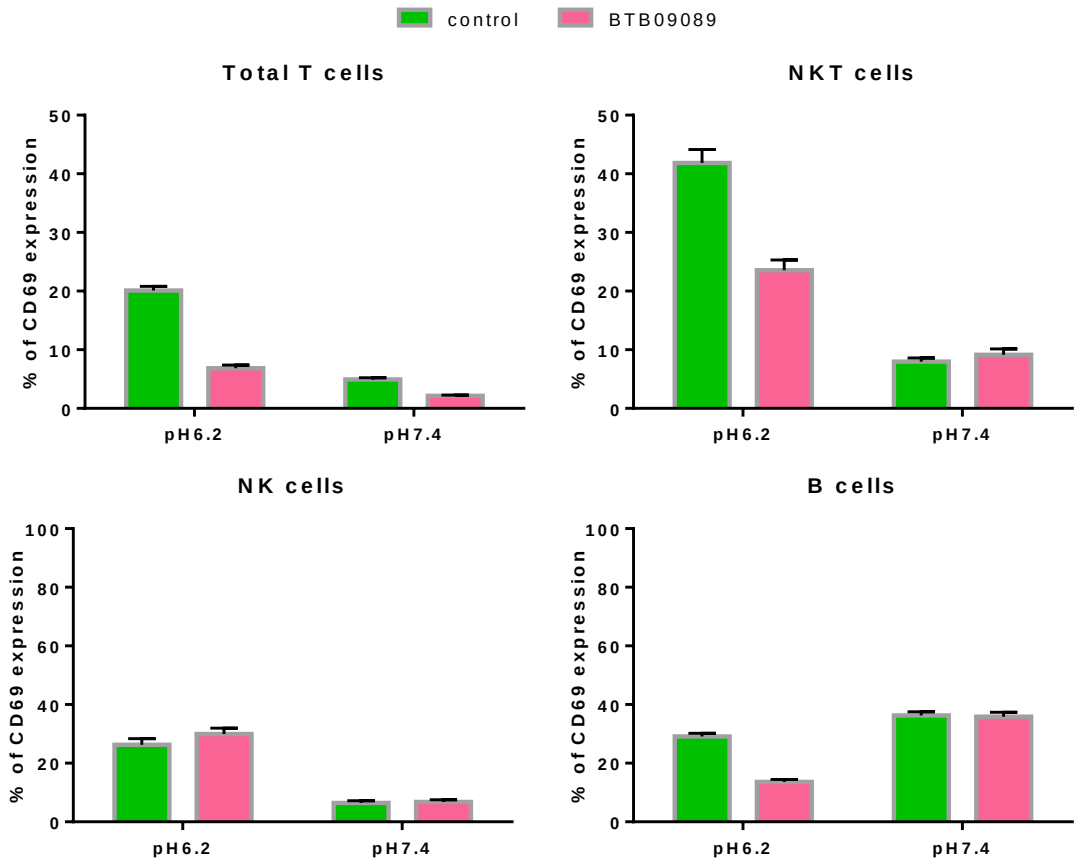

Figure 8. 8: Mean CD69 expression across all 60 individuals in lymphocyte subtypes after culture. Sample specific expression was measured in triplicate.

8.4.1 Ex-vivo lymphocyte subtypes

Unfortunately, in this replication set I found no evidence that the protective allele of rs74796499 (A) has any effect on the expression of LacCer in any of the ex-vivo lymphocyte subtypes (Figure 8.9). These data indicate that the nominally significant observation that carrying the protective allele reduced expression of LacCer was a false positive finding. As anticipated there was no evidence that genotype influenced the expression of CD69 expression in any of the ex-vivo lymphocytes subtypes (Figure 8.10). Similarly, I found no evidence that the rs74796499 genotype influenced the balance of CD4+ T and CD8+ T cells in ex-vivo lymphocytes (Figure 8.11). Association analysis for the rs74796499 SNP was completed using the logistic regression option in PLINK, including the pair ID as categorical covariates.

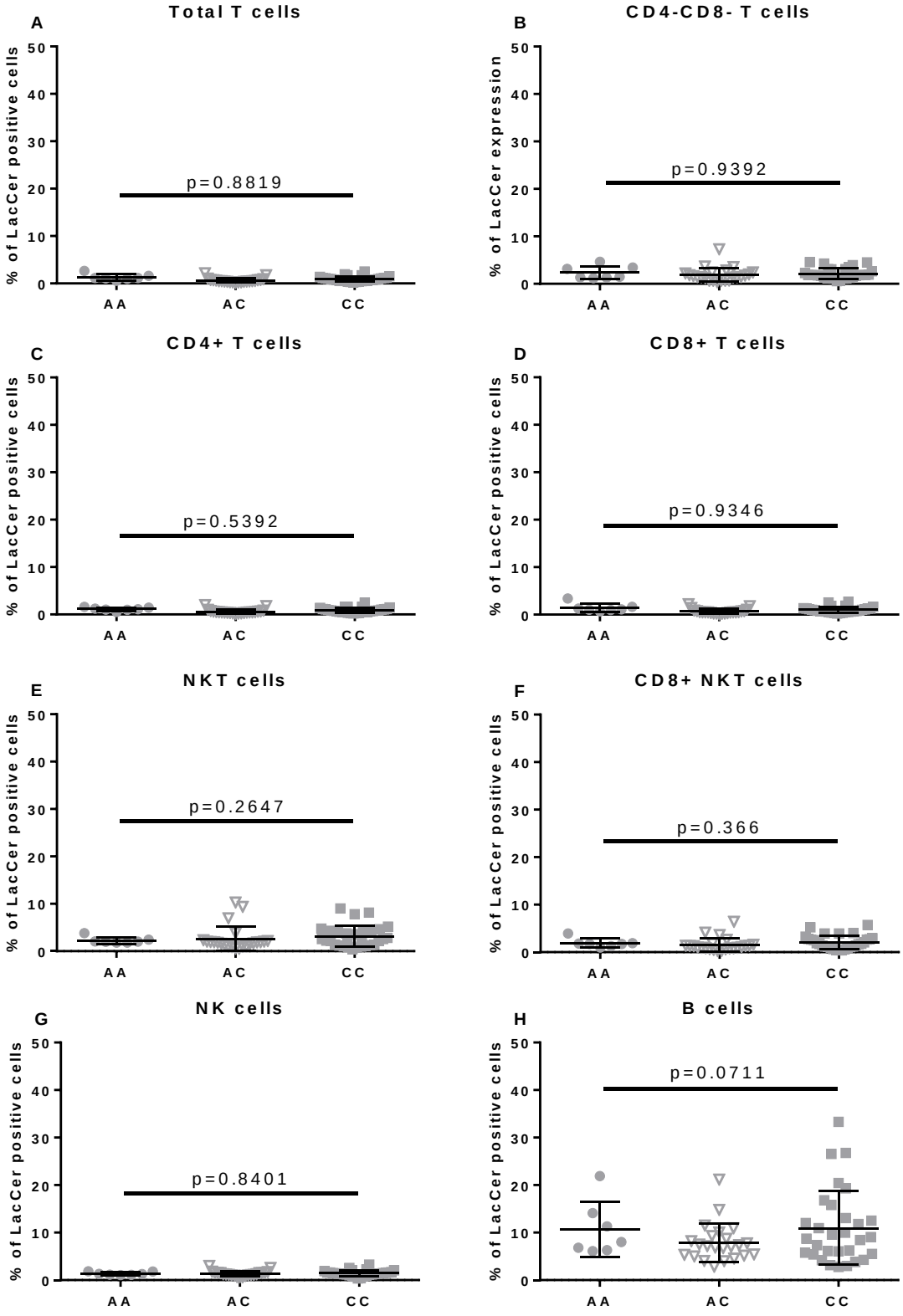

Figure 8. 9: LaCer expression on ex-vivo lymphocyte subtypes by genotype at rs74796499: protective allele homozygotes (A/A), heterozygotes (A/C) and risk allele homozygotes (C/C) are compared for total T cells (A), CD4-CD8- T cells (B), CD4+ T cells (C), CD8+ T cells (D), NKT cells (E), CD8+ NKT cells (F), NK cells (G) and B cells (H).

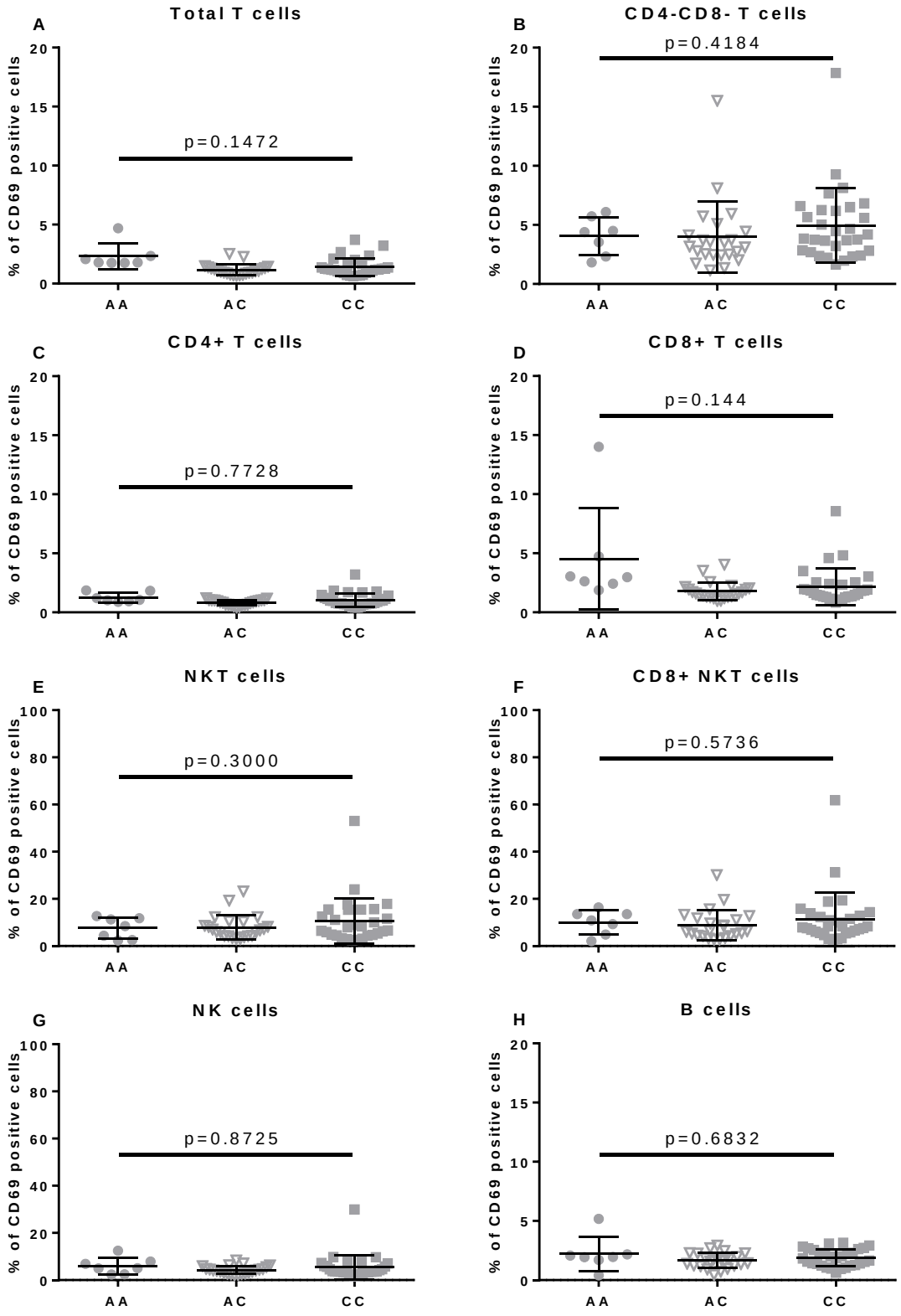

Figure 8. 10: CD69 expression on ex-vivo lymphocyte subtypes by genotype at rs74796499; protective allele homozygotes (A/A), heterozygotes (A/C) and risk allele homozygotes (C/C) are compared for total T cells (A), CD4-CD8- T cells (B), CD4+ T cells (C), CD8+ T cells (D), NKT cells (E), CD8+ NKT cells (F), NK cells (G) and B cells (H).

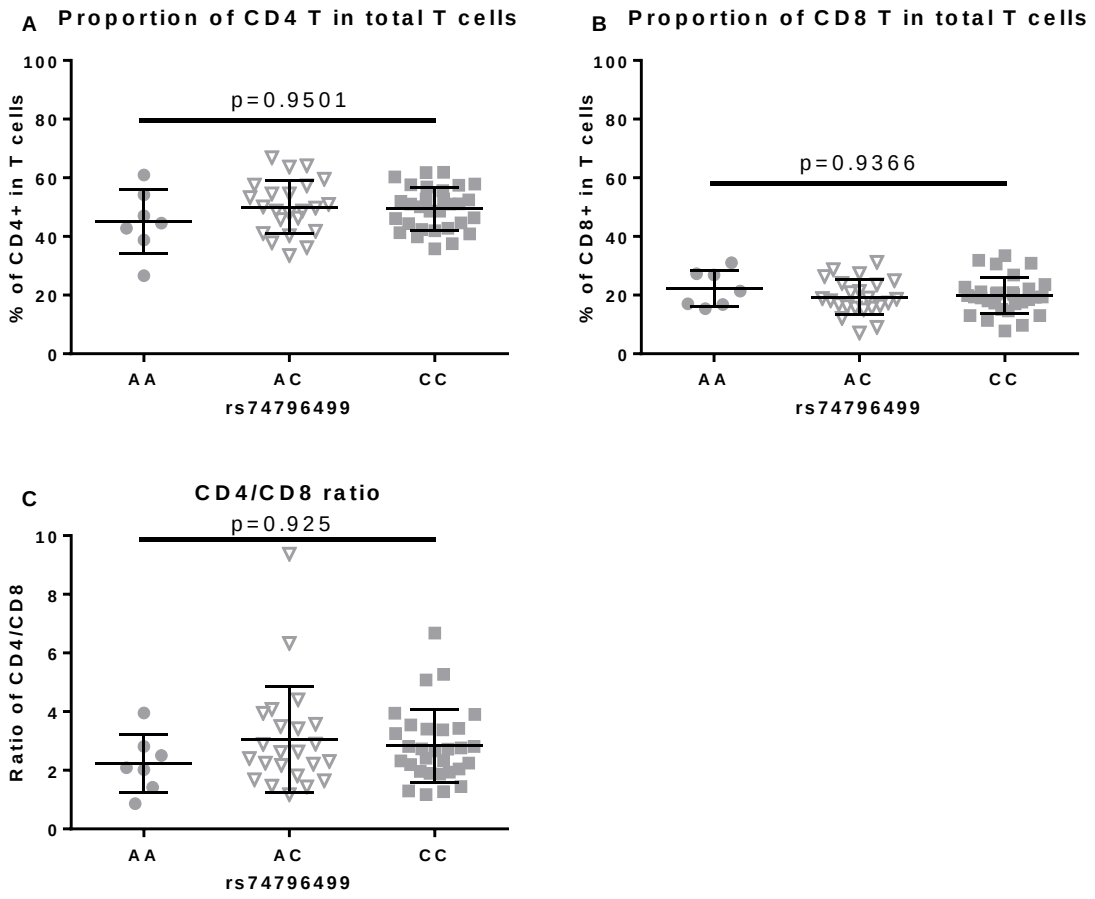

Figure 8. 11: Proportion of T cells that are CD4+ (A) or CD8+ (B) and the ratio of CD4+/CD8+ T cells (C) in protective allele homozygotes (circles), heterozygotes (inverted triangles) and risk allele homozygotes (squares) in ex-vivo cells.

8.4.2 LacCer expression after culture

Figures 8.12, 8.13, 8.14, 8.15, 8.16, 8.17, 8.18 and 8.19 show LacCer expression by rs74796499 genotype in acidic (pH=6.2) and physiological (pH=7.4) conditions for total T cells, CD4-CD8- T cells, CD4+ T cells, CD8+ T cells, NKT cells, CD8+ NKT cells, NK cells and B cells respectively. As for ex-vivo cells I found no evidence to support any influence of the MS associated SNP rs74796499 on LacCer expression.

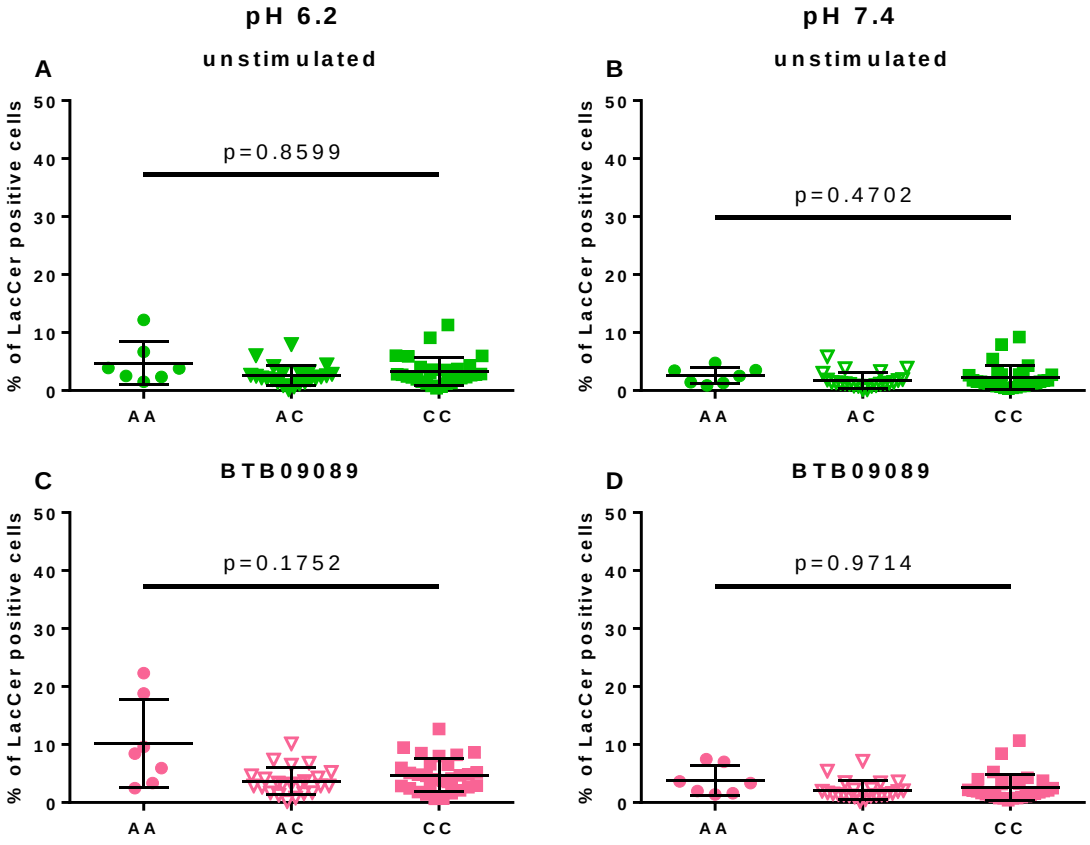

Figure 8. 12: Expression of LacCer on total T cells in protective allele homozygotes (circles), heterozygotes (inverted triangles) and risk allele homozygotes (squares) after 18 hours culture at pH 6.2 and pH 7.4 with and without BTB09089.

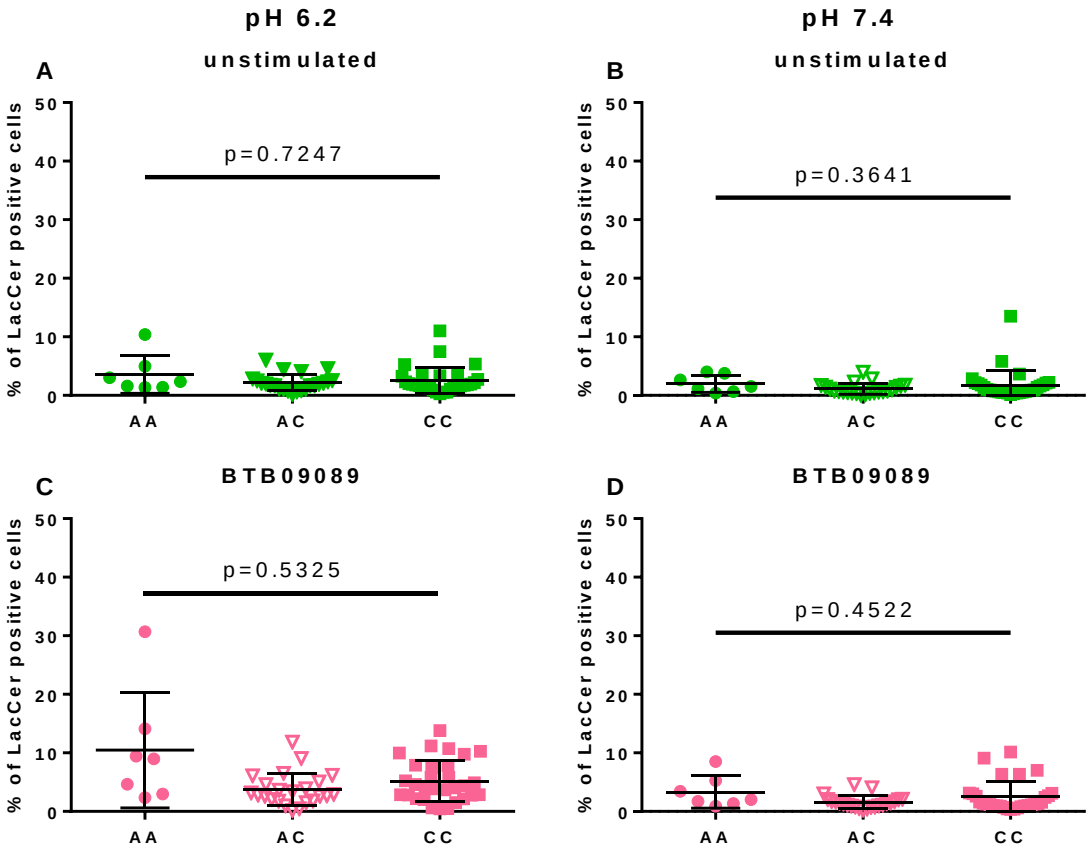

Figure 8. 13: Expression of LacCer on CD4- CD8- T cells ("double negative" cells) in protective allele homozygotes (circles), heterozygotes (inverted triangles) and risk allele homozygotes (squares) after 18 hours culture at pH 6.2 and pH 7.4 with and without BTB09089.

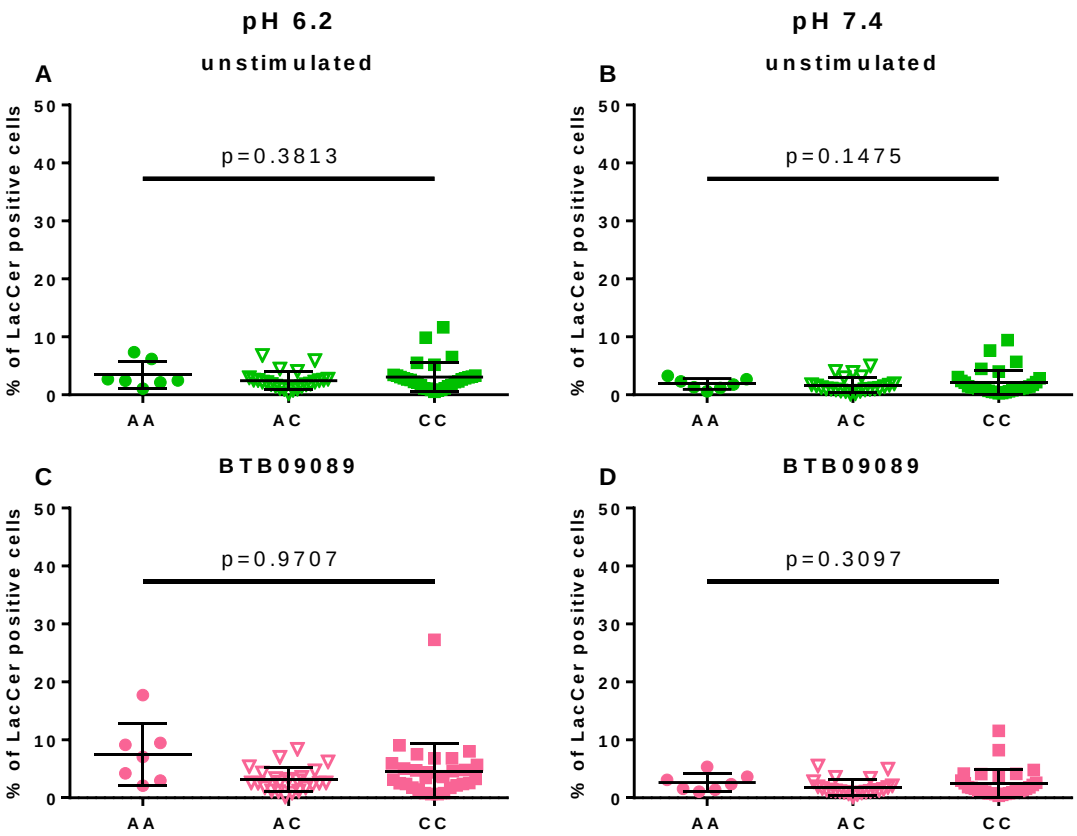

Figure 8. 14: Expression of LacCer on CD4+ T cells in protective allele homozygotes (circles), heterozygotes (inverted triangles) and risk allele homozygotes (squares) after 18 hours culture at pH 6.2 and pH 7.4 with and without BTB09089.

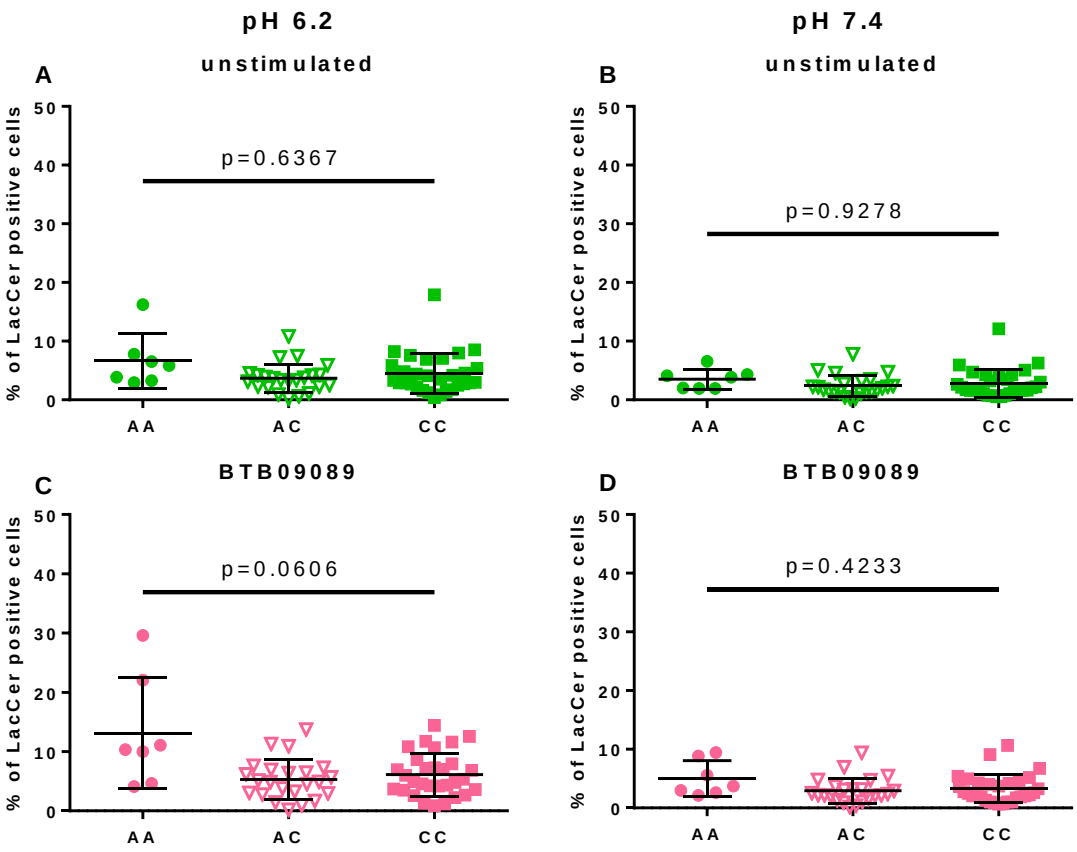

Figure 8. 15: Expression of LacCer on CD8+ T cells in protective allele homozygotes (circles), heterozygotes (inverted triangles) and risk allele homozygotes (squares) after 18 hours culture at pH 6.2 and pH 7.4 with and without BTB09089.

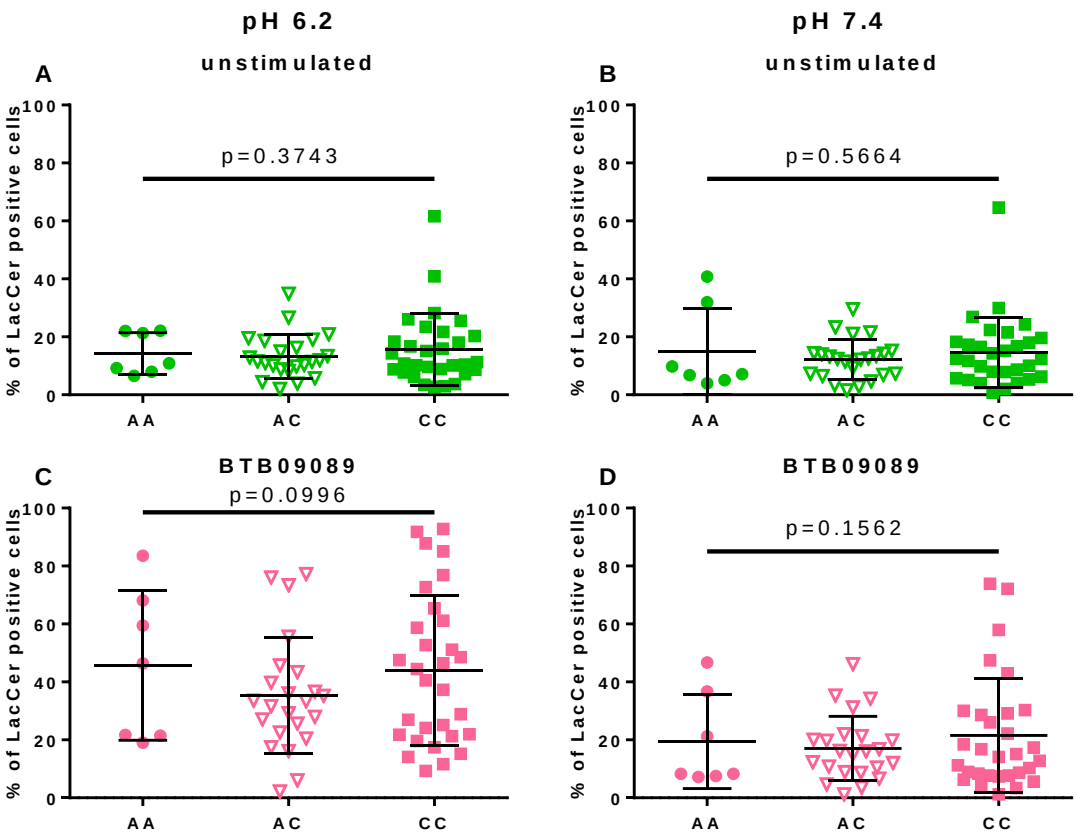

Figure 8. 16: Expression of LacCer on NKT cells in protective allele homozygotes (circles), heterozygotes (inverted triangles) and risk allele homozygotes (squares) after 18 hours culture at pH 6.2 and pH 7.4 with and without BTB09089.

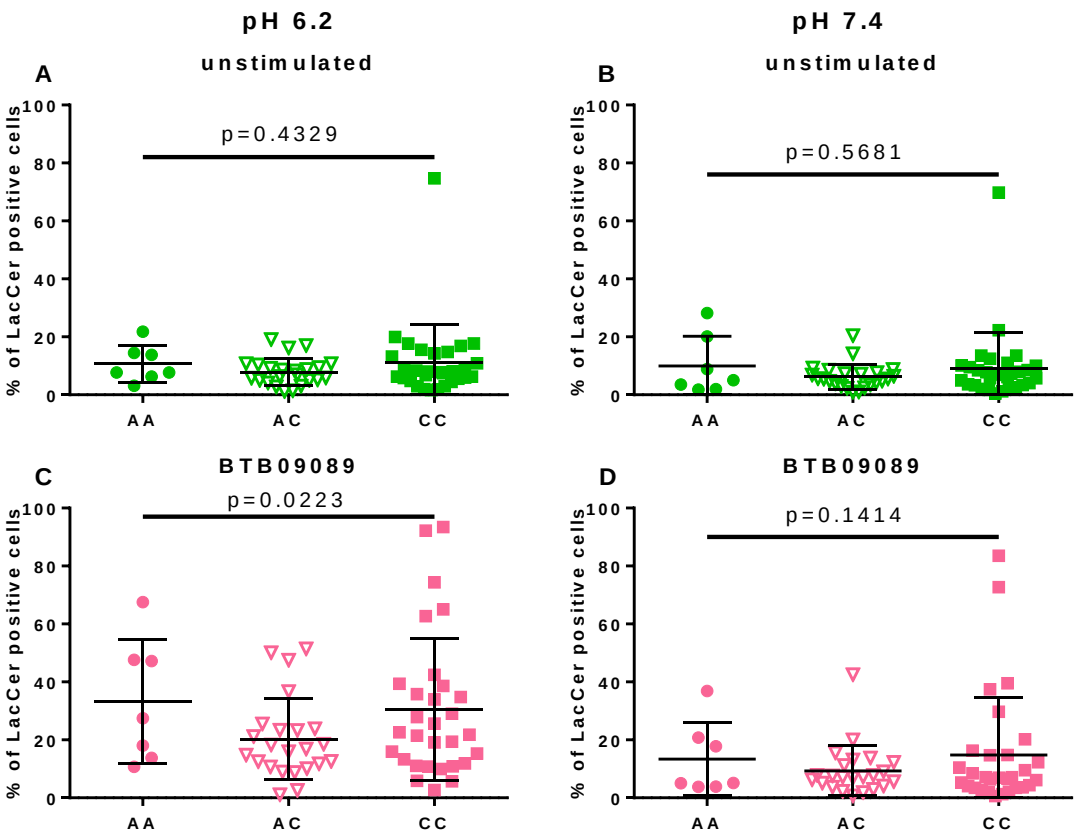

Figure 8. 17: Expression of LacCer on CD8+ NKT cells in protective allele homozygotes (circles), heterozygotes (inverted triangles) and risk allele homozygotes (squares) after 18 hours culture at pH 6.2 and pH 7.4 with and without BTB09089.

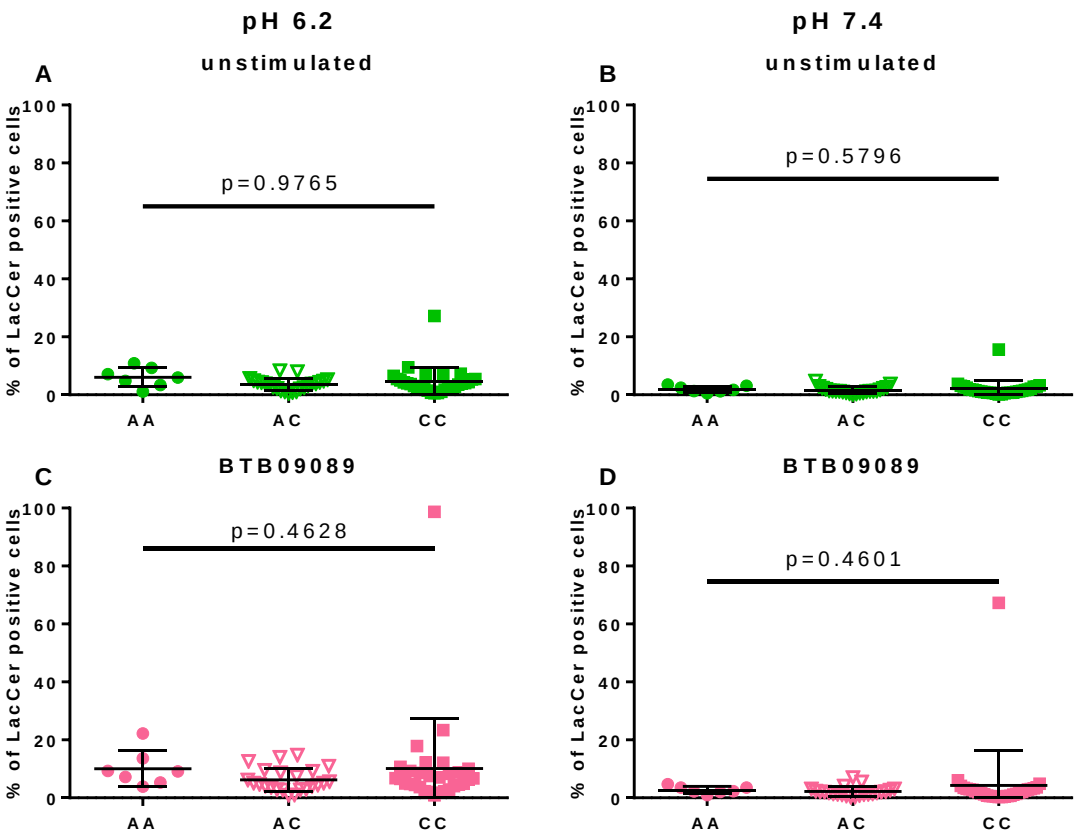

Figure 8. 18: Expression of LacCer on NK cells in protective allele homozygotes (circles), heterozygotes (inverted triangles) and risk allele homozygotes (squares) after 18 hours culture at pH 6.2 and pH 7.4 with and without BTB09089.

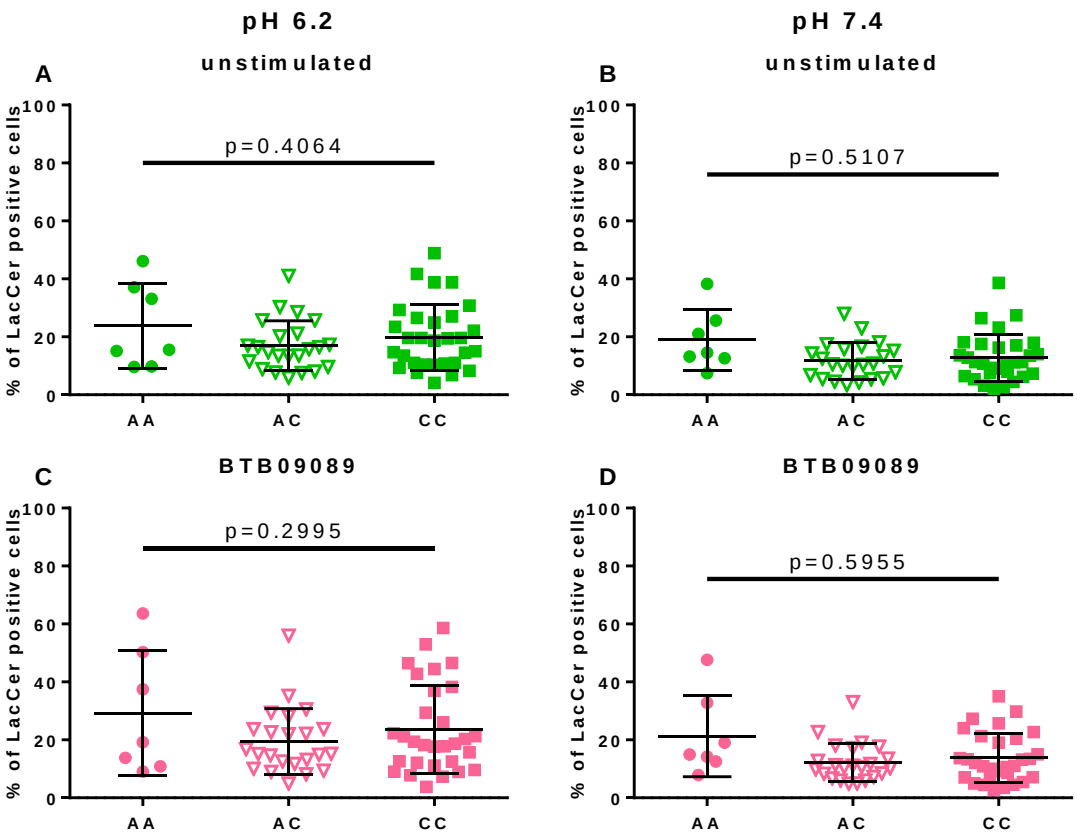

Figure 8. 19: Expression of LacCer on B cells in protective allele homozygotes (circles), heterozygotes (inverted triangles) and risk allele homozygotes (squares) after 18 hours culture at pH 6.2 and pH 7.4 with and without BTB09089.

8.4.3 CD69 expression after culture

Figures 8.20, 8.21, 8.22, 8.23, 8.24, 8.25, 8.26 and 8.27 show CD69 expression by rs74796499 genotype in acidic (pH=6.2) and physiological (pH=7.4) conditions for total T cells, CD4-CD8- T cells, CD4+ T cells, CD8+ T cells, NKT cells, CD8+ NKT cells, and NK cells and B cells respectively. Unfortunately, here I saw a trend towards greater expression of CD69 in protective allele carriers from cells cultured in acidic conditions (unstimulated) but this was not even nominally significant. This failure of replication suggests that these previous observations were also false positives.

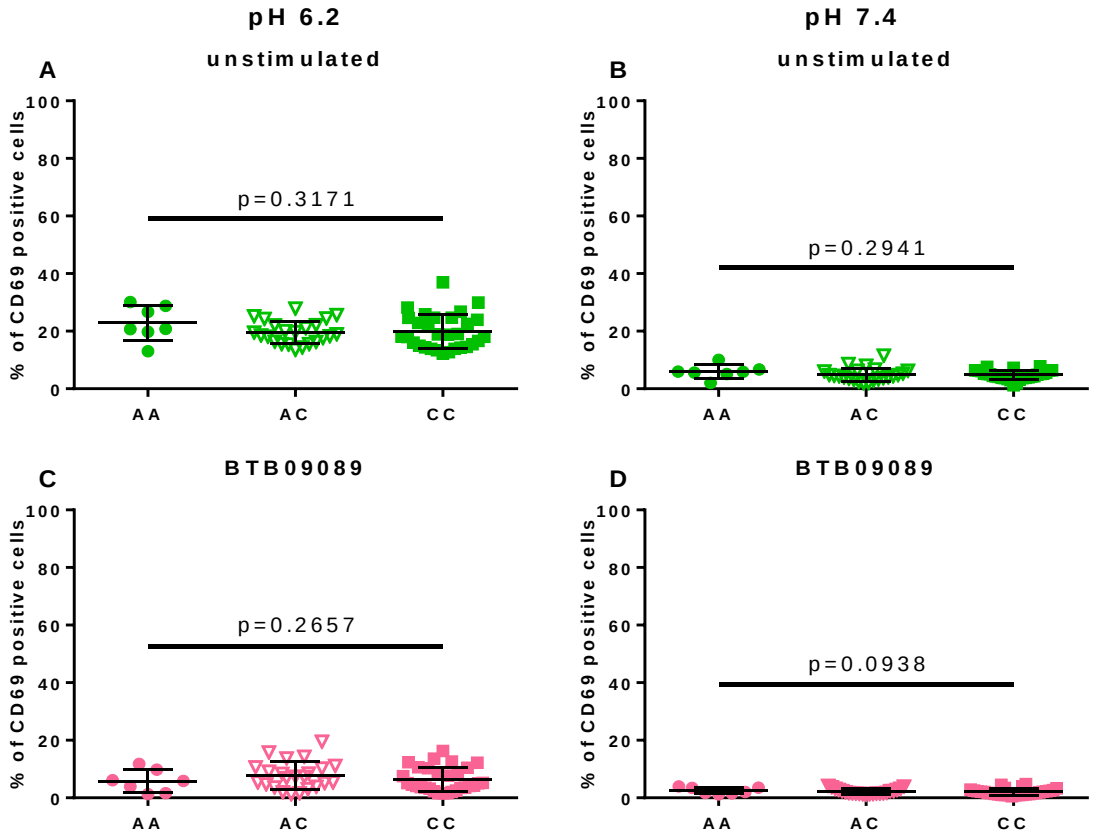

Figure 8. 20: Expression of CD69 on total T cells in protective allele homozygotes (circles), heterozygotes (inverted triangles) and risk allele homozygotes (squares) after 18 hours culture at pH 6.2 and pH 7.4 with and without BTB09089.

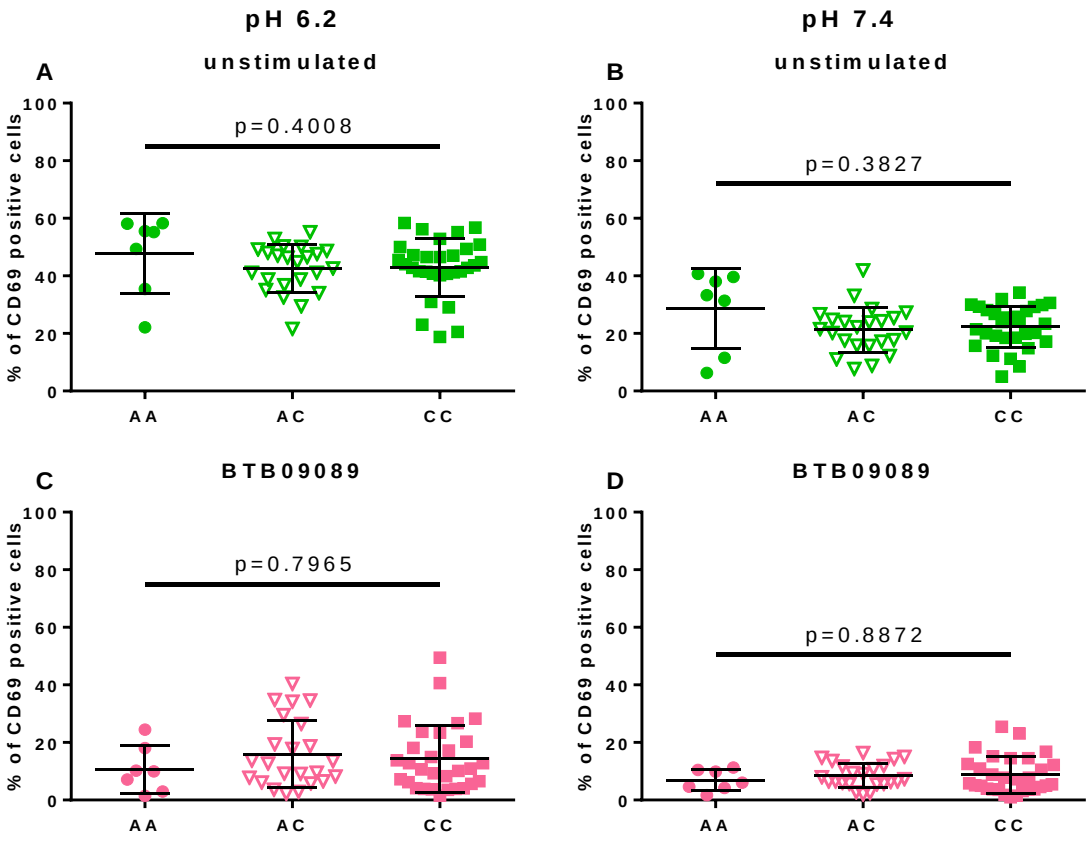

Figure 8. 21: Expression of CD69 on total CD4- CD8- T cells ("double negative" cells) in protective allele homozygotes (circles), heterozygotes (inverted triangles) and risk allele homozygotes (squares) after 18 hours culture at pH 6.2 and pH 7.4 with and without BTB09089.

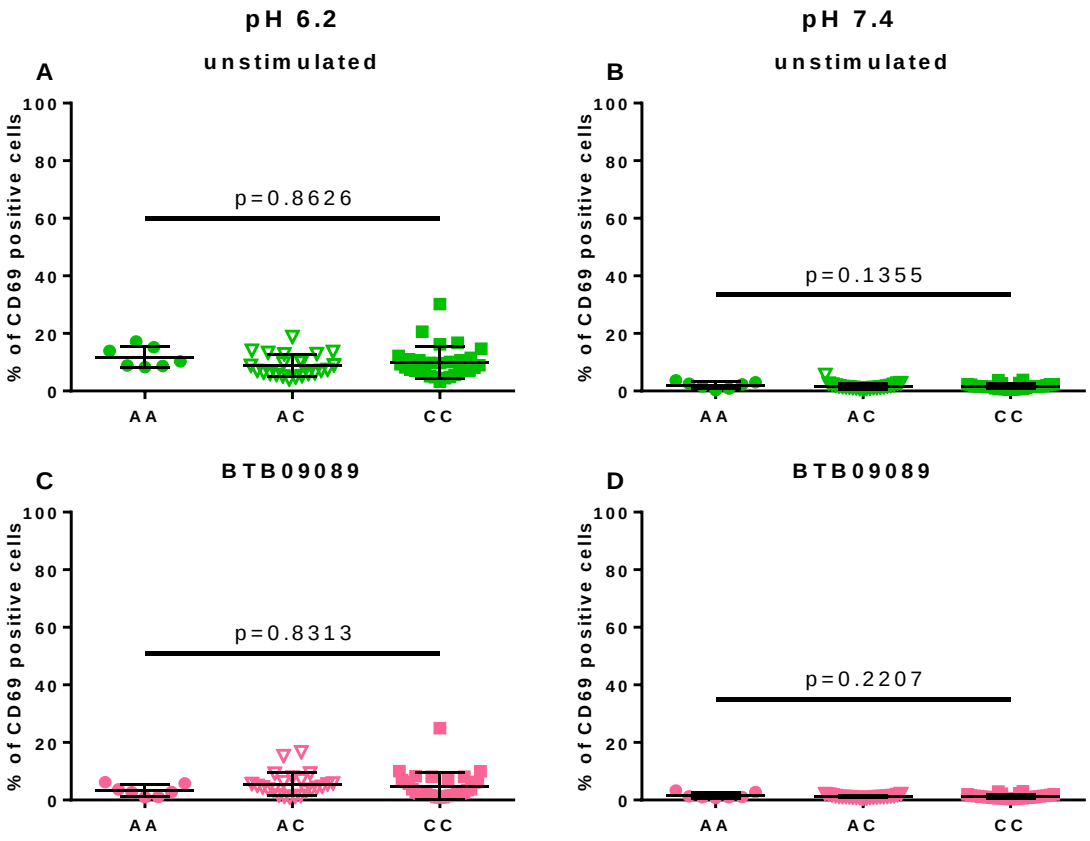

Figure 8. 22: Expression of CD69 on total CD4+ T cells in protective allele homozygotes (circles), heterozygotes (inverted triangles) and risk allele homozygotes (squares) after 18 hours culture at pH 6.2 and pH 7.4 with and without BTB09089.

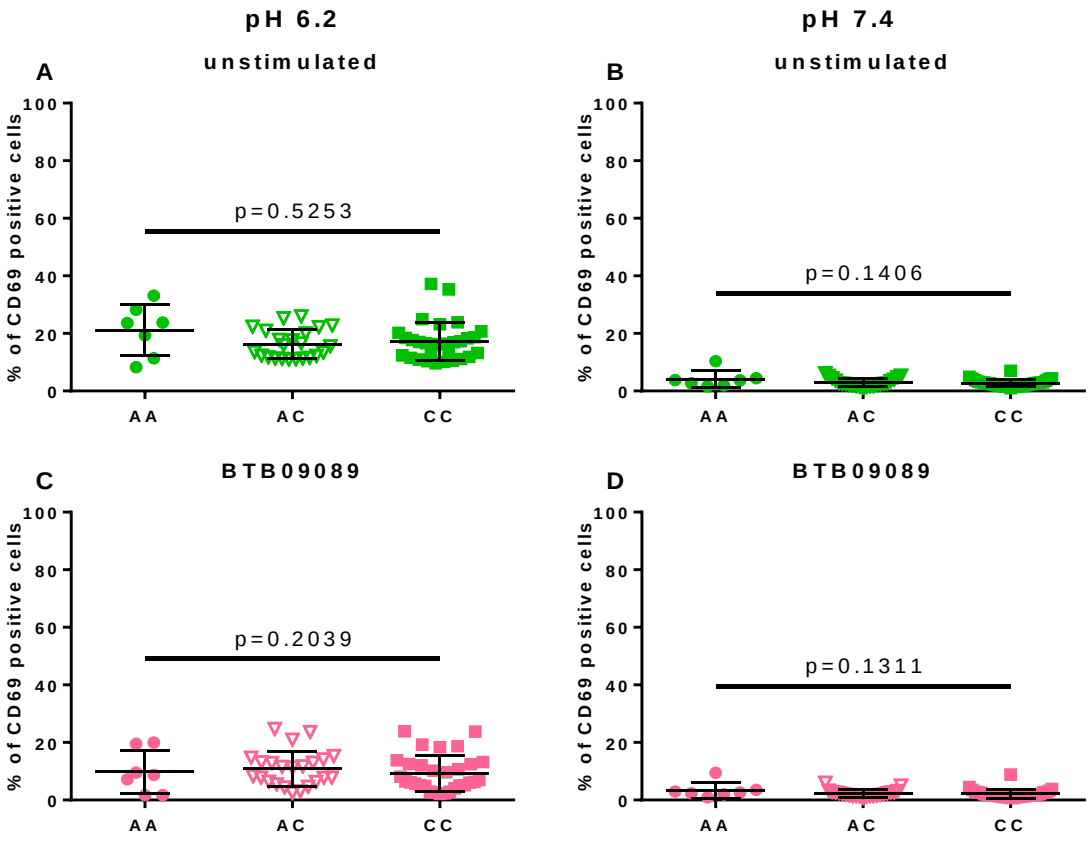

Figure 8. 23: Expression of CD69 on total CD8+ T cells in protective allele homozygotes (circles), heterozygotes (inverted triangles) and risk allele homozygotes (squares) after 18 hours culture at pH 6.2 and pH 7.4 with and without BTB09089.

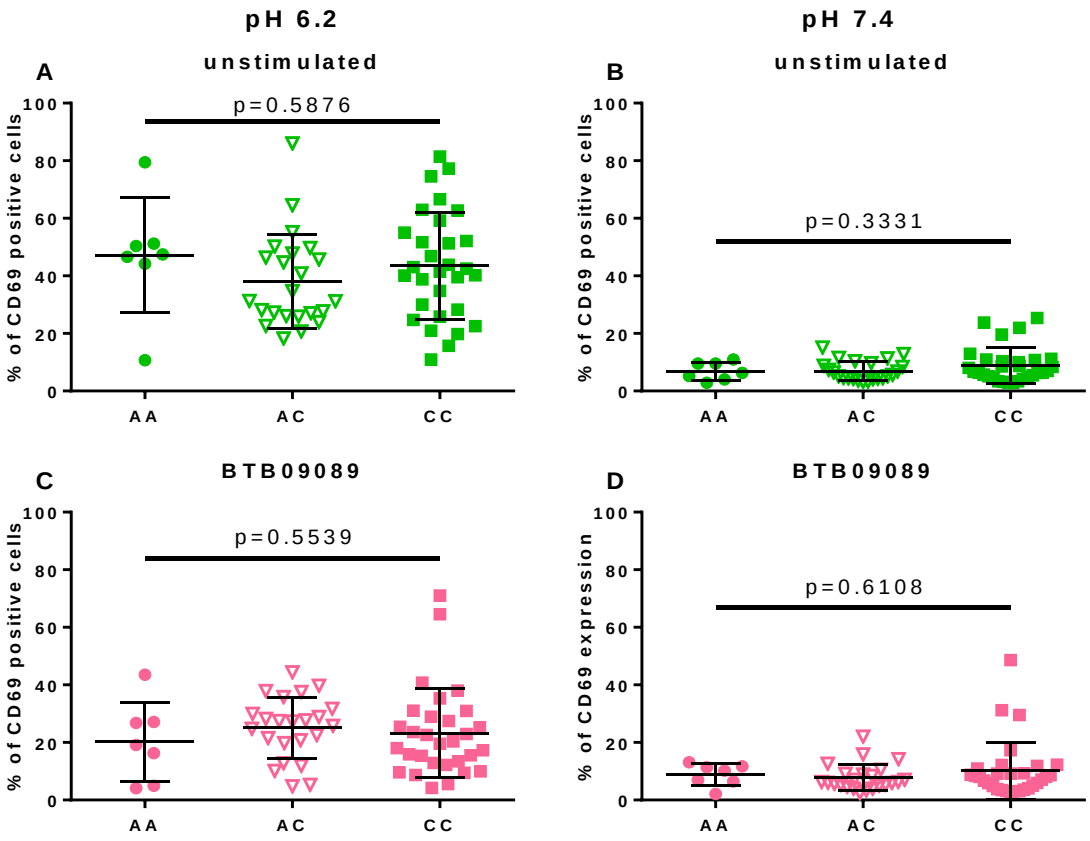

Figure 8. 24: Expression of CD69 on total NKT cells in protective allele homozygotes (circles), heterozygotes (inverted triangles) and risk allele homozygotes (squares) after 18 hours culture at pH 6.2 and pH 7.4 with and without BTB09089.

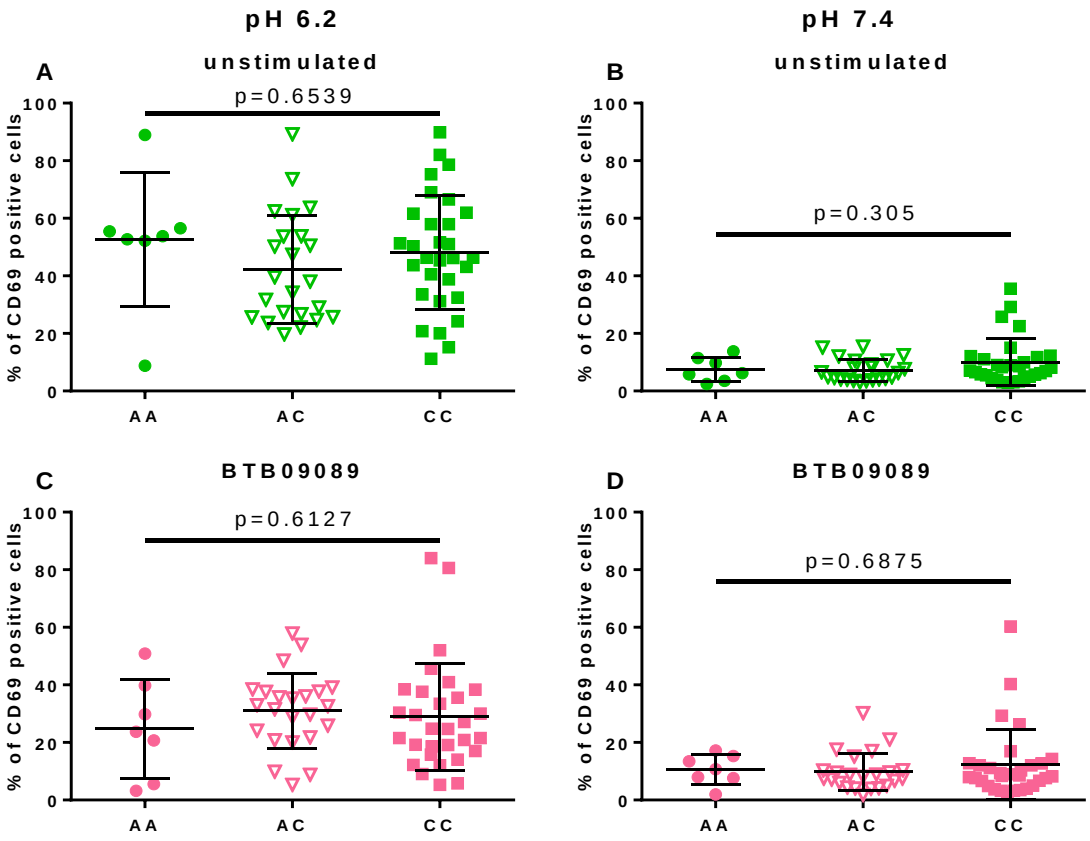

Figure 8. 25: Expression of CD69 on total CD8+ NKT cells in protective allele homozygotes (circles), heterozygotes (inverted triangles) and risk allele homozygotes (squares) after 18 hours culture at pH 6.2 and pH 7.4 with and without BTB09089.

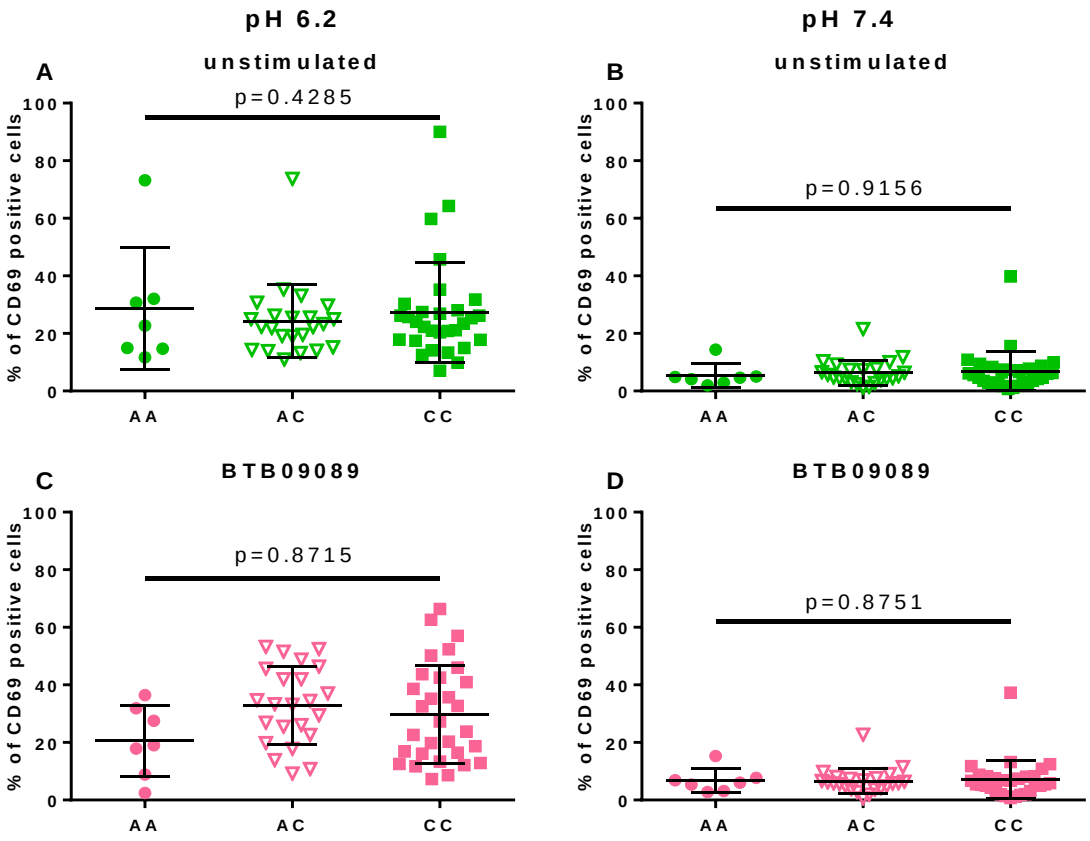

Figure 8. 26: Expression of CD69 on total NK cells in protective allele homozygotes (circles), heterozygotes (inverted triangles) and risk allele homozygotes (squares) after 18 hours culture at pH 6.2 and pH 7.4 with and without BTB09089.

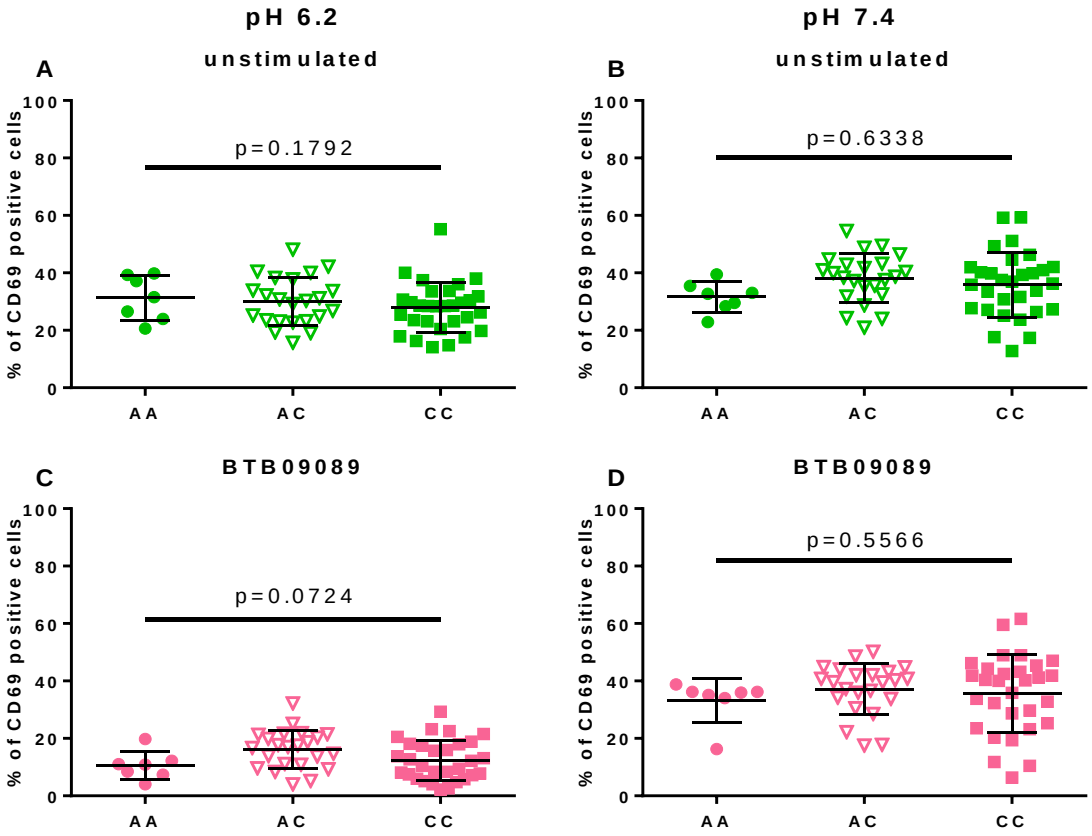

Figure 8. 27: Expression of CD69 on B cells in protective allele homozygotes (circles), heterozygotes (inverted triangles) and risk allele homozygotes (squares) after 18 hours culture at pH 6.2 and pH 7.4 with and without BTB09089.

8.5 Second independent MS associated variant - rs11052877

Genotyping rs11052877 in the 60 individuals studied above revealed that this cohort included 17 protective allele homozygotes (A/A), 35 heterozygotes (A/G) and 8 risk allele homozygotes (G/G). As in Chapter 6 I did not include recruitment pair specific covariates in the analysis of this SNP. For SNPs other than rs74796499 many of the recruitment pairs have the same genotype and therefore including these covariates would effectively exclude these pairs and thereby reduces the power of the analysis. Figure 8.28, 8.29, 8.30, 8.31, 8.32, 8.33, 8.34, 8.35, and 8.36 show CD69 expression by rs11052877 genotype in ex-vivo and cultured cells. Although no association surviving correction for multiple testing was seen, nominally significant association was seen for the higher expression of CD69 in those individuals carrying the rs11052877 protective allele.

In addition, no significant associations were seen with any of the other SNPs tested in Chapter 6 (rs1163251, rs17785991, rs28533072, rs3742074, rs3943657 and rs6020055).

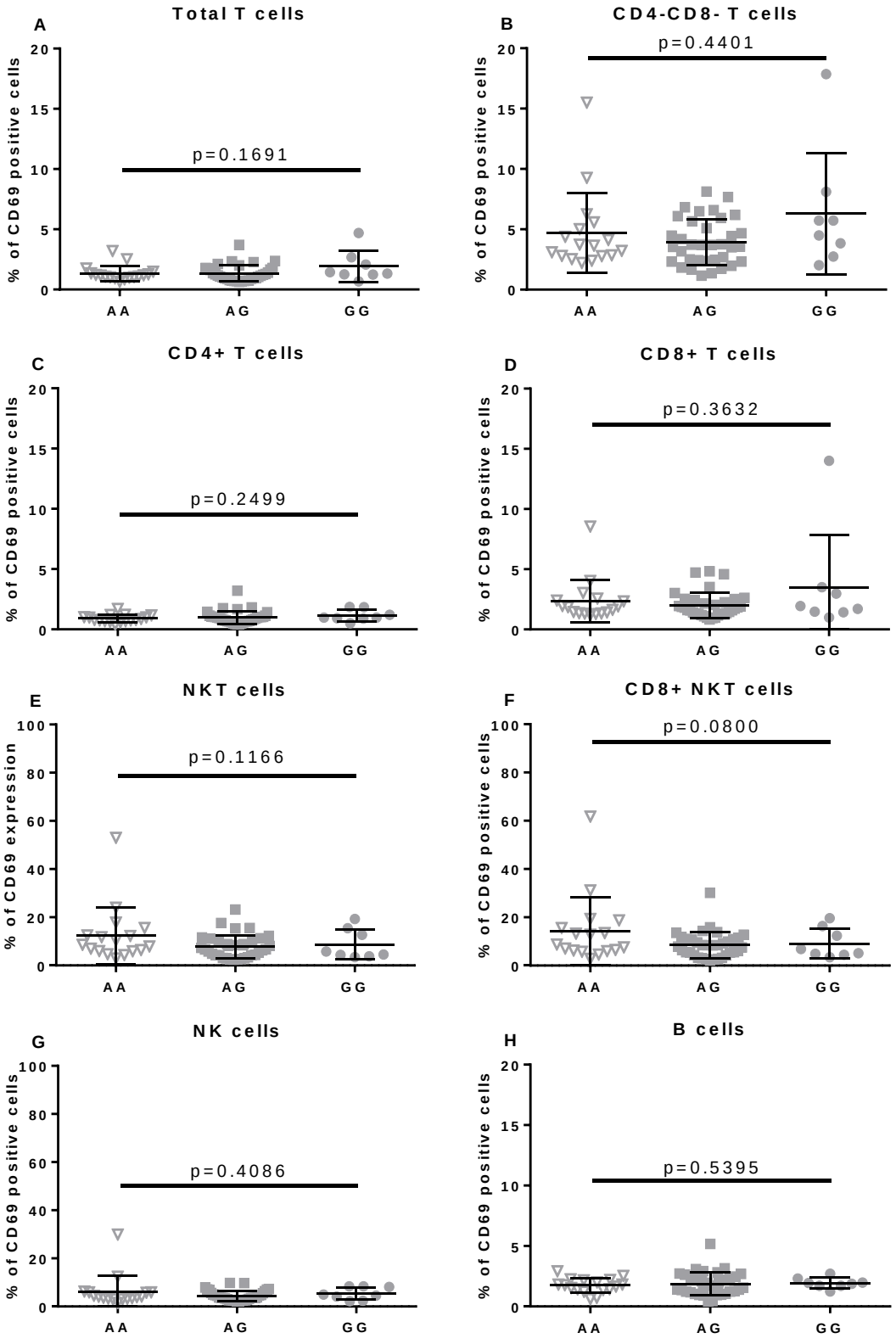

Figure 8. 28: CD69 expression on ex-vivo lymphocyte subtypes by genotype at rs11052877; protective allele homozygotes (circles), heterozygotes (inverted triangles) and risk allele homozygotes (squares).

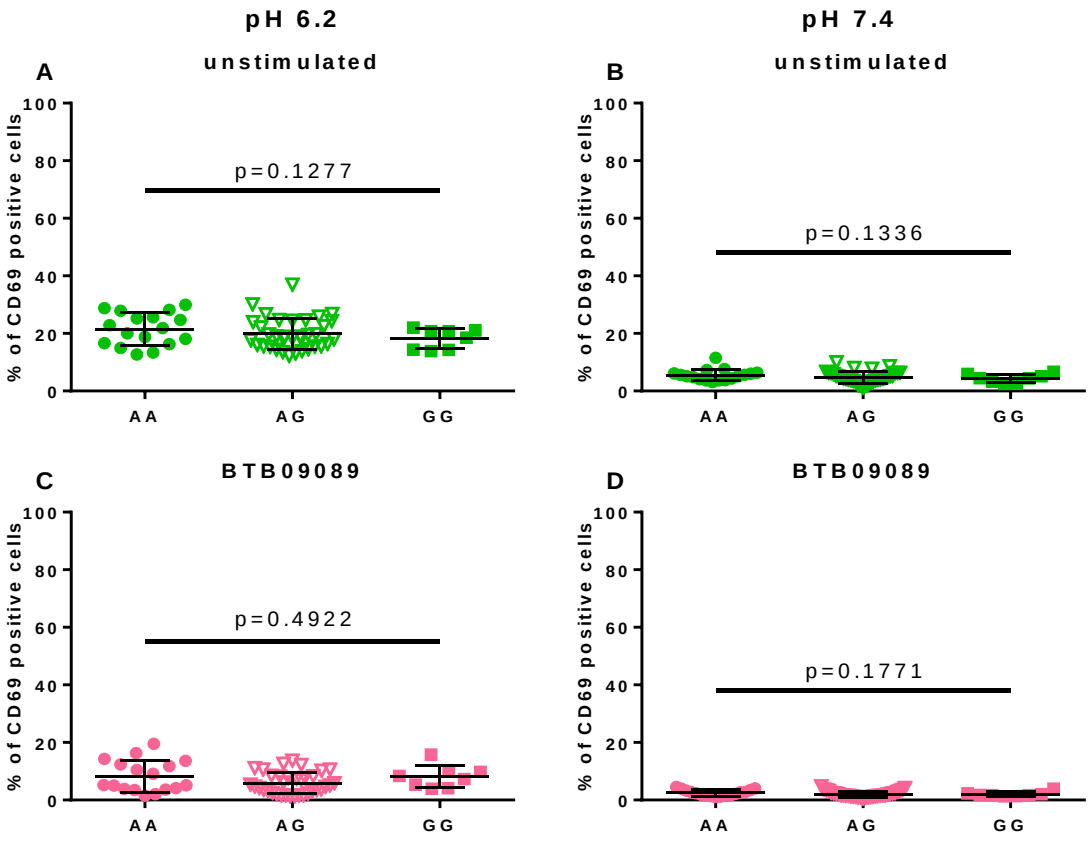

Figure 8. 29: Expression of CD69 on total T cells in protective allele homozygotes (circles), heterozygotes (inverted triangles) and risk allele homozygotes (squares) for rs11052877 after 18 hours culture at pH 6.2 and pH 7.4 with and without BTB09089.

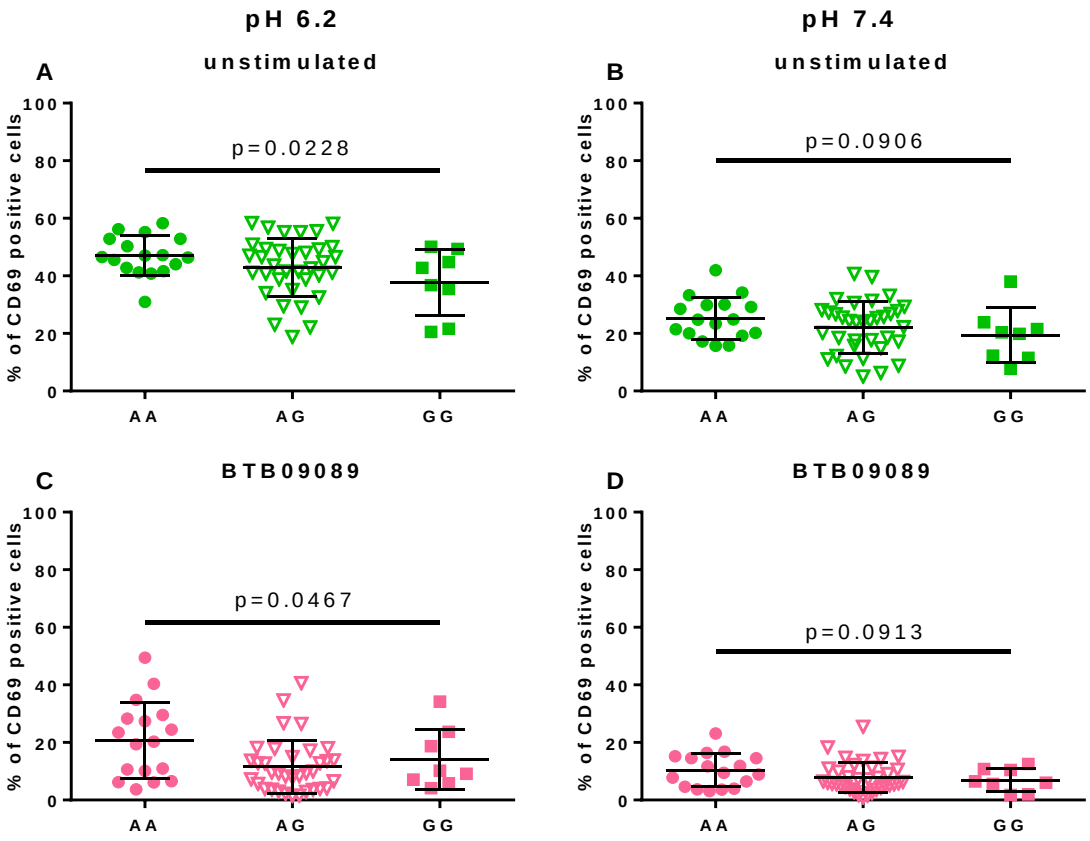

Figure 8. 30: Expression of CD69 on CD4- CD8- T cells ("double negative" cells) in protective allele homozygotes (circles), heterozygotes (inverted triangles) and risk allele homozygotes (squares) for rs11052877 after 18 hours culture at pH 6.2 and pH 7.4 with and without BTB09089.

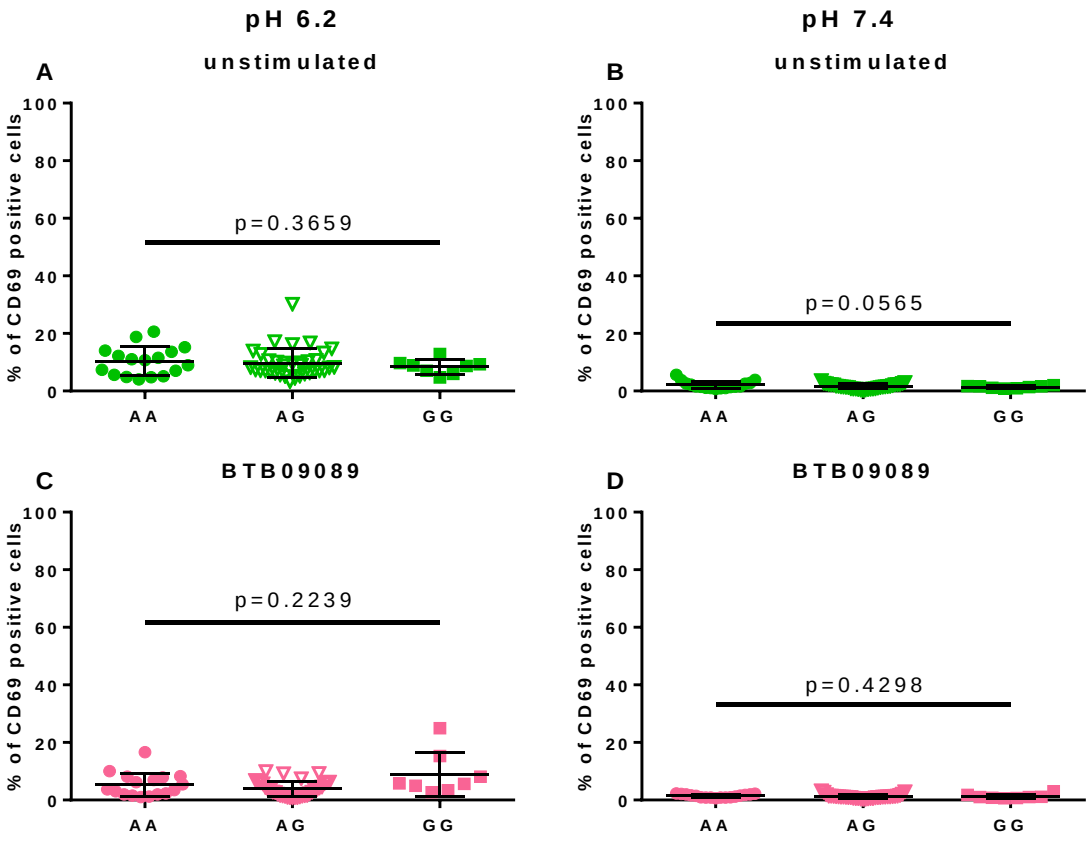

Figure 8. 31: Expression of CD69 on CD4+ T cells in protective allele homozygotes (circles), heterozygotes (inverted triangles) and risk allele homozygotes (squares) for rs11052877 after 18 hours culture at pH 6.2 and pH 7.4 with and without BTB09089.

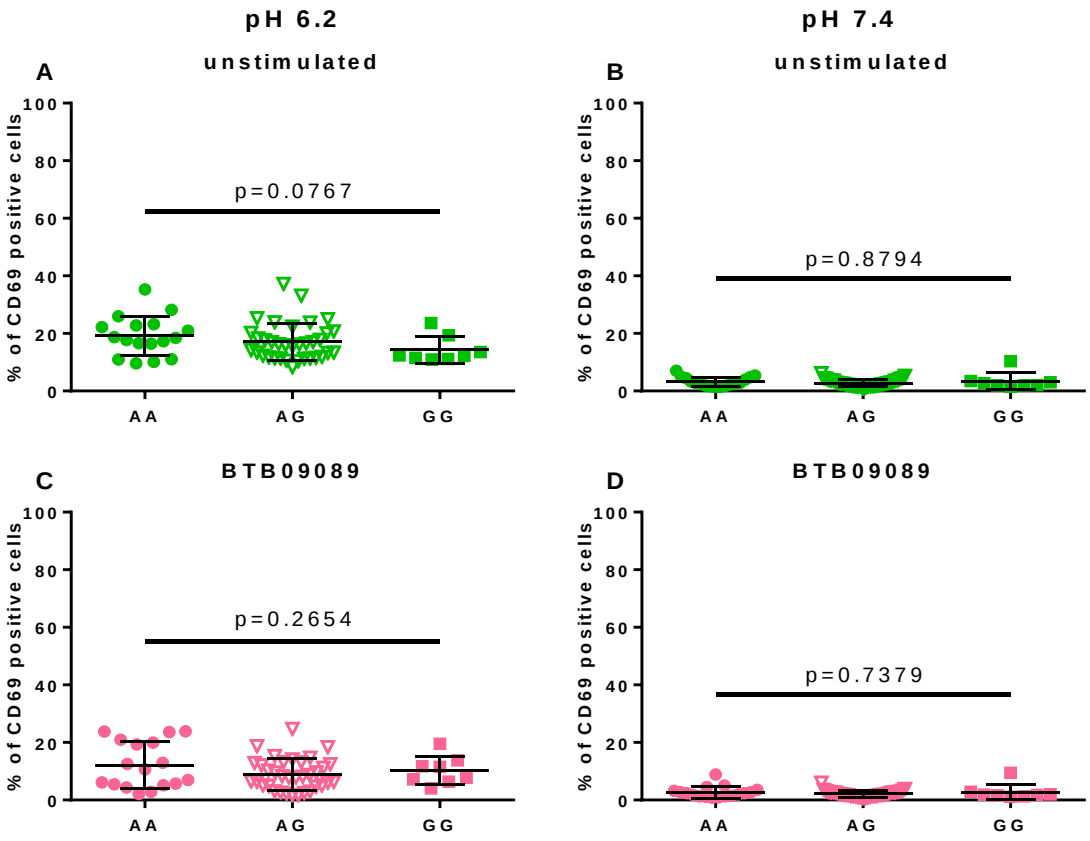

Figure 8. 32: Expression of CD69 on CD8+ T cells in protective allele homozygotes (circles), heterozygotes (inverted triangles) and risk allele homozygotes (squares) for rs11052877 after 18 hours culture at pH 6.2 and pH 7.4 with and without BTB09089.

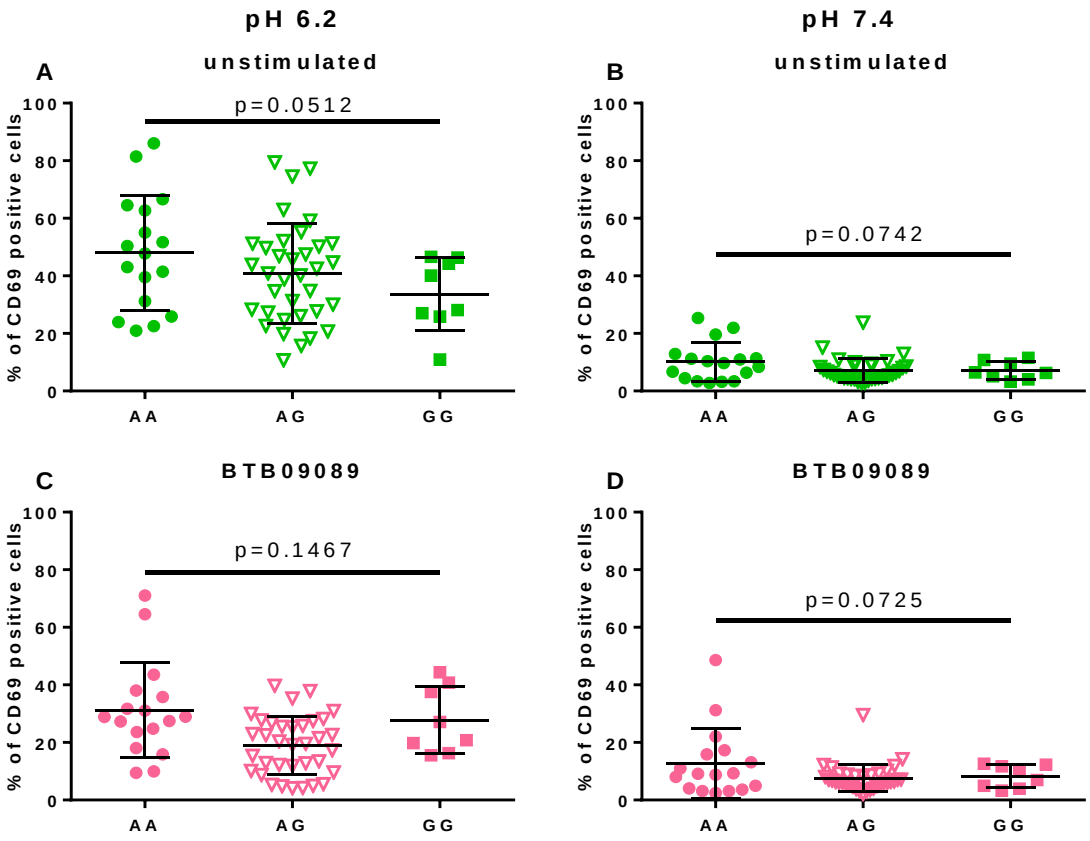

Figure 8. 33: Expression of CD69 on NKT cells in protective allele homozygotes (circles), heterozygotes (inverted triangles) and risk allele homozygotes (squares) for rs11052877 after 18 hours culture at pH 6.2 and pH 7.4 with and without BTB09089.

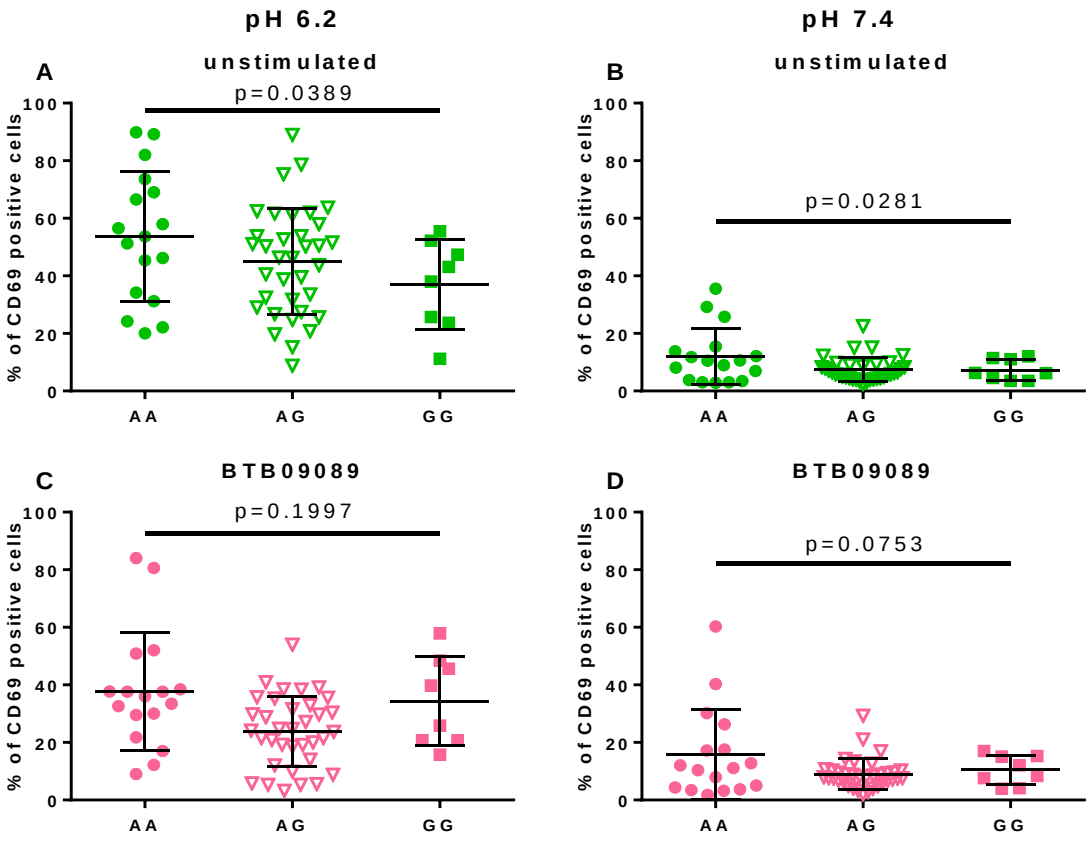

Figure 8. 34: Expression of CD69 on CD8+ NKT cells in protective allele homozygotes (circles), heterozygotes (inverted triangles) and risk allele homozygotes (squares) for rs11052877 after 18 hours culture at pH 6.2 and pH 7.4 with and without BTB09089.

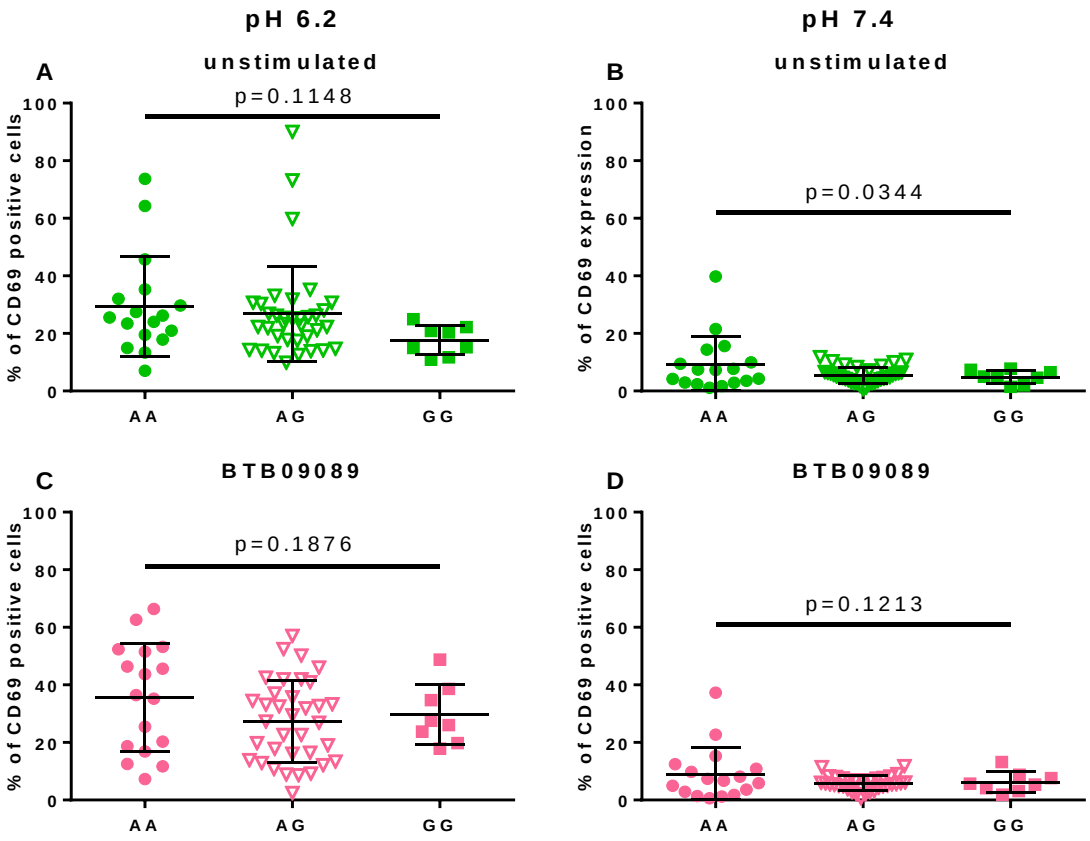

Figure 8. 35: Expression of CD69 on NK cells in protective allele homozygotes (circles), heterozygotes (inverted triangles) and risk allele homozygotes (squares) for rs11052877 after 18 hours culture at pH 6.2 and pH 7.4 with and without BTB09089.

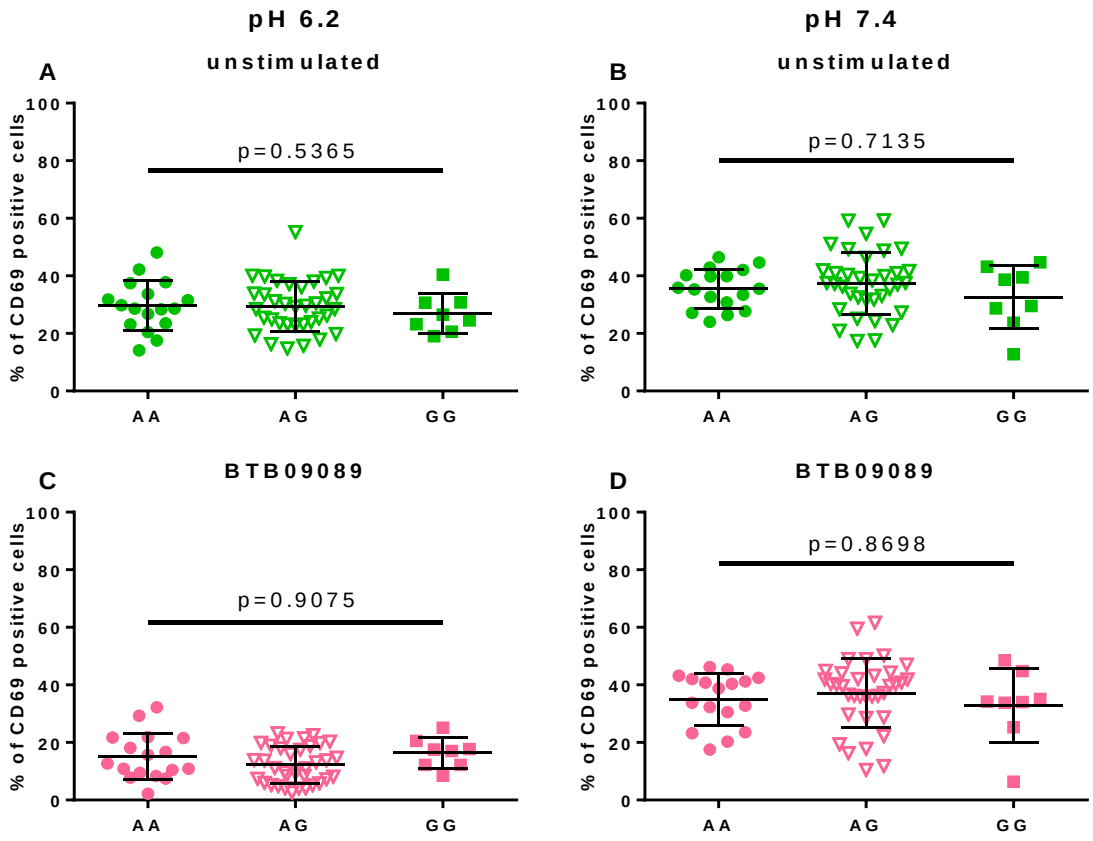

Figure 8. 36: Expression of CD69 on B cells in protective allele homozygotes (circles), heterozygotes (inverted triangles) and risk allele homozygotes (squares) for rs11052877 after 18 hours culture at pH 6.2 and pH 7.4 with and without BTB09089**.**

8.6 mRNA expression in ex-vivo cells

I collected mRNA from CD3+ and CD3- ex-vivo cells and measured transcriptional expression of *GPR65* using two primer pairs. Primer pair 1 (also be used in Chapter 6) extends from exon 1 to exon 2 and therefore includes the exon 1-2 boundary; whereas primer pair 2 is contained entirely within exon 2 (this pair is distinct from the primers used in Chapter 6). Figure 8.37 shows the results for both primer pairs in both cell subtypes, which reveals a trend (nominally significant in CD3- cells) towards higher expression of *GPR65* in individuals carrying the protective allele. The same trend was seen in Chapter 6, but no protective allele homozygotes were included in that earlier analysis. However, after conditioning these data on the known eQTL rs3943657 there was no residual evidence of association, confirming that this modest apparent association with expression is the result of LD between rs74796499 and rs3943657 (D'=1.0 in the CEU population, with the minor allele of rs74796499 always carried on

chromosomes carrying the major allele at rs3943657, the difference in allele frequency means that r^2 is necessarily low). In addition, I also measured the mRNA expression of *GALC*, *CD69*, *RORC* and non-coding RNA *LINC01146* (Figure 8.38) and found evidence that carrying the protective allele of rs74796499 increased the expression of *GALC* and *CD69*; again these effects disappeared after conditioning rs3943657. All expressions levels were quantified relative to the housekeeping gene *β-ACTIN* using the standard curve method. Analysis was performed as for surface expression but with additional covariates related to batching for RNA extraction, RNA clean-up and cDNA conversion.

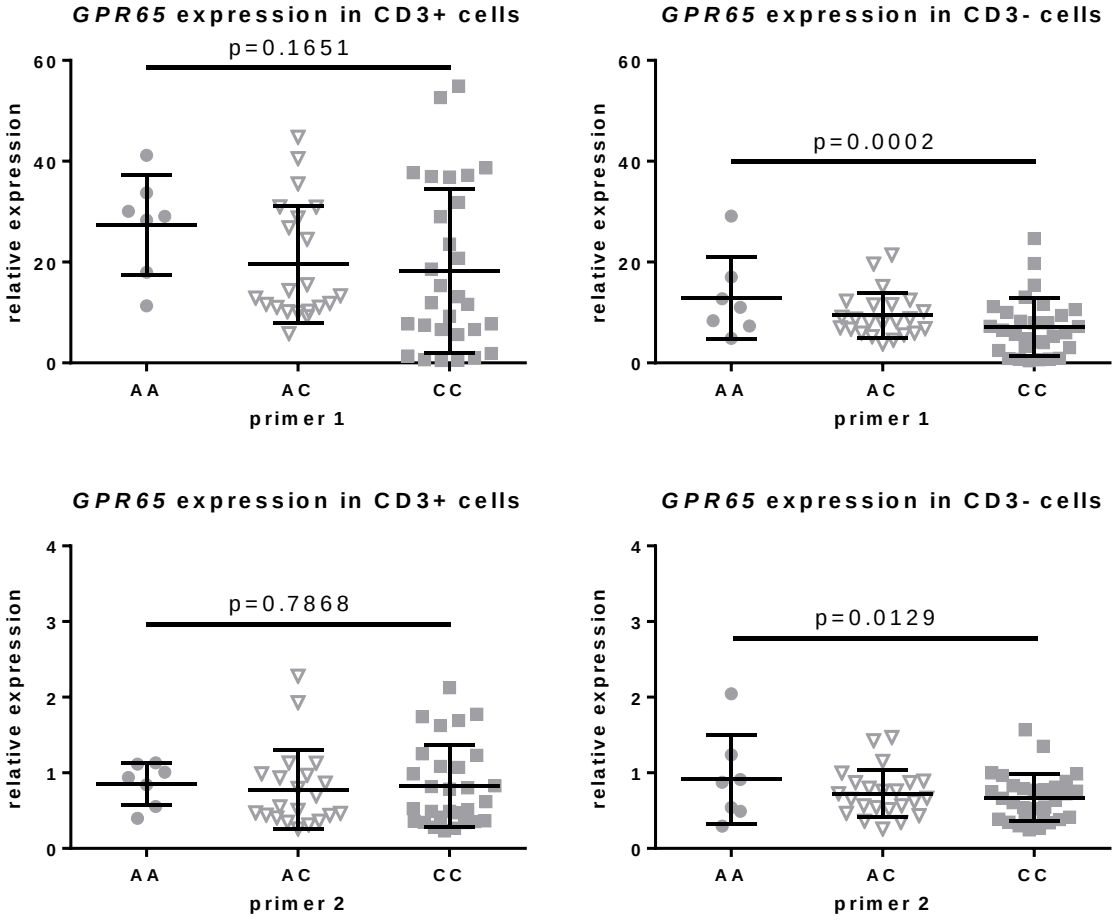

Figure 8. 37: *GPR65* mRNA expression using primer pair 1 (top row) and primer pair 2 (bottom row) in CD3+ (left hand panels) and CD3- cells (right hand panels) comparing rs74796499 protective allele homozygotes (circles), heterozygotes (inverted triangles) and risk allele homozygotes (squares).

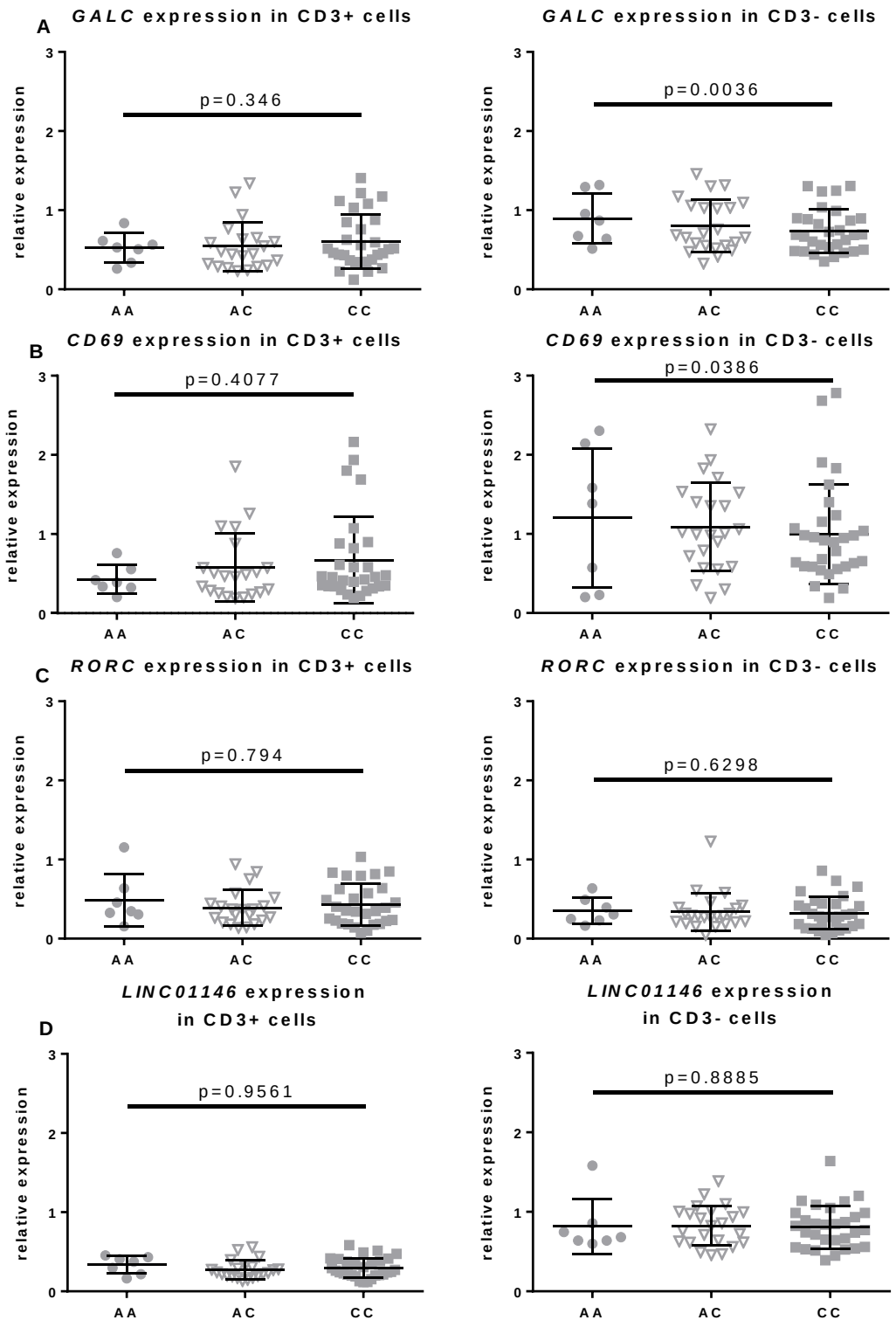

Figure 8. 38: *GALC* (A), *CD69* (B) and *RORC* (C) and *LINC01146* (D) mRNA expression in CD3+ (left hand panels) and CD3- cells (right hand panels) comparing rs74796499 protective allele homozygotes (circles), heterozygotes (inverted triangles) and risk allele homozygotes (squares).

8.6.1 *GPR65* expression and rs3943657

Given that rs3943657 is an established eQTL for GPR65 [271], I genotyped this SNP in these 60 individuals and tested for association with the data from both GPR65 primer pairs as a positive control (Figure 8.39). The result was as expected with lower expression of the minor allele (G) (and the clearest difference seen for primer pair 1 in CD3- cells). Pair IDs were not included as covariates.

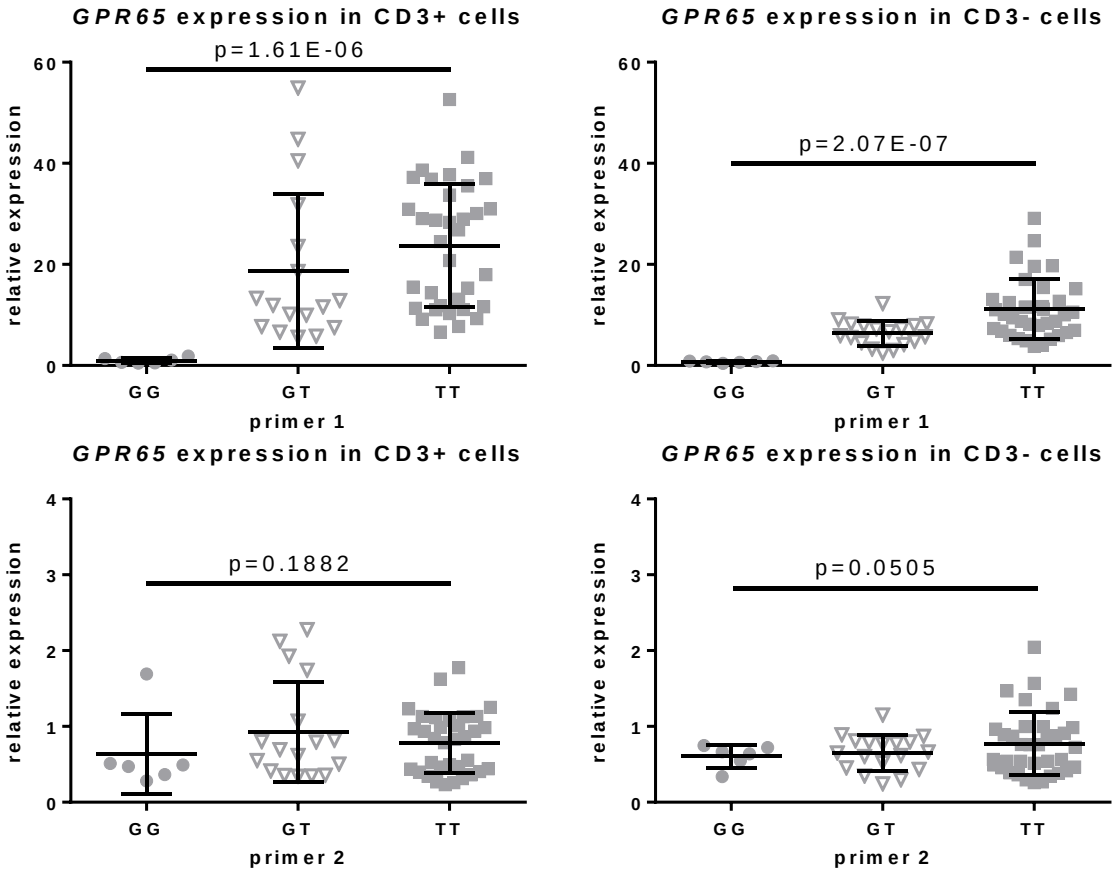

Figure 8. 39: *GPR65* mRNA expression using primer pair 1 (top row) and primer pair 2 (bottom row) in CD3+ (left hand panels) and CD3- cells (right hand panels) comparing rs3943657 minor allele homozygotes (circles, n=6), heterozygotes (inverted triangles, n=18) and major allele homozygotes (squares, n=36).

8.7 Discussion

In this final stage of my thesis I unfortunately failed to replicate either of the observations I had made earlier regarding the effects of carrying the protective allele of rs74796499; lower levels of LacCer in ex-vivo cells and higher level of CD69 on cells cultured in acidic conditions. There are several factors that may have confounded this final round of experiments, in particular technical effects relating to differences in the flow cytometry antibody panel used and the possibility of regression to the mean. However, the evidence supporting these effects from my earlier work was rather preliminary, only just surviving correction for multiple testing, and thus these earlier observations are most likely to have been false positive associations. The fact that I saw the expected effect of rs3943657 on the mRNA expression of *GPR65* provides a positive control indicating that my study had adequate power. However, it is clear that I would need a very much larger study to definitively confirm or refute whether or not the effects I highlighted in earlier chapters are genuine.

The low frequency of the rs74796499 protective allele meant that it became increasingly difficult for the Cambridge BioResource to recruit completely healthy volunteers and in the final set of experiments described in this chapter a small proportion of those recruited were receiving treatments for immunologically minor conditions, such as depression and eczema. Those receiving treatment for such conditions (e.g. anti-histamine, anti-depressants etc.) were over represented in the protective allele carriers (the more difficult group to recruit) and therefore it is conceivable that these could have confounded my results. However, it seems unlikely that such treatments would have undermined the demonstration of both of these effects, especially the increase in CD69 seen in cultured cells, where it seems unlikely that any drug related effects would have persisted.

Because I did not observe any evidence for genotype dependent effects on expression (as had been suggested by the work in earlier chapters) it was not possible to infer whether GPR65 might be involved through the effects of BTB09089. I confirmed the toxic effect of psychosine reported by others [159, 321] and saw substantial effects of BTB09089 on surface expression in cultured cells which certainly suggests that GPR65 is involved in modulating the response of immune cells in acidic conditions, but the relevance of this to the modulation of MS risk resulting from rs74796499 genotype cannot be inferred.

Chapter 9: Conclusion and Future work

The research I undertook during my PhD was prompted by my predecessor's provisional observations that extracellular pH influences T cell activation and that the extent of this influence was dependent upon MS associated variation on chromosome 14q31.3 [33, 151]. Given the known immune regulatory effects and acid sensing properties of GPR65 [193], I hypothesised that this gene might be involved in mediating these effects. It seems reasonable to imagine that acid induced activation of GPR65 might have an important role in limiting the inflammatory response within MS lesions, and therefore that the allele carried at the nearby MS associated SNP rs74796499 might exert its effects on risk by altering GPR65's involvement in this process. Unfortunately, although, I was able to confirm with high statistical confidence that T cell activation is indeed affected by extracellular pH, I found no evidence to support the suggestion that rs74796499 genotype influences these effects.

In his original pilot work my predecessor, Dr Tom Button, only considered the late activation marker CD25. However, in my experiments I also assessed the early activation marker CD69 and the functionally important membrane lipid lactosylceramide (LacCer, CD17). This extended analysis revealed that the expression of CD69 is increased after culturing in acidic conditions, even in the absence of any stimulation. In my initial experiments I found evidence that rs74796499 genotype might influence this acid induced expression of CD69, and also the expression of LacCer in ex-vivo cells. Unfortunately, neither of these nominally significant provisional trends were confirmed in my replication experiments. Including BTB09089, the synthetic agonist of GPR65, in cultures dramatically changed the expression of CD25, CD69 and LacCer in a range of cell types, but once again did not reveal any genotype dependent effects. In total despite processing samples from over 160 individuals I found no convincing evidence that the genotype at the MS associated SNP rs74796499 exerts any effects on lymphocyte activation, regardless of pH, anti-CD3/CD28 stimulation or GPR65 activation.

My research was based exclusively on samples from healthy volunteers recruited through the Cambridge BioResource. This increased the power of my analysis by ensuring higher than expected representation of the lower frequency genotypes, but meant that I have not assessed the influence of rs74796499 in the context of the disease. I had intended to extend my work into considering patient samples once a genotype dependent effect was demonstrated but in retrospect I probably should have included patient samples in parallel with healthy controls. It

is possible that genotype dependent effects might have emerged if I had sufficient resources to consider alternate GPR65 negative modulators, such as ZINC62678696 [322], more refined cell subtypes, such as iNKT cells [323-325], or had measured cytokine profiles, for example by using the human Th1/Th2/Th17A cytokine kit (BD Bioscience, US) (which including IL-2, IL-4, IL-5, IL-10, TNF, IFN-γ and IL-17A). It might also have been profitable to further explore the effects of genotype on apoptosis, especially since GPR65 has already been shown to have a functionally important role in the survival and apoptosis in other cell types and disease contexts [185, 326]. In my experiments I only employed a simple fixable viability stain so that dead cells could be excluded. It could have been relevant to extend the analysis to include a fuller assessment of survival and apoptosis.

Given more time I would like to have further optimised and refined my efforts to localise and quantify GPR65 which would also have enabled me to explore the effects of knocking down this gene. The fact that I easily replicated the eQTL effects of rs3943657 confirms the validity of my RNA quantification [271].

Given the importance of CD69 signalling in establishing the balance between pro inflammatory (Th17) and anti-inflammatory (Treg) cells [237, 301, 302, 319], even though I saw no evidence that rs74796499 genotype influences the expression of *RORC* in ex-vivo lymphocytes I think it would have been interesting to also consider this key transcription factor in cultured cells. Considering the Treg master transcription factor *FOXP3* could also have been informative.

I found no evidence that either the MS associated SNP rs74796499 [151] or the IBD associated SNP rs3742704 [320] influences lysosomal pH. However, lysosomes are highly heterogeneous, so it might be that genotype is only relevant in some of the individual classes of lysosome. It would also have been interesting to try and establish a way to use the dual dye LysoSensor system so that absolute, rather than relative, pH could have been measured.

In my research I established a culture system capable of maintaining a stable pH and used this to explore the influence of extracellular pH on human T cell activation. I found marked effects of pH on the expression of both early (CD69) and late (CD25) activation markers, and also, unexpectedly, observed that in an acid environment the expression of CD69 increased even without stimulation. Unfortunately, I could find no evidence to support my predecessor's suggestion that the MS associated variant rs74796499 influenced these processes. His

preliminary data nominated the acid sensing receptor GPR65 as the candidate gene in this region but unfortunately, I have not been able to find any GPR65 dependent effects that are influenced by the MS associated SNP. The lead MS associated variant, rs74796499, is in tight LD with a coding variant in the other protein coding gene from this region, *GALC*. This synonymous coding variant is predicted to be a splice variant and so the role of GALC should be further investigated.

Reference

1. Compston, A. and A. Coles, *Multiple sclerosis.* Lancet, 2008. **372**(9648): p. 1502-17.
2. Taylor, B.V., et al., *Latitudinal variation in incidence and type of first central nervous system demyelinating events.* Mult Scler, 2010. **16**(4): p. 398-405.
3. Nakahara, J., et al., *Current concepts in multiple sclerosis: autoimmunity versus oligodendrogliopathy.* Clin Rev Allergy Immunol, 2012. **42**(1): p. 26-34.
4. Patzold, U. and P.R. Pocklington, *Course of multiple sclerosis. First results of a prospective study carried out of 102 MS patients from 1976-1980.* Acta Neurol Scand, 1982. **65**(4): p. 248-66.
5. Lublin, F.D. and S.C. Reingold, *Defining the clinical course of multiple sclerosis: results of an international survey. National Multiple Sclerosis Society (USA) Advisory Committee on Clinical Trials of New Agents in Multiple Sclerosis.* Neurology, 1996. **46**(4): p. 907-11.
6. Sawcer, S., R.J. Franklin, and M. Ban, *Multiple sclerosis genetics.* Lancet Neurol, 2014. **13**(7): p. 700-9.
7. Noseworthy, J.H., et al., *Multiple sclerosis.* N Engl J Med, 2000. **343**(13): p. 938-52.
8. Ascherio, A. and K.L. Munger, *Environmental risk factors for multiple sclerosis. Part II: Noninfectious factors.* Ann Neurol, 2007. **61**(6): p. 504-13.
9. Ahlgren, C., et al., *High risk of MS in Iranian immigrants in Gothenburg, Sweden.* Mult Scler, 2010. **16**(9): p. 1079-82.
10. Cabre, P., et al., *Role of return migration in the emergence of multiple sclerosis in the French West Indies.* Brain, 2005. **128**(Pt 12): p. 2899-910.
11. Dean, G. and M. Elian, *Age at immigration to England of Asian and Caribbean immigrants and the risk of developing multiple sclerosis.* J Neurol Neurosurg Psychiatry, 1997. **63**(5): p. 565-8.
12. Elian, M. and G. Dean, *Multiple sclerosis among the United Kingdom-born children of immigrants from the West Indies.* J Neurol Neurosurg Psychiatry, 1987. **50**(3): p. 327-32.
13. O'Gorman, C., R. Lucas, and B. Taylor, *Environmental Risk Factors for Multiple Sclerosis: A Review with a Focus on Molecular Mechanisms.* International Journal of Molecular Sciences, 2012. **13**(9): p. 11718-11752.
14. Ebers, G.C., *Environmental factors and multiple sclerosis.* The Lancet Neurology. **7**(3): p. 268-277.
15. Ascherio, A. and M. Munch, *Epstein-Barr virus and multiple sclerosis.* Epidemiology, 2000. **11**(2): p. 220-4.
16. Sumaya, C.V., et al., *Increased prevalence and titer of Epstein-Barr virus antibodies in patients with multiple sclerosis.* Ann Neurol, 1985. **17**(4): p. 371-7.
17. Ascherio, A., et al., *Epstein-Barr virus antibodies and risk of multiple sclerosis: a prospective study.* Jama, 2001. **286**(24): p. 3083-8.
18. Lindsey, J.W., et al., *The antibody response to Epstein-Barr virions is altered in multiple sclerosis.* J Neuroimmunol, 2013. **254**(1-2): p. 146-53.
19. Pender, M.P. and S.R. Burrows, *Epstein-Barr virus and multiple sclerosis: potential opportunities for immunotherapy.* Clin Transl Immunology, 2014. **3**(10): p. e27.
20. Ortega-Madueño, I., et al., *Anti-Human Herpesvirus 6A/B IgG Correlates with Relapses and Progression in Multiple Sclerosis.* PLOS ONE, 2014. **9**(8): p. e104836.
21. Challoner, P.B., et al., *Plaque-associated expression of human herpesvirus 6 in multiple sclerosis.* Proceedings of the National Academy of Sciences of the United States of America, 1995. **92**(16): p. 7440-7444.

22. van der Mei, I.A., et al., *Past exposure to sun, skin phenotype, and risk of multiple sclerosis: case-control study.* Bmj, 2003. **327**(7410): p. 316.
23. Hanwell, H.E. and B. Banwell, *Assessment of evidence for a protective role of vitamin D in multiple sclerosis.* Biochim Biophys Acta, 2011. **1812**(2): p. 202-12.
24. Farez, M.F., et al., *Sodium intake is associated with increased disease activity in multiple sclerosis.* J Neurol Neurosurg Psychiatry, 2015. **86**(1): p. 26-31.
25. Ebers, G.C., et al., *A population-based study of multiple sclerosis in twins.* N Engl J Med, 1986. **315**(26): p. 1638-42.
26. Hansen, T., et al., *Risk for multiple sclerosis in dizygotic and monozygotic twins.* Mult Scler, 2005. **11**(5): p. 500-3.
27. Mumford, C.J., et al., *The British Isles survey of multiple sclerosis in twins.* Neurology, 1994. **44**(1): p. 11-5.
28. Ristori, G., et al., *Multiple sclerosis in twins from continental Italy and Sardinia: A nationwide study.* Annals of Neurology, 2006. **59**(1): p. 27-34.
29. Ebers, G.C., A.D. Sadovnick, and N.J. Risch, *A genetic basis for familial aggregation in multiple sclerosis. Canadian Collaborative Study Group.* Nature, 1995. **377**(6545): p. 150-1.
30. Compston, D.A., J.R. Batchelor, and W.I. McDonald, *B-lymphocyte alloantigens associated with multiple sclerosis.* Lancet, 1976. **2**(7998): p. 1261-5.
31. Terasaki, P.I., et al., *Multiple sclerosis and high incidence of a B lymphocyte antigen.* Science, 1976. **193**(4259): p. 1245-7.
32. Jersild, C., A. Svejgaard, and T. Fog, *HL-A antigens and multiple sclerosis.* Lancet, 1972. **1**(7762): p. 1240-1.
33. Sawcer, S., et al., *Genetic risk and a primary role for cell-mediated immune mechanisms in multiple sclerosis.* Nature, 2011. **476**(7359): p. 214-9.
34. Dean, G., et al., *HLA-DRB1 and multiple sclerosis in Malta.* Neurology, 2008. **70**(2): p. 101-5.
35. Olerup, O. and J. Hillert, *HLA class II-associated genetic susceptibility in multiple sclerosis: a critical evaluation.* Tissue Antigens, 1991. **38**(1): p. 1-15.
36. Oksenberg, J.R., et al., *Mapping multiple sclerosis susceptibility to the HLA-DR locus in African Americans.* Am J Hum Genet, 2004. **74**(1): p. 160-7.
37. Patsopoulos, N., et al., *The Multiple Sclerosis Genomic Map: Role of peripheral immune cells and resident microglia in susceptibility.* bioRxiv, 2017.
38. Hafler, D.A., et al., *Risk alleles for multiple sclerosis identified by a genomewide study.* N Engl J Med, 2007. **357**(9): p. 851-62.
39. Gregory, S.G., et al., *Interleukin 7 receptor alpha chain (IL7R) shows allelic and functional association with multiple sclerosis.* Nat Genet, 2007. **39**(9): p. 1083-91.
40. Galarza-Munoz, G., et al., *Human Epistatic Interaction Controls IL7R Splicing and Increases Multiple Sclerosis Risk.* Cell, 2017. **169**(1): p. 72-84.e13.
41. Kemppinen, A., S. Sawcer, and A. Compston, *Genome-wide association studies in multiple sclerosis: lessons and future prospects.* Brief Funct Genomics, 2011. **10**(2): p. 61-70.
42. Zang, Y.C.Q., et al., *Regulation of chemokine receptor CCR5 and production of RANTES and MIP-1alpha by interferon-beta.* Journal of Neuroimmunology. **112**(1): p. 174-180.
43. Dhib-Jalbut, S., et al., *Immune response during interferon beta-1b treatment in patients with multiple sclerosis who experienced relapses and those who were relapse-free in the START study.* Journal of Neuroimmunology, 2013. **254**(1): p. 131-140.
44. Cheng, W. and G. Chen, *Chemokines and Chemokine Receptors in Multiple Sclerosis.* Mediators of Inflammation, 2014. **2014**: p. 8.

45. Dhib-Jalbut, S. and S. Marks, *Interferon-beta mechanisms of action in multiple sclerosis.* Neurology, 2010. **74 Suppl 1**: p. S17-24.
46. Airas, L., et al., *Mechanism of action of IFN-beta in the treatment of multiple sclerosis: a special reference to CD73 and adenosine.* Ann N Y Acad Sci, 2007. **1110**: p. 641-8.
47. Hu, Y., et al., *Investigation of the mechanism of action of alemtuzumab in a human CD52 transgenic mouse model.* Immunology, 2009. **128**(2): p. 260-270.
48. Martin, R., *Anti-CD25 (daclizumab) monoclonal antibody therapy in relapsing-remitting multiple sclerosis.* Clin Immunol, 2012. **142**(1): p. 9-14.
49. Pfender, N. and R. Martin, *Daclizumab (anti-CD25) in multiple sclerosis.* Exp Neurol, 2014. **262 Pt A**: p. 44-51.
50. Chun, J. and H.-P. Hartung, *Mechanism of Action of Oral Fingolimod (FTY720) in Multiple Sclerosis.* Clinical neuropharmacology, 2010. **33**(2): p. 91-101.
51. McGinley, M.P., B.P. Moss, and J.A. Cohen, *Safety of monoclonal antibodies for the treatment of multiple sclerosis.* Expert Opin Drug Saf, 2017. **16**(1): p. 89-100.
52. Reddy, V., et al., *Optimising B-cell depletion in autoimmune disease: is obinutuzumab the answer?* Drug Discovery Today, 2016. **21**(8): p. 1330-1338.
53. Montalban, X., et al., *Ocrelizumab versus Placebo in Primary Progressive Multiple Sclerosis.* New England Journal of Medicine, 2016. **376**(3): p. 209-220.
54. Sospedra, M. and R. Martin, *IMMUNOLOGY OF MULTIPLE SCLEROSIS.* Annual Review of Immunology, 2004. **23**(1): p. 683-747.
55. Boppana, S., et al., *Immunologic aspects of multiple sclerosis.* Mt Sinai J Med, 2011. **78**(2): p. 207-20.
56. Stromnes, I.M. and J.M. Goverman, *Passive induction of experimental allergic encephalomyelitis.* Nat Protoc, 2006. **1**(4): p. 1952-60.
57. Brostoff, S.W. and D.W. Mason, *Experimental allergic encephalomyelitis: successful treatment in vivo with a monoclonal antibody that recognizes T helper cells.* J Immunol, 1984. **133**(4): p. 1938-42.
58. van Oosten, B.W., et al., *Treatment of multiple sclerosis with the monoclonal anti-CD4 antibody cM-T412: results of a randomized, double-blind, placebo-controlled, MR-monitored phase II trial.* Neurology, 1997. **49**(2): p. 351-7.
59. Berge, T., et al., *The multiple sclerosis susceptibility genes TAGAP and IL2RA are regulated by vitamin D in CD4+ T cells.* Genes Immun, 2016. **17**(2): p. 118-27.
60. Börnsen, L., et al., *Effect of Natalizumab on Circulating CD4+ T-Cells in Multiple Sclerosis.* PLOS ONE, 2012. **7**(11): p. e47578.
61. Hellberg, S., et al., *Dynamic Response Genes in CD4+ T Cells Reveal a Network of Interactive Proteins that Classifies Disease Activity in Multiple Sclerosis.* Cell Rep, 2016. **16**(11): p. 2928-2939.
62. Cohen, J.A., et al., *Alemtuzumab versus interferon beta 1a as first-line treatment for patients with relapsing-remitting multiple sclerosis: a randomised controlled phase 3 trial.* Lancet, 2012. **380**(9856): p. 1819-28.
63. Lowenstein, H., et al., *Different mechanisms of Campath-1H-mediated depletion for CD4 and CD8 T cells in peripheral blood.* Transpl Int, 2006. **19**(11): p. 927-36.
64. Moutsianas, L., et al., *Class II HLA interactions modulate genetic risk for multiple sclerosis.* Nat Genet, 2015. **47**(10): p. 1107-1113.
65. Huseby, E.S., et al., *A pathogenic role for myelin-specific CD8(+) T cells in a model for multiple sclerosis.* J Exp Med, 2001. **194**(5): p. 669-76.
66. Huseby, E.S., et al., *Pathogenic CD8 T Cells in Multiple Sclerosis and Its Experimental Models.* Frontiers in Immunology, 2012. **3**: p. 64.
67. Hauser, S.L., et al., *Immunohistochemical analysis of the cellular infiltrate in multiple sclerosis lesions.* Ann Neurol, 1986. **19**(6): p. 578-87.

68. Salou, M., et al., *Expanded CD8 T-cell sharing between periphery and CNS in multiple sclerosis.* Ann Clin Transl Neurol, 2015. **2**(6): p. 609-22.
69. Friese, M.A. and L. Fugger, *Autoreactive CD8+ T cells in multiple sclerosis: a new target for therapy?* Brain, 2005. **128**(Pt 8): p. 1747-63.
70. Gold, R., C. Linington, and H. Lassmann, *Understanding pathogenesis and therapy of multiple sclerosis via animal models: 70 years of merits and culprits in experimental autoimmune encephalomyelitis research.* Brain, 2006. **129**(Pt 8): p. 1953-71.
71. Harrington, L.E., et al., *Interleukin 17-producing CD4+ effector T cells develop via a lineage distinct from the T helper type 1 and 2 lineages.* Nat Immunol, 2005. **6**(11): p. 1123-32.
72. Brucklacher-Waldert, V., et al., *Phenotypical and functional characterization of T helper 17 cells in multiple sclerosis.* Brain, 2009. **132**(12): p. 3329-3341.
73. Etesam, Z., et al., *Altered Expression of Specific Transcription Factors of Th17 (RORγt, RORα) and Treg Lymphocytes (FOXP3) by Peripheral Blood Mononuclear Cells from Patients with Multiple Sclerosis.* Journal of Molecular Neuroscience, 2016. **60**(1): p. 94-101.
74. Langrish, C.L., et al., *IL-23 drives a pathogenic T cell population that induces autoimmune inflammation.* J Exp Med, 2005. **201**(2): p. 233-40.
75. Kuwabara, T., et al., *CCR 7 Ligands Are Required for Development of Experimental Autoimmune Encephalomyelitis through Generating IL-23-Dependent Th17 Cells.* The Journal of Immunology, 2009. **183**(4): p. 2513.
76. Cua, D.J., et al., *Interleukin-23 rather than interleukin-12 is the critical cytokine for autoimmune inflammation of the brain.* Nature, 2003. **421**(6924): p. 744-8.
77. Komiyama, Y., et al., *IL-17 plays an important role in the development of experimental autoimmune encephalomyelitis.* J Immunol, 2006. **177**(1): p. 566-73.
78. Chatenoud, L. and J.F. Bach, *Regulatory T cells in the control of autoimmune diabetes: the case of the NOD mouse.* Int Rev Immunol, 2005. **24**(3-4): p. 247-67.
79. Morgan, M.E., et al., *Effective treatment of collagen-induced arthritis by adoptive transfer of CD25+ regulatory T cells.* Arthritis Rheum, 2005. **52**(7): p. 2212-21.
80. Hori, S., T. Nomura, and S. Sakaguchi, *Control of regulatory T cell development by the transcription factor Foxp3.* Science, 2003. **299**(5609): p. 1057-61.
81. Kohm, A.P., et al., *Cutting edge: CD4+CD25+ regulatory T cells suppress antigen-specific autoreactive immune responses and central nervous system inflammation during active experimental autoimmune encephalomyelitis.* J Immunol, 2002. **169**(9): p. 4712-6.
82. McGeachy, M.J., L.A. Stephens, and S.M. Anderton, *Natural recovery and protection from autoimmune encephalomyelitis: contribution of CD4+CD25+ regulatory cells within the central nervous system.* J Immunol, 2005. **175**(5): p. 3025-32.
83. Brunkow, M.E., et al., *Disruption of a new forkhead/winged-helix protein, scurfin, results in the fatal lymphoproliferative disorder of the scurfy mouse.* Nat Genet, 2001. **27**(1): p. 68-73.
84. Haas, J., et al., *Reduced suppressive effect of CD4+CD25high regulatory T cells on the T cell immune response against myelin oligodendrocyte glycoprotein in patients with multiple sclerosis.* Eur J Immunol, 2005. **35**(11): p. 3343-52.
85. Chofflon, M., et al., *Loss of functional suppression is linked to decreases in circulating suppressor inducer (CD4+ 2H4+) T cells in multiple sclerosis.* Ann Neurol, 1988. **24**(2): p. 185-91.
86. Kumar, M., et al., *CD4+CD25+FoxP3+ T lymphocytes fail to suppress myelin basic protein-induced proliferation in patients with multiple sclerosis.* J Neuroimmunol, 2006. **180**(1-2): p. 178-84.

87. Strowig, T., F. Brilot, and C. Munz, *Noncytotoxic functions of NK cells: direct pathogen restriction and assistance to adaptive immunity.* J Immunol, 2008. **180**(12): p. 7785-91.
88. Xu, W., et al., *Mechanism of natural killer (NK) cell regulatory role in experimental autoimmune encephalomyelitis.* J Neuroimmunol, 2005. **163**(1-2): p. 24-30.
89. Segal, B.M., *The role of natural killer cells in curbing neuroinflammation.* J Neuroimmunol, 2007. **191**(1-2): p. 2-7.
90. Benczur, M., et al., *Dysfunction of natural killer cells in multiple sclerosis: a possible pathogenetic factor.* Clin Exp Immunol, 1980. **39**(3): p. 657-62.
91. Merrill, J., et al., *Decreased NK killing in patients with multiple sclerosis: an analysis on the level of the single effector cell in peripheral blood and cerebrospinal fluid in relation to the activity in the disease.* Clin Exp Immunol, 1982. **47**(2): p. 419-30.
92. Chanvillard, C., et al., *The role of natural killer cells in multiple sclerosis and their therapeutic implications.* Front Immunol, 2013. **4**: p. 63.
93. Kastrukoff, L.F., et al., *Clinical relapses of multiple sclerosis are associated with 'novel' valleys in natural killer cell functional activity.* J Neuroimmunol, 2003. **145**(1-2): p. 103-14.
94. Hao, J., et al., *Interleukin-2/interleukin-2 antibody therapy induces target organ natural killer cells that inhibit central nervous system inflammation.* Ann Neurol, 2011. **69**(4): p. 721-34.
95. Perini, P., et al., *Effect of IFNbeta and anti-IFNbeta antibodies on NK cells in multiple sclerosis patients.* J Neuroimmunol, 2000. **105**(1): p. 91-5.
96. Saraste, M., H. Irjala, and L. Airas, *Expansion of CD56Bright natural killer cells in the peripheral blood of multiple sclerosis patients treated with interferon-beta.* Neurol Sci, 2007. **28**(3): p. 121-6.
97. Vandenbark, A.A., et al., *Interferon-beta-1a treatment increases CD56bright natural killer cells and CD4+CD25+ Foxp3 expression in subjects with multiple sclerosis.* J Neuroimmunol, 2009. **215**(1-2): p. 125-8.
98. Martinez-Rodriguez, J.E., et al., *Natural killer receptors distribution in multiple sclerosis: Relation to clinical course and interferon-beta therapy.* Clin Immunol, 2010. **137**(1): p. 41-50.
99. Bendelac, A., P.B. Savage, and L. Teyton, *The biology of NKT cells.* Annu Rev Immunol, 2007. **25**: p. 297-336.
100. Godfrey, D.I., et al., *NKT cells: what's in a name?* Nat Rev Immunol, 2004. **4**(3): p. 231-7.
101. Van Kaer, L., V.V. Parekh, and L. Wu, *Invariant natural killer T cells: bridging innate and adaptive immunity.* Cell Tissue Res, 2011. **343**(1): p. 43-55.
102. Jahng, A.W., et al., *Activation of Natural Killer T Cells Potentiates or Prevents Experimental Autoimmune Encephalomyelitis.* The Journal of Experimental Medicine, 2001. **194**(12): p. 1789-1799.
103. Gigli, G., et al., *Innate immunity modulates autoimmunity: type 1 interferon-β treatment in multiple sclerosis promotes growth and function of regulatory invariant natural killer T cells through dendritic cell maturation.* Immunology, 2007. **122**(3): p. 409-417.
104. Engelhardt, B. and R.M. Ransohoff, *Capture, crawl, cross: the T cell code to breach the blood-brain barriers.* Trends Immunol, 2012. **33**(12): p. 579-89.
105. Yamazaki, T., et al., *CCR6 Regulates the Migration of Inflammatory and Regulatory T Cells.* The Journal of Immunology, 2008. **181**(12): p. 8391.
106. Reboldi, A., et al., *C-C chemokine receptor 6-regulated entry of TH-17 cells into the CNS through the choroid plexus is required for the initiation of EAE.* Nat Immunol, 2009. **10**(5): p. 514-523.

107. Teleshova, N., et al., *Multiple sclerosis and optic neuritis: CCR5 and CXCR3 expressing T cells are augmented in blood and cerebrospinal fluid.* J Neurol, 2002. **249**(6): p. 723-9.
108. Horuk, R., *Chemokine receptor antagonists: overcoming developmental hurdles.* Nat Rev Drug Discov, 2009. **8**(1): p. 23-33.
109. Sutton, C., et al., *A crucial role for interleukin (IL)-1 in the induction of IL-17-producing T cells that mediate autoimmune encephalomyelitis.* J Exp Med, 2006. **203**(7): p. 1685-91.
110. Sutton, C., et al., *A crucial role for interleukin (IL)-1 in the induction of IL-17–producing T cells that mediate autoimmune encephalomyelitis.* The Journal of Experimental Medicine, 2006. **203**(7): p. 1685-1691.
111. Jacobs, C.A., et al., *Experimental autoimmune encephalomyelitis is exacerbated by IL-1 alpha and suppressed by soluble IL-1 receptor.* J Immunol, 1991. **146**(9): p. 2983-9.
112. Petitto, J.M., et al., *Interleukin-2 gene deletion produces a robust reduction in susceptibility to experimental autoimmune encephalomyelitis in C57BL/6 mice.* Neurosci Lett, 2000. **285**(1): p. 66-70.
113. Renner, K., et al., *IL-3 promotes the development of experimental autoimmune encephalitis.* JCI Insight, 2016. **1**(16): p. e87157.
114. Falcone, M., et al., *A critical role for IL-4 in regulating disease severity in experimental allergic encephalomyelitis as demonstrated in IL-4-deficient C57BL/6 mice and BALB/c mice.* J Immunol, 1998. **160**(10): p. 4822-30.
115. Liblau, R., L. Steinman, and S. Brocke, *Experimental autoimmune encephalomyelitis in IL-4-deficient mice.* Int Immunol, 1997. **9**(5): p. 799-803.
116. Keating, P., et al., *Protection from EAE by IL-4R[alpha]-/- macrophages depends upon T regulatory cell involvement.* Immunol Cell Biol, 2009. **87**(7): p. 534-545.
117. Samoilova, E.B., et al., *IL-6-deficient mice are resistant to experimental autoimmune encephalomyelitis: roles of IL-6 in the activation and differentiation of autoreactive T cells.* J Immunol, 1998. **161**(12): p. 6480-6.
118. Gijbels, K., et al., *Administration of neutralizing antibodies to interleukin-6 (IL-6) reduces experimental autoimmune encephalomyelitis and is associated with elevated levels of IL-6 bioactivity in central nervous system and circulation.* Mol Med, 1995. **1**(7): p. 795-805.
119. Serada, S., et al., *IL-6 blockade inhibits the induction of myelin antigen-specific Th17 cells and Th1 cells in experimental autoimmune encephalomyelitis.* Proceedings of the National Academy of Sciences, 2008. **105**(26): p. 9041-9046.
120. Bettelli, E., et al., *IL-10 is critical in the regulation of autoimmune encephalomyelitis as demonstrated by studies of IL-10- and IL-4-deficient and transgenic mice.* J Immunol, 1998. **161**(7): p. 3299-306.
121. Klose, J., et al., *Suppression of experimental autoimmune encephalomyelitis by interleukin-10 transduced neural stem/progenitor cells*. Vol. 10. 2013. 117.
122. Becher, B., B.G. Durell, and R.J. Noelle, *Experimental autoimmune encephalitis and inflammation in the absence of interleukin-12.* The Journal of Clinical Investigation, 2002. **110**(4): p. 493-497.
123. Zhang, G.-X., et al., *Role of IL-12 Receptor β1 in Regulation of T Cell Response by APC in Experimental Autoimmune Encephalomyelitis.* The Journal of Immunology, 2003. **171**(9): p. 4485.
124. Xie, C., et al., *IL-12Rbeta2 has a protective role in relapsing-remitting experimental autoimmune encephalomyelitis.* Journal of Neuroimmunology. **291**: p. 59-69.

125. Bright, J.J., M. Rodriguez, and S. Sriram, *Differential influence of interleukin-12 in the pathogenesis of autoimmune and virus-induced central nervous system demyelination.* J Virol, 1999. **73**(2): p. 1637-9.
126. Haak, S., et al., *IL-17A and IL-17F do not contribute vitally to autoimmune neuro-inflammation in mice.* J Clin Invest, 2009. **119**(1): p. 61-9.
127. Lee, Y., et al., *IL-21R signaling is critical for induction of spontaneous experimental autoimmune encephalomyelitis.* The Journal of Clinical Investigation, 2015. **125**(11): p. 4011-4020.
128. Coquet, J.M., et al., *Cutting edge: IL-21 is not essential for Th17 differentiation or experimental autoimmune encephalomyelitis.* J Immunol, 2008. **180**(11): p. 7097-101.
129. Kreymborg, K., et al., *IL-22 is expressed by Th17 cells in an IL-23-dependent fashion, but not required for the development of autoimmune encephalomyelitis.* J Immunol, 2007. **179**(12): p. 8098-104.
130. Thakker, P., et al., *IL-23 Is Critical in the Induction but Not in the Effector Phase of Experimental Autoimmune Encephalomyelitis.* The Journal of Immunology, 2007. **178**(4): p. 2589.
131. Espejo, C., et al., *Treatment with anti-interferon-gamma monoclonal antibodies modifies experimental autoimmune encephalomyelitis in interferon-gamma receptor knockout mice.* Exp Neurol, 2001. **172**(2): p. 460-8.
132. Duong, T.T., et al., *Effect of anti-interferon-gamma monoclonal antibody treatment on the development of experimental allergic encephalomyelitis in resistant mouse strains.* J Neuroimmunol, 1994. **53**(1): p. 101-7.
133. Willenborg, D.O., et al., *IFN-gamma plays a critical down-regulatory role in the induction and effector phase of myelin oligodendrocyte glycoprotein-induced autoimmune encephalomyelitis.* J Immunol, 1996. **157**(8): p. 3223-7.
134. Espejo, C., et al., *Interferon-gamma regulates oxidative stress during experimental autoimmune encephalomyelitis.* Exp Neurol, 2002. **177**(1): p. 21-31.
135. Axtell, R.C., et al., *T helper type 1 and 17 cells determine efficacy of interferon-beta in multiple sclerosis and experimental encephalomyelitis.* Nat Med, 2010. **16**(4): p. 406-12.
136. Teige, I., et al., *IFN-beta gene deletion leads to augmented and chronic demyelinating experimental autoimmune encephalomyelitis.* J Immunol, 2003. **170**(9): p. 4776-84.
137. Galligan, C.L., et al., *Interferon-β is a key regulator of proinflammatory events in experimental autoimmune encephalomyelitis.* Multiple Sclerosis Journal, 2010. **16**(12): p. 1458-1473.
138. Liu, J., et al., *TNF is a potent anti-inflammatory cytokine in autoimmune-mediated demyelination.* Nat Med, 1998. **4**(1): p. 78-83.
139. Kassiotis, G. and G. Kollias, *Uncoupling the proinflammatory from the immunosuppressive properties of tumor necrosis factor (TNF) at the p55 TNF receptor level: implications for pathogenesis and therapy of autoimmune demyelination.* J Exp Med, 2001. **193**(4): p. 427-34.
140. Batoulis, H., et al., *Blockade of tumour necrosis factor-alpha in experimental autoimmune encephalomyelitis reveals differential effects on the antigen-specific immune response and central nervous system histopathology*. Clin Exp Immunol, 2014. **175**(1): p. 41-8.
141. Pierson, E.R. and J.M. Goverman, *GM-CSF is not essential for experimental autoimmune encephalomyelitis but promotes brain-targeted disease.* JCI Insight, 2017. **2**(7): p. e92362.
142. Martinez, N.E., et al., *RORgammat, but not T-bet, overexpression exacerbates an autoimmune model for multiple sclerosis.* J Neuroimmunol, 2014. **276**(1-2): p. 142-9.

143. Bettelli, E., et al., *Loss of T-bet, but not STAT1, prevents the development of experimental autoimmune encephalomyelitis.* J Exp Med, 2004. **200**(1): p. 79-87.
144. Altmüller, J., et al., *Genomewide Scans of Complex Human Diseases: True Linkage Is Hard to Find.* American Journal of Human Genetics, 2001. **69**(5): p. 936-950.
145. Sawcer, S., et al., *A high-density screen for linkage in multiple sclerosis.* Am J Hum Genet, 2005. **77**(3): p. 454-67.
146. *Genome-wide association study of 14,000 cases of seven common diseases and 3,000 shared controls.* Nature, 2007. **447**(7145): p. 661-78.
147. Slatkin, M., *Linkage disequilibrium--understanding the evolutionary past and mapping the medical future.* Nat Rev Genet, 2008. **9**(6): p. 477-85.
148. Johnson, G.C., et al., *Haplotype tagging for the identification of common disease genes.* Nat Genet, 2001. **29**(2): p. 233-7.
149. The International HapMap, C., *A haplotype map of the human genome.* Nature, 2005. **437**(7063): p. 1299-1320.
150. Frazer, K.A., et al., *Human genetic variation and its contribution to complex traits.* Nat Rev Genet, 2009. **10**(4): p. 241-251.
151. Beecham, A.H., et al., *Analysis of immune-related loci identifies 48 new susceptibility variants for multiple sclerosis.* Nat Genet, 2013. **45**(11): p. 1353-60.
152. Kyaw, H., et al., *Cloning, characterization, and mapping of human homolog of mouse T-cell death-associated gene.* DNA Cell Biol, 1998. **17**(6): p. 493-500.
153. De Jager, P.L., et al., *Meta-analysis of genome scans and replication identify CD6, IRF8 and TNFRSF1A as new multiple sclerosis susceptibility loci.* Nat Genet, 2009. **41**(7): p. 776-82.
154. *Genome-wide association study identifies new multiple sclerosis susceptibility loci on chromosomes 12 and 20.* Nat Genet, 2009. **41**(7): p. 824-8.
155. Jakkula, E., et al., *Genome-wide association study in a high-risk isolate for multiple sclerosis reveals associated variants in STAT3 gene.* Am J Hum Genet, 2010. **86**(2): p. 285-91.
156. Sanna, S., et al., *Variants within the immunoregulatory CBLB gene are associated with multiple sclerosis.* Nat Genet, 2010. **42**(6): p. 495-7.
157. Patsopoulos, N.A., et al., *Genome-wide meta-analysis identifies novel multiple sclerosis susceptibility loci.* Ann Neurol, 2011. **70**(6): p. 897-912.
158. Andlauer, T.F., et al., *Novel multiple sclerosis susceptibility loci implicated in epigenetic regulation.* Sci Adv, 2016. **2**(6): p. e1501678.
159. Hawkins-Salsbury, J.A., et al., *Psychosine, the cytotoxic sphingolipid that accumulates in globoid cell leukodystrophy, alters membrane architecture.* Journal of Lipid Research, 2013. **54**(12): p. 3303-3311.
160. Lee, W.C., et al., *Molecular Characterization of Mutations that Cause Globoid Cell Leukodystrophy and Pharmacological Rescue Using Small Molecule Chemical Chaperones.* The Journal of Neuroscience, 2010. **30**(16): p. 5489-5497.
161. Cannizzaro, L.A., et al., *Regional mapping of the human galactocerebrosidase gene (GALC) to 14q31 by in situ hybridization.* Cytogenet Cell Genet, 1994. **66**(4): p. 244-5.
162. Deane, J.E., et al., *Insights into Krabbe disease from structures of galactocerebrosidase.* Proc Natl Acad Sci U S A, 2011. **108**(37): p. 15169-73.
163. Jackman, N., A. Ishii, and R. Bansal, *Oligodendrocyte development and myelin biogenesis: parsing out the roles of glycosphingolipids.* Physiology (Bethesda), 2009. **24**: p. 290-7.

164. Coetzee, T., J.L. Dupree, and B. Popko, *Demyelination and altered expression of myelin-associated glycoprotein isoforms in the central nervous system of galactolipid-deficient mice.* J Neurosci Res, 1998. **54**(5): p. 613-22.
165. Jatana, M., S. Giri, and A.K. Singh, *Apoptotic positive cells in Krabbe brain and induction of apoptosis in rat C6 glial cells by psychosine.* Neurosci Lett, 2002. **330**(2): p. 183-7.
166. White, A.B., et al., *Psychosine accumulates in membrane microdomains in the brain of krabbe patients, disrupting the raft architecture.* J Neurosci, 2009. **29**(19): p. 6068-77.
167. Svennerholm, L., M.T. Vanier, and J.E. Mansson, *Krabbe disease: a galactosylsphingosine (psychosine) lipidosis.* J Lipid Res, 1980. **21**(1): p. 53-64.
168. Haq, E., et al., *Molecular mechanism of psychosine-induced cell death in human oligodendrocyte cell line.* J Neurochem, 2003. **86**(6): p. 1428-40.
169. Zaka, M. and D.A. Wenger, *Psychosine-induced apoptosis in a mouse oligodendrocyte progenitor cell line is mediated by caspase activation.* Neurosci Lett, 2004. **358**(3): p. 205-9.
170. Sueyoshi, N., T. Maehara, and M. Ito, *Apoptosis of Neuro2a cells induced by lysosphingolipids with naturally occurring stereochemical configurations.* J Lipid Res, 2001. **42**(8): p. 1197-202.
171. Malone, M.H., Z. Wang, and C.W. Distelhorst, *The glucocorticoid-induced gene tdag8 encodes a pro-apoptotic G protein-coupled receptor whose activation promotes glucocorticoid-induced apoptosis.* J Biol Chem, 2004. **279**(51): p. 52850-9.
172. Potter, G.B., et al., *Missense mutation in mouse GALC mimics human gene defect and offers new insights into Krabbe disease.* Hum Mol Genet, 2013. **22**(17): p. 3397-414.
173. Luzi, P., et al., *Effects of treatments on inflammatory and apoptotic markers in the CNS of mice with globoid cell leukodystrophy.* Brain research, 2009. **1300**: p. 146-158.
174. Maghazachi, A.A., et al., *D-galactosyl-beta1-1'-sphingosine and D-glucosyl-beta1-1'-sphingosine induce human natural killer cell apoptosis.* Biochem Biophys Res Commun, 2004. **320**(3): p. 810-5.
175. Formichi, P., et al., *Psychosine-induced apoptosis and cytokine activation in immune peripheral cells of Krabbe patients.* J Cell Physiol, 2007. **212**(3): p. 737-43.
176. LeVine, S.M. and D.C. Brown, *IL-6 and TNFalpha expression in brains of twitcher, quaking and normal mice.* J Neuroimmunol, 1997. **73**(1-2): p. 47-56.
177. Pedchenko, T.V. and S.M. LeVine, *IL-6 deficiency causes enhanced pathology in Twitcher (globoid cell leukodystrophy) mice.* Exp Neurol, 1999. **158**(2): p. 459-68.
178. Waubant, E., *Biomarkers indicative of blood-brain barrier disruption in multiple sclerosis.* Dis Markers, 2006. **22**(4): p. 235-44.
179. Franke, A., et al., *Genome-wide meta-analysis increases to 71 the number of confirmed Crohn's disease susceptibility loci.* Nat Genet, 2010. **42**(12): p. 1118-25.
180. Cortes, A., et al., *Identification of multiple risk variants for ankylosing spondylitis through high-density genotyping of immune-related loci.* Nat Genet, 2013. **45**(7): p. 730-8.
181. Choi, J.W., S.Y. Lee, and Y. Choi, *Identification of a putative G protein-coupled receptor induced during activation-induced apoptosis of T cells.* Cell Immunol, 1996. **168**(1): p. 78-84.
182. Radu, C.G., et al., *Normal immune development and glucocorticoid-induced thymocyte apoptosis in mice deficient for the T-cell death-associated gene 8 receptor.* Mol Cell Biol, 2006. **26**(2): p. 668-77.
183. Wang, J.Q., et al., *TDAG8 is a proton-sensing and psychosine-sensitive G-protein-coupled receptor.* J Biol Chem, 2004. **279**(44): p. 45626-33.

184. McGuire, J., et al., *Acid-sensing by the T cell death-associated gene 8 (TDAG8) receptor cloned from rat brain.* Biochem Biophys Res Commun, 2009. **386**(3): p. 420-5.
185. Kottyan, L.C., et al., *Eosinophil viability is increased by acidic pH in a cAMP- and GPR65-dependent manner.* Blood, 2009. **114**(13): p. 2774-82.
186. Abrahamsen, H., et al., *TCR- and CD28-mediated recruitment of phosphodiesterase 4 to lipid rafts potentiates TCR signaling.* J Immunol, 2004. **173**(8): p. 4847-58.
187. Vang, T., et al., *Activation of the Cooh-Terminal Src Kinase (Csk) by Camp-Dependent Protein Kinase Inhibits Signaling through the T Cell Receptor*. The Journal of Experimental Medicine, 2001. **193**(4): p. 497-508.
188. Tasken, K. and A.J. Stokka, *The molecular machinery for cAMP-dependent immunomodulation in T-cells.* Biochem Soc Trans, 2006. **34**(Pt 4): p. 476-9.
189. Skalhegg, B.S., et al., *Location of cAMP-dependent protein kinase type I with the TCR-CD3 complex.* Science, 1994. **263**(5143): p. 84-7.
190. Wen, A.Y., K.M. Sakamoto, and L.S. Miller, *The Role of the Transcription Factor CREB in Immune Function.* The Journal of Immunology, 2010. **185**(11): p. 6413.
191. Polansky, J.K., et al., *Methylation matters: binding of Ets-1 to the demethylated Foxp3 gene contributes to the stabilization of Foxp3 expression in regulatory T cells.* J Mol Med (Berl), 2010. **88**(10): p. 1029-40.
192. Kim, H.-P. and W.J. Leonard, *CREB/ATF-dependent T cell receptor-induced FoxP3 gene expression: a role for DNA methylation.* The Journal of Experimental Medicine, 2007. **204**(7): p. 1543.
193. Onozawa, Y., et al., *Activation of T cell death-associated gene 8 regulates the cytokine production of T cells and macrophages in vitro.* Eur J Pharmacol, 2012. **683**(1-3): p. 325-31.
194. Ryder, C., et al., *Acidosis promotes Bcl-2 family-mediated evasion of apoptosis: involvement of acid-sensing G protein-coupled receptor Gpr65 signaling to Mek/Erk.* The Journal of Biological Chemistry, 2012. **287**(33): p. 27863-27875.
195. Ishii, S., Y. Kihara, and T. Shimizu, *Identification of T cell death-associated gene 8 (TDAG8) as a novel acid sensing G-protein-coupled receptor*. J Biol Chem, 2005. **280**(10): p. 9083-7.
196. Ludwig, M.G., et al., *Proton-sensing G-protein-coupled receptors.* Nature, 2003. **425**.
197. Mogi, C., et al., *Involvement of proton-sensing TDAG8 in extracellular acidification-induced inhibition of proinflammatory cytokine production in peritoneal macrophages.* J Immunol, 2009. **182**(5): p. 3243-51.
198. Friese, M.A., et al., *Acid-sensing ion channel-1 contributes to axonal degeneration in autoimmune inflammation of the central nervous system.* Nat Med, 2007. **13**(12): p. 1483-9.
199. Ihara, Y., et al., *The G protein-coupled receptor T-cell death-associated gene 8 (TDAG8) facilitates tumor development by serving as an extracellular pH sensor.* Proc Natl Acad Sci U S A, 2010. **107**.
200. Li, Z., et al., *Acidosis decreases c-Myc oncogene expression in human lymphoma cells: a role for the proton-sensing G protein-coupled receptor TDAG8.* Int J Mol Sci, 2013. **14**(10): p. 20236-55.
201. Im, D.S., et al., *Identification of a molecular target of psychosine and its role in globoid cell formation.* J Cell Biol, 2001. **153**(2): p. 429-34.
202. Tosa, N., et al., *Critical function of T cell death-associated gene 8 in glucocorticoid-induced thymocyte apoptosis.* Int Immunol, 2003. **15**(6): p. 741-9.
203. Lassen, K.G., et al., *Genetic Coding Variant in GPR65 Alters Lysosomal pH and Links Lysosomal Dysfunction with Colitis Risk.* Immunity, 2016. **44**(6): p. 1392-405.

204. Tanaka, D., et al., *Essential role of neutrophils in anti-type II collagen antibody and lipopolysaccharide-induced arthritis.* Immunology, 2006. **119**(2): p. 195-202.
205. Onodera, S., et al., *A novel DNA vaccine targeting macrophage migration inhibitory factor protects joints from inflammation and destruction in murine models of arthritis.* Arthritis Rheum, 2007. **56**(2): p. 521-30.
206. Onozawa, Y., T. Komai, and T. Oda, *Activation of T cell death-associated gene 8 attenuates inflammation by negatively regulating the function of inflammatory cells.* Eur J Pharmacol, 2011. **654**(3): p. 315-9.
207. Gaublomme, J.T., et al., *Single-cell Genomics Unveils Critical Regulators of Th17 cell Pathogenicity.* Cell, 2015. **163**(6): p. 1400-1412.
208. Ciofani, M., et al., *A validated regulatory network for Th17 cell specification.* Cell, 2012. **151**(2): p. 289-303.
209. Schroeder, A., et al., *The RIN: an RNA integrity number for assigning integrity values to RNA measurements.* BMC Molecular Biology, 2006. **7**: p. 3-3.
210. Milstein, C., *The hybridoma revolution: an offshoot of basic research.* Bioessays, 1999. **21**(11): p. 966-73.
211. Alkan, S.S., *Monoclonal antibodies: the story of a discovery that revolutionized science and medicine.* Nat Rev Immunol, 2004. **4**(2): p. 153-156.
212. Zhang, L., et al., *Proteomic analysis of PBMCs: characterization of potential HIV-associated proteins.* Proteome Science, 2010. **8**(1): p. 12.
213. Moll, R., M. Divo, and L. Langbein, *The human keratins: biology and pathology.* Histochemistry and Cell Biology, 2008. **129**(6): p. 705-733.
214. Hodge, K., et al., *Cleaning up the masses: Exclusion lists to reduce contamination with HPLC-MS/MS.* Journal of Proteomics, 2013. **88**: p. 92-103.
215. Gao, X., et al., *GATA Factor-G-Protein-Coupled Receptor Circuit Suppresses Hematopoiesis.* Stem Cell Reports, 2016. **6**(3): p. 368-382.
216. Rosko, A.E., et al., *Acidosis Sensing Receptor GPR65 Correlates with Anti-Apoptotic Bcl-2 Family Member Expression in CLL Cells: Potential Implications for the CLL Microenvironment.* Journal of leukemia (Los Angeles, Calif.), 2014. **2**(5): p. 160.
217. Warburg, O., K. Posener, and E. Negelein, *Über den Stoffwechsel der Tumoren (On metabolism of tumors).* Biochem Z, 1924. **152**.
218. Cummings, N.A. and G.L. Nordby, *Measurement of synovial fluid pH in normal and arthritic knees.* Arthritis Rheum, 1966. **9**(1): p. 47-56.
219. Treuhaft, P.S. and M.C. DJ, *Synovial fluid pH, lactate, oxygen and carbon dioxide partial pressure in various joint diseases.* Arthritis Rheum, 1971. **14**(4): p. 475-84.
220. Lardner, A., *The effects of extracellular pH on immune function.* J Leukoc Biol, 2001. **69**(4): p. 522-30.
221. Dubos, R.J., *The micro-environment of inflammation or Metchnikoff revisited.* Lancet, 1955. **269**(6879): p. 1-5.
222. Helmlinger, G., et al., *Interstitial pH and pO2 gradients in solid tumors in vivo: high-resolution measurements reveal a lack of correlation.* Nat Med, 1997. **3**.
223. Loeffler, D.A., P.L. Juneau, and S. Masserant, *Influence of tumour physico-chemical conditions on interleukin-2-stimulated lymphocyte proliferation.* Br J Cancer, 1992. **66**(4): p. 619-22.
224. Loeffler, D.A., P.L. Juneau, and G.H. Heppner, *Natural killer-cell activity under conditions reflective of tumor micro-environment.* Int J Cancer, 1991. **48**(6): p. 895-9.
225. Park, S.-Y., et al., *Extracellular Low pH Modulates Phosphatidylserine-dependent Phagocytosis in Macrophages by Increasing Stabilin-1 Expression.* The Journal of Biological Chemistry, 2012. **287**(14): p. 11261-11271.

226. McDowell, C.L. and E.T. Papoutsakis, *Decreasing extracellular pH increases CD13 receptor surface content and alters the metabolism of HL60 cells cultured in stirred tank bioreactors.* Biotechnol Prog, 1998. **14**(4): p. 567-72.
227. Coakley, R.J., et al., *Cytosolic pH and the inflammatory microenvironment modulate cell death in human neutrophils after phagocytosis.* Blood, 2002. **100**(9): p. 3383-3391.
228. McAdams, T.A., W.M. Miller, and E.T. Papoutsakis, *pH is a potent modulator of erythroid differentiation.* British Journal of Haematology, 1998. **103**(2): p. 317-325.
229. Carswell, K.S. and E.T. Papoutsakis, *Extracellular pH affects the proliferation of cultured human T cells and their expression of the interleukin-2 receptor.* J Immunother, 2000. **23**(6): p. 669-74.
230. Nakagawa, Y., et al., *Effects of extracellular pH and hypoxia on the function and development of antigen-specific cytotoxic T lymphocytes.* Immunology Letters, 2015. **167**(2): p. 72-86.
231. Becknell, B. and M.A. Caligiuri, *Interleukin-2, interleukin-15, and their roles in human natural killer cells.* Adv Immunol, 2005. **86**: p. 209-39.
232. Lehmann, C., M. Zeis, and L. Uharek, *Activation of natural killer cells with interleukin 2 (IL-2) and IL-12 increases perforin binding and subsequent lysis of tumour cells.* Br J Haematol, 2001. **114**(3): p. 660-5.
233. Schmidt, R.E., et al., *A subset of natural killer cells in peripheral blood displays a mature T cell phenotype.* J Exp Med, 1986. **164**(1): p. 351-6.
234. Díaz, F.E., et al., *Fever-range hyperthermia improves the anti-apoptotic effect induced by low pH on human neutrophils promoting a proangiogenic profile.* Cell Death & Disease, 2016. **7**(10): p. e2437.
235. Radulovic, K., et al., *The Early Activation Marker CD69 Regulates the Expression of Chemokines and CD4 T Cell Accumulation in Intestine.* PLOS ONE, 2013. **8**(6): p. e65413.
236. Han, Y., et al., *CD69+ CD4+ CD25- T cells, a New Subset of Regulatory T Cells, Suppress T Cell Proliferation through Membrane-Bound TGF-β1.* The Journal of Immunology, 2009. **182**(1): p. 111-120.
237. de la Fuente, H., et al., *The leukocyte activation receptor CD69 controls T cell differentiation through its interaction with galectin-1.* Mol Cell Biol, 2014. **34**(13): p. 2479-87.
238. Martín, P., et al., *CD69 Association with Jak3/Stat5 Proteins Regulates Th17 Cell Differentiation.* Molecular and Cellular Biology, 2010. **30**(20): p. 4877-4889.
239. Borrego, F., J. Peña, and R. Solana, *Regulation of CD69 expression on human natural killer cells: differential involvement of protein kinase C and protein tyrosine kinases.* European Journal of Immunology, 1993. **23**(5): p. 1039-1043.
240. Lanier, L.L., et al., *Interleukin 2 activation of natural killer cells rapidly induces the expression and phosphorylation of the Leu-23 activation antigen.* J Exp Med, 1988. **167**(5): p. 1572-85.
241. Gerosa, F., et al., *Interferon alpha induces expression of the CD69 activation antigen in human resting NK cells, while interferon gamma and tumor necrosis factor alpha are ineffective.* Int J Cancer, 1991. **48**(3): p. 473-5.
242. Borrego, F., J. Pena, and R. Solana, *Regulation of CD69 expression on human natural killer cells: differential involvement of protein kinase C and protein tyrosine kinases.* Eur J Immunol, 1993. **23**(5): p. 1039-43.
243. Müller, B., B. Fischer, and W. Kreutz, *An acidic microenvironment impairs the generation of non-major histocompatibility complex-restricted killer cells.* Immunology, 2000. **99**(3): p. 375-384.

244. Islam, A., et al., *An Acidic Microenvironment Increases NK Cell Killing of Cryptococcus neoformans and Cryptococcus gattii by Enhancing Perforin Degranulation.* PLOS Pathogens, 2013. **9**(7): p. e1003439.
245. Lingueglia, E., *Acid-sensing ion channels in sensory perception.* J Biol Chem, 2007. **282**(24): p. 17325-9.
246. Deval, E., et al., *ASIC3, a sensor of acidic and primary inflammatory pain.* The EMBO Journal, 2008. **27**(22): p. 3047-3055.
247. Bertin, S., et al., *Novel immune function for the TRPV1 channel in T lymphocytes.* Channels, 2014. **8**(6): p. 479-480.
248. Samivel, R., et al., *The role of TRPV1 in the CD4+ T cell-mediated inflammatory response of allergic rhinitis.* Oncotarget, 2016. **7**(1): p. 148-60.
249. Dong, L., et al., *Acidosis activation of the proton-sensing GPR4 receptor stimulates vascular endothelial cell inflammatory responses revealed by transcriptome analysis.* PLoS One, 2013. **8**(4): p. e61991.
250. Chandra, V., et al., *Extracellular acidification stimulates GPR68 mediated IL-8 production in human pancreatic β cells.* Scientific Reports, 2016. **6**: p. 25765.
251. Le, L.Q., et al., *Mice lacking the orphan G protein-coupled receptor G2A develop a late-onset autoimmune syndrome.* Immunity, 2001. **14**(5): p. 561-71.
252. Seuwen, K., M.G. Ludwig, and R.M. Wolf, *Receptors for protons or lipid messengers or both?* J Recept Signal Transduct Res, 2006. **26**(5-6): p. 599-610.
253. Ichimonji, I., et al., *Extracellular acidification stimulates IL-6 production and Ca(2+) mobilization through proton-sensing OGR1 receptors in human airway smooth muscle cells.* Am J Physiol Lung Cell Mol Physiol, 2010. **299**(4): p. L567-77.
254. de Vallière, C., et al., *G Protein-coupled pH-sensing Receptor OGR1 Is a Regulator of Intestinal Inflammation.* Inflammatory Bowel Diseases, 2015. **21**(6): p. 1269-1281.
255. D'Souza, C.A., et al., *OGR1/GPR68 Modulates the Severity of Experimental Autoimmune Encephalomyelitis and Regulates Nitric Oxide Production by Macrophages.* PLOS ONE, 2016. **11**(2): p. e0148439.
256. Rajendran, L. and K. Simons, *Lipid rafts and membrane dynamics.* Journal of Cell Science, 2005. **118**(6): p. 1099-1102.
257. Allen, J.A., R.A. Halverson-Tamboli, and M.M. Rasenick, *Lipid raft microdomains and neurotransmitter signalling.* Nat Rev Neurosci, 2007. **8**(2): p. 128-40.
258. Michel, V. and M. Bakovic, *Lipid rafts in health and disease.* Biology of the Cell, 2007. **99**(3): p. 129-140.
259. Simons, K. and D. Toomre, *Lipid rafts and signal transduction.* Nature Reviews Molecular Cell Biology, 2000. **1**: p. 31.
260. Varshney, P., V. Yadav, and N. Saini, *Lipid rafts in immune signalling: current progress and future perspective.* Immunology, 2016. **149**(1): p. 13-24.
261. Cherukuri, A., M. Dykstra, and S.K. Pierce, *Floating the raft hypothesis: lipid rafts play a role in immune cell activation.* Immunity, 2001. **14**(6): p. 657-60.
262. Huwiler, A., et al., *Physiology and pathophysiology of sphingolipid metabolism and signaling.* Biochimica et Biophysica Acta (BBA) - Molecular and Cell Biology of Lipids, 2000. **1485**(2–3): p. 63-99.
263. Arai, T., et al., *Lactosylceramide stimulates human neutrophils to upregulate Mac-1, adhere to endothelium, and generate reactive oxygen metabolites in vitro.* Circ Res, 1998. **82**(5): p. 540-7.
264. Mayo, L., et al., *B4GALT6 regulates astrocyte activation during CNS inflammation.* Nature medicine, 2014. **20**(10): p. 1147-1156.
265. McDonald, G., et al., *Normalizing glycosphingolipids restores function in CD4+ T cells from lupus patients.* J Clin Invest, 2014. **124**(2): p. 712-24.

266. Jury, E.C., et al., *Altered lipid raft-associated signaling and ganglioside expression in T lymphocytes from patients with systemic lupus erythematosus.* J Clin Invest, 2004. **113**(8): p. 1176-87.
267. Zhu, K., et al., *Sphingosylphosphorylcholine and lysophosphatidylcholine are ligands for the G protein-coupled receptor GPR4.* J Biol Chem, 2001. **276**(44): p. 41325-35.
268. Kloverpris, H., et al., *Dimethyl sulfoxide (DMSO) exposure to human peripheral blood mononuclear cells (PBMCs) abolish T cell responses only in high concentrations and following coincubation for more than two hours.* Journal of Immunological Methods, 2010. **356**(1): p. 70-78.
269. Timm, M., et al., *Considerations regarding use of solvents in in vitro cell based assays.* Cytotechnology, 2013. **65**(5): p. 887-894.
270. Kahler, C.P., *Evaluation of the use of the solvent dimethyl sulfoxide in chemiluminescent studies.* Blood Cells Mol Dis, 2000. **26**(6): p. 626-33.
271. Pala, M., et al., *Population- and individual-specific regulatory variation in Sardinia.* Nat Genet, 2017. **49**(5): p. 700-707.
272. Liu, J.Z., et al., *Association analyses identify 38 susceptibility loci for inflammatory bowel disease and highlight shared genetic risk across populations.* Nature Genetics, 2015. **47**: p. 979.
273. Shin, S.-Y., et al., *An atlas of genetic influences on human blood metabolites.* Nature genetics, 2014. **46**(6): p. 543-550.
274. Bertin, S., et al., *The ion channel TRPV1 regulates the activation and proinflammatory properties of CD4+ T cells.* Nat Immunol, 2014. **15**(11): p. 1055-1063.
275. Wang, C., et al., *CD5L/AIM Regulates Lipid Biosynthesis and Restrains Th17 Cell Pathogenicity.* Cell, 2015. **163**(6): p. 1413-27.
276. Zhu, Y., et al., *Lowering glycosphingolipid levels in CD4+ T cells attenuates T cell receptor signaling, cytokine production, and differentiation to the Th17 lineage.* J Biol Chem, 2011. **286**(17): p. 14787-94.
277. Pannu, R., A.K. Singh, and I. Singh, *A novel role of lactosylceramide in the regulation of tumor necrosis factor alpha-mediated proliferation of rat primary astrocytes. Implications for astrogliosis following neurotrauma.* J Biol Chem, 2005. **280**(14): p. 13742-51.
278. Bhunia, A.K., et al., *Lactosylceramide mediates tumor necrosis factor-alpha-induced intercellular adhesion molecule-1 (ICAM-1) expression and the adhesion of neutrophil in human umbilical vein endothelial cells.* J Biol Chem, 1998. **273**(51): p. 34349-57.
279. Martin, S.F., N. Williams, and S. Chatterjee, *Lactosylceramide is required in apoptosis induced by N-Smase.* Glycoconj J, 2006. **23**(3-4): p. 147-57.
280. Bodas, M., T. Min, and N. Vij, *Lactosylceramide-accumulation in lipid-rafts mediate aberrant-autophagy, inflammation and apoptosis in cigarette smoke induced emphysema.* Apoptosis, 2015. **20**(5): p. 725-39.
281. Rostami, A. and B. Ciric, *Astrocyte-derived lactosylceramide implicated in multiple sclerosis.* Nat Med, 2014. **20**(10): p. 1092-3.
282. Wenger, D.A., M.A. Rafi, and P. Luzi, *Molecular genetics of Krabbe disease (globoid cell leukodystrophy): diagnostic and clinical implications.* Hum Mutat, 1997. **10**(4): p. 268-79.
283. Ziegler, S.F., et al., *Molecular characterization of the early activation antigen CD69: a type II membrane glycoprotein related to a family of natural killer cell activation antigens.* Eur J Immunol, 1993. **23**.
284. Marzio, R., J. Mauel, and S. Betz-Corradin, *CD69 and regulation of the immune function.* Immunopharmacol Immunotoxicol, 1999. **21**.

285. Testi, R., et al., *The CD69 receptor: a multipurpose cell-surface trigger for hematopoietic cells.* Immunol Today, 1994. **15**(10): p. 479-83.
286. Sancho, D., M. Gómez, and F. Sánchez-Madrid, *CD69 is an immunoregulatory molecule induced following activation.* Trends in Immunology, 2005. **26**(3): p. 136-140.
287. Sancho, D., et al., *CD69 downregulates autoimmune reactivity through active transforming growth factor-beta production in collagen-induced arthritis.* J Clin Invest, 2003. **112**.
288. Cruz-Adalia, A., et al., *CD69 limits the severity of cardiomyopathy after autoimmune myocarditis.* Circulation, 2010. **122**(14): p. 1396-404.
289. González-Amaro, R., et al., *Is CD69 an effective brake to control inflammatory diseases?* Trends in molecular medicine, 2013. **19**(10): p. 625-632.
290. Shiow, L.R., et al., *CD69 acts downstream of interferon-alpha/beta to inhibit S1P1 and lymphocyte egress from lymphoid organs.* Nature, 2006. **440**(7083): p. 540-4.
291. Liu, G., et al., *The receptor S1P1 overrides regulatory T cell-mediated immune suppression through Akt-mTOR.* Nat Immunol, 2009. **10**(7): p. 769-77.
292. Garris, C.S., et al., *Sphingosine-1-phosphate receptor 1 signalling in T cells: trafficking and beyond.* Immunology, 2014. **142**(3): p. 347-53.
293. Fyrst, H. and J.D. Saba, *An update on sphingosine-1-phosphate and other sphingolipid mediators.* Nat Chem Biol, 2010. **6**(7): p. 489-97.
294. Prieschl, E.E. and T. Baumruker, *Sphingolipids: second messengers, mediators and raft constituents in signaling.* Immunology Today. **21**(11): p. 555-560.
295. O'Sullivan, C. and K.K. Dev, *Galactosylsphingosine (psychosine)-induced demyelination is attenuated by sphingosine 1-phosphate signalling.* Journal of Cell Science, 2015. **128**(21): p. 3878-3887.
296. Wu, Y.P., et al., *Sphingosine kinase 1/S1P receptor signaling axis controls glial proliferation in mice with Sandhoff disease.* Hum Mol Genet, 2008. **17**(15): p. 2257-64.
297. Chun, J. and V. Brinkmann, *A Mechanistically Novel, First Oral Therapy for Multiple Sclerosis: The Development of Fingolimod (FTY720, Gilenya).* Discovery medicine, 2011. **12**(64): p. 213-228.
298. Brinkmann, V., *FTY720 (fingolimod) in Multiple Sclerosis: therapeutic effects in the immune and the central nervous system.* Br J Pharmacol, 2009. **158**(5): p. 1173-82.
299. Viola, A., et al., *T Lymphocyte Costimulation Mediated by Reorganization of Membrane Microdomains.* Science, 1999. **283**(5402): p. 680-682.
300. Simons, K. and E. Ikonen, *Functional rafts in cell membranes.* Nature, 1997. **387**(6633): p. 569-72.
301. Martín, P. and F. Sánchez-Madrid, *CD69: an unexpected regulator of TH17 cell-driven inflammatory responses.* Science Signaling, 2011. **4**(165): p. pe14.
302. Cortes, J.R., et al., *Maintenance of immune tolerance by Foxp3+ regulatory T cells requires CD69 expression.* J Autoimmun, 2014. **55**: p. 51-62.
303. Kornfeld, S. and I. Mellman, *The biogenesis of lysosomes.* Annu Rev Cell Biol, 1989. **5**: p. 483-525.
304. Jmoudiak, M. and A.H. Futerman, *Gaucher disease: pathological mechanisms and modern management.* Br J Haematol, 2005. **129**(2): p. 178-88.
305. Vitner, E.B., A.H. Futerman, and N. Platt, *Innate immune responses in the brain of sphingolipid lysosomal storage diseases.* Biol Chem, 2015. **396**(6-7): p. 659-67.
306. Itoh, H., et al., *The fine structure of cytoplasmic inclusions in brain and other visceral organs in Sandhoff disease.* Brain Dev, 1984. **6**(5): p. 467-74.
307. Mellman, I., R. Fuchs, and A. Helenius, *Acidification of the endocytic and exocytic pathways.* Annu Rev Biochem, 1986. **55**: p. 663-700.

308. Mindell, J.A., *Lysosomal acidification mechanisms.* Annu Rev Physiol, 2012. **74**: p. 69-86.
309. Funato, K., et al., *Reconstitution of phagosome-lysosome fusion in streptolysin O-permeabilized cells.* J Biol Chem, 1997. **272**(26): p. 16147-51.
310. Lawrence, B.P. and W.J. Brown, *Autophagic vacuoles rapidly fuse with pre-existing lysosomes in cultured hepatocytes.* J Cell Sci, 1992. **102 (Pt 3)**: p. 515-26.
311. Cuervo, A.M. and J.F. Dice, *A receptor for the selective uptake and degradation of proteins by lysosomes.* Science, 1996. **273**(5274): p. 501-3.
312. Jaishy, B. and E.D. Abel, *Lipids, lysosomes, and autophagy.* J Lipid Res, 2016. **57**(9): p. 1619-35.
313. McKeown, S.R. and I.V. Allen, *The fragility of cerebral lysosomes in multiple sclerosis.* Neuropathol Appl Neurobiol, 1979. **5**(5): p. 405-15.
314. Kim, I., et al., *Excess Lipid Accumulation in Cortical Neurons in Multiple Sclerosis May Lead to Autophagic Dysfunction and Neurodegeneration (P5.237).* Neurology, 2015. **84**(14 Supplement).
315. Cuzner, M.L. and A.N. Davison, *Changes in cerebral lysosomal enzyme activity and lipids in multiple sclerosis.* Journal of the Neurological Sciences, 1973. **19**(1): p. 29-36.
316. Riekkinen, P., J. Palo, and I. Asikainen, *Lysosomal enzymes in the lymphocytes and granulocytes of patients with multiple sclerosis.* Acta Neurol Scand, 1977. **56**(1): p. 83-6.
317. Folts, C.J., et al., *Lysosomal Re-acidification Prevents Lysosphingolipid-Induced Lysosomal Impairment and Cellular Toxicity.* PLoS Biology, 2016. **14**(12): p. e1002583.
318. Dendrou, C.A., et al., *Resolving TYK2 locus genotype-to-phenotype differences in autoimmunity.* Sci Transl Med, 2016. **8**(363): p. 363ra149.
319. Martin, P., et al., *The leukocyte activation antigen CD69 limits allergic asthma and skin contact hypersensitivity.* J Allergy Clin Immunol, 2010. **126**(2): p. 355-65, 365.e1-3.
320. Lassen, K.G., et al., *Genetic Coding Variant in GPR65 Alters Lysosomal pH and Links Lysosomal Dysfunction with Colitis Risk.* Immunity, 2016. **44**(6): p. 1392-1405.
321. Formichi, P., et al., *Psychosine-induced apoptosis and cytokine activation in immune peripheral cells of Krabbe patients.* Journal of Cellular Physiology, 2007. **212**(3): p. 737-743.
322. Huang, X.P., et al., *Allosteric ligands for the pharmacologically dark receptors GPR68 and GPR65.* Nature, 2015. **527**(7579): p. 477-83.
323. Wirasinha, R.C., et al., *GPR65 inhibits experimental autoimmune encephalomyelitis through CD4+ T cell independent mechanisms that include effects on iNKT cells.* Immunology and Cell Biology, 2017.
324. Godfrey, D.I., et al., *NKT cells: facts, functions and fallacies.* Immunol Today, 2000. **21**(11): p. 573-83.
325. Sag, D., et al., *Improved Detection of Cytokines Produced by Invariant NKT Cells.* Sci Rep, 2017. **7**(1): p. 16607.
326. Ihara, Y., et al., *The G protein-coupled receptor T-cell death-associated gene 8 (TDAG8) facilitates tumor development by serving as an extracellular pH sensor.* Proceedings of the National Academy of Sciences, 2010. **107**(40): p. 17309-17314.

Appendix

1. The MS associated SNP rs74796499 in the *GALC* coding gene is in tight LD with other 4 SNPs.

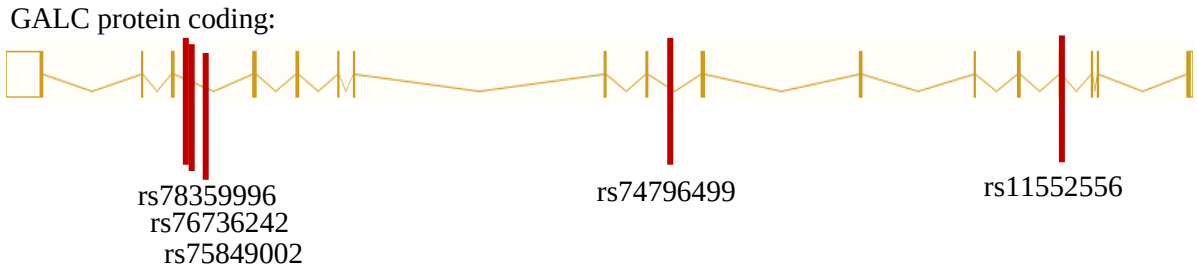

2. Influence of standard antibody volume (A), compensation and Compbeads volume (B) on the standard fluorescence.